



**KTH Electrical Engineering**

# **Multiantenna Cellular Communications**

Channel Estimation, Feedback, and Resource Allocation

EMIL BJÖRNSON

Doctoral Thesis in Telecommunications  
Stockholm, Sweden 2011

TRITA-EE 2011:072  
ISSN 1653-5146  
ISBN 978-91-7501-114-1

KTH Royal Institute of Technology  
School of Electrical Engineering  
Signal Processing Laboratory  
SE-100 44 Stockholm, SWEDEN

Akademisk avhandling som med tillstånd av Kungliga Tekniska högskolan framlägges till offentlig granskning för avläggande av teknologie doktorsexamen i telekommunikation torsdag den 17 november 2011 klockan 13.15 i hörsal K2, Teknikringen 28, Stockholm.

© Emil Björnson, November 2011, except where otherwise stated.

Many of the results have previously been published under IEEE copyright.

Tryck: Universitetsservice US-AB

*Tillägnad alla E:n i mitt liv*



## Abstract

The use of multiple antennas at base stations and user devices is a key component in the design of cellular communication systems that can meet the capacity demands of tomorrow. The downlink transmission from base stations to users is particularly limiting, both from a theoretical and a practical perspective, since user devices should be simple and power-efficient, and because many applications primarily create downlink traffic (e.g., video streaming). The potential gain of employing multiple antennas for downlink transmission is well recognized: the total data throughput increases linearly with the number of transmit antennas if the spatial dimension is exploited for simultaneous transmission to multiple users. In the design of practical cellular systems, the actual benefit of multiuser multiantenna transmission is limited by a variety of factors, including acquisition and accuracy of channel information, transmit power, channel conditions, cell density, user mobility, computational complexity, and the level of cooperation between base stations in the transmission design.

The thesis considers three main components of downlink communications: 1) estimation of current channel conditions using training signaling; 2) efficient feedback of channel estimates; and 3) allocation of transmit resources (e.g., power, time and spatial dimensions) to users. In each area, the thesis seeks to provide a greater understanding of the interplay between different system properties. This is achieved by generalizing the underlying assumptions in prior work and providing both extensions of previous outcomes and entirely new mathematical results, along with supporting numerical examples. Some of the main thesis contributions can be summarized as follows.

A framework is proposed for estimation of different channel quantities using a common optimized training sequence. Furthermore, it is proved that each user should only be allocated one data stream and utilize its antennas for receive combining and interference rejection, instead of using the antennas for reception of multiple data streams. This fundamental result is proved under both exact channel acquisition and under imperfections from channel estimation and limited feedback. This also has positive implications on the hardware and system design.

Next, a general mathematical model is proposed for joint analysis of cellular systems with different levels of base station cooperation. The optimal multicell resource allocation can in general only be found with exponential computational complexity, but a systematic algorithm is proposed to find the optimal solution for the purpose of offline benchmarking. A parametrization of the optimal solution is also derived, creating a foundation for heuristic low-complexity algorithms that can provide close-to-optimal performance. This is exemplified by proposing centralized and distributed multicell transmission strategies and by evaluating these using multicell channel measurements.



## Acknowledgements

I am grateful to my supervisor Prof. Björn Ottersten for giving me the opportunity to pursue doctoral studies in Telecommunications. Since the very beginning, you gave me the freedom and encouragement to explore whatever scientific challenges I found interesting. You have always pointed me in good directions and connected me to the right people, and I know by experience that you were always ready to step up for me when I needed someone to defend me. Likewise, I would like to acknowledge my co-advisor Prof. Mats Bengtsson for always having excellent answers to my questions. You have a unique ability to find weaknesses in my research at the very last moment, as well as to discover ways to rectify them.

I would like to thank some other distinguished researchers who have mentored me over the years: Dr. David Hammarwall took great care of me during my Master Degree project and shared his insights on limited feedback design; Prof. Eduard Jorswieck introduced me to majorization theory and has inspired me through his own research; and Prof. David Gesbert taught me the basics of multicell communications—which eventually became the main part of this thesis. Conversations with Prof. Joakim Jaldén and Prof. Per Zetterberg have impacted my research in unexpected ways. I am also very thankful to Dr. Niklas Jaldén, Dr. Randa Zakhour, Dr. Gan Zheng, Dr. Pandu Devarakota, Xueying Hou, Samer Medawar, Konstantinos Ntontin, and Jinghong Yang for our fruitful scientific collaborations and for surviving the process of writing papers with me.

The fourth floor on Osquldas väg 10 has provided an outstanding creative environment and social atmosphere—thanks to all past and present colleagues. Someone told me that coffee is a necessary condition for research; I resisted for four years, but I am writing this acknowledgement under the influence of espresso. I would like to give special thanks to Mattias Andersson and Simon Järmyr, who have endured sharing offices with me over the years. I am indebted to Rasmus Brandt, Nafiseh Shariati, Jinghong Yang, and Dr. Jiaheng Wang for their careful proofreading of the thesis. I also thank the computer support group for providing reliable resources, and Annika Augustsson and Tove Schwartz for always taking care of administrative issues.

I wish to thank Prof. Marios Kountouris for taking time to serve as opponent for this thesis, and also Prof. Håkan Hjalmarsson, Prof. Arogyaswami Paulraj, and Prof. Tommy Svensson for participating in the evaluation committee.

Most importantly, my family deserves a special mention. I want to thank my parents for always supporting my studies in whatever aspect. It is amusing that you still seem to feel bad for no longer being qualified to tutor me. I am also grateful that my brother has helped proofreading my scientific texts, although he is not an engineer. His early interest in cell phones has certainly influenced my choice of research area. Finally, the most remarkable thing is the love and patience shown, and sacrifices made, by my wife Emma. Without your wonderful support and suggestion of KTH for doctoral studies, finishing a thesis of this quality would not have been possible.

*Emil Björnson*

Stockholm, November 2011



# Contents

<b>Nomenclature</b>	<b>xi</b>
<b>1 Introduction</b>	<b>1</b>
1.1 Digital Communication . . . . .	1
1.2 Wireless Channels . . . . .	3
1.3 Cellular Networks . . . . .	7
1.4 System Operation . . . . .	14
<b>2 Problem Formulation: Background &amp; Contributions</b>	<b>17</b>
2.1 System Model . . . . .	17
2.2 System Operation . . . . .	27
2.3 Problem Formulation: Training-Based Estimation . . . . .	30
2.4 Problem Formulation: Feedback Design . . . . .	33
2.5 Problem Formulation: Multicell Transmission . . . . .	38
2.6 Contributions Outside the Scope of the Thesis . . . . .	45
<b>3 Training-Based Channel Estimation</b>	<b>47</b>
3.1 Training-Based Channel Estimation . . . . .	47
3.2 MMSE Channel Estimation . . . . .	48
3.3 Training Sequence Optimization . . . . .	51
3.4 Impact of Spatial Correlation . . . . .	60
3.5 Numerical Examples . . . . .	62
3.6 Summary . . . . .	68
3.A Collection of Proofs . . . . .	69
<b>4 Fundamental Properties of Feedback Design</b>	<b>81</b>
4.1 Introduction to Linear Precoding . . . . .	81
4.2 Receive Combining vs. Multistream Multiplexing . . . . .	86
4.3 $\epsilon$ -Outage Sum Rate and Feedback Design . . . . .	101
4.4 Low-Complexity Feedback Quantization . . . . .	105
4.5 Summary . . . . .	115
4.A Collection of Proofs . . . . .	116

<b>5</b>	<b>Framework for General Multicell Coordination</b>	<b>127</b>
5.1	Extending Multiuser MIMO to Multicell MIMO . . . . .	127
5.2	Multicell Performance Measures . . . . .	132
5.3	Basic Properties of Optimal Strategies . . . . .	136
5.4	Summary . . . . .	138
5.A	Collection of Proofs . . . . .	139
<b>6</b>	<b>Optimal Solutions to Multicell Resource Allocation</b>	<b>143</b>
6.1	Multicell Resource Allocation . . . . .	143
6.2	Fairness-Profile Optimization . . . . .	144
6.3	Multicell Monotonic Optimization . . . . .	149
6.4	Extensions to the System Model . . . . .	155
6.5	Numerical Illustrations . . . . .	161
6.6	Summary . . . . .	166
6.A	Collection of Proofs . . . . .	167
<b>7</b>	<b>Practical Solutions to Multicell Resource Allocation</b>	<b>171</b>
7.1	Multicell Resource Allocation . . . . .	172
7.2	Characterization of Optimal Resource Allocation . . . . .	172
7.3	Low-Complexity Multicell Resource Allocation . . . . .	177
7.4	Summary . . . . .	186
7.A	Collection of Proofs . . . . .	187
<b>8</b>	<b>Evaluation of Strategies for Multicell Resource Allocation</b>	<b>191</b>
8.1	Evaluation on Simple Synthetic Channels . . . . .	191
8.2	Evaluation on Channel Measurements . . . . .	195
8.3	Summary . . . . .	202
<b>9</b>	<b>Conclusions</b>	<b>205</b>
9.1	Future Work . . . . .	206
	<b>Bibliography</b>	<b>209</b>

# Nomenclature

## Abbreviations and Acronyms

The following abbreviations and acronyms are used in the thesis:

3GPP	3rd Generation Partnership Project
4G	Fourth Generation of Cellular Wireless Standards
BD	Block-Diagonalization
BER	Bit Error Rate
BRB	Branch-Reduce-and-Bound
BS	Base Station
c.u.	channel use
CDF	Cumulative Distribution Function
CDI	Channel Directional Information
CoMP	Coordinated Multipoint
COOPCOM	Cooperative and Opportunistic Communications in Wireless Networks
CQI	Channel Quality Information
CSI	Channel State Information
CVSINR	Centralized Virtual SINR
DVSINR	Distributed Virtual SINR
ECM	Exponential Correlation Model
FDD	Frequency Division Duplex
FM	Frequency Modulation
FPO	Fairness-Profile Optimization
GPS	Global Positioning System
HARQ	Hybrid Automatic Repeat Request
KKT	Karush-Kuhn-Tucker
LMMSE	Linear Minimum Mean Square Error
LSM	Local Scattering Model
LTE	3GPP Long Term Evolution
MAP	Maximum A Posteriori
MESC	Maximum Estimated SINR Combiner
MIMO	Multiple-Input Multiple-Output

MISO	Multiple-Input Single-Output
ML	Maximum Likelihood
MMSE	Minimum Mean Squared Error
MRC	Maximum Ratio Combining
MRT	Maximum Ratio Transmission
MS	Mobile Station (i.e., user device)
MSE	Mean Squared Error
MVDR	Minimum-Variance Distortionless Response
MVU	Minimum Variance Unbiased
NP-hard	Non-Deterministic Polynomial-Time hard
NS	Norm-Supported
OFDM	Orthogonal Frequency-Division Multiplexing
PAM	Pulse Amplitude Modulation
PDF	Probability Density Function
PSK	Phase-Shift Keying
QAM	Quadrature Amplitude Modulation
QBC	Quantization-Based Combining
QoS	Quality-of-Service
RVQ	Random Vector Quantization
SDMA	Space Division Multiple Access
SER	Symbol Error Rate
SINR	Signal-to-Interference-and-Noise Ratio
SLNR	Signal-to-Leakage-and-Noise Ratio
SNR	Signal-to-Noise Ratio
TDD	Time Division Duplex
TDMA	Time Division Multiple Access
UCA	Uniform Circular Array
ULA	Uniform Linear Array
WINNER+	Wireless World Initiative New Radio+
WLAN	Wireless Local Area Network
ZF	Zero-Forcing
ZFC	Zero-Forcing with Receive Combining

## Mathematical Notation

Upper-case boldface letters are used to denote matrices (e.g.,  $\mathbf{X}$ ,  $\mathbf{Y}$ ), while (column) vectors are denoted with lower-case boldface letters (e.g.,  $\mathbf{x}$ ,  $\mathbf{y}$ ). Scalars are denoted by italic letters (e.g.,  $X$ ,  $Y$ ) and sets by calligraphic letters (e.g.,  $\mathcal{X}$ ,  $\mathcal{Y}$ ). The following mathematical notations are used:

$\mathbb{C}^{N \times M}$	The set of complex-valued $N \times M$ matrices.
$\mathbb{R}^{N \times M}$	The set of real-valued $N \times M$ matrices.
$\mathbb{R}_+^{N \times M}$	The set of non-negative real-valued $N \times M$ matrices.

$\mathbb{Z}_+^{N \times M}$	The set of non-negative integer $N \times M$ matrices.
$x_i = [\mathbf{x}]_i$	Two ways of writing the $i$ th element of a vector $\mathbf{x}$ .
$x_{ij} = [\mathbf{X}]_{ij}$	Two ways of writing the $i, j$ th element of a matrix $\mathbf{X}$ .
$\text{diag}(x_1, \dots, x_N)$	The diagonal matrix with $x_1, \dots, x_N$ at the diagonal.
$\text{diag}(\mathbf{X}_1, \dots, \mathbf{X}_N)$	The block-diagonal matrix with $\mathbf{X}_1, \dots, \mathbf{X}_N$ at the diagonal.
$\mathbf{X}^T$	The transpose of $\mathbf{X}$ .
$\mathbf{X}^*$	The conjugate of a each element of $\mathbf{X}$ .
$\mathbf{X}^H$	The conjugate transpose of $\mathbf{X}$ .
$\mathbf{X}^{-1}$	The inverse of a square matrix $\mathbf{X}$ .
$\mathbf{X}^\dagger$	The Moore-Penrose pseudo inverse of $\mathbf{X}$ .
$\mathbf{\Pi}_{\mathbf{X}}$	The orthogonal projection matrix onto the column space of $\mathbf{X}$ (i.e., $\mathbf{\Pi}_{\mathbf{X}} = \mathbf{X}(\mathbf{X}^H \mathbf{X})^{-1} \mathbf{X}^H$ ).
$\mathbf{\Pi}_{\mathbf{X}}^\perp$	Projection matrix onto the orthogonal complement of the column space of $\mathbf{X}$ (i.e., $\mathbf{\Pi}_{\mathbf{X}}^\perp = \mathbf{I} - \mathbf{\Pi}_{\mathbf{X}}$ ).
$\Re\{x\}$	Real part of a scalar $x$ .
$\Im\{x\}$	Imaginary part of a scalar $x$ .
$ x $	Absolute value of a scalar $x$ .
$\angle x$	Phase of a complex-valued scalar $x$ .
$\lceil x \rceil$	The smallest integer not less than the scalar $x \in \mathbb{R}$ .
$\log_a(x)$	Logarithm of $x$ using the base $a \in \mathbb{R}_+$ .
$\mathcal{O}(\cdot)$	Big O notation where $f(x) = \mathcal{O}(g(x))$ means that it exist $c \in \mathbb{R}_+$ and $x_0 \in \mathbb{R}$ such that $ f(x)  \leq c g(x) $ for $x > x_0$ .
$\text{tr}\{\mathbf{X}\}$	The trace of a square matrix $\mathbf{X}$ .
$\text{rank}\{\mathbf{X}\}$	The rank of a matrix $\mathbf{X}$ (i.e., non-zero singular values).
$\text{span}\{\mathbf{X}\}$	Orthonormal basis for the row space of $\mathbf{X}$ .
$\text{null}\{\mathbf{X}\}$	Orthonormal basis for the null space to the rows of $\mathbf{X}$ .
$\text{radius}\{\mathbf{X}\}$	The spectral radius of a matrix $\mathbf{X}$ .
$\text{vec}(\mathbf{X})$	The vector obtained by stacking the columns of $\mathbf{X}$ .
$\mathcal{N}(\mathbf{x}, \mathbf{R})$	The multivariate Gaussian distribution with mean $\mathbf{x}$ and covariance matrix $\mathbf{R}$ .
$\mathcal{CN}(\mathbf{x}, \mathbf{R})$	The circular symmetric complex Gaussian counterpart.
$\mathbb{E}\{\mathbf{X}\}$	The mathematical expectation of a stochastic $\mathbf{X}$ .
$\ \mathbf{x}\ _p$	The $L_p$ -norm $\ \mathbf{x}\ _p = (\sum_i  x_i ^p)^{1/p}$ of $\mathbf{x}$ .
$\ \mathbf{X}\ _F$	The Frobenius norm $\ \mathbf{X}\ _F = \sqrt{\sum_{i,j}  x_{ij} ^2}$ of $\mathbf{X}$ .
$ \mathcal{S} $	The cardinality (i.e., number of members) of a set $\mathcal{S}$ .
$\mathcal{S} \setminus \{k\}$	The remaining set when member $k$ is removed.
$\mathcal{S}_1 \cup \mathcal{S}_2$	Union set with all members which are in $\mathcal{S}_1$ and/or $\mathcal{S}_2$ .
$\mathcal{S}_1 \cap \mathcal{S}_2$	Intersection set with all members which are in <i>both</i> $\mathcal{S}_1$ and $\mathcal{S}_2$ .
$\mathcal{S}(n)$	The $n$ th member of a set $\mathcal{S}$ .
$\forall x$	Means that a statement holds for all $x$ (in the set that $x$ belongs to).

$x \in \mathcal{S}$	If $\mathcal{S}$ is a set: $x$ is a member. If $\mathcal{S}$ a stochastic distribution: $x$ is a realization.
$\mathbf{X} \otimes \mathbf{Y}$	The Kronecker product of two matrices $\mathbf{X}$ and $\mathbf{Y}$ .
$\mathbf{X} \succ \mathbf{Y}$	Means that $\mathbf{X} - \mathbf{Y}$ is positive definite.
$\mathbf{X} \succeq \mathbf{Y}$	Means that $\mathbf{X} - \mathbf{Y}$ is positive semi-definite.
$\mathbf{x} \succeq \mathbf{y}$	Means that the vector $\mathbf{x}$ majorizes $\mathbf{y}$ (see (2.14)).
$\mathbf{x} > \mathbf{y}$ ( $\mathbf{x} \geq \mathbf{y}$ )	Means that $x_i > y_i$ ( $x_i \geq y_i$ ) for all vector indices $i$ .
$\mathbf{I}_N$	The $N \times N$ identity matrix.
$\mathbf{1}_N$	The $N \times 1$ matrix (i.e., vector) of only ones.
$\mathbf{0}_N$	The $N \times N$ matrix of only zeros.
$\mathbf{0}_{N \times M}$	The $N \times M$ matrix of only zeros.

## Thesis Specific Notation

Symbols and functions that are commonly used in the thesis are summarized as follows:

$\mathbf{a}$	Lowest performance levels in a FPO problem.
$\boldsymbol{\alpha}$	Fairness-profile vector in a FPO problem.
$B$	Total number of channel feedback bits per user.
$B_d$	Number of feedback bits for CDI per user.
$B_q$	Number of feedback bits for CQI per user.
$\text{BS}_j$	Base station $j$ .
$\mathcal{C}_j$	Set of users that $\text{BS}_j$ coordinates interference to.
$\mathbf{C}_k$	Diagonal matrix such that $\mathbf{h}_k^H \mathbf{C}_k$ is the channel that carries non-negligible interference to user $k$ .
$\mathbf{C}_{jk}$	Equal to $\mathbf{I}_{N_j}$ if $\text{BS}_j$ coordinates interference to user $k$ .
$\mathcal{D}_j$	Set of users that $\text{BS}_j$ can send data to.
$\mathbf{C}_{jk}$	Equal to $\mathbf{I}_{N_j}$ if $\text{BS}_j$ can send data to user $k$ .
$\mathbf{D}_k$	Diagonal matrix such that $\mathbf{h}_k^H \mathbf{D}_k$ is the channel that carries data.
$d(\cdot, \cdot)$	Chordal distance between the spaces spanned by two matrices.
$\delta$	Predefined accuracy of the solution to FPO problems.
$\varepsilon$	Predefined accuracy of the solution in the BRB algorithm.
$\mathbf{e}_k$	Denotes the $k$ th column of an identity matrix.
$\mathbf{E}_k$	Error covariance matrix for channel estimation to user $k$ .
$f(\cdot)$	System performance function.
$g_k(\cdot)$	Performance function of user $k$ .
$\hat{g}_k(\cdot)$	Performance function of user $k$ under worst-case robustness.
$\mathcal{G}_{N, \bar{M}}$	Complex Grassmannian manifold with all $\bar{M}$ -dimensional subspaces passing through the origin of an $N$ -dimensional space.
$\mathbf{h}_k$	Effective channel vector from all transmit antennas to user $k$ (i.e., $\mathbf{h}_k = \mathbf{H}_k^H \mathbf{r}_k$ if $M > 1$ ).
$\mathbf{h}_{jk}$	Effective channel vector from $\text{BS}_j$ to user $k$ .
$\mathbf{H}_k$	Channel matrix from all transmit antennas to a

	multi-antenna user $k$ .
$\bar{\mathbf{H}}_k$	Mean value of the channel matrix for user $k$ .
$K_r$	Number of receiving users.
$K_t$	Number of transmitting base stations.
$L$	Total number of constraints in the system.
$L_p$	Number of power constraints in the system.
$L_k$	Number of soft-shaping constraints for user $k$ .
$\mathcal{M}_\infty$	Multiplexing gain of a transmit strategy.
$m$	Equal to $\min(N, B)$ in channel estimation.
$M_k$	Number of antennas at the $k$ th user.
$\text{MS}_k$	User $k$ .
$\text{MSE}_k$	Mean squared error for user $k$ .
$\widetilde{\text{MSE}}_k$	Worst-case robust mean squared error for user $k$ .
$N$	Total number of transmit antennas in the system.
$N_j$	Number of antennas at the $j$ th base station.
$\mathcal{N}$	Set of boxes in the BRB algorithm.
$\varrho$	Total training power for channel estimation.
$\mathbf{P}_k$	Training matrix designated for user $k$ .
$\tilde{\mathbf{P}}_k$	Kronecker version ( $\mathbf{P}_k^T \otimes \mathbf{I}_M$ ) of the training matrix.
$\mathbf{Q}_l$	Weighting matrix for the $l$ th power constraint.
$q_l$	Upper limit for the $l$ th power constraint.
$\mathbf{r}_k$	Receive combining vector for user $k$ .
$r_k$	Equalizing coefficient for user $k$ .
$\mathcal{R}$	Performance region.
$\tilde{\mathcal{R}}$	Robust performance region under worst-case robustness.
$\mathcal{R}_\infty$	Asymptotic rate offset of a transmit strategy.
$\mathbf{R}_k$	Channel covariance matrix for user $k$ .
$\mathbf{R}_{T,k}$	Transmit-side channel covariance matrix for user $k$ .
$\mathbf{R}_{R,k}$	Receive-side channel covariance matrix for user $k$ .
$\mathbf{S}_k$	Signal correlation matrix for user $k$ .
$\sigma_k^2$	Noise variance for user $k$ (if white noise).
$\bar{\Sigma}_Q$	Temporal disturbance covariance matrix.
$\bar{\Sigma}_R$	Received spatial covariance matrix of disturbance.
$\Sigma_k$	Covariance matrix of the (colored) disturbance for user $k$ .
$\text{SINR}_k$	Signal-to-interference-and-noise ratio of user $k$ .
$t$	Index of current time instant.
$\mathcal{T}$	Set of time instants with a static channel under block fading.
$\mathbf{T}_{ik}$	The $i$ th soft-shaping matrix of user $k$ .
$\tau_{ik}$	Upper limit for the $i$ th soft-shaping constraint of user $k$ .
$\mathbf{v}_k$	Precoding vector for user $k$ .
$\mathbf{y}_k$	Received data signal at user $k$ .
$\mathbf{Y}_k$	Received training signal at user $k$ .



# Chapter 1

## Introduction

This chapter gives a basic introduction to the topics of this thesis: digital communication, wireless channels, multiantenna transmission, and the physical operation of cellular networks. The purpose of the chapter is to provide sufficient background to be able to understand the basic research problems that are considered herein and how the thesis contributes to these areas. The mathematical system model, research background, and exact problem formulations are given in Chapter 2.

### 1.1 Digital Communication

The purpose of digital communication is to transfer some kind of information from one device to another. Digital information is represented by a (finite) sequence of bits—that is, digits that are either zero or one. These bits can be used to describe any kind of information, either exactly or approximately. Written language contains a limited number of letters and can therefore be perfectly described with bits; a sequence of 8 bits can have  $2^8 = 256$  different appearances and represent all letters/symbols in Western languages. This was recognized by Samuel Morse and his fellow inventors in the 19th century when they created the Morse code for transmission of textual information using the electrical telegraph. Each letter in the Morse code was represented by a sequence of short and long tones, which corresponds exactly to a bit sequence.

As opposed to written language, sound and pictures can only be approximately described by a (finite) sequence of bits, as they are not limited in their sound or appearance. The digital approximation of such information consists of two steps: *sampling* and *quantization*. As an example, sampling makes a picture consist of a certain number of pixels (i.e., points having a certain color), while quantization approximates the color of each pixel using a limited color palette (e.g., 24 bits can represent millions of

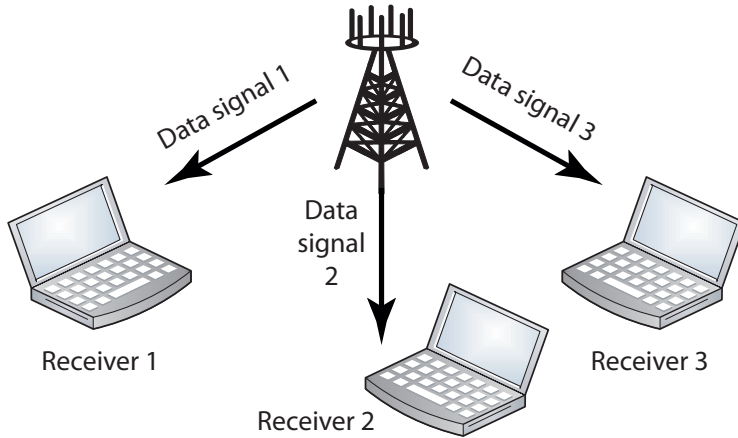


Figure 1.1: This thesis considers a scenario where one transmitter sends (independent) data signals wirelessly to multiple user devices.

different colors). Similarly, sampling means that sound is only recorded a certain number of times per second (e.g., 44,100 times/second on a CD), while quantization approximates the sound at each recorded time instant using a limited number of bits (e.g., 16 bits on a CD). If the sampling and quantization is fine enough, meaning that the number of bits is large enough, it is almost impossible for a human to perceive the difference between the original information and the approximate version described by the bit sequence.

In this thesis, each sequence of bits is called a *data signal* and it might describe any kind of information (i.e., the information source is not important in this thesis). We consider a scenario where one transmitting device should provide a set of wireless user devices with independent data signals; see Figure 1.1. The signals are sent as radio waves and the overall goal is to transfer each data signal to its designated receiver as fast and efficiently as possible. The transfer speed is called the *data rate* and describes how many bits that can be transferred to a certain user per second. It is desirable to have high data rates since that means fast transmissions, but it also makes the transmission more vulnerable to disturbances (e.g., interference from other systems and background noise). The data rate basically depends on the amount of power used to transmit the data signal divided by the power level of the disturbances. The power resources are limited, by factors such as power supplies, national frequency spectrum regulations, and money. From an engineering perspective, efficient transmission therefore means using the available power to achieve as high data rates as possible.

The data rate is not a perfect way of describing the performance. At any data rate, there is a risk that the disturbances happen to be so strong that the receiving device cannot recover the exact transmitted data signal; certain zeros might be incorrectly interpreted as ones, and *vice versa*. One can imagine this as listening to a Morse code transmission; in a silent room, it is easy to hear if the tones are long or short, but if a jet plane happens to fly over the roof you will not hear anything of the Morse code.

The risk of errors increases with the data rate and errors can have large consequences, for example making “yes” seem like “no”. These mistakes can be avoided by adding a mechanism to detect errors. If we send a text message, we can for example add a few *error control bits* that describe how many times each letter occurs. The receiver can then check if the received message contains the right set of letters. If not, the receiver knows that some error has occurred and can request that the message is retransmitted. The error control design is a rich research area by itself and is not covered by the thesis, but it clarifies one of the main motivations behind sending digital information (although it might be an approximation of the original information): with error control, we can be sure that user will receive exactly the same information as was originally transmitted. Since retransmissions create delays, efficient transmission means finding a good balance between having a high (original) data rate and a low risk of error.

## 1.2 Wireless Channels

When digital information is transferred from one device to another, it passes through some kind of physical medium called the *channel*. There are basically two types of channels: wired and wireless. In the former category, data signals are sent as electrical impulses in cables or as light impulses in optical fibers. In this thesis, we concentrate on the category of wireless channels where the data is sent through the air as electromagnetic radio waves. Cellular telephony and WLAN (i.e., wireless computer networks) are examples of communication systems that operate over wireless channels. Wireless communication is more flexible than its wired counterpart, since wireless devices are allowed to move around freely. The downside is that the properties of the wireless channel will change as the user is moving around, making it harder to adapt the transmission by, for example, finding the appropriate data rate.

The following properties provide understanding of wireless channels:

- **Path loss:** When radio waves are emitted from an antenna, they spread in all directions as the water from a sprinkler would do. Therefore, one can imagine that the further apart the transmitter and the receiver are, the less signal power (or similarly, water) will arrive at the receiver (or similarly, the plants). This decay is called the *path*

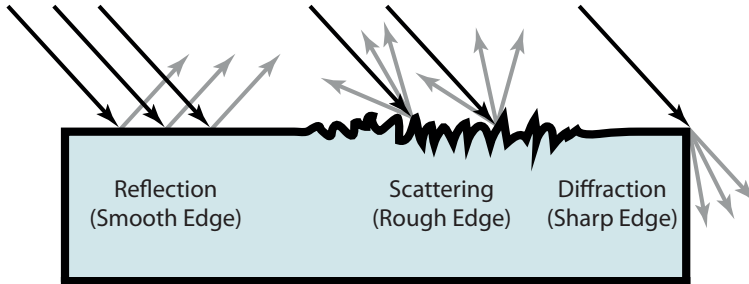


Figure 1.2: Illustration of three propagation effects for radio waves.

*loss* and decides how large portion of the transmitted power that will be received. This portion decays rapidly with distance: as the squared distance if the transmitter and receiver can “see” each other and with even larger exponents (e.g., 2 – 6) in urban areas with only multipath propagation (described next).

- Multipath propagation:** Since radio waves propagate in all directions, they will reach many objects in the surroundings: buildings, streets, cars, trees, etc. These objects will absorb parts of the signal power carried by the radio waves. Depending on the geometry and material of the objects, the waves will also be reflected (on flat surfaces), scattered (on rough surfaces), or diffracted (if the object has sharp edges). These phenomena are illustrated in Figure 1.2. The implication is that the transmitted radio waves can bounce on a multitude of different objects and arrive at the receiver through different paths, see Figure 1.3. At a first glance, multipath propagation is advantageous since more signal power arrives at the receiver (each path component carries some signal power). However, the components have traveled different distances and might arrive with unsynchronized phases, meaning that they interfere with (rather than support) each other. This is illustrated in Figure 1.4 and one can think of it as waves in the ocean: the receiver wants to be at a location where the water waves are large. But just as the water waves are constantly moving and changing, multipath propagation creates continuous variations in the received signal power. Even if the device is not in motion, other objects will move around and influence the different paths.
- Shadowing:** In certain environments, there are large buildings or hills that block the way from the transmitter to the receiver. This phenomenon is called shadowing and basically means that the re-

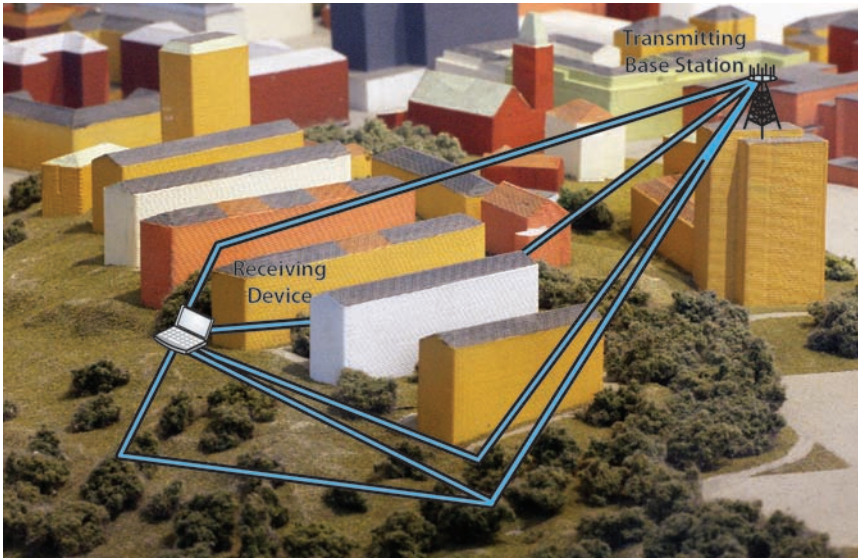


Figure 1.3: Schematic illustration of a wireless channel in an urban environment. There is no direct path between the transmitting base station and the receiving device, but the signal reaches the receiver through multipath propagation (e.g., reflections in buildings, scattering in trees, etc.).

ceived power in a certain area can be much worse than described by the path loss. As opposed to multipath propagation, shadowing typically creates slow variations in the received signal power—one needs to leave the shadowed area before the situation improves.

In principle, the wireless channel can be perfectly described by calculating exactly how the radio waves propagate between the transmitter and receiver. But this is not very meaningful since the environment is rapidly changing. Instead, it is common to summarize the channel properties as

- **Large-scale fading:** Slow variations as the device moves over a large area (e.g., path loss and shadowing).
- **Small-scale fading:** Rapid variations that occurs all the time (e.g., multipath propagation).

This thesis assumes that the large-scale fading properties are known for each user (i.e., its slow variations can be tracked), to concentrate the analysis on some methods for acquiring accurate knowledge of the current small-scale fading. To simplify the analysis, we assume that the small-scale fading

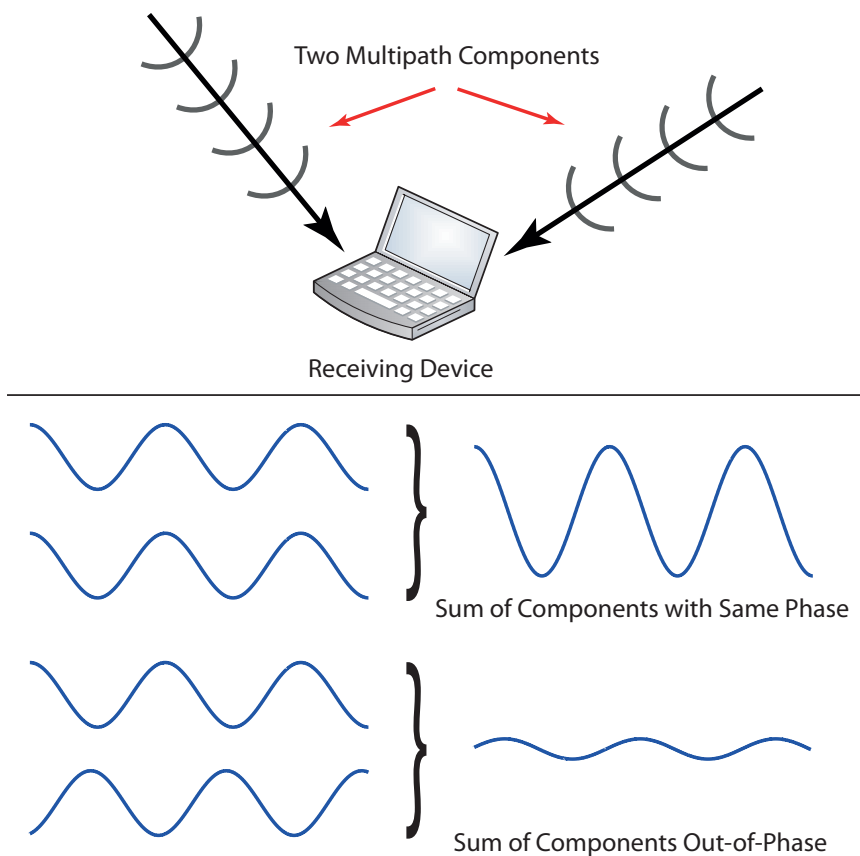


Figure 1.4: Illustration of multipath propagation, where the radio signal arrives at the receiver through multiple paths. If all components arrive with the same phase, the received signal becomes stronger. However, the components have traveled different distances and might cancel out each other by being out-of-phase. The rapid channel variations induced by changes in the phases of the multipath components are called small-scale fading.

is constant for a short period called the *coherence time* (e.g., a few milliseconds) and only needs to be estimated once per such time period.

### 1.2.1 Frequency Spectrum: Narrowband and Wideband

The radio frequency spectrum is a global resource used for many different things: FM radio, television broadcasting, mobile communications, WLAN, satellite services, navigation, amateur radio, military applications, etc. In other words, the frequency spectrum is very crowded and it is difficult to find unused frequency bands that can be used for new wireless services. Recently, many countries have replaced analog television broadcasting with more spectrally efficient digital techniques. This has allowed for reallocation of some frequency bands to enable the deployment of emerging 4G wireless communication systems. But the frequency resources are still scarce, which makes licensing of radio spectrum a major cost for network operators. From an engineering perspective, wireless communication systems should therefore be designed to use their assigned frequency bands as efficiently as possible.

Most wireless communication systems operate at a center frequency somewhere in the band of 0.7–5 GHz and has a total system bandwidth of about 10–40 MHz around their center frequency. Such large bandwidths are called *wideband* and are complicated since the small-scale fading behaves differently in different parts of the frequency band. Therefore, it is common to divide the bandwidth into many smaller frequency bands that are *narrowband*, meaning that the channel properties are approximately the same in the whole band and thereby easier to acquire. Recent wireless standards, such as LTE/4G and WLAN, use a technique called *orthogonal frequency-division multiplexing* (OFDM) to divide a wideband channel into many narrowband subchannels. This thesis considers narrowband channels and the analysis can be applied directly to each of the subchannels of an OFDM system.

## 1.3 Cellular Networks

In principle, two mobile devices can send wireless signals directly to each other (as walkie-talkies do), but this is often impractical since the distance should be small or else they will consume massive amounts of transmit power. The common solution is to divide a geographic area into cells, where each cell is governed by a base station. These base stations are placed on fixed locations, preferably at roof-tops or other elevated places where radio waves more easily find their ways to devices everywhere in the cell (i.e., to limit the risk of shadowing). Base stations are connected to each other by a *backhaul network*, which could consist of both cables and fixed wireless links.

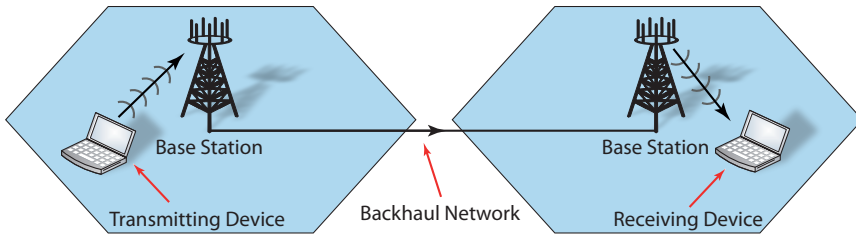


Figure 1.5: Schematic illustration of cellular communication from one user to another: The transmitting user sends data to its base station, the data is forwarded to another base station through the backhaul network, and the receiving user obtains the data from its base station.

When a device wants to send a data signal to another device, it will first send it wirelessly to the nearest base station. This station forwards the signal over the backhaul network to the base station closest to the receiving device. Finally, the receiving base station sends the signal wirelessly to the receiving device. This example is illustrated in Figure 1.5.

Cellular networks have many advantages over direct transmission:

1. Shorter distances imply higher data rates and lower power usage;
2. Efficient use of frequency resources since the same frequency band can be used simultaneously in multiple cells that are geographically separated (with only limited interference);
3. It is simple to connect wireless devices to regular corded telephones and to access Internet services.

This thesis considers cellular networks and studies how the transmissions within a cell should be designed to optimize the performance and how to coordinate the operation of multiple cells. The main focus is on transmission from a base station to multiple user devices, which is commonly viewed as more difficult than transmission in the opposite direction.

### 1.3.1 Multiantenna Transmission

The performance of cellular systems can be improved by employing more than one antenna at each base station and user device. Such systems are called *multiple-input multiple-output* (MIMO). Each transmit antenna can be viewed as a mouth and each receive antenna as an ear. The extra mouths and ears can be used for diversity or multiplexing:

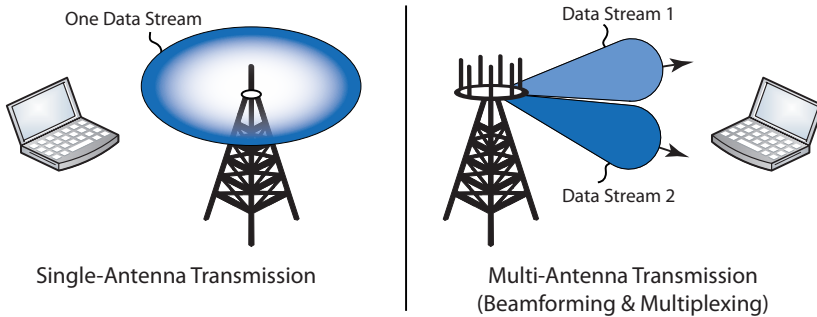


Figure 1.6: Comparison of single-antenna and multi-antenna transmission. With a single antenna, the signal propagates in all directions (and most directions will not lead to the user). With multiple antennas, the signal can be directed towards the users (called beamforming). Multiple signals can be sent in parallel using different beamforming (called multiplexing).

- Diversity:** The multipath propagation between each pair of transmit and receive antennas will be different. This creates a diversity of routes that the transmitted signal can travel to the destination. One of these routes will carry the strongest signal and should be used for transmission. Certainly, by selecting the best route out of many possibilities we will achieve better performance than if we are stuck with only one possibility (as in the single antenna case). The result can be viewed as speaking with many mouths in such a way that the voice is directed towards the user and using the ears to listen carefully in this direction. Note that the best route is usually not to select one antenna/mouth at the transmitter and one antenna/ear at the receiver, but to combine *all* of them in a smart way to achieve one strong voice that is easy to hear. This directing is called *beamforming* since it forms a directed signal beam towards the receiver, instead of sending in all directions as with a single antenna; see Figure 1.6. The best beamforming direction can be quite different from a line drawn between the transmitter and the receiver, because there are often no direct path in cellular systems but only (indirect) multipath propagation (see Figure 1.3).
- Multiplexing:** Instead of using only the best route as in the diversity case, MIMO techniques can be used to send multiple data signals in parallel. The idea can be viewed as listening to different voices with each ear and is called *multiplexing*. It can be achieved by directing the signals toward different ears using the beamforming idea in Figure 1.6. To multiplex four data signals, both the transmitter and the receiver

need to have four antennas—it is the minimum of the number of mouths and the number of ears that decides how many signals that can be multiplexed.

It is not obvious whether the antennas should be used to achieve diversity or to perform multiplexing, or a little bit of both. Diversity reduces the risk of errors in the transmission (since all ears are focused on the same signal), while multiplexing increases the total data rate (since ears are listening to different signals). Beamforming requires knowledge of how the channel behaves; otherwise the desirable beam direction will remain unknown. Therefore, multiplexing is preferred if the channel knowledge is accurate (so we can be sure that each ear will hear a different voice), while diversity can protect against inaccuracies. How to achieve reliable channel knowledge is one of the main topics of the thesis.

The advantages of multiantenna transmission all depend on whether the channels from each transmit antenna to each receive antenna experience different multipath propagation (i.e., the signals travel different routes). This is not necessarily the case: if the transmitter and receiver are located in a tunnel that acts like a waveguide, there is basically just one route between them irrespectively of how many antennas we employ. Fortunately, such closed environments are rare in practice. Instead, the important thing is that the antennas are sufficiently separated to be able to observe different signal routes. The wavelength decides what is a good separation, and it is short when the frequency is high and *vice versa*. For frequencies in the range of 0.7 – 5 GHz, a good separation is one or a few decimeters. Thus, we can expect the next generation of communication systems to employ, for example, two antennas in handheld devices, up to four antennas in laptops, and perhaps even more at the base stations (which are less size-constrained). Of course, there will always be some similarities between the antennas; this is called *spatial correlation*. Geometrically, it means that transmissions in some spatial directions are more probable to arrive at the receiver and that the receiver is more probable to hear strong signals from certain directions. This behavior is natural; if the base station is placed on a roof top, it is probably better to use beamforming to send signals along a street leading towards the receiver than to send it in a completely different direction; see Figure 1.3. This thesis analyzes how spatial correlation impacts on various aspects of cellular networks.

### 1.3.2 Multiuser MIMO

There are often many users in a cell that would like to communicate at a given time instant. The demand for data traffic is continuously growing since both the number of user devices and the use of them increase rapidly. This puts cellular networks under pressure and motivates the de-

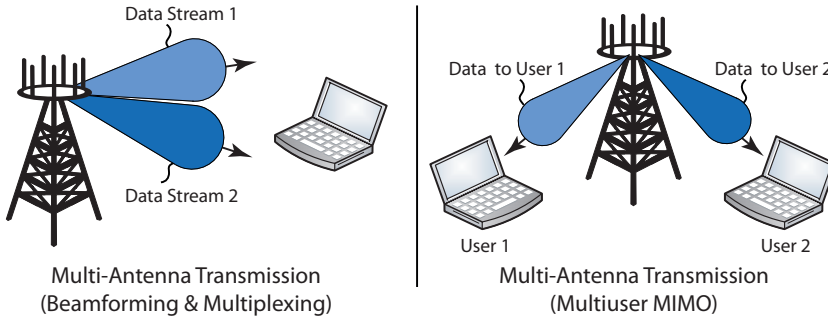


Figure 1.7: Two types of multi-antenna transmission: Send many streams to one users or one stream each to many users. The latter can make user devices less complex and is more resilient to bad channel properties, but accurate channel knowledge is required to find the user directions.

sign of efficient methods for dividing the available transmit resources between users. Such *resource allocation* should allocate users to time slots, frequency subchannels, spatial beamforming directions, and different portions of the transmit power.

An advantage of having many users is that it creates a *multiuser diversity*, meaning that we can decide to transmit to a given user when the small-scale fading makes the channel strong. We can also select users that are evenly distributed in the cell, to make their respective beamforming directions as different as possible. By prioritizing users with strong channel conditions and select spatially separated users, the total performance can be greatly improved. In general, resource allocation is a very complex and difficult problem to solve, since it involves both finding strong users and maintain some kind of fairness between users that are located at different distances from the base station (so that users in the cell center will not “steal” all transmission resources).

At a given time and subchannel, the base station has to decide whether it should serve one of the users (perhaps with multiplexing) or if multiple users should be served in different spatial directions; see Figure 1.7. The latter is known as *multiuser MIMO* and has several practical advantages over single-user transmission (described in Section 1.3.1):

- **Simple user devices:** Recall that the number of parallel signals in the single-user case was limited by the minimum of the number of transmit antennas (mouths) and receive antennas (ears). In multiuser MIMO, there are very many ears located at different user devices and all of these receive antennas are counted. The same total performance can therefore be achieved by having many simple user devices with few antennas and limited processing power, instead of

one large and complicated device with many antennas. In addition, multiuser MIMO could enable more parallel data signals since the number of streams is no longer limited by the number of antennas at each user, but mainly depends on how many antennas that are placed at the base station.

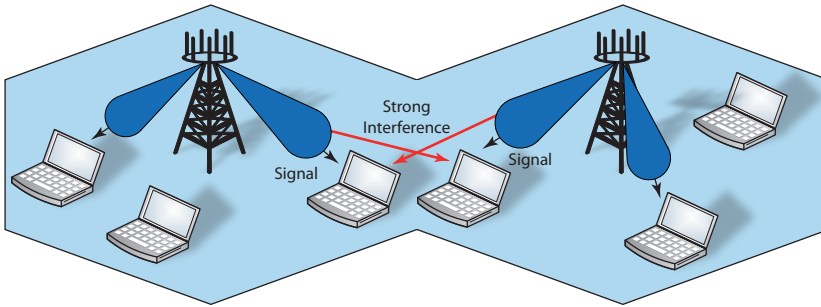
- **Better channel properties:** Each user is located in a certain direction from the base station, thus there will naturally only be a few beamforming directions that lead to this user. Even if the receive antennas are sufficiently separated, they can only hear signals that arrive to a small part of the cell; it is hard to imagine an environment where the base station can send signals in any direction and expect them all to arrive at the user (with equal strength). With multiuser MIMO, we can select users that are located in completely different directions (from the base station) and thereby have ears all over the cell. Beamforming can be used to direct each signal towards its user, without creating much interference between users; see Figure 1.7.

Recall that multiplexing required knowledge of how the channel behaves, to enable proper beamforming selection. The downside of multiuser MIMO is that this requirement becomes even more critical. We would like each user to only hear its designated signal, but the base station must have accurate knowledge of the direction of the user to achieve low interference. If the channel knowledge is uncertain, the signals will be mixed up and each user will only hear a clutter of interfering signals. The thesis analyzes how the accuracy of channel knowledge impacts the performance and how to improve the accuracy in scenarios with many users.

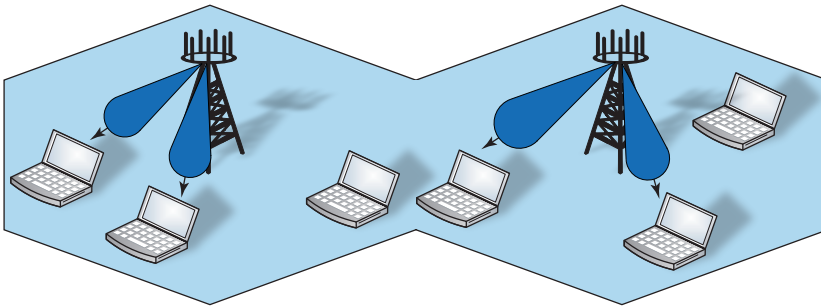
### 1.3.3 Multicell Coordination

A cellular network consists of a large number of cells and each user connects to the closest base station (i.e., the one with the strongest channel). Thus, there are invisible edges between each cell where user devices switch between the corresponding base stations. The activities in one cell will be influenced by activities in neighboring cells. The extreme case is that two users are next to each other, but at different sides of the cell edge and thus belong to different cells. If these users are served in parallel (at the same subchannel), their respective data signals will cause severe interference to each other; see Figure 1.8a. In other words, there needs to be some kind of coordination of resource allocation between adjacent cells.

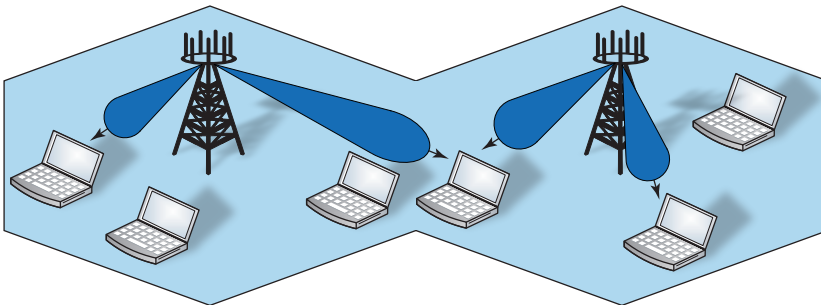
The simplest coordination scheme would be to forbid adjacent cells to use the same subchannels. This will basically remove the interference between cells, but leads to poor exploitation of the scarce frequency resources. Multiantenna transmission enables more intricate coordination



(a) Uncoordinated Multicell: Strong interference might be caused to cell edge users.



(b) Coordinated Interference: Base stations cooperate by only sending parallel transmissions to users in different directions.



(c) Coordinated Multipoint Transmission: Base stations cooperate and jointly serve cell edge users from both base stations.

Figure 1.8: Three levels of multicell coordination. More coordination leads to lower interference and higher performance, but requires more signaling between base stations and more accurate channel knowledge.

schemes where base stations avoid allocating the same time/frequency-resource to adjacent users at the cell edge; see Figure 1.8b. Such schemes require that base stations share decisions with neighboring base stations. In addition, each base station needs to know the channels to all users in adjacent cells that they might cause interference to.

In addition to interference avoidance, multicell coordination can also be used to jointly serve certain users through multiple base stations and thereby remove the strict cell edges; see Figure 1.8c. Joint transmission to a user is called *coordinated multipoint* (CoMP) transmission and will ideally make all the cells act as just one cell (with transmit antennas at different locations). This has great potential as it makes the the number of parallel data signals limited by the total number of antennas (mouths) at all base stations. But just as every other advanced transmission scheme, CoMP transmission requires very accurate channel knowledge and good backhaul networks between base stations to enable fast coordination.

This thesis shows how to jointly model and analyze different level of multicell coordination. We derive a method for finding the optimal transmission scheme (which requires extensive computations) and propose more practical schemes that still achieves good performance.

## 1.4 System Operation

There are two transmission directions in cellular systems; transmission from the base station to the users is called the *downlink*, while transmission from the users to the base station is known as the *uplink*. As mentioned earlier, this thesis concentrates on downlink transmission on a single subchannel, but we assume that there also exist uplink subchannels so that the base station and the users can exchange information and decisions.

The MIMO techniques and multicell coordination schemes described in Section 1.3 all require accurate channel knowledge. At the same time, the channels are constantly changing due to small-scale fading. It is therefore necessary to have a mechanism that acquires channel knowledge at a regular intervals to keep it up-to-date. The common way is to use so-called *training signaling*; that is, sending a known signal and trying to estimate channel properties by comparing the transmitted signal with the received signal. Training signaling provides the receiver with channel knowledge. This information can be fed back to the base station, but it should be done in a concise way to save resources. When both the base station and the users have learned the channel, this information is used for resource allocation, multiuser MIMO transmission, multicell coordination, and processing of the received data signals. After a while (e.g., a few milliseconds), the small-scale fading has changed the channel and made the acquired channel

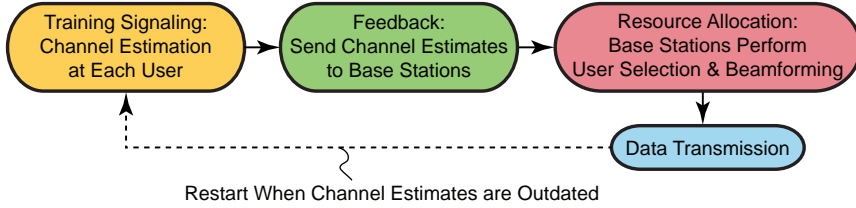


Figure 1.9: Schematic illustration of the system operation in a wireless communication system. The three main components are training signaling for channel estimation, feedback of channel information, and resource allocation. These are also the three main topics of the thesis.

information outdated. It is time for new training signaling and the system operation starts all over again.

The cyclic operation is illustrated in Figure 1.9. This thesis follows the basic system operation structure in that figure and analyzes its components: 1) training signaling for channel estimation; 2) limited feedback of channel information; and 3) resource allocation for multicell systems.

#### 1.4.1 Aim and Contributions of the Thesis

The aim of the thesis is to analyze channel estimation, channel feedback, and resource allocation aspects of multi-antenna cellular networks. Using optimization theory, we study the optimal solution to a collection of problems and then use the obtained insights to propose practical solutions. More details and background are given in Chapter 2, but this chapter will be concluded with a brief description of the thesis contributions.

- **Training signaling for channel estimation:** Multiuser MIMO and multicell coordination require very accurate channel knowledge. Estimation of the channel propagation is a well-studied area and it is known that the estimation performance can be improved by having a good statistical model of the channel. While prior works have concentrated on a small set of specific statistical structures, this thesis shows how these results can be gathered in a joint framework with more general conditions. It is shown how the design and length of the training signaling depends on the statistical model. It is also shown how to estimate other properties than the channel propagation, which for example might be the total received power.
- **Limited feedback of channel information:** The feedback of channel information needs to be very concise and accurate, so that the transmission can start as quickly as possible. The thesis investigates

how to maximize the amount of information that each feedback bit provides and analyze the relative importance of knowing user directions and the strength of the channels. In addition, we prove that each user should only receive one data signal and that the additional user antennas should be used to improve the feedback accuracy.

- **Resource allocation in multicell systems:** A general multicell coordination framework is proposed to emulate practical conditions and enable joint analysis of basically any type of multicell coordination scheme. The optimal resource allocation in such systems is very complicated to calculate; it requires huge computational resources and cannot be applied in practical systems. However, we propose an algorithm that calculates the optimal resource allocation for the purpose of comparing it with practical approaches. We also extract certain properties of the optimal solution and show how these can be used to achieve simple but well-performing practical algorithms for resource allocation. Finally, the performance is evaluated under practical conditions, based on real channel measurements.

## Chapter 2

# Problem Formulation: Background & Contributions

In this chapter, we introduce the mathematical system model, describe our system operation, and formulate the problems that are considered in the thesis. We provide an extensive background to the research on these topics and outline the main contributions of the thesis, including references to our published and submitted articles.

The fundamental system assumptions are given in Section 2.1, along with preliminaries on how to measure performance, on different statistical models, and on the concept of spatial correlation. The cyclic system operation is described in Section 2.2 and consists of three main components. The thesis analyzes and tries to optimize these components. The first part is training-based channel estimation and this area is outlined in Section 2.3. The second part is feedback design and a survey is provided in Section 2.4. The third component is resource allocation in multicell systems, which is discussed in Section 2.5. Finally, research results that have not been included in the thesis are summarized in Section 2.6.

### 2.1 System Model

We consider a downlink multiuser MIMO system where a base station with  $N$  antennas communicates with  $K_r$  users; see Figure 2.1. We assume that there are many users in the system, such that  $K_r \geq N$  is satisfied. The  $k$ th user is denoted  $\text{MS}_k$  and has  $M_k$  antennas. The channel to  $\text{MS}_k$  is narrowband and represented in the complex baseband by the matrix  $\mathbf{H}_k \in \mathbb{C}^{M_k \times N}$ . The complex-valued element  $[\mathbf{H}_k]_{ij}$  describes the channel from the  $j$ th transmit antenna to the  $i$ th receive antenna. Its norm represents the strength/gain of the channel, while its argument describes the phase-shift created by the channel. For tractability, the multipath propagation

is modeled as *quasi-static block fading*; that is, the channel matrix  $\mathbf{H}_k$  is constant for a set of consecutive discrete time instants  $\mathcal{T} \subset \mathbb{Z}_+$  and then replaced with a new independent realization.<sup>1</sup> The number of time instants,  $|\mathcal{T}|$ , is called the *coherence time*. The transceiver hardware is assumed to be ideal, without other impairments or distortions than can be included in the channel matrix and background noise (cf. [GGLF08, SWB10]).

At the discrete time instant  $t \in \mathcal{T}$ , the symbol-sampled complex-baseband received signal at MS $_k$  is  $\mathbf{y}_k(t) \in \mathbb{C}^{M_k \times 1}$  and is given by the linear input-output model

$$\mathbf{y}_k(t) = \mathbf{H}_k \mathbf{x}(t) + \mathbf{n}_k(t) \quad (2.1)$$

where  $\mathbf{n}_k(t) \in \mathbb{C}^{M_k \times 1}$  is the combined vector of additive noise and interference. It is modeled as circular symmetric complex Gaussian distributed with  $\mathbf{n}_k(t) \in \mathcal{CN}(\bar{\mathbf{n}}_k(t), \mathbf{\Sigma}_k(t))$ , where  $\bar{\mathbf{n}}_k(t) \in \mathbb{C}^{M_k \times 1}$  is the mean value and  $\mathbf{\Sigma}_k(t) \in \mathbb{C}^{M_k \times M_k}$  is the covariance matrix. Further statistical details and motivations are provided in Section 2.1.2.

The transmitted signal  $\mathbf{x}(t) \in \mathbb{C}^{N \times 1}$  contains data signals intended for each of the users and is given by

$$\mathbf{x}(t) = \sum_{k=1}^{K_r} \mathbf{s}_k(t) \quad (2.2)$$

where  $\mathbf{s}_k(t) \in \mathbb{C}^{N \times 1}$  is the signal designated to MS $_k$ . These stochastic data signals are modeled as zero-mean and having *signal correlation matrices*

$$\mathbf{S}_k(t) = \mathbb{E}\{\mathbf{s}_k(t)\mathbf{s}_k^H(t)\} \in \mathbb{C}^{N \times N}. \quad (2.3)$$

These matrices are important design parameters that are used in the thesis to optimize the system performance. The selection of  $\mathbf{S}_1(t), \dots, \mathbf{S}_{K_r}(t)$  is called *resource allocation* and implicitly includes selecting which users to transmit to at a given time instant, the design of beamforming directions, and power allocation. Basically,  $\text{tr}\{\mathbf{S}_k(t)\}$  describes the power allocated for transmission to MS $_k$ , while the eigenvectors and eigenvalues of  $\mathbf{S}_k(t)$  describe the spatial distribution of this power. The general case when multiple users are served simultaneously is called *space division multiple access* (SDMA), while the special case when only one user is given non-zero power at each time instant is known as *time division multiple access* (TDMA). To enable efficient multiuser SDMA transmission, the resource allocation should preferably be based on the current *channel state information* (CSI)—that is, the collection of current channel matrices  $\mathbf{H}_k$ .

Multiuser transmission is a main focus of the thesis and we assume that there is an infinite queue of data to be sent to each user; thus, all users are

---

<sup>1</sup>The actual channel may be time-correlated, but we assume that this correlation cannot be modeled and tracked in a reliable way.

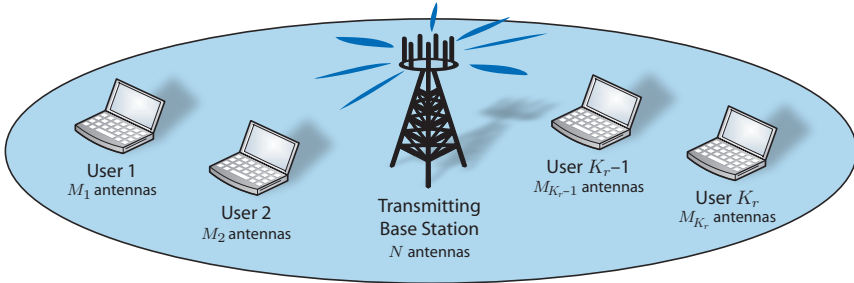


Figure 2.1: Illustration of the downlink multiuser MIMO system in this thesis. A base station with  $N$  antennas serves  $K_r$  multi-antenna users.

available for transmission at every time instant and using any data rate. The data is delivered to the base station through a *backhaul network*, which also will be used for multicell coordination when we extend the single-cell model of this section to a general multicell model in Chapter 5.

The transmission resources need to be limited somehow to model the inherent restrictions of practical systems. We assume that there are  $L$  linear constraints, which are divided into two categories:  $L_p$  power constraints and  $\sum_{k=1}^{K_r} L_k$  user-specific shaping constraints. The power constraints are defined as

$$\sum_{k=1}^{K_r} \text{tr}\{\mathbf{Q}_l \mathbf{S}_k\} \leq q_l \quad l = 1, \dots, L_p, \quad (2.4)$$

where  $\mathbf{Q}_l \in \mathbb{C}^{N \times N}$  are Hermitian positive semi-definite weighting matrices and  $q_l \geq 0$  for all  $l$ . To ensure that the power is constrained in all spatial directions, these matrices satisfy  $\sum_{l=1}^{L_p} \mathbf{Q}_l \succ \mathbf{0}_N$ . These power constraints are given in advance and are based on, for example,

- physical limitations (e.g., dynamic range of power amplifiers);
- regulatory constraints (e.g., radiated power in different directions);
- economical decisions (e.g., long-term cost of running a base station).

Two simple examples are a total power constraint (i.e.,  $L_p = 1$  and  $\mathbf{Q}_1 = \mathbf{I}_N$ ) and per-antenna constraints (i.e.,  $L_p = N$  and  $\mathbf{Q}_l$  is only non-zero at the  $l$ th diagonal element). While these examples can be viewed as two extremes, practical systems can certainly be limited in both respects.

The second category of constraints is user-specific and controls the shape of the transmission to this user.  $\mathbf{MS}_k$  has  $L_k$  constraints

$$\text{tr}\{\mathbf{T}_{ik} \mathbf{S}_k\} \leq \tau_{ik} \quad i = 1, \dots, L_k, \quad (2.5)$$

where  $\mathbf{T}_{ik} \in \mathbb{C}^{N \times N}$  are Hermitian positive semi-definite matrices and  $\tau_{ik} \geq 0$  for all  $i$ . Each matrix  $\mathbf{T}_{ik} \succeq \mathbf{0}_N$  identifies a subspace where the output power should be kept below a certain threshold (e.g., to not disturb neighboring systems [HP10]). These constraints are called soft-shaping, because the shape of the transmission is only affected if the power is above the threshold defined by  $\tau_{ik}$ . In the extreme case, these constraints can be used to prohibit transmission to  $\text{MS}_k$  from certain antennas, which will be used in Chapter 5 to turn the single-cell system in (2.1) into a multicell system. The total number of constraints is  $L = L_p + \sum_{k=1}^{K_r} L_k$ .

*Remark 2.1.* This thesis concentrates on the design of downlink multiuser MIMO transmission (also known as the *broadcast channel*). This problem is commonly viewed as more challenging than uplink transmission (also known as the *multiple access channel*) [GKH<sup>+</sup>07], and there many good arguments supporting this statement. Firstly, efficient multiantenna transmission requires accurate channel knowledge at both sides in the downlink (to achieve the full multiplexing gain, see the next section), while channel information is only critically needed at the base station during uplink transmission [Tel99,GJJV03]. Secondly, user devices should have power-efficient hardware and are therefore limited to low-complexity signal processing algorithms, while the base station can apply advanced algorithms for signal reception in the uplink. Thirdly, many services primarily create downlink traffic (i.e., video streaming), making the downlink throughput the limiting factor for the user experience. However, there are important connections between the downlink and uplink, which have enabled researchers to gain intuition on the design of downlink transmission by solving mathematically more convenient uplink problems [BS02,VT03]. Many results in this thesis could therefore be useful also for the design of uplink transmissions.

*Remark 2.2.* The input-output model in (2.1) can describe many other types of systems than narrowband MIMO communication. In OFDM systems, (2.1) can model each of the subchannels [Böl04]. In addition, transmission over frequency-selective channels using filterbanks [SGB99], wireless wideband MIMO channels [RC98], and transmission over bundles of cables with crosstalk [HSG90] can all be expressed in the form of (2.1). Thus, the analysis in this thesis can be applied to a much wider range of problems than narrowband communication. In those parts of the thesis where we assume certain statistical properties, one should keep in mind that the alternative applications listed above may impose certain structures on  $\mathbf{H}_k$  (e.g., it being Toeplitz) and on  $\mathbf{n}_k(t)$  that may be possible to exploit to improve on our results. In addition, the Rician statistical model defined in Section 2.1.2 is not necessarily a good model for all applications.

### 2.1.1 Data Rate and Multiplexing Gain

The performance of a downlink multiuser MIMO system can be measured in a variety of ways, which we discuss in detail in Chapter 5. As a preliminary, and to support the analysis in Chapter 4, we consider the concepts of mutual information, sum rate, and multiplexing gain in this section.

The data throughput of the downlink system in (2.1) can be characterized using information theory, which is an area pioneered by Claude Shannon in his seminal work of [Sha48]. The mutual information between the transmitted signal  $\mathbf{x}(t)$  and the received signal  $\mathbf{y}_k(t)$  at  $\text{MS}_k$  is

$$\mathcal{I}_k(\mathbf{S}_1(t), \dots, \mathbf{S}_{K_r}(t)) = \log_2 \left( \frac{\det \left( \boldsymbol{\Sigma}_k(t) + \sum_{\bar{k}=1}^{K_r} \mathbf{H}_k \mathbf{S}_{\bar{k}}(t) \mathbf{H}_k^H \right)}{\det \left( \boldsymbol{\Sigma}_k(t) + \sum_{\bar{k} \neq k} \mathbf{H}_k \mathbf{S}_{\bar{k}}(t) \mathbf{H}_k^H \right)} \right), \quad (2.6)$$

for a fixed  $\mathbf{H}_k$  and under the assumption of Gaussian distributed data signals (i.e.,  $\mathbf{s}_k(t) \in \mathcal{CN}(\mathbf{0}, \mathbf{S}_k(t)) \forall k$ ) [Tel99, VVH03]. We will call  $\mathcal{I}_k$  the *data rate* for  $\text{MS}_k$ , as the mutual information represents the number of bits that can be conveyed to user  $k$  (per time instant  $t \in \mathcal{T}$ ) with an arbitrarily low probability of decoding error [CT91]. The data rate is a very common way of measuring performance, but its definition hinges on many idealized assumptions: perfect CSI at the receiver, data signals from infinite constellations, error-control coding over very long data blocks, and no computational complexity constraints (see [DHL<sup>+</sup>11] for a further discussion). Therefore, alternative performance measures such as the signal-to-interference-and-noise ratio (SINR), mean squared error, and bit/symbol error rates are studied in Chapter 5.

The data rate in (2.6) is a function of the transmit correlation matrices  $\mathbf{S}_1(t), \dots, \mathbf{S}_{K_r}(t)$ . Thus, the performance of  $\text{MS}_k$  depends on the transmissions to all other users. The total data throughput is the achievable sum rate

$$f_{\text{sum}}(\mathbf{S}_1(t), \dots, \mathbf{S}_{K_r}(t)) = \sum_{k=1}^{K_r} \mathcal{I}_k(\mathbf{S}_1(t), \dots, \mathbf{S}_{K_r}(t)). \quad (2.7)$$

The sum rate can be optimized by finding the signal correlation matrices  $\mathbf{S}_1(t), \dots, \mathbf{S}_{K_r}(t)$  that maximizes (2.7), while satisfying the power constraints in (2.4) and the soft-shaping constraints in (2.5). Instead of maximizing the sum of each user's performance, other functions such as the geometric/harmonic mean or the worst-user performance can be used. A framework with general performance functions is introduced in Chapter 5.

*Remark 2.3.* In the mutual information expression of (2.6), it was implicitly assumed that the base station applies linear precoding and that each

user only decodes its own data signal, while treating co-user interference as part of the background noise. The sum rate can be improved by allowing non-linear interference pre-subtraction at the base station; the *dirty paper coding* approach in [CS03, VT03, WSS06] achieves the single-cell sum capacity (i.e., the largest sum rate over all transmission strategies). The mutual information can also be improved if each user decodes and subtracts signals intended for other users (e.g., using superposition coding and successive interference cancellation) [LG01, SCG06]; for example, we can achieve the sum capacity if all users are allowed to collaborate. If transmission in multiple interfering cells is considered, the exact sum capacity is typically unknown but the recent area of *interference alignment* has demonstrated that the optimal sum rate scaling (when the transmit power grows large) can be attained with linear precoding by expanding the transmission dimension over, for instance, a collection of channel realizations [CJ08]. However, all these potential improvements come at the cost of a higher sensitivity to inaccurate CSI at the transmitter, require complicated signal processing, and may cause delays and additional signaling overhead. To achieve practically appealing transmit strategies and low-complexity receivers, this thesis assumes linear precoding over a single subchannel (and coherence time) and users that treat co-user interference as noise.

The advantage of multiantenna and multiuser transmission can be characterized in terms of how the sum rate scales with the total transmit power. This scaling is of great importance as practical systems preferably operate at large *signal-to-noise ratios* (SNRs). Similar to [ZT03], we give the following definition.

*Definition 2.1.* Let the parameters  $q_l, \tau_{ik}$  of all constraints in (2.4) and (2.5) be linearly increasing (i.e., non-decreasing) functions of  $q$ . Assume that we have a strategy for selecting  $\mathbf{S}_1(t), \dots, \mathbf{S}_{K_r}(t)$  for every given set of constraints. This strategy achieves the *multiplexing gain*<sup>2</sup> of  $\mathcal{M}_\infty$  if the sum rate satisfies

$$\lim_{q \rightarrow \infty} \frac{f_{\text{sum}}(\mathbf{S}_1(t), \dots, \mathbf{S}_{K_r}(t))}{\log_2(q)} = \mathcal{M}_\infty. \quad (2.8)$$

This means that the sum rate behaves as  $\mathcal{M}_\infty \log_2(q) + \text{constant}$  when the transmit power is large. If we apply TDMA and only transmit to a single user (say  $\text{MS}_k$ ) having a total power constraint, the multiplexing gain is limited by  $\min(N, M_k)$ ; that is, the minimum of the number of transmit and receive antennas. This typically means that  $\mathcal{M}_\infty^{\text{TDMA}} = M_k$  because the user device is small and therefore has fewer antennas than the

---

<sup>2</sup>The multiplexing gain was originally introduced for spatial multiplexing in single-user systems, and the generalization to multiuser systems has sometimes been referred to as the *spatial division multiplexing gain*; see for example [ZKAH11]. The multiplexing gain has also been named *degrees of freedom* and *pre-log factor*.

base station. If we instead transmit to many users in parallel using SDMA, the largest/full multiplexing gain is  $\mathcal{M}_\infty^{\text{SDMA}} = \min(N, \sum_k M_k)$  and can be achieved using both non-linear techniques (e.g., dirty paper coding) and linear precoding (e.g., block diagonalization) [LJ07, SP09]. Recall that we have assumed that there are more users than transmit antennas (i.e.,  $K_r \geq N$ ), which simplifies the full multiplexing gain into  $\mathcal{M}_\infty^{\text{SDMA}} = N$ . In other words, a benefit of multiuser SDMA transmission over single-user TDMA transmission is that the multiplexing gain is limited by the number of transmit antennas instead of the number of antennas at the selected user. The drawback is that the base station requires perfect CSI to realize this benefit in practice [GKH<sup>+</sup>07]. The good news is that linear precoding can achieve the optimal sum rate scaling, which further motivates why this thesis only considers the use of practical linear precoding techniques.

In this thesis, we use the notion of multiplexing gain to investigate how inaccurate CSI affects the performance (see Chapter 4). We will also propose low-complexity multicell precoding strategies in Chapter 7 and analyze the achievable multiplexing gains of these strategies.

### 2.1.2 Rician Statistical Model

When a probabilistic system model is required in the thesis, we model the small-scale fading by having a channel matrix  $\mathbf{H}_k$  with circular-symmetric complex Gaussian elements. Although very simple, this model makes sense in scenarios with rich multipath propagation (e.g., based on the Lindeberg Central Limit Theorem [Zab95]) and has been validated by extensive measurements (see e.g., [WJ01, KSP<sup>+</sup>02, CLW<sup>+</sup>03, YBO<sup>+</sup>04, WHOB06]).

To achieve a proper multivariate channel distribution, we first transform  $\mathbf{H}_k$  into a vector by stacking its columns and denote it by  $\text{vec}(\mathbf{H}_k)$ . We then let

$$\text{vec}(\mathbf{H}_k) \in \mathcal{CN}(\text{vec}(\bar{\mathbf{H}}_k), \mathbf{R}_k) \quad (2.9)$$

where the mean  $\bar{\mathbf{H}}_k \in \mathbb{C}^{M_k \times N}$  describes the line-of-sight component. The positive definite covariance matrix  $\mathbf{R}_k \in \mathbb{C}^{NM_k \times NM_k}$  describes the spatial properties of the multipath propagation. This matrix depends on the large-scale fading and varies at a much slower pace than the small-scale fading. Throughout the thesis, we therefore assume that both the base station and  $\text{MS}_k$  can keep track of  $\bar{\mathbf{H}}_k$  and  $\mathbf{R}_k$  perfectly, either using a negligible feedback overhead or reverse-link estimation [AFFM98, CHC04, WJ09a] (e.g., exploiting that the large-scale fading is relatively frequency independent).

The statistical model in (2.9) is known as *Rician fading*, because the magnitude of each element in  $\mathbf{H}_k$  is Rician distributed. In many urban scenarios, there is no line-of-sight link between the base station and  $\text{MS}_k$  meaning that  $\bar{\mathbf{H}}_k = \mathbf{0}_{M_k \times N}$ . This important special case is called *Rayleigh fading*, because the magnitude of each element in  $\mathbf{H}_k$  is Rayleigh distributed.

It is also common to model the additive noise and interference,  $\mathbf{n}_k(t)$ , as circular-symmetric complex Gaussian distributed, because white Gaussian noise is a safe worst-case assumption and since interfering signals from other communication systems with Gaussian signaling also experience rich multipath propagation. To achieve a general model, we consequently let

$$\mathbf{n}_k(t) \in \mathcal{CN}(\bar{\mathbf{n}}_k(t), \mathbf{\Sigma}_k(t)) \quad (2.10)$$

where  $\bar{\mathbf{n}}_k(t)$  is the mean disturbance and  $\mathbf{\Sigma}_k(t)$  is a positive definite covariance matrix. We will call this stochastic model *Rician disturbance*, because the magnitude of each element in  $\mathbf{n}_k(t)$  is Rician distributed. The disturbance is statistically independent from the channel. Throughout the thesis, we assume that both the base station and  $\text{MS}_k$  can keep track of  $\bar{\mathbf{n}}_k(t)$  and  $\mathbf{\Sigma}_k(t)$  perfectly, through estimation at the user and a negligible low-rate feedback overhead. Observe that we have implicitly assumed that the disturbance is an ergodic process, which is not necessarily satisfied if unknown communication systems with fast adaptive resource allocation strategies are creating the interference; a further discussion is available in [YBB11].

### 2.1.3 Spatial Correlation and Majorization

The channel distribution in (2.9) was defined using an arbitrary covariance matrix  $\mathbf{R}_k$ , but physical channels have certain characteristics that are not captured by just any arbitrary covariance matrix. The *virtual channel representation* in [Say02] and the *jointly-correlated model* in [WHOB06] (also known as the Weichselberger model) have both shown that realistic physical propagation can be well-modeled using simple rules on the eigenstructure of  $\mathbf{R}_k$ . For analytical and simulation purposes, we will sometimes use a special case of the jointly-correlated model known as the *Kronecker model*. This model assumes that the antenna correlation at the transmitter and the receiver are separable, such that the structure of the antenna array at one side does not affect the spatial properties at the other side. This general property is formalized into mathematical conditions on  $\mathbf{R}_k$  in [Oes06], but we concentrate on the following definition:

*Definition 2.2.* Under the *Kronecker model*, the channel covariance matrix  $\mathbf{R}_k$  can be factorized as

$$\mathbf{R}_k = \mathbf{R}_{T,k}^T \otimes \mathbf{R}_{R,k} \quad (2.11)$$

where  $\mathbf{R}_{T,k} \in \mathbb{C}^{N \times N}$  and  $\mathbf{R}_{R,k} \in \mathbb{C}^{M_k \times M_k}$  represent the spatial covariance matrices at the transmitter and receiver side, respectively.

Observe that there is a scaling ambiguity in the covariance matrices  $\mathbf{R}_{T,k}, \mathbf{R}_{R,k}$  of the Kronecker model, but this has no impact on the

analysis of the thesis since these matrices are assumed to be given. The Kronecker model has been verified by field measurements (see e.g., [CLW<sup>+</sup>03, YBO<sup>+</sup>04]), but is not necessarily applicable in all highly correlated scenarios [OCVJP05, Oes06]. However, the Kronecker model enables separate analysis of the impact of *spatial correlation* at the transmitter and the receiver (i.e., the correlation between channel direction and channel quality). In urban cellular systems, base stations are typically elevated and exposed to little near-field scattering, thus large antenna separations are necessary to achieve low spatial correlation. The receiving users might on the other hand be exposed to rich local scattering and thereby experience weak spatial correlation (if the antenna spacing is sufficiently large [ECS<sup>+</sup>98] or polarized antennas are used [ABH<sup>+</sup>07]).

One way to study the impact of spatial correlation is to use a model for the channel covariance matrices  $\mathbf{R}_{T,k}, \mathbf{R}_{R,k}$  that explicitly includes the correlation. There are a variety of ways to generate synthetic channel covariance matrices, based on different assumptions on the scattering environment, the angle between transmitter and receiver, the antenna array geometry, and antenna spacing. The *exponential correlation model* (ECM) in [Loy01] is among the simplest models as it only depends on a single complex-valued parameter  $r$ . The covariance matrix  $\mathbf{R}_{\text{ECM}}(r)$  is given by

$$[\mathbf{R}_{\text{ECM}}(r)]_{kl} = \begin{cases} r^{l-k}, & k \leq l, \\ ([\mathbf{R}_{\text{ECM}}(r)]_{lk})^*, & k > l, \end{cases} \quad |r| \leq 1. \quad (2.12)$$

This model approximates a uniform linear array (ULA) where the antennas are equally spaced on a line. The magnitude  $|r|$  of the correlation coefficient  $r$  can be interpreted as the correlation between adjacent antennas in the array, while the phase  $\angle r$  describes the angle of arrival/departure (depending on the use of the array). A main advantage of the ECM is that we can vary between no correlation ( $|r| = 0$ ) and full correlation ( $|r| = 1$ ) by simply changing the magnitude of  $r$ , but it should be noted that the scale between these extremes is non-linear; typical spatially correlated environments correspond to  $|r| \approx 0.9$  [BHO09].

Another channel covariance model is the *local scattering model* (LSM) that considers a scenario where the antenna array is exposed to little scattering, while the other side is surrounded by rich local scattering. In this highly correlated scenario it is valid to model the multipath components as Gaussian distributed around an angle of arrival/departure  $\theta$  and with a standard deviation  $\sigma_\theta$  which is called the *angular spread* [ZO95, TO96, Str03]. Observe that high spatial correlation corresponds to having a small angular spread. We consider a uniform circular array (UCA) where  $N$  antennas are equally distributed on a circle with radius  $\vartheta$  (measured in fractions of the carrier wavelength). If the angular spread is small [Str03, Bjö07], the corresponding covariance matrix  $\mathbf{R}_{\text{LSM}}(\theta, \sigma_\theta, \vartheta)$  is

well-approximated by

$$\begin{aligned} & [\mathbf{R}_{\text{LSM}}(\theta, \sigma_\theta, \vartheta)]_{kl} \\ &= e^{j4\pi\vartheta \sin(\pi \frac{k-l}{N}) \sin(\pi \frac{k+l-2}{N} - \theta)} e^{-\frac{\sigma_\theta^2}{2} (4\pi\vartheta \sin(\pi \frac{k-l}{N}) \cos(\pi \frac{k+l-2}{N} - \theta))^2}. \end{aligned} \quad (2.13)$$

This covariance model has three real-valued parameters and should provide more accurate results in highly correlated scenarios than the ECM in (2.12), but the LSM lacks the ability to move between no correlation and full correlation. Therefore, both models will be used for numerical evaluation in the thesis. Note that (2.12) and (2.13) will give covariance matrices with  $\text{tr}\{\mathbf{R}_{\text{ECM}}\} = \text{tr}\{\mathbf{R}_{\text{LSM}}\} = N$ , thus the scaling of these matrices needs to be adapted to the large-scale fading (e.g., path loss) when used for analysis.

Instead of assuming a certain covariance matrix model, one can analyze the spatial correlation in terms of the eigenvalue distribution of  $\mathbf{R}_{T,k}$  and  $\mathbf{R}_{R,k}$ ; weak correlation is represented by almost identical eigenvalues, while strong correlation means that a few eigenvalues dominate. Thus, in a highly correlated system, the channel is approximately confined to a small eigensubspace, while all eigenvectors are equally important in an uncorrelated environment.

The notion of majorization in [MO79, JB07] provides a useful measure of the spatial correlation and will be used herein for various purposes. Let  $\mathbf{x} = [x_1, \dots, x_n]^T$  and  $\mathbf{y} = [y_1, \dots, y_n]^T$  be two non-negative real-valued vectors of arbitrary length  $n$ . We say that  $\mathbf{x}$  majorizes  $\mathbf{y}$  if

$$\begin{aligned} \sum_{k=1}^l x_{[k]} &\geq \sum_{k=1}^l y_{[k]}, \quad \text{for } l=1, \dots, n-1, \text{ and} \\ \sum_{k=1}^n x_k &= \sum_{k=1}^n y_k, \end{aligned} \quad (2.14)$$

where  $x_{[k]}$  and  $y_{[k]}$  are the  $k$ th largest ordered elements of  $\mathbf{x}$  and  $\mathbf{y}$ , respectively. This majorization property is denoted as  $\mathbf{x} \succeq \mathbf{y}$  and is illustrated in Figure 2.2. If  $\mathbf{x}$  and  $\mathbf{y}$  contain eigenvalues of channel covariance matrices, then  $\mathbf{x} \succeq \mathbf{y}$  corresponds to that  $\mathbf{x}$  is more spatially correlated than  $\mathbf{y}$ . Majorization only provides a partial order of vectors, but is still very powerful due to its connection to certain order-preserving functions:

*Definition 2.3.* A function  $f(\cdot) : \mathbb{R}^n \rightarrow \mathbb{R}$  is said to be<sup>3</sup>

- *Schur-convex* if  $\mathbf{x} \succeq \mathbf{y}$  implies that  $f(\mathbf{x}) \geq f(\mathbf{y})$ .
- *Schur-concave* if  $\mathbf{x} \succeq \mathbf{y}$  implies that  $f(\mathbf{x}) \leq f(\mathbf{y})$ .

---

<sup>3</sup>This definition is consistent with [MO79, JB07], while alternative definitions of Schur-convexity have appeared in other works.

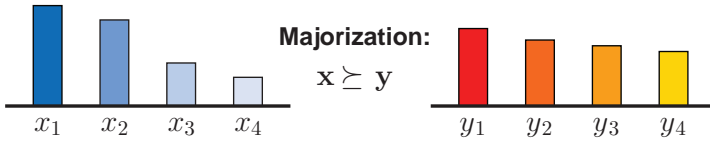


Figure 2.2: Illustration of a majorization relationship between  $\mathbf{x} = [x_1, \dots, x_4]^T$  and  $\mathbf{y} = [y_1, \dots, y_4]^T$ . The total height of all piles (i.e., sum of all elements) is the same for both vectors, but  $\mathbf{x}$  *majorizes*  $\mathbf{y}$  since the total height is more spread out between the piles.

Thus, Schur-convex functions increase with the spatial correlation, while Schur-concave functions decrease. We will use Schur-convexity in the thesis to analyze how the system performance varies with correlation.

#### 2.1.4 Summary of System Assumptions

To be concise, the following are main assumptions of the thesis:

- Downlink transmission in one (or multiple) cells with many users.
- Multiple transmit antennas and more users than transmit antennas.
- Each user has one or multiple antennas and infinite data queues.
- Narrowband channels with ideal distortionless transceivers.
- Block fading channels with coherence time  $|\mathcal{T}|$ .
- Linear precoding and users that treat co-user interference as noise.
- Rapid resource allocation with tight delay-constraints, which motivates alternative performance measures to the mutual information.
- When needed, the channel and interference plus noise are complex Gaussian distributed with known mean and covariance matrices.

## 2.2 System Operation

The performance at a given time instant depends on the resource allocation (i.e., selection of  $\mathbf{S}_1(t), \dots, \mathbf{S}_{K_r}(t)$ ). If the base station can achieve some instantaneous channel knowledge, it can select users to serve in parallel based on their current channel conditions and spatial separability. The signal correlation matrices of the selected users are designed to maximize the sum rate in (2.7), or some other system performance measure. Based

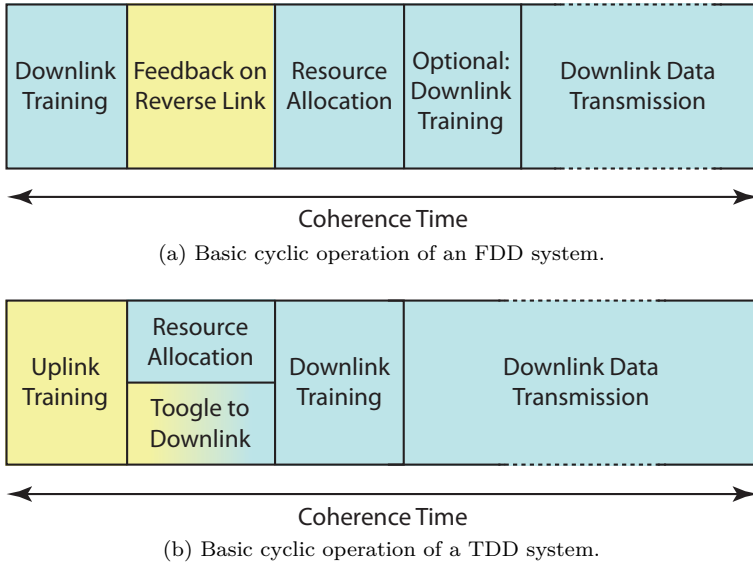


Figure 2.3: Illustration of the system operation for FDD systems and TDD systems. The main components are training signaling, feedback, and resource allocation. These will be considered in the thesis, one at the time.

on the block fading assumption, the channel matrices  $\mathbf{H}_k$  are constant during the coherence time  $|\mathcal{T}|$ . In this time period, we should first try to obtain accurate estimates of  $\mathbf{H}_k$  at user  $k$  and at the base station and then use it for resource allocation and data transmission until the end of the coherence time. The common way of obtaining CSI is to send a known *training sequence* and compare it with the received signal.

Block fading makes it easy to describe the system operation as a cyclic process that is restarted every time the channel matrices are updated. This thesis focus on two types of systems: Frequency Division Duplex (FDD) and Time Division Duplex (TDD). The main difference is that each subchannel in an FDD systems is used for *either* downlink or uplink transmission, while each subchannel in a TDD system switches between downlink and uplink transmission. Thus, TDD systems can send training sequences in both directions,<sup>4</sup> while FDD systems only can send it in the downlink direction and needs another way to achieve CSI at the base station.

<sup>4</sup>The physical channel in the downlink and the uplink are reciprocal [VP07, And09]; that is, the multipath propagation of the radio waves are reversed but otherwise identical. However, the transceiver hardware is typically different between the downlink and the uplink, which requires careful calibration when exploiting the channel reciprocity.

First, we describe the basic operation of FDD systems. It is illustrated in Figure 2.3a and consists of five steps [VP07, LHL<sup>+</sup>08, CJKR10]:

1. **Training:** The base station sends a training sequence that enables each user to estimate its channel.
2. **Feedback:** Each active user feeds back a quantized version of its channel estimate to the base station, using an uplink subchannel.
3. **Resource Allocation:** The base station perform resource allocation (i.e., selects users and their signal correlation matrices). The allocation is either fixed throughout the coherence time or consists of a collection of scheduling/precoding strategies.
4. **Training:** The base station can send a second training sequence, to enable selected users to adapt to the signal correlation matrices (both their own and the interfering ones). This is often necessary to achieve coherent reception.
5. **Data:** Transmission of data until the end of the coherence time.

FDD systems enable parallel downlink and uplink transmissions at different subchannels, which implies short communication delays. The drawback is that the antennas are used for transmission of strong signals and reception of weak signals (due to path losses) in parallel. To avoid interference within the hardware, the downlink and uplink subchannels need to be sufficiently separated in frequency. FDD systems can handle asymmetric data traffic (e.g., access to webpages and video streaming) by using more subchannels for downlink transmission, but cannot adapt to traffic variations (e.g., users that switch between symmetric voice calls and asymmetric internet traffic).

Next, we describe the basic operation of TDD systems. It is illustrated in Figure 2.3b and consists of four steps [VP07, GPS08, And09, JAWV11]:

1. **Training:** Each active user sends training sequences in the uplink direction that enables the base station to estimate the downlink channels using the reciprocity between the uplink and downlink channels.
2. **Resource Allocation:** The base station performs resource allocation, while the system switches from uplink to downlink transmission. The allocation is either fixed throughout the coherence time or consists of a collection of scheduling/precoding strategies.
3. **Training:** The base station sends a training sequence that enables the selected users to estimate their effective channels (with the selected signal correlation matrices), to enable coherent reception.
4. **Data:** Data is transmitted until the end of the coherence time.

TDD systems can be very flexible to asymmetric data traffic, since more time can be used for the downlink when needed. It also reduces the hardware complexity, because devices can concentrate on either transmitting or receiving at a given time. The drawback is the need for silent so-called *guard periods* when switching direction, to make sure that the signal has reached the destination before it starts transmitting in the opposite direction. The communication delays are longer in TDD systems than in FDD, as only one transmission direction is active at a time.

Both FDD and TDD are used in current cellular networks and is supported by the emerging 4G-standards. The choice of system operation depends on many other considerations than described in this section, including regulatory aspects that make certain frequency bands suitable for FDD and others for TDD. It is worth noting that the described FDD and TDD operations are idealized. In practical systems, adjacent cycles are overlapping (e.g., data transmission using old CSI takes place during the feedback step) and there is a variety of control signaling. However, our point is that the basic system operation has three main components: 1) channel estimation based on training signaling; 2) quantized channel feedback (not in TDD systems that exploit channel reciprocity); and 3) resource allocation based on instantaneous channel information. This thesis considers all these components, one at the time. For analytical convenience, it will often be assumed that the previous components have been performed perfectly (e.g., feedback quantization of perfect CSI instead of estimated CSI and resource allocation based on perfect instead of estimated/quantized CSI). The next three sections provide an overview of the state-of-the-art on each of these three areas, along with details on the thesis contributions.

## 2.3 Problem Formulation: Training-Based Estimation

### 2.3.1 Background

The seminal works of [MF70, FG98, Tel99] provide the motivation behind multi-antenna communication; the data rate in single-user MIMO systems increases rapidly with the number of antennas (with a multiplexing gain of  $\mathcal{M}_\infty = \min(N, M_k)$ ). Similar encouraging results for the multiuser downlink (also known as broadcast channels) were developed in [CS03, VT03]. All these results are based on the idealized assumption of having full channel state information (CSI)—that is, perfect knowledge of the channel matrix  $\mathbf{H}_k$  for all users  $k$ . In practice, the channel statistics can often be regarded as known (see Section 2.1.2), but the instantaneous realization of  $\mathbf{H}_k$  needs to be estimated with limited resources (e.g., few time instants and constrained power) due to short-term fading, interference, and noise. Having accurate CSI is critical for multiuser downlink transmission, since this information is required for spatial separation of users [Jin06, SH07,

GKH<sup>+</sup>07]. The gain of having multiple antennas can easily be lost under CSI errors, which motivates research on channel estimation that exploits the available resources efficiently.

Channel estimation is a type of system identification [Gev05, Hja05] where the quasi-constant channel matrix  $\mathbf{H}_k$  should be identified. Common channel estimation techniques can be divided into three categories: training-based, semi-blind, and blind. In the former, the estimation is entirely based on transmission of training sequences (known *a priori* to both the transmitter and the receiver). The other extreme is blind estimation, which only exploits some known structure of the received data signals. The combination of these techniques is called semi-blind estimation. None of the approaches is overall superior; training improves the estimation quality, but the time and power spent on training is taken away from the actual data transmission. It is indicated in [CS97] that the semi-blind approach is preferable over blind estimation, but the optimal choice certainly depend on the coherence time of the channel (i.e., we can spend more resources on estimation if  $|\mathcal{T}|$  is large). In this thesis, we consider training-based estimation since this is the common approach in wireless standards [DPSB08].

By nature, the channel matrix is stochastic, which motivates Bayesian estimation—that is, modeling of the current channel state as a realization from a known multi-variate probability density function (PDF). However, there is a large amount of literature on estimation of deterministic MIMO channels which are analytically tractable but in general provide less accurate channel estimates, as shown in [DU05, BG06]. Early works on Bayesian minimum mean square error (MMSE) estimation of the channel matrix are provided in [KS04] and [MYG05], where the authors considered noise-limited systems with  $\mathbf{\Sigma}_k(t) = \mathbf{I}_{M_k}$ . A first step towards MMSE estimation under colored interference was taken in [LWH07], where the authors disregard the noise and consider an interference-limited system where the interference has similar statistical properties as the channel (which is a rather limiting assumption, but enables analysis).

The estimation can be based on any known training sequence, but the training can also be adapted to optimize the estimation accuracy. Under their respective system conditions, [KS04, MYG05, LWH07] optimize the training sequence to minimize the MSE of the estimation at a certain user. Interestingly, they all derive similar structures of the optimal training sequence. Note that finding the training sequence that minimizes the MSE of the channel matrix estimate will not necessarily result in the best system performance, which typically corresponds to some other function of the channel. The alternative approach of maximizing the entropy between the channel and the received training signal is taken in [BGS09]. Training sequence design with robustness to imperfect statistical knowledge is considered in [SB11b]. When mentioning previous work, it is worth noting that simplified channel matrix estimators have been developed

in [BG06,KKT07,NMB09] and claimed to be linear MMSE estimators, but we show in the thesis that these estimators are in general restrictive.

The optimal length of the training sequence (i.e., the sufficient number of time instants to minimize the MSE) was analyzed in [HH03] for uncorrelated channels and white noise. Under these conditions, the training sequence length should be at least equal to the number of transmit antennas,  $N$ , and can be even longer if the maximum training power per time instant is limited. This result was clarified in [KCJ08] by showing that either the length of the training sequence or the power per time instant should optimally be scaled proportionally to  $\sqrt{|\mathcal{T}|}$ , when the coherence time  $|\mathcal{T}|$  is large. For general spatially correlated channels, the optimal length can be smaller than the number of transmit antennas [PLZL07].

### 2.3.2 Contributions of the Thesis

The main contributions of the thesis in the channel estimation area are:

- We consider MMSE estimation of the channel matrix under arbitrary Rician channel statistics and Rician disturbance. This enables joint analysis of channel estimation under different types of disturbances, including the noise-limited and interference-limited scenarios in the prior work of [KS04,MYG05,LWH07,JJZ<sup>+</sup>08]. We clarify under which conditions the MSE minimizing training sequence can be calculated by solving a convex optimization problem and when it can be solved in closed form. Based on this insight, we propose a heuristic training sequence that can be used for arbitrary Rician statistics.
- We prove that the MSE decreases with the spatial correlation at both the transmitter and the receiver side. Based on this observation, we show that the optimal length of the training sequence can be considerably shorter than the number of transmit antennas.
- We extend the framework by deriving MMSE estimators of the squared Frobenius norm of the channel and the received SNR, which all can be calculated using the same training sequence. We illustrate numerically that direct estimation of such channel quantities yield more accurate results than indirect calculation using an estimated channel matrix. It is also shown how the training sequence can be optimized to minimize the estimation error of such channel quantities.

These novel results are presented in Chapter 3 (*Training-Based Channel Estimation under Arbitrary Rician Statistics*) and most of the results have previously appeared in:

- [BO10] E. Björnson and B. Ottersten, “A framework for training-based estimation in arbitrarily correlated Rician MIMO channels with Rician disturbance,” *IEEE Trans. Signal Process.*, vol. 58, no. 3, pp. 1807–1820, 2010
- [BO09b] E. Björnson and B. Ottersten, “Training-based Bayesian MIMO channel and channel norm estimation,” in *Proc. IEEE ICASSP’09*, 2009, pp. 2701–2704
- [BO08b] E. Björnson and B. Ottersten, “Pilot-based Bayesian channel norm estimation in Rayleigh fading multi-antenna systems,” in *Proc. Nordic Radio Science and Commun. (RVK’08)*, 2008

The research articles [BO09b] and [BO10] are published under © 2009-2010 IEEE. Textual material and illustrations are reprinted with permission.

Some of the results were developed within the European project Wireless World Initiative New Radio+ (WINNER+) and have been republished in deliverables of that project and in:

- [KTS<sup>+</sup>10] P. Komulainen, A. Tölli, B. Song, F. Roemer, E. Björnson, and M. Bengtsson, “CSI acquisition concepts for advanced antenna schemes in the WINNER+ project,” in *Proc. Future Network and MobileSummit*, 2010

## 2.4 Problem Formulation: Feedback Design

### 2.4.1 Background

The optimal data throughput can only be achieved in multiuser MIMO systems with perfect CSI at both the base station and the users [GKH<sup>+</sup>07], but a bounded performance loss is achievable if sufficient resources are allocated for CSI estimation and feedback [Jin06, CJKR10]. The channel matrix  $\mathbf{H}_k$  can be estimated at user  $k$  by analyzing the received signal (see Section 2.3), but the base station cannot make similar channel observations. In FDD systems, the base station and users have fixed roles at each subchannel and thus the base station can only achieve CSI of downlink channels

if users feed it back over uplink subchannels. Downlink multiuser systems require accurate CSI at the base station to benefit from multiuser diversity or achieve the full multiplexing gain [Jin06,SH07,GKH<sup>+</sup>07], but every time instant used for channel feedback is also removed from data transmission on the reverse links. In block fading systems, the data throughput of each block can be optimized by finding the optimal tradeoff between acquiring accurate CSI and having enough time left to benefit from efficient data transmission; see [SH06,KCJ08]. In this thesis, we are not seeking the optimal tradeoff since it highly depends on channel characteristics such as the coherence time  $|T|$ , channel statistics, user distribution, available transmit power, etc. Instead, we assume that  $B$  bits are available for CSI feedback per user and analyze how to use them efficiently. We refer to this as *limited feedback* because  $B$  is typically small and finite [LHL<sup>+</sup>08], but  $B$  naturally increases with the SNR since the SNR improves the uplink throughput.

Continuous multidimensional variables, such as  $\mathbf{H}_k$ , need to be quantized to be described by a finite number of bits. When the number of feedback bits is very limited, the quantization should concentrate on channel properties that are essential for data transmission and exploit the available statistical information [LHS04]. For example, if only a single data stream should be sent to a user, it is more efficient to quantize the preferred beamforming direction and its corresponding channel quality (i.e., the dominating eigenvector and eigenvalue of  $\mathbf{H}_k^H \mathbf{H}_k$ , respectively) than trying to quantize the complete channel matrix [LHS03].

CSI is often divided into two categories: *channel directional information* (CDI) and *channel quality information* (CQI). The directional part is useful for user selection and precoding [KKGK09], while the quality part is used for user selection and rate adaptation [ZJOP09]. Spatial correlation makes CDI and CQI correlated, since the average channel quality is larger in some directions than in others. However, it is convenient to quantize the CDI and CQI separately to simplify the adaptation to statistical variations [LH06, HBO08b] and enable the CQI feedback to account for CDI quantization errors when reporting the anticipated channel quality [TBT07, KdFG<sup>+</sup>07, dFS08]. It also reduces the quantization complexity.

The common approach to CDI quantization is to have a finite codebook of vectors, determine which element in the codebook that best describes the preferred beamformer, and then feed back this index to the base station [LHL<sup>+</sup>08]. The simplest approach is to generate the codebook randomly, using the same distribution as the vector that should be quantized [AYL07]. This gives a lower bound in terms of performance, but the randomness provides a simple structure that can be exploited for analysis [Jin06, YJG07, Jin08, RJ08a]. The optimal choice of codebook depends on how the quantization distortion is defined and can be calculated numerically using the generalized Lloyd algorithm [LBG80]. For uncorrelated Rayleigh fading channels (i.e.,  $\mathbf{R}_k \propto \mathbf{I}$ ), the beamforming direction that

maximizes the received signal power (i.e., the dominating right singular vector of  $\mathbf{H}_k$ ) is uniformly distributed over the unit sphere and it makes sense to distribute the codeword vectors over the same sphere such that the worst-case Euclidean distance to a codeword is minimized. This distortion measure leads to the *Grassmannian codebook* of [LHS03], which can be calculated numerically using the algorithm in [DHST08].

The design of good CDI quantization codebooks is more complicated under general spatial correlation. For a given statistical scenario, an optimal codebook can be designed through computationally expensive algorithms. Such optimization needs to be performed offline, meaning that a large set of fixed codebooks are required to cover any possible statistical scenario. This is infeasible in practice and motivates the design of suboptimal codebooks that can adapt to statistical variations under a minor performance loss. Such algorithms have been proposed for single-user transmission in [LH06, RHS07, KBLS08] by basically having preliminary codebooks that are rotated in different ways depending on the current channel statistics. In principle, the codebook design can also exploit properties of multiuser systems [CMJH08], but it is hard to define proper distortion measures in these scenarios.

The CQI feedback can be based on the actual coding rates supported by the system [LTE10], but it is hard for a user to predict the interference level under multiuser transmission—it depends on user selection in both the own cell and neighboring cells. In addition, only parts of such a list are relevant for each user if their channel statistics are known. Intuitively, the CQI variable should describe the channel norm (i.e., the channel power gain), but better practical performance can often be achieved by feeding back some SINR-like variable that also includes the loss in channel gain and the amount of interference leakage that is expected due to quantization errors [TBT07, KdFG<sup>+</sup>07, YJG07, dFS08]. Any scalar CQI variable needs to be quantized to enable feedback, which typically is achieved by dividing the range of possible values into disjoint intervals based on its statistics [KdFG06, BO08c, YRT09, KY12].

An alternative to CQI feedback is to select an optimistic data rate (e.g., based on the statistics) and reduce it iteratively if the data signal is incorrectly decoded. Using a hybrid automatic repeat request (HARQ) protocol to combine the received signal over multiple time instants, this approach can ideally achieve the same average performance as with perfect CQI feedback in single-antenna single-user systems [SLF09]. Since retransmissions are performed until all data signals can be correctly decoded, the worst-case delay is very long. In addition, multiuser diversity cannot be properly exploited without having some explicit CQI feedback [YJG07]. Thus, it is necessary to combine quantized CQI feedback with HARQ protocols in delay-sensitive multiuser MIMO systems, which is the approach taken in many existing wireless standards. It has recently been shown that the ma-

majority of bits should be used to achieve fairly accurate CQI, while HARQ with a few retransmission takes care of CQI errors [YRT09,ME10]. In this thesis, CQI feedback is utilized for efficient user selection and to find data rates that are supported with a given probability, while the few cases with unsupported rates are assumed to be handled by an HARQ protocol.

If the total number of feedback bits is limited but can be allocated freely among the users, the system should concentrate on achieving accurate CSI from a few users [RJ08b]. Multiuser diversity can still be achieved by first obtaining coarse CSI feedback from many users and then request refinements for the selected users [ZG07]. When the number of bits per user,  $B$ , has been determined, an important question is how these bits should be divided between CDI and CQI feedback. This tradeoff is often ignored by assuming perfect CQI feedback [SH05, HBO08a, YJG07] or long-term averaging without CQI feedback [Jin06, LH06, RJ08a], but can have a substantial impact on the multiplexing gain and the ability to exploit multiuser diversity [KdFG06]. By applying zero-forcing precoding on uncorrelated Rayleigh fading channels, it has been shown that the number of CDI feedback bits needs to increase with the transmit power to achieve the full multiplexing gain [Jin06, Jin08]. This result was improved in [KdFG06, YJG07] by showing that the optimal portion of CDI bits increases with the transmit power, but decreases with the number of users that feed back. A similar setup was used in [KY12] to analyze the asymptotic regime when  $B \rightarrow \infty$ , with given SINR constraints and outage probability constraints. This analysis shows that  $2(N - 1)$  times more CDI bits than CQI bits should be used. Thus, [Jin06, YJG07, KY12] are aligned in the view that CDI feedback should be prioritized under zero-forcing precoding. But other conclusions are possible if we broaden the perspective to other precoding strategies. Random beamforming with SINR-based feedback and a few bits indicating the preferable beamforming direction can achieve the optimal sum rate scaling if the number of users is large [SH05], while additional CQI feedback can be used to achieve reasonable performance at practical number of users [KGS08]. Similarly, CDI feedback can be completely excluded in spatially correlated channels if eigenbeamforming is applied and the number of users is large [HBO08a].

## 2.4.2 Contributions of the Thesis

The main contributions of this thesis in the feedback quantization area are:

- We analyze whether the system should send one stream per scheduled user (i.e., utilize receive antennas for receive diversity) or selecting a smaller number of users and multiplex multiple streams to each of them. This affects the number of channel directions that the base station needs to acquire per user. The former alternative is repre-

sented by zero-forcing precoding with receive combining, while the latter is represented by block-diagonalization precoding. We show both analytically and numerically that zero-forcing with receive combining is the better choice as it is more resilient to spatial correlation and benefits more from multiuser diversity. A notable exception is when the CSI accuracy is poor, but single-user TDMA transmission is the best choice in these scenarios.

- We define the  $\epsilon$ -outage sum rate as a robust estimate of the achievable performance that only exploits CSI available at the transmitter. We explain why this is a more practical performance measure, under imperfect CSI and the considered system operation, than the highest achievable sum rate. We show how the low-complexity precoding strategies of maximum estimated SINR combiner (MESC) from [TBH08] and norm-supported minimum-variance distortionless response (NS-MVDR) from [HBO08a, HBO08b] can be adapted to optimize the  $\epsilon$ -outage sum rate.
- We investigate how  $B$  feedback bits per user should be split between conveying CDI and CQI, under more general condition than in [Jin06, KdFG06, KY12]. We show that the  $\epsilon$ -outage sum rate can achieve the full multiplexing gain if only CDI feedback, only CQI feedback, or neither is available at the base station—all depending on the number of users, number of receive antennas, and the spatial correlation. Thus, asymptotic analysis can be used to draw very different conclusions depending on the system conditions and studied precoding strategy. This analysis is complemented with numerical examples that show the impact of spatial correlation and the number of users on the optimal division of feedback bits at practical values on SNR,  $B$ ,  $M$ , and  $K_r$ . The results show that the asymptotic conclusions in [Jin06, KdFG06, KY12] are quite reasonable under practical system conditions.

These novel results are presented in Chapter 4 (*Fundamental Properties of Feedback Design*) and most of the results have previously appeared in:

- [BHO09] E. Björnson, D. Hammarwall, and B. Ottersten, “Exploiting quantized channel norm feedback through conditional statistics in arbitrarily correlated MIMO systems,” *IEEE Trans. Signal Process.*, vol. 57, no. 10, pp. 4027–4041, 2009
- [BBO11b] E. Björnson, M. Bengtsson, and B. Ottersten, “Receive combining vs. multistream multiplexing in multiuser MIMO systems,” in *Proc. IEEE Swe-CTW’11*, 2011, pp. 109–114

- [BNO10] E. Björnson, K. Ntontin, and B. Ottersten, “Channel quantization design in multiuser MIMO systems: Asymptotic versus practical conclusions,” in *Proc. IEEE ICASSP’11*, 2010, pp. 3072–3075
- [BO08c] E. Björnson and B. Ottersten, “Post-user-selection quantization and estimation of correlated Frobenius and spectral channel norms,” in *Proc. IEEE PIMRC’08*, 2008
- [BO08a] E. Björnson and B. Ottersten, “Exploiting long-term statistics in spatially correlated multi-user MIMO systems with quantized channel norm feedback,” in *Proc. IEEE ICASSP’08*, 2008, pp. 3117–3120

These research articles are published under © 2008-2011 IEEE. Textual material and illustrations are reprinted with permission.

Some of the results on feedback design (and also on multicell transmission) were developed within the FP6 project Cooperative and Opportunistic Communications in Wireless Networks (COOPCOM) and have been republished in deliverables of that project and in:

- [BHZ<sup>+</sup>08] E. Björnson, D. Hammarwall, R. Zakhour, M. Bengtsson, D. Gesbert, and B. Ottersten, “Feedback design in multiuser MIMO systems using quantization splitting and hybrid instantaneous/statistical channel information,” in *Proc. ICT Mobile and Wireless Communications Summit*, 2008

## 2.5 Problem Formulation: Multicell Transmission

### 2.5.1 Background

In conventional cellular systems, each user belongs to one cell at a time and resource allocation is performed autonomously by its base station. Multiple users can be assigned to each subchannel using space division multiple access (SDMA) and MIMO techniques that manage co-user interference within the cell [GKH<sup>+</sup>07]. However, with base stations performing autonomous *single-cell processing*, the performance is fundamentally limited by interference from other cells—especially for users close to cell edges.

The limiting inter-cell interference can be handled by cooperation between base stations. By sharing CSI over the backhaul network, base stations can take the interference caused to adjacent cells into consideration in

the resource allocation. The *interference channel* is among the simplest examples of multicell coordination and represents the special case when each base station only serves a single unique user, but can share CSI to manage intercell interference [HK81, ETW08, LDL11, SCP11]. *Coordinated beamforming* represents the more practical scenario when each base station can serve multiple users in its cell, but still coordinates the resource allocation with other cells to limit the interference [RL06, GKGØ07, KK08, DY10]. By sharing both data and CSI over the backhaul, cell edge users can be jointly served through multiple base stations [SZ01, ZD04, KFV06, GHH<sup>+</sup>10]. This advanced level of cooperation has recently been termed *network MIMO* [VLV07] and *coordinated multi-point transmission* (CoMP) [PDF<sup>+</sup>08], and it basically transforms the multicell system into a single wide-area cell with distributed antenna arrays. The sum capacity of ideal network MIMO systems was derived in [WSS06], while more practical performance gains over conventional single-cell processing were reported in [MF08, SSPS09] under constrained backhaul signaling.

In practical multicell systems, only a small subset of base stations will take the interference generated at a given user into consideration (to limit the backhaul signaling and computational complexity, and to avoid estimating negligibly weak channels). Static disjoint cooperation clusters were considered in [MF08, HTH<sup>+</sup>09, ZCA<sup>+</sup>09] to coordinate transmissions within each cluster. While easily implementable for co-located base stations (such as sectors connected to the same eNodeB in an LTE system), each cluster only becomes a fully coordinated super-cell with distributed antenna arrays. Thus, fixed clustering can only remove some of the interference; the performance will still be limited by out-of-cluster interference. More dynamic approaches were taken in [TCJ08, KK10] where each base station has its own set of users to serve and these sets are partially overlapping. However, these works still consider global interference coordination, making their approaches infeasible in large networks. This thesis extends previous work and proposes multicell system models that are feasible in practice.

The selection of the signal correlation matrices  $\mathbf{S}_1(t), \dots, \mathbf{S}_{K_r}(t)$  should be based on some system performance measure, which creates a mathematical resource allocation problem. There are two particular multicell resource allocation problems that can be solved exactly and efficiently (i.e., in polynomial time). The first one is based on minimizing the power necessary to fulfill pre-defined quality-of-service (QoS) constraints for all users (which is a very strong assumption, because it is not easy to find good QoS constraints). This problem was shown to be convex in [BO01] and the convex formulation has gradually been extended in [WES06, YL07, DY10, BJBO11] to include general power constraints and multicell conditions. These convex problems can be solved in polynomial time using general-purpose implementations of interior-point methods [TTT03, GB10, Löf04], while fixed point algorithms can be used under certain conditions to achieve even faster

convergence [SB04, SB05]. The second problem that can be solved efficiently is to maximize the worst performance among all users (also known as max-min fairness), which can be formulated as solving a series of convex QoS problems [WES06, YL07, SB04, SB05]. This approach provides a kind of absolute fairness, which could be a reasonable goal of resource allocation but cannot really exploit that cellular users often are highly heterogeneous (both in average channel gain and delay sensitivity [HCML10]). These two resource allocation problems are normally studied under perfect CSI, but can also be solved under CSI uncertainty. Exact results under worst-case robustness (with ellipsoidal uncertainty regions) were considered in [SD09, VBS09, TPW11], while approximations under probabilistically uncertainty (i.e., with outage probabilities) were considered in [CSCG07, SD08, WCWKM11].

Apart from the two aforementioned problems, most resource allocation problems in multiantenna multicell systems are non-convex and NP-hard [LDL11], meaning that the optimal solution cannot be obtained in polynomial time. Thus, only heuristic suboptimal precoding strategies can be applied in practice when trying to optimize, for example, the sum performance, proportional fairness, or harmonic mean. Still, it is very important to compute the optimal solution to use it as a benchmark and to characterize its properties. The key to solving non-convex resource allocation problems systematically is to find a suitable parameter space that represents all feasible and some infeasible strategies, and then apply some global optimization technique to iteratively reduce this space with guaranteed convergence to a global optimum [Tuy00, TAKT05]. Recently, parameter spaces have been proposed based on precoding parametrizations [JL10], power allocation [ESV<sup>+</sup>10], user data rates [BU10], and received interference [RTSH11]. In these works, the global optimization was either based on the outer polyblock approximation algorithm [JL10, BU10] or the branch-and-bound algorithm [ESV<sup>+</sup>10, RTSH11]. In addition, only [BU10, RTSH11] handle arbitrary multicell systems and all of the mentioned papers assume perfect CSI between *all* base stations and *all* users in the system, which is unreasonable in practice.

The set of all achievable combinations of user performance is called the achievable *performance region*. The solution to any (reasonable) resource allocation problem thus corresponds to a point on the upper boundary of this region, which is called the *Pareto boundary*.<sup>5</sup> Many suboptimal iterative algorithms have been suggested for handling various non-convex multicell resource allocation problems in practice; see for example [CACC08, ZWN08b, TCJ08, TPK09, NSGS10, VPW10]. These algo-

---

<sup>5</sup>To be correct, the Pareto boundary is only a subset of the upper boundary where the performance cannot be improved for any user without degrading for other users. But it is only in certain special cases that the Pareto boundary is a strict subset, see Chapter 5.

gorithms can be viewed as search procedures in the performance region and have shown good performance on synthetic channels, but the choice of starting point will of course have great impact since these algorithms only have local convergence. The search for good starting points (or non-iterative low-complexity strategies in general) can be simplified by the Pareto boundary parameterizations in [JLD08, SCP11, ZC10, MJ11a, MJ11b, LKL11]. These provide necessary conditions for strategies that attain the Pareto boundary (except for the necessary and sufficient conditions for two-user interference channel in [MJ11b, LKL11]), which greatly reduce the search-space for optimal strategies. For general multicell systems with  $K_t$  base stations and  $K_r$  users, the characterization in [MJ11a] requires  $K_t(K_r - 1)$  parameters from the interval  $[0, 1]$  for beamforming directions (and additional power-control parameters). The special case of the multiple-input single-output (MISO)  $K_r$ -user interference channel has received particular attention. A characterization with  $K_t(K_r - 1)$  complex-valued parameters was derived in [JLD08] and it was improved in [SCP11] to  $[0, 1]$ -parameters. Later, a similar<sup>6</sup> characterization was proposed in [ZC10].

A major consideration in the design of practical multicell transmission strategies is to which extent the cooperation is managed centrally. Centralized resource allocation requires both sharing of CSI over the backhaul network and a central station with high computational power for analyzing the joint CSI. In other words, centralized multicell coordination is not really feasible in large cellular networks. There is therefore a great interest in distributed forms of cooperation that reduce the backhaul signaling and precoding complexity, while still benefiting from efficient interference coordination. In the initial work of [JTS<sup>+</sup>08, NEHA08], base stations were assumed to only affect immediate neighboring cells. The impact of having a limited backhaul capacity for sharing CSI and data was analyzed in [SSPS09, MF09, ZG10b, ZG11]. In addition, centralized user selection schemes that only require partial CSI were considered in [SGH08, KDB09] and combined with distributed precoding that only require local CSI (i.e., for channels from the base station to all users). While these works represent partially distributed resource allocation, a fully distributed resource allocation strategy was proposed in [HBYB11] based on having local CSI and base stations that inform neighboring cells of their scheduling decisions.

Finally, it is worth noting that the performance of downlink multicell resource allocation strategies have mainly been evaluated on synthetic channels. However, synthetic and real channels usually differ due to the simplifications used in the channel model assumptions. Thus, the impact of characteristics such as the correlation between channels from different base stations have not been properly analyzed [JZOG07].

---

<sup>6</sup>Positive parameters are used in [ZC10] instead of  $[0, 1]$ -parameters, but there are bijective functions from  $[0, \infty)$  to  $[0, 1]$  making the parameter complexity identical.

### 2.5.2 Contributions of the Thesis

The main contributions of this thesis in the multicell resource allocation area are presented in a collection of chapters.

#### Chapter 5 (Framework for General Multicell Coordination):

- We propose a general multicell cooperation framework with dynamic overlapping clusters that enables unified analysis of everything from interference channels to ideal network MIMO systems. The main characteristic is that each base station is responsible for the interference caused to a set of users (those with non-negligible channel gains), while only serving a subset of them with data (to limit backhaul signaling). This framework also supports arbitrary monotonic user performance functions (e.g., representing data rates, error rates, or mean square errors) and arbitrary monotonic system performance functions (e.g., sum performance, proportional fairness, or max-min fairness).
- The concept of performance regions is extended to our multicell framework. We prove that the performance region is compact and normal, and that the global optimum to any system optimization lies on its upper boundary. In addition, we prove that the upper boundary always can be attained by strategies that use single-stream beamforming and satisfy some constraints with equality.

#### Chapter 6 (Optimal Solutions to Multicell Resource Allocation):

- We introduce a novel extension to classic max-min performance optimization problems that we call *fairness-profile optimization*. It includes both a lowest acceptable performance level for each user and a division of the remaining resources with predefined proportions. This multicell problem is shown to be quasi-convex under both perfect CSI and worst-case robustness, thus it can be solved in polynomial time.
- We propose a systematic multicell algorithm for solving arbitrary resource allocation problems with monotonic user performance functions. Convergence to the global optimum of these NP-hard problems is achieved by an adaptation of the *branch-reduce-and-bound* (BRB) algorithm in [TAKT05]. A fairness-profile optimization is performed in each iteration, meaning that the framework can be applied whenever this problem can be solved efficiently. As the BRB algorithm solves a problem with exponential worst-case complexity, it is mainly useful as a benchmark in system level evaluations of suboptimal low-complexity algorithms, although good lower bounds on the

optimum are achieved in quite few iterations. We show by simulations that the proposed BRB algorithm has faster convergence than the outer polyblock approximation algorithm, confirming observations in [TAKT05].

### Chapter 7 (Practical Solutions to Multicell Resource Allocation):

- We show that the optimal beamforming directions for each base station belong to certain subspace defined using only local CSI; thus, the difficulty of multicell coordination is not the lack of CSI but the need for coordinated decision making. In addition, we parameterize the optimal resource allocation strategy by deriving a new explicit Pareto characterization. This parametrization is based on the idea of uplink-downlink duality [WES06, YL07, BJBO11] and requires  $K_r + L - 1$  parameters in the interval  $[0, 1]$ , where  $L$  is the total number of power and soft-shaping constraints. This is fewer parameters than in the prior work of [MJ11a, JLD08, SCP11, ZC10] (with exception for the two-user MISO interference channel in [MJ11b, LKL11]). Interestingly, the signal-to-leakage-and-noise ratio (SLNR) beamforming of [STS07, HSHS08, LJS<sup>+</sup>08, ZG10a] is achieved by simple parameter selection, which explains why many papers have achieved good performance with this heuristic approach.
- Two low-complexity strategies for resource allocation are proposed based on our new parametrization of optimal resource allocation and a multicell extension of the efficient ProSched scheduling algorithm of [FGH06, FGH07]. The first strategy is centralized and provides close-to-optimal performance, while the distributed version is suitable for large systems with limited computational complexity and backhaul signaling.

### Chapter 8 (Evaluation of Multicell Resource Allocation):

- The proposed low-complexity strategies for resource allocation are evaluated under both synthetic and realistic channel conditions, using measured channels from a typical urban macro-cell environment. The proposed BRB algorithm is used for benchmarking of the proposed low-complexity strategies. It is shown that a large portion of the optimal performance can be achieved by simple means. Important properties of coordinated multicell transmission are revealed by comparing the average cell performance with random user locations and the performance with fixed user locations. We also evaluate the robustness to synchronization imperfections.

These novel results have previously appeared in:

- [BZGO10] E. Björnson, R. Zakhour, D. Gesbert, and B. Ottersten, “Cooperative multicell precoding: Rate region characterization and distributed strategies with instantaneous and statistical CSI,” *IEEE Trans. Signal Process.*, vol. 58, no. 8, pp. 4298–4310, 2010
- [BJBO11] E. Björnson, N. Jaldén, M. Bengtsson, and B. Ottersten, “Optimality properties, distributed strategies, and measurement-based evaluation of coordinated multicell OFDMA transmission,” *IEEE Trans. Signal Process.*, 2011, to appear
- [BZBO11] E. Björnson, G. Zheng, M. Bengtsson, and B. Ottersten, “Robust monotonic optimization framework for multicell MISO systems,” *IEEE Trans. Signal Process.*, mar 2011, submitted, arXiv:1104.5240v2
- [BBO11a] E. Björnson, M. Bengtsson, and B. Ottersten, “Pareto characterization of the multicell MIMO performance region with simple receivers,” *IEEE Trans. Signal Process.*, may 2011, submitted, arXiv:1105.4880v1

The research articles [BZGO10] and [BJBO11] are published under © 2010-2011 IEEE. Textual material and illustrations are reprinted with permission. Preliminary versions of the results have also appeared in:

- [BBO10] E. Björnson, M. Bengtsson, and B. Ottersten, “Optimality properties and low-complexity solutions to coordinated multicell transmission,” in *Proc. IEEE GLOBECOM’10*, 2010
- [BZGO09] E. Björnson, R. Zakhour, D. Gesbert, and B. Ottersten, “Distributed multicell and multiantenna precoding: Characterization and performance evaluation,” in *Proc. IEEE GLOBECOM’09*, 2009
- [BO09a] E. Björnson and B. Ottersten, “On the principles of multicell precoding with centralized and distributed cooperation,” in *Proc. WCSP’09*, 2009

## 2.6 Contributions Outside the Scope of the Thesis

Certain results that were achieved during my doctoral studies have not been included in the thesis, mainly to achieve a coherency among the system assumptions and transmit strategies used herein. Based on my Master of science thesis, a generalization of the norm-supported precoding strategies of [HBO08a, HBO08b] was proposed in [BHO07] to enable the use of multiple receive antennas. A framework for CQI codebook design was proposed in [BO08c] and applied for quantization of the Frobenius norm and the spectral norm of a Rayleigh fading channel matrix. This framework tries to maximize the feedback-entropy by making every codeword equally probable to be fed back by those users that are eventually scheduled. In addition, the BRB algorithm in Chapter 6 was applied in [BBZO11] to coordinated beamforming systems. By assuming perfect CSI from the serving base station and uncertain CSI from all other base stations, a more efficient type of convex subproblem formulations was achieved. Next, some of the precoding parametrization results and low-complexity strategies proposed in Chapter 7 have been extended for systems where the base station only have statistical CSI; see [BO09a, BZGO10]

We have analyzed the impact of spatial correlation under system conditions that are quite different from those in this thesis: one transmitter and one receiver, the transmitter has either statistical or no CSI, and the transmission is based on linear precoded orthogonal space-time block codes. These assumptions enable analysis based on majorization theory (see Section 2.1.3). We have proved that spatial correlation at the receive antennas always degrades the performance, while correlation is actually advantageous at the transmitter side if transmitter has statistical CSI. In addition, conditions were given for the optimality of single-stream beamforming (i.e., rank-one signal correlation matrices) in these systems. These results are published in:

- [BJO10] E. Björnson, E. Jorswieck, and B. Ottersten, “Impact of spatial correlation and precoding design in OSTBC MIMO systems,” *IEEE Trans. Wireless Commun.*, vol. 9, no. 11, pp. 3578–3589, 2010
- [BOJ09] E. Björnson, B. Ottersten, and E. Jorswieck, “On the impact of spatial correlation and precoder design in MIMO systems with space-time block coding,” in *Proc. IEEE ICASSP’09*, 2009, pp. 2741–2744

- [BDMJ08] E. Björnson, P. Devarakota, S. Medawar, and E. Jorswieck, “Schur-convexity of the symbol error rate in correlated MIMO systems with precoding and space-time coding,” in *Proc. Nordic Radio Science and Commun. (RVK’08)*, 2008

Finally, the collaboration with fellow doctoral students has resulted in:

- [YBB11] J. Yang, E. Björnson, and M. Bengtsson, “Receive beamforming design based on a multiple-state interference model,” in *Proc. IEEE ICC’11*, 2011
- [HBYB11] X. Hou, E. Björnson, C. Yang, and M. Bengtsson, “Cell-grouping based distributed beamforming and scheduling for multi-cell cooperative transmission,” in *Proc. IEEE PIMRC’11*, 2011

In [YBB11], we recognize the variability in interference characteristics that appears when neighboring wireless systems apply scheduling and other resource allocation strategies with fast channel-adaptivity. This is modeled by a multiple-state interference model and the usefulness of such a model is illustrated through two receive beamforming problems: maximization of the average data rate and of the worst-case data rate. We observe that exploiting such a interference structure can improve the performance, especially for cell-edge users in interference-limited systems.

In [HBYB11], we analyze the special coordinated beamforming case of the multicell cooperation framework in Chapter 5. The cells are divided into groups such that neighboring cells (i.e., those that create interference to each other) belong to different groups. Thus, the base stations in a given cell-group will not impact each other and can perform resource allocation independently and in parallel. Since the number of cell-groups can be small and does not depend on the network size, the cell-groups can perform resource allocation in an iterative fashion with limited backhaul signaling. This approach achieves similar performance as previous low-complexity centralized resource allocation strategies, but requires less backhaul signaling and computational complexity.

## Chapter 3

# Training-Based Channel Estimation under Arbitrary Rician Statistics

In this chapter, we propose a framework for training-based estimation of instantaneous channel information under Rician channel and Rician disturbance statistics. This framework unifies and generalizes results that have appeared in prior work. We focus on estimation at a certain user and drop all user indices for notational convenience.

The model for training-based estimation is given in Section 3.1. The preliminaries of minimum mean squared error (MMSE) estimation are given in Section 3.2, where we also derive closed-form MMSE estimators for the channel matrix, its squared Frobenius norm, and the received SNR. In Section 3.3, we show how the training sequence can be designed to maximize the estimation performance. Analytical results on the optimal training structure are achieved under the Kronecker model and these results are used to propose heuristic strategies that can be applied under arbitrary statistics. The optimal length of the training sequence and the impact of spatial correlation are investigated in Section 3.4. Finally, the results are illustrated and evaluated numerically in Section 3.5.

### 3.1 Training-Based Channel Estimation

In this chapter, both the transmitter and the receiver are assumed to know the long-term statistics of the channel and of the disturbance. In order to estimate properties of the current channel realization  $\mathbf{H} \in \mathbb{C}^{M \times N}$ , the transmitter can send a sequence of known training vectors. We consider sequences of arbitrary length  $B \geq 1$ , represented by the training matrix  $\mathbf{P} \in \mathbb{C}^{N \times B}$ . This matrix fulfills a total training power constraint

$\text{tr}(\mathbf{P}^H \mathbf{P}) \leq \varrho$  and its maximal rank is  $m = \min(N, B)$ , which represents the maximal number of spatial channel directions that the training sequence can excite. The columns of  $\mathbf{P}$  are used as transmit signals in the system model of (2.1) for  $B$  time instants, which are not necessarily consecutive and thus denoted  $t = \mathcal{T}(1), \dots, \mathcal{T}(B)$ . The collective received matrix  $\mathbf{Y} = [\mathbf{y}(\mathcal{T}(1)), \dots, \mathbf{y}(\mathcal{T}(B))] \in \mathbb{C}^{M \times B}$  from the training transmission is

$$\mathbf{Y} = \mathbf{H}\mathbf{P} + \mathbf{N} \quad (3.1)$$

where  $\mathbf{N} = [\mathbf{n}(\mathcal{T}(1)), \dots, \mathbf{n}(\mathcal{T}(B))] \in \mathbb{C}^{M \times B}$  is the collective disturbance matrix. In Section 2.1.2, the disturbance at each time instant was modeled as  $\mathbf{n}(t) \in \mathcal{CN}(\bar{\mathbf{n}}(t), \bar{\boldsymbol{\Sigma}}(t))$ . The training signaling lasts over  $B$  time instants, and to allow the disturbance to contain temporally correlated interference we extend the statistical model by assuming that

$$\text{vec}(\mathbf{N}) \in \mathcal{CN}(\text{vec}(\bar{\mathbf{N}}), \bar{\boldsymbol{\Sigma}}) \quad (3.2)$$

where  $\bar{\boldsymbol{\Sigma}} \in \mathbb{C}^{BM \times BM}$  is the positive definite covariance matrix and  $\bar{\mathbf{N}} \in \mathbb{C}^{M \times B}$  is the mean disturbance.

## 3.2 MMSE Channel Estimation

Suppose that we would like to estimate some function  $h(\cdot)$  of the channel matrix  $\mathbf{H}$ . This might, for example, be the channel matrix itself  $h(\mathbf{H}) = \mathbf{H}$  (useful to improve the receive processing) or the total received SNR  $h(\mathbf{H}) = \text{tr}\{\mathbf{H}\mathbf{S}\mathbf{H}^H\}$  for a given signal correlation matrix  $\mathbf{S}$  (useful for rate adaptation and precoding selection). The estimation of  $h(\mathbf{H})$  should be based on all available information; that is, the observation  $\mathbf{Y}$  and the long-term statistics. We consider MMSE estimation, which minimizes the average estimation error and is one of the principal estimators in practice [Kay93].

In general, the MMSE estimate of a function  $h(\mathbf{h})$  of a random vector  $\mathbf{h}$  (with known statistics) is

$$\hat{h}_{\text{MMSE}} = \mathbb{E}\{h(\mathbf{h})|\mathbf{y}\} = \int h(\mathbf{h})p(\mathbf{h}|\mathbf{y})d\mathbf{h} \quad (3.3)$$

where  $\mathbf{y}$  is the observation and  $p(\mathbf{h}|\mathbf{y})$  is the conditional (posterior) PDF of  $\mathbf{h}$  given  $\mathbf{y}$ . Thus, the MMSE estimator is the conditional mean of  $h(\mathbf{H})$  and it minimizes the mean squared error (MSE) defined as

$$\text{MSE} = \mathbb{E}\left\{\|h(\mathbf{h}) - \hat{h}_{\text{MMSE}}\|_F^2\right\}, \quad (3.4)$$

where the expectation is taken over *both* the random vector  $\mathbf{h}$  and the observation  $\mathbf{y}$ . The MMSE estimator can be viewed as the Bayesian counterpart to the minimum variance unbiased (MVU) estimator developed for deterministic channels [Kay93, Section 3.4].

### 3.2.1 Estimation of the Channel Matrix

By vectorizing the received signal in (3.1) and applying the rule  $\text{vec}(\mathbf{ABC}) = (\mathbf{C}^T \otimes \mathbf{A})\text{vec}(\mathbf{B})$ , the observation in our system becomes

$$\text{vec}(\mathbf{Y}) = \tilde{\mathbf{P}}\text{vec}(\mathbf{H}) + \text{vec}(\mathbf{N}) \quad (3.5)$$

where  $\tilde{\mathbf{P}} = (\mathbf{P}^T \otimes \mathbf{I}_M)$ . By pre-subtracting the mean disturbance  $\text{vec}(\bar{\mathbf{N}})$  from  $\text{vec}(\mathbf{Y})$ , it is straightforward to apply the results of [Kay93, Chapter 15.8] to conclude that the conditional PDF is

$$p(\text{vec}(\mathbf{H})|\text{vec}(\mathbf{Y})) = \frac{e^{-(\text{vec}(\mathbf{H})-\mathbf{m})^H \mathbf{E}^{-1}(\text{vec}(\mathbf{H})-\mathbf{m})}}{\pi^{NM} \det(\mathbf{E})}, \quad (3.6)$$

which is a circular symmetric complex Gaussian distribution with

$$\begin{aligned} \mathbf{m} &= \text{vec}(\bar{\mathbf{H}}) + \mathbf{E}\tilde{\mathbf{P}}^H \bar{\boldsymbol{\Sigma}}^{-1}(\text{vec}(\mathbf{Y}) - \tilde{\mathbf{P}}\text{vec}(\bar{\mathbf{H}}) - \text{vec}(\bar{\mathbf{N}})), \\ \mathbf{E} &= \left( \mathbf{R}^{-1} + \tilde{\mathbf{P}}^H \bar{\boldsymbol{\Sigma}}^{-1} \tilde{\mathbf{P}} \right)^{-1} \end{aligned} \quad (3.7)$$

as mean value and covariance matrix, respectively. Using the conditional PDF, it is trivial to achieve the MMSE estimator of the channel matrix.

*Lemma 3.1.* The MMSE estimate,  $\hat{\mathbf{H}}_{\text{MMSE}}$ , of the channel matrix  $\mathbf{H}$  and its corresponding MSE are

$$\begin{aligned} \text{vec}(\hat{\mathbf{H}}_{\text{MMSE}}) &= \mathbf{m}, \\ \text{MSE}_{\hat{\mathbf{H}}} &= \text{tr}\{\mathbf{E}\}, \end{aligned} \quad (3.8)$$

respectively, where  $\mathbf{m}$  and  $\mathbf{E}$  are defined in (3.7).

We stress that the *general* MMSE estimator in (3.8) is in fact linear (affine), but nonetheless it has repeatedly been referred to as the *linear* MMSE (LMMSE) estimator (see e.g., [KS04, MYG05, LWH07]) which is correct but could lead to the incorrect conclusion that there may exist better non-linear estimators. The MMSE estimator in (3.8) is also the maximum a posteriori (MAP) estimator of  $\mathbf{H}$  [Kay93, Chapter 15.8] and the LMMSE estimator in the case of non-Gaussian fading and disturbance (with known first and second order statistics, independent fading and disturbance, and arbitrary types of distributions [Kay93, Chapter 12.3]).

Note that the computation of the MMSE estimate in (3.8) only requires a multiplication of  $\text{vec}(\mathbf{Y})$  with a matrix and adding a vector, which both only depend on the system statistics. Thus, the computational complexity of the estimator is small.

*Remark 3.1.* For Rayleigh fading channels, the MMSE estimator in (3.8) has the general linear form  $\text{vec}(\hat{\mathbf{H}}_{\text{MMSE}}) = \mathbf{A}\text{vec}(\mathbf{Y})$ . A special kind of

linear estimators with the alternative structure  $\widehat{\mathbf{H}} = \mathbf{Y}\mathbf{A}_o$  were studied in [BG06,KKT07,NMB09] and claimed to give rise to LMMSE estimators. In general, this claim is incorrect, which is seen by vectorizing the estimate:  $\text{vec}(\widehat{\mathbf{H}}) = (\mathbf{A}_o^T \otimes \mathbf{I})\text{vec}(\mathbf{Y})$ . Thus, the estimators in [BG06,KKT07,NMB09] belong to a subset of linear estimators with  $\mathbf{A} = (\mathbf{A}_o^T \otimes \mathbf{I})$ . The general MMSE estimator belongs to this subset when applied to Kronecker-structured systems with identical receiver-side channel and disturbance covariance matrices,<sup>1</sup> while the difference between  $\text{vec}(\widehat{\mathbf{H}}_{\text{MMSE}})$  and  $\text{vec}(\widehat{\mathbf{H}})$  increases with the difference in receive-side correlation and how far from Kronecker-structured the statistics are.

*Remark 3.2.* The MSE in (3.8) is independent of the channel mean  $\bar{\mathbf{H}}$  and the disturbance mean  $\bar{\mathbf{N}}$ , thus the estimation quality is identical under Rician and Rayleigh statistics (with the same covariance matrices). Observe that we consider general Rician fading and not the special case with a Rician  $K$ -factor (see [TV05]). The  $K$ -factor represents the ratio between the average power in the direct path (i.e., the squared mean value  $\bar{\mathbf{H}}^H\bar{\mathbf{H}}$ ) and in the scattered paths (i.e., the covariance matrix  $\mathbf{R}$ ) under a fixed total power  $\|\bar{\mathbf{H}}\|_F^2 + \text{tr}\{\mathbf{R}\}$ . Increasing the  $K$ -factor will therefore make the channel more deterministic and easier to estimate; the MSE in (3.8) decreases if we reduce all elements of  $\mathbf{R}$  with a common factor. This natural result was also illustrated in [NMB09].

### 3.2.2 Estimation of the Squared Frobenius Norm and the Received SNR

Using the conditional PDF in (3.6), we can also achieve a closed-form MMSE estimator of the total channel power, represented by the squared Frobenius norm  $h(\mathbf{H}) = \|\mathbf{H}\|_F^2$ . This channel quantity corresponds directly to the SINR in space-time block coded systems and has a large impact on the performance of many other types of systems [BO08c].

*Lemma 3.2.* The MMSE estimate,  $\widehat{\rho}_{\text{MMSE}}$ , of the squared channel norm  $\|\mathbf{H}\|_F^2$  and its corresponding MSE are

$$\begin{aligned}\widehat{\rho}_{\text{MMSE}} &= \|\mathbf{m}\|_2^2 + \text{tr}\{\mathbf{E}\}, \\ \text{MSE}_{\widehat{\rho}} &= \text{tr}\{\mathbf{E}(2\mathbf{R} - \mathbf{E})\} + 2\text{vec}(\bar{\mathbf{H}})^H \mathbf{E} \text{vec}(\bar{\mathbf{H}}),\end{aligned}\tag{3.9}$$

respectively, where  $\mathbf{m}$  and  $\mathbf{E}$  are defined in (3.7).

*Proof.* The proof is given in Appendix 3.A.2. □

Based on this result, we can also achieve a closed-form MMSE estimator of the received SNR  $h(\mathbf{H}) = \text{tr}\{\mathbf{H}\mathbf{S}\mathbf{H}^H\}$ .

<sup>1</sup>In this special case, the estimation of each row of  $\mathbf{H}$  can be separated into independent problems with identical statistics.

*Lemma 3.3.* Consider the received SNR  $\text{tr}\{\mathbf{H}\mathbf{S}\mathbf{H}^H\}$  for a fixed deterministic signal correlation matrix  $\mathbf{S} \succeq \mathbf{0}_N$ . The MMSE estimate,  $\widehat{\text{SNR}}_{\text{MMSE}}$ , and its corresponding MSE are

$$\begin{aligned}\widehat{\text{SNR}}_{\text{MMSE}} &= \mathbf{m}^H \tilde{\mathbf{S}} \mathbf{m} + \text{tr} \left\{ \tilde{\mathbf{S}} \mathbf{E} \right\}, \\ \text{MSE}_{\widehat{\text{SNR}}} &= \text{tr} \left\{ \tilde{\mathbf{S}} \mathbf{E} \tilde{\mathbf{S}} (2\mathbf{R} - \mathbf{E}) \right\} + 2\text{vec}(\bar{\mathbf{H}})^H (\tilde{\mathbf{S}} \mathbf{E} \tilde{\mathbf{S}}) \text{vec}(\bar{\mathbf{H}}),\end{aligned}\tag{3.10}$$

respectively, where  $\tilde{\mathbf{S}} = (\mathbf{S}^T \otimes \mathbf{I}_M)$  and with  $\mathbf{m}$  and  $\mathbf{E}$  from (3.7).

*Proof.* Observe that  $\|\mathbf{H}\|_F^2 = \text{tr}\{\mathbf{H}\mathbf{H}^H\}$  and thus Lemma 3.2 derives the MMSE estimator of the received SNR in the special case of  $\mathbf{S} = \mathbf{I}_N$ . For a general  $\mathbf{S} \succeq \mathbf{0}_N$ , we can apply the proof of Lemma 3.2 to estimate the squared Frobenius norm of  $\mathbf{H}\mathbf{S}^{1/2}$ . The conditional distribution of  $\mathbf{H}\mathbf{S}^{1/2}$  is easily achieved from the conditional PDF of  $\text{vec}(\mathbf{H})$  in (3.6).  $\square$

The estimators of the squared Frobenius norm and the received SNR have rather different properties than the estimator of the channel matrix in Lemma 3.1. Firstly, the estimators are not linear but quadratic in  $\mathbf{m}$  (and thereby in the observation vector  $\mathbf{Y}$ ). Secondly, the MSE performance depends on the mean value  $\bar{\mathbf{H}}$  of the channel, which was not the case for the channel matrix estimate.

Observe that we use the same training signaling and observation  $\mathbf{Y}$  to estimate different channel quantities. The message is that if the system requires estimates of several arbitrary functions  $h_1(\mathbf{H}), h_2(\mathbf{H}), \dots$ , of the channel, we should calculate the MMSE estimate of each of them separately (as in Lemma 3.1-3.3). For example, we show in Section 3.5 that  $\hat{\rho}_{\text{MMSE}}$  yield much better MSE performance than indirect estimation as  $\|\hat{\mathbf{H}}_{\text{MMSE}}\|_F^2$ . For general functions  $h(\cdot)$ , it might be difficult to find a closed-form MMSE estimator, but the simple posterior PDF in (3.6) enables efficient numerical integration.

### 3.3 Training Sequence Optimization

The MMSE estimators in Section 3.2 can be used with any training matrix  $\mathbf{P}$ , but their error covariance matrices depend on the selection of  $\mathbf{P}$ . We will try to select the training matrix to minimize the estimation error. In multi-user systems where users with different statistical properties want to estimate their channels simultaneously, any unitary matrix (scaled to fit the power constraint) can be used;<sup>2</sup> the reason is that the training sequence needs to be based on information available at all receivers. Alternatively,

<sup>2</sup>If the base station only covers a certain cell sector, there might be other matrices that better describe the average characteristics of this area.

a codebook of training matrices can be used, but this requires additional codeword signaling.

In this section, we consider a training sequence dedicated to a single user and we try to tailor it for the considered estimator and the statistical properties and of this user. This is called *experiment design* in the area of system identification [Gev05,Hja05] and should ideally shape the inevitable estimation errors such that the final system performance is maximized. In multi-antenna transmission, this typically means allocating more power to estimate the channel along strong eigendirections of  $\mathbf{R}$  than along weak eigendirections. Dedicated training is useful to achieve very accurate CSI for certain users.<sup>3</sup>

Motivated by analytical convenience, rather than claiming any optimality, this chapter considers training sequences that minimize the MSE for MMSE estimation of some function  $h(\mathbf{H})$ . If this function represents the channel matrix itself,  $h(\mathbf{H}) = \mathbf{H}$ , the training sequence should be selected to minimize the MSE in Lemma 3.1. This problem can be formulated as

$$\begin{aligned} & \underset{\mathbf{P}}{\text{minimize}} \quad \text{tr} \left\{ (\mathbf{R}^{-1} + (\mathbf{P}^T \otimes \mathbf{I}_M)^H \bar{\mathbf{\Sigma}}^{-1} (\mathbf{P}^T \otimes \mathbf{I}_M))^{-1} \right\} \\ & \text{subject to} \quad \text{tr}(\mathbf{P}^H \mathbf{P}) \leq \varrho. \end{aligned} \quad (3.11)$$

This MSE only depends on the training matrix  $\mathbf{P}$  and on the covariance matrices of the channel and disturbance statistics. Thus, the MSE-minimizing training matrix in (3.11) will be a function of the second-order statistics (as in [KS04,MYG05,JJZ<sup>+</sup>08,LWH07]). For general channel and disturbance statistics, the problem in (3.11) is non-convex and the MSE-minimizing training matrix will not have any special structure that can be used for simplification. However, if the covariance matrices  $\mathbf{R}$  and  $\bar{\mathbf{\Sigma}}$  are structured, the optimal  $\mathbf{P}$  may inherit this structure.

### 3.3.1 MSE Optimization under the Kronecker Model

From the training model in (3.1), we see that the training matrix  $\mathbf{P}$  only affects the channel matrix,  $\mathbf{H}$ , from the right hand (transmitter) side. Therefore it is convenient to analyze the special case when the covariance matrices also can be separated between the transmitter and receiver side. This is achieved by the well-known Kronecker model (see Section 2.1.3). Under this model, it has previously been shown that for both noise-limited [KS04,MYG05,JJZ<sup>+</sup>08] and interference-limited systems [LWH07], the optimal training matrix has a certain structure that can be exploited to

---

<sup>3</sup>In practice, a common training sequence can be used to achieve preliminary channel estimates for all users and select the best ones for transmission. These estimates are then improved by sending dedicated sequences to the selected users. The estimation framework herein can be applied also in this scenario, by simply letting  $\bar{\mathbf{H}}$  be the preliminary MMSE estimate and  $\mathbf{R}$  be the corresponding error covariance matrix.

convexify (3.11). In this chapter, these results are generalized by showing that the same optimal structure appears in systems with *both* noise and interference. In our notation, the Kronecker model means that

$$\mathbf{R} = \mathbf{R}_T^T \otimes \mathbf{R}_R \quad (3.12)$$

where  $\mathbf{R}_T \in \mathbb{C}^{N \times N}$  and  $\mathbf{R}_R \in \mathbb{C}^{M \times M}$  represent the spatial covariance matrices at the transmitter and receiver side, respectively. In addition, we assume that the disturbance covariance  $\bar{\Sigma}$  is Kronecker-structured as

$$\bar{\Sigma} = \bar{\Sigma}_Q^T \otimes \bar{\Sigma}_R \quad (3.13)$$

where  $\bar{\Sigma}_Q \in \mathbb{C}^{B \times B}$  and  $\bar{\Sigma}_R \in \mathbb{C}^{M \times M}$  represent the temporal covariance matrix and the received spatial covariance matrix, respectively. For analytical tractability, we also assume that  $\mathbf{R}_R$  and  $\bar{\Sigma}_R$  have identical eigenvectors. This means that the disturbance is either spatially uncorrelated or shares the spatial signature of the channel (e.g., arriving from the same spatial directions). This assumption was first made in [LWH07] for estimation in interference-limited systems. Under this assumption, we can jointly describe several types of disturbance, including the following examples:

- **Noise-limited:**  
 $\bar{\Sigma} = \sigma^2 \mathbf{I}_{BM}$  with some noise variance  $\sigma^2$ .
- **Interference-limited** (with a set  $\mathcal{S}$  of interferers):  
 $\bar{\Sigma} = (\sum_{l \in \mathcal{S}} \tilde{\Sigma}_l) \otimes \mathbf{R}_R$  with  $\tilde{\Sigma}_l$  as temporal covariance of interferer  $l$ .<sup>4</sup>
- **Noise plus temporally uncorrelated interference:**  
 $\bar{\Sigma} = \sigma^2 \mathbf{I}_{BM} + (\sum_{l \in \mathcal{S}} \Sigma_l \mathbf{I}_B) \otimes \mathbf{R}_R = \mathbf{I}_B \otimes (\sigma^2 \mathbf{I}_M + \sum_{l \in \mathcal{S}} \Sigma_l \mathbf{R}_R)$ .
- **Noise plus spatially uncorrelated interference:**  
 $\bar{\Sigma} = \sigma^2 \mathbf{I}_{BM} + (\sum_{l \in \mathcal{S}} \tilde{\Sigma}_l) \otimes \mathbf{I}_M = (\sigma^2 \mathbf{I}_B + \sum_{l \in \mathcal{S}} \tilde{\Sigma}_l) \otimes \mathbf{I}_M$ .

To simplify the notation, we use the following eigen decompositions

$$\mathbf{R}_T = \mathbf{U}_T \mathbf{\Lambda}_T \mathbf{U}_T^H, \quad \mathbf{R}_R = \mathbf{U}_R \mathbf{\Lambda}_R \mathbf{U}_R^H, \quad (3.14)$$

$$\bar{\Sigma}_Q = \mathbf{V}_Q \mathbf{\Upsilon}_Q \mathbf{V}_Q^H, \quad \bar{\Sigma}_R = \mathbf{U}_R \mathbf{\Upsilon}_R \mathbf{U}_R^H, \quad (3.15)$$

where  $\mathbf{\Lambda}_T = \text{diag}(\lambda_1^{(T)}, \dots, \lambda_N^{(T)})$  and  $\mathbf{\Upsilon}_Q = \text{diag}(\sigma_1^{(Q)}, \dots, \sigma_B^{(Q)})$  contain eigenvalues in *decreasing* and *increasing* order, respectively. The eigenvalue matrices  $\mathbf{\Lambda}_R = \text{diag}(\lambda_1^{(R)}, \dots, \lambda_M^{(R)})$  and  $\mathbf{\Upsilon}_R = \text{diag}(\sigma_1^{(R)}, \dots, \sigma_M^{(R)})$  can be ordered arbitrarily.

---

<sup>4</sup>It worth noting that since a flat and block fading channel model was assumed in Chapter 2, the potential unequal temporal covariance in  $\tilde{\Sigma}_l$  primarily originates from the interfering signals and not from their channels. Also observe that if  $\mathbf{R}_R \neq \mathbf{I}_M$ , the interference will be received from the same spatial direction as the training signal.

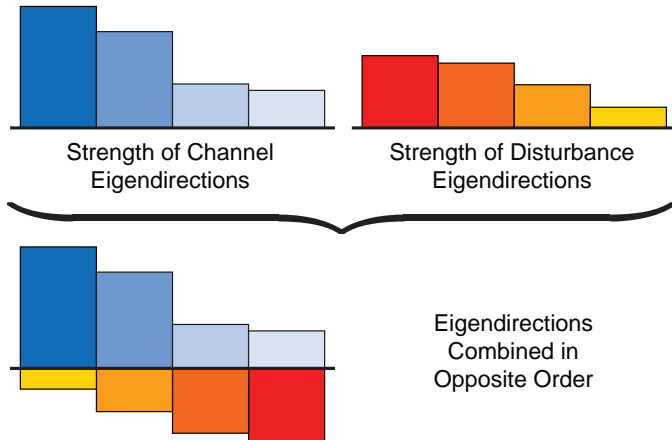


Figure 3.1: Illustration of the optimal training structure in Kronecker-structured systems. Each pile represents an eigendirections and the height is proportional to the corresponding eigenvalue. Theorem 3.1 proves that eigendirections of the channel and the disturbance are assigned to each other, but in opposite order of magnitude.

Based on these assumptions, we search for a feasible  $\mathbf{P}$  that minimizes the MSE for estimation of  $h(\mathbf{H}) = \mathbf{H}$  (other functions are considered in Section 3.3.3). The following theorem solves the training optimization in (3.11) by transferring it into a convex problem. It also provides the optimal structure of the MSE-minimizing training matrix.

*Theorem 3.1.* Under the Kronecker-structured assumptions, the solution to (3.11) has the singular value decomposition  $\mathbf{P} = \mathbf{U}_T \mathbf{D} \mathbf{V}_Q^H$ , where  $\mathbf{D} \in \mathbb{C}^{N \times B}$  has  $\sqrt{p_1}, \dots, \sqrt{p_m}$  on its main diagonal. The MSE-minimizing training power allocation  $p_1, \dots, p_m$  is achieved by solving the convex problem

$$\begin{aligned}
 & \underset{p_1 \geq 0, \dots, p_m \geq 0}{\text{minimize}} && \sum_{j=1}^m \sum_{l=1}^M \frac{\lambda_j^{(T)} \lambda_l^{(R)}}{1 + p_j \frac{\lambda_j^{(T)} \lambda_l^{(R)}}{\sigma_j^{(Q)} \sigma_l^{(R)}}} + \text{tr}(\mathbf{R}_R) \sum_{j=m+1}^N \lambda_j^{(T)} \\
 & \text{subject to} && \sum_{j=1}^m p_j \leq \varrho.
 \end{aligned} \tag{3.16}$$

The solution to (3.16) allocates power such that  $p_j / \sigma_j^{(Q)}$  decreases with  $j$  (i.e., it has the same order as  $\lambda_j^{(T)}$ ).

*Proof.* The proof is given in Appendix 3.A.3. □

This theorem proves that the MSE-minimizing training matrix  $\mathbf{P}$  in Kronecker-structured systems has a special structure based on the eigenvectors of the channel at the transmitter side and the temporal disturbance; the  $j$ th strongest channel eigendirection is assigned to the  $j$ th weakest disturbance eigendirection (i.e., in opposite order of magnitude). In other words, the strongest channel direction is estimated when the disturbance is as weak as possible (and *vice versa*); see Figure 3.1. This was proved in [LWH07] for interference-limited systems, while the noise-limited counterpart was shown in [KS04, MYG05]. Theorem 3.1 generalizes these results to cover various combinations of noise and interference.

Theorem 3.1 has transferred the non-convex optimization problem in (3.11) into a convex power allocation problem. The convex structure is very useful since it means that the global solution can be achieved through efficient general-purpose algorithms (e.g., the interior-point method [BV04]) with polynomial computational complexity. For real-time applications, it might still be necessary to have closed-form solutions. The following corollary states the necessary and sufficient conditions for the optimal power allocation and provides closed-form asymptotical expressions.

*Corollary 3.1.* The MSE-minimizing power allocation,  $p_1, \dots, p_m$ , for (3.16) is achieved from the following system of equations:

$$\alpha = \sum_{l=1}^M \frac{(\lambda_j^{(T)} \lambda_l^{(R)})^2 \sigma_j^{(Q)} \sigma_l^{(R)}}{(\sigma_j^{(Q)} \sigma_l^{(R)} + p_j \lambda_j^{(T)} \lambda_l^{(R)})^2} \quad (3.17)$$

for all  $j$  with  $\alpha < \sum_{l=1}^M (\lambda_j^{(T)} \lambda_l^{(R)})^2 / (\sigma_j^{(Q)} \sigma_l^{(R)})$  and  $p_j = 0$  otherwise. The Lagrange multiplier  $\alpha > 0$  is chosen to fulfill the constraint with equality.

The limiting power allocation at high power  $\varrho$  is given by

$$p_j = \varrho \frac{\sqrt{\sigma_j^{(Q)}}}{\sum_{i=1}^m \sqrt{\sigma_i^{(Q)}}} \quad \forall j. \quad (3.18)$$

At low power  $\varrho$ , let  $\tilde{m}$  be the minimum of the multiplicities of the largest  $\lambda_j^{(T)}$  and the smallest  $\sigma_j^{(Q)}$ . Then, the limiting training matrix is given by allocating all power in an arbitrary manner among  $p_1, \dots, p_{\tilde{m}}$ , while  $p_j = 0$  for all  $j > \tilde{m}$ .

*Proof.* The proof is given in Appendix 3.A.4. □

At high training power, non-zero power should be allocated to the  $m$  statistically strongest eigendirections of the channel, and the power allocation is proportional to the square root of the  $m$  weakest eigendirections of the disturbance. At low training power, all power can be allocated in the

strongest eigendirection. These asymptotic results unify previous results, including the special cases with uncorrelated noise in [KS04, JJZ<sup>+</sup>08] and with single-antenna receivers in [HLW06].

Under certain additional conditions, the system of equations in (3.17) can be solved in closed form. These conditions are summarized by the following corollary.

*Corollary 3.2.* If  $\mathbf{R}_T = \mathbf{I}_N$  and  $\bar{\Sigma}_Q = \mathbf{I}_B$ , then equal power allocation ( $p_j = \frac{\rho}{m}$  for all  $j$ ) minimizes the MSE.

If  $\mathbf{R}_R = \bar{\Sigma}_R$ , then the MSE-minimizing power allocation is given by

$$p_j = \max \left( \sqrt{\frac{\sigma_j^{(Q)}}{\alpha}} - \frac{\sigma_j^{(Q)}}{\lambda_j^{(T)}}, 0 \right) \quad \forall j \quad (3.19)$$

where the Lagrange multiplier  $\alpha > 0$  is chosen to use all available power.

*Proof.* In the first case, the conditions in (3.17) are identical for all  $j$  and thus all power allocation coefficients are equal. In the second case, an explicit expression for each  $p_j$  can be achieved from (3.17) since each term of the sum is identical. See [LWH07, Theorem 5.3] for details.  $\square$

This corollary unifies and generalizes the closed-form solutions derived in prior work. The first part of the corollary represents the case of uncorrelated transmit antennas and temporal disturbance, and has previously been analyzed in [JJZ<sup>+</sup>08] for noise-limited systems. The waterfilling solution in the second part of the corollary was derived in [LWH07] for interference-limited disturbance, but is also valid in noise-limited systems with uncorrelated receive antennas as shown in [KS04, MYG05, JJZ<sup>+</sup>08].

### 3.3.2 MSE Optimization under Arbitrary Statistics

In the previous section, the non-convex training optimization problem in (3.11) was reformulated into a convex problem under the Kronecker model assumption. Based on these analytical results, we now propose a heuristic training matrix that can be used under arbitrary statistics.

*Strategy 3.1.* Let  $\tilde{\mathbf{R}}_T = \mathbb{E}\{\mathbf{H}^H \mathbf{H}\}$  and  $\tilde{\Sigma}_Q = \mathbb{E}\{\mathbf{N}^H \mathbf{N}\}$ . Let their eigen decompositions be  $\tilde{\mathbf{R}}_T = \tilde{\mathbf{U}}_T \tilde{\Lambda}_T \tilde{\mathbf{U}}_T^H$  and  $\tilde{\Sigma}_Q = \tilde{\mathbf{V}}_Q \tilde{\Upsilon}_Q \tilde{\mathbf{V}}_Q^H$  where the eigenvalues are ordered decreasingly and increasingly, respectively. We propose to use the training matrix  $\mathbf{P} = \tilde{\mathbf{U}}_T \tilde{\mathbf{D}} \tilde{\mathbf{V}}_Q^H$ , where the elements  $\sqrt{p_1}, \dots, \sqrt{p_m}$  of the rectangular diagonal matrix  $\tilde{\mathbf{D}}$  are calculated by inserting the eigenvalues of  $\tilde{\Lambda}_T$  and  $\tilde{\Upsilon}_Q$  into (3.19).

This strategy minimizes the MSE if the Kronecker-structured conditions in Corollary 3.2 are satisfied. Its performance under general Rician statistics is evaluated in Section 3.5 and the conclusion is that it performs well,

even when the covariance matrices are clearly non-Kronecker-structured. This was also validated in [SB11a] under statistics that are as far from Kronecker-structured as possible. An explanation of the good performance is that approximations are only applied to the training matrix, while the MMSE estimator in (3.8) is used without approximations.

### 3.3.3 MSE Optimization for Squared Norm Estimation

The training sequence optimization in Section 3.3.1 and 3.3.2 considered minimization of the MSE for estimation of  $h(\mathbf{H}) = \mathbf{H}$ . However, the training sequence can also be optimized towards some other criteria, which might be closer coupled to the actual performance of data transmission. In this section, we try to select  $\mathbf{P}$  to minimize the MSE in Lemma 3.2 for estimation of the squared Frobenius norm,  $\|\mathbf{H}\|_F^2$ , of the channel. This problem can be formulated as

$$\begin{aligned} & \underset{\mathbf{P}}{\text{minimize}} \quad \text{tr}\{\mathbf{E}(2\mathbf{R} - \mathbf{E})\} + 2\text{vec}(\bar{\mathbf{H}})^H \mathbf{E} \text{vec}(\bar{\mathbf{H}}), \\ & \text{subject to} \quad \mathbf{E} = (\mathbf{R}^{-1} + (\mathbf{P}^T \otimes \mathbf{I}_M)^H \bar{\mathbf{\Sigma}}^{-1} (\mathbf{P}^T \otimes \mathbf{I}_M))^{-1}, \\ & \quad \text{tr}(\mathbf{P}^H \mathbf{P}) \leq \varrho. \end{aligned} \quad (3.20)$$

This problem is considerably more involved than the corresponding problem for the channel matrix estimation, because the objective of (3.20) has multiple terms and depends on the mean value  $\bar{\mathbf{H}}$ . To achieve analytical tractability, we make the same Kronecker-structured assumptions as in Section 3.3.1. We also limit the analysis to training matrices with the structure  $\mathbf{P} = \mathbf{U}_T \mathbf{D} \mathbf{V}_Q^H$  (i.e., the optimal structure under channel matrix estimation). It is our conjecture that this is the optimal structure for (3.20).<sup>5</sup>

Based on these assumptions, the following theorem reformulates the training optimization in (3.20) into a power allocation problem.

*Theorem 3.2.* Consider a Kronecker-structured systems with a training matrix structure  $\mathbf{P} = \mathbf{U}_T \mathbf{D} \mathbf{V}_Q^H$ , where the rectangular diagonal  $\mathbf{D} \in \mathbb{C}^{N \times B}$  has  $\sqrt{p_1}, \dots, \sqrt{p_m}$  on its diagonal. The training power allocation  $p_1, \dots, p_m$

---

<sup>5</sup>If the mean channel component  $\bar{\mathbf{H}}$  is strong and has different directivity than the strongest eigenvectors, it might be necessary to permute the eigenvectors in  $\mathbf{U}_T$  when constructing the MSE-minimizing training matrix  $\mathbf{P}$ . To simplify the notation, this has been ignored herein, but it is only a matter of reordering the eigenvalues in (3.14).

that minimizes (3.20) is achieved by solving the problem

$$\begin{aligned}
& \underset{p_1 \geq 0, \dots, p_m \geq 0}{\text{minimize}} && \sum_{l=1}^M \sum_{j=1}^m \left( \frac{(\lambda_j^{(T)} \lambda_l^{(R)})^2 + \frac{2p_j (\lambda_j^{(T)} \lambda_l^{(R)})^3}{\sigma_j^{(Q)} \sigma_l^{(R)}}}{\left( \frac{p_j \lambda_j^{(T)} \lambda_l^{(R)}}{\sigma_j^{(Q)} \sigma_l^{(R)}} + 1 \right)^2} + \frac{2|\tilde{h}_{lj}|^2 \lambda_j^{(T)} \lambda_l^{(R)}}{\frac{p_j \lambda_j^{(T)} \lambda_l^{(R)}}{\sigma_j^{(Q)} \sigma_l^{(R)}} + 1} \right) \\
& && + \sum_{l=1}^M \sum_{j=m+1}^N (\lambda_j^{(T)} \lambda_l^{(R)})^2 + 2|\tilde{h}_{lj}|^2 \lambda_j^{(T)} \lambda_l^{(R)}, \\
& \text{subject to} && \sum_{j=1}^m p_j \leq \varrho,
\end{aligned} \tag{3.21}$$

where  $\tilde{y}_{lj}$  and  $\tilde{h}_{lj}$  are the  $lj$ th elements of  $\tilde{\mathbf{Y}} = \mathbf{U}_R^H (\mathbf{Y} - \bar{\mathbf{N}}) \mathbf{V}_Q$  and  $\tilde{\tilde{\mathbf{H}}} = \mathbf{U}_R^H \tilde{\mathbf{H}} \mathbf{U}_T$ , respectively. This problem is convex in  $p_j$  if  $2|\tilde{h}_{lj}|^2 \geq \lambda_j^{(T)} \lambda_l^{(R)}$  for all  $l$ . In general, the MSE can however be non-convex in certain training powers, but the set of  $p_j$  that minimizes the MSE is always given as one of the solutions to the following system of equations:

$$\alpha = \sum_{l=1}^M \frac{2 \frac{(\lambda_j^{(T)} \lambda_l^{(R)})^4}{(\sigma_j^{(Q)} \sigma_l^{(R)})^2} \left( p_j + |\tilde{h}_{lj}|^2 \left( \frac{p_j}{\lambda_j^{(T)} \lambda_l^{(R)}} + \frac{\sigma_j^{(Q)} \sigma_l^{(R)}}{(\lambda_j^{(T)} \lambda_l^{(R)})^2} \right) \right)}{\left( p_j \frac{\lambda_j^{(T)} \lambda_l^{(R)}}{\sigma_j^{(Q)} \sigma_l^{(R)}} + 1 \right)^3} \tag{3.22}$$

for all  $p_j > 0$  and  $p_j = 0$  otherwise. The Lagrange multiplier  $\alpha > 0$  is chosen to fulfill the power constraint with equality.

*Proof.* The proof is given in Appendix 3.A.5.  $\square$

In contrast to training sequence optimization for estimation of  $h(\mathbf{H}) = \mathbf{H}$ , the power allocation problem in (3.21) for  $h(\mathbf{H}) = \|\mathbf{H}\|_F^2$  is not always convex. The convexity only holds if the mean value is almost as strong as the covariance (or stronger), in each spatial eigendirection. Although the MSE cannot be guaranteed to be convex, the next corollary shows that the limiting power allocation at high and low training power can always be derived in closed form.

*Corollary 3.3.* The limiting power allocation in (3.21) at high power  $\varrho$  is given by  $p_j = \varrho \sqrt{c_j} / \sum_{i=1}^m \sqrt{c_i}$ , where  $c_i = \sum_{l=1}^M \sigma_i^{(Q)} \sigma_l^{(R)} (\lambda_i^{(T)} \lambda_l^{(R)} + |\tilde{h}_{li}|^2)$ .

At low power  $\varrho$ , the limiting solution is given by  $p_{j^*} = \varrho$  for  $j^* = \arg \max_j \sum_{l=1}^M \frac{\lambda_j^{(T)} \lambda_l^{(R)}}{\sigma_j^{(Q)} \sigma_l^{(R)}} (\lambda_j^{(T)} \lambda_l^{(R)} + 2|\tilde{h}_{lj}|^2)$  and  $p_j = 0$  for all  $j \neq j^*$ . If there are multiple  $j^*$ , the power can be allocated arbitrarily among these  $p_{j^*}$ .

*Proof.* The proof is given in Appendix 3.A.6.  $\square$

When comparing Corollary 3.3 with the asymptotic results for channel matrix estimation in Corollary 3.1, we see that the limiting solutions are similar in the sense that all power is allocated to a single eigendirection at low training power and are spread in all  $m$  spatial directions at high power. The definition of the strongest direction at low power and the relative power distribution at high power are however different, which means that the MSE-minimizing training matrices usually are different between estimation of  $\mathbf{H}$  and  $\|\mathbf{H}\|_F^2$ .

Irrespective of whether the problem in (3.21) is convex or not, the system of equations in (3.22) provides necessary conditions that can be used to find a set of solutions that contain the global optimum. The next corollary shows that under certain conditions, all possible solutions have explicit expressions and can thus be tested with relatively low complexity.

*Corollary 3.4.* If  $\mathbf{R}_R = \bar{\Sigma}_R$ , then the solution to (3.21) is given by either  $p_j = 0$  or

$$p_j = \sqrt{\frac{8\sigma_j^{(Q)}(\gamma_j + \nu_j)}{3\lambda_j^{(T)}\alpha}} \cos\left(\frac{\pi(-1)^k - \phi_j}{3}\right) - \frac{\sigma_j^{(Q)}}{\lambda_j^{(T)}} \quad (3.23)$$

for  $k = 0$  or  $k = 1$ , where

$$\begin{aligned} \gamma_j &= \sum_{l=1}^M (\lambda_j^{(T)} \lambda_l^{(R)})^2, \\ \nu_j &= \sum_{l=1}^M \lambda_j^{(T)} \lambda_l^{(R)} |\tilde{h}_{lj}|^2, \end{aligned} \quad (3.24)$$

$$\phi_j = \arctan \sqrt{\frac{8\lambda_j^{(T)}(\gamma_j + \nu_j)^3}{27\sigma_j^{(Q)}\gamma_j^2\alpha}} - 1.$$

The Lagrange multiplier  $\alpha > 0$  is chosen to use all power and the solutions in (3.23) are only feasible if  $\alpha \leq \frac{8\lambda_j^{(T)}(\gamma_j + \nu_j)^3}{27\sigma_j^{(Q)}\gamma_j^2}$  and when they are positive. Depending on  $\alpha$ , the potential solutions in (3.23) belong to the intervals

$$\frac{\sigma_j^{(Q)}(\gamma_j - 2\nu_j)}{2\lambda_j^{(T)}(\gamma_j + \nu_j)} \leq p_j < \infty \quad \text{for } k = 0 \text{ and} \quad (3.25)$$

$$-\frac{\sigma_j^{(Q)}}{\lambda_j^{(T)}} < p_j \leq \frac{\sigma_j^{(Q)}(\gamma_j - 2\nu_j)}{2\lambda_j^{(T)}(\gamma_j + \nu_j)} \quad \text{for } k = 1. \quad (3.26)$$

Thus, if  $\gamma_j - 2\nu_j < 0$  for some  $j$ , then  $k = 1$  cannot give an optimal  $p_j$ .

*Proof.* The proof is given in Appendix 3.A.7.  $\square$

In an interference-limited system or when the receive antennas are uncorrelated, the implication of Corollary 3.4 is that the optimal solution can be achieved by testing three possibilities for each training power. Thus, the worst case complexity of finding the optimal solution to the (potentially) non-convex problem scales with  $N$  and  $B$  as  $3^m$ .

The power allocation problem in (3.22) can be convexified by adding a constraint on the minimal amount of training power in each eigendirection.

*Corollary 3.5.* Problem (3.22) becomes convex if we add the constraints

$$p_j \geq \max \left( \frac{\sigma_j^{(Q)} \sigma_l^{(R)} (\lambda_j^{(T)} \lambda_l^{(R)} - 2|\tilde{h}_{lj}|^2)}{2\lambda_j^{(T)} \lambda_l^{(R)} (\lambda_j^{(T)} \lambda_l^{(R)} + |\tilde{h}_{lj}|^2)}, 0 \right) \quad \forall l, j. \quad (3.27)$$

In the special case  $\mathbf{R}_R = \bar{\Sigma}_R$ , this new constraint can be tightened to

$$p_j \geq \max \left( \frac{\sigma_j^{(Q)} (\gamma_j - 2\nu_j)}{2\lambda_j^{(T)} (\gamma_j + \nu_j)}, 0 \right) \quad (3.28)$$

and the optimal power allocation is given by  $k = 0$  in (3.23) for all active  $p_j$  (i.e., those larger than the new lower bound).

*Proof.* The proof is given in Appendix 3.A.8.  $\square$

Observe that in some cases (e.g., for channels with strong mean components), the suggested additional constraints in Corollary 3.5 are identical to  $p_j \geq 0$  for some  $j$  and then the MSE is convex with respect to these  $p_j$  without the need of imposing any additional constraints.

### 3.4 Impact of Spatial Correlation

In this section, we will analyze the impact of spatial correlation on the MSE and on the optimal length of the training sequence. For analytical simplicity, we concentrate on estimation of  $h(\mathbf{H}) = \mathbf{H}$  and make the same Kronecker-structured assumptions as in Section 3.3.1. Under these conditions, we have the following impact of spatial correlation.

*Theorem 3.3.* If an MSE-minimizing training matrix is used under the Kronecker model, then the MSE for channel matrix estimation is Schur-concave<sup>6</sup> with respect to the eigenvalues of  $\mathbf{R}_T$  (for fixed  $\mathbf{R}_R$ ). If  $\bar{\Sigma}_R = \mathbf{I}_M$ , then the MSE is also Schur-concave with respect to the eigenvalues of  $\mathbf{R}_R$  (for fixed  $\mathbf{R}_T$ ).

<sup>6</sup>The definition of Schur-convexity is given in Section 2.1.3.

*Proof.* The proof is given in Appendix 3.A.9.  $\square$

The interpretation of Theorem 3.3 is that the MSE with an optimal training matrix decreases with increasing spatial correlation. This result is intuitive if we consider the extreme: it is easier to estimate the channel in one eigendirection with full training power, than in two eigendirections where each direction receive half the training power. If combined with Corollary 3.2, Theorem 3.3 provides insight to the selection of the total training power  $\varrho$ ; as the spatial correlation increases, less power is required to achieve a given MSE and this power will be concentrated in the most important eigendirections of the channel.

Next, we provide guidance on how to select the training sequence length  $B$  under different system statistics and based on the rank of  $\mathbf{P}$ . Recall from Corollary 3.1 that all power is allocated in a single eigendirection for low  $\varrho$  (i.e.,  $\text{rank}(\mathbf{P}) = 1$ ). Corollary 3.2 derived a waterfilling power allocation—that is, strong eigendirections receive more power than weak and only a subset of  $p_1, \dots, p_m$  with cardinality  $\tilde{m} \leq m$  will receive non-zero power. Under these conditions, the rank of  $\mathbf{P}$  is equal to  $\tilde{m}$ , which basically means that the training power is spread in the temporal dimension at the  $\tilde{m}$  best time instants out of the  $B$  allocated for training. Unless the disturbance varies heavily over time, it is not worth wasting  $B - \tilde{m}$  time instants just to find slightly better disturbance conditions. Thus, we should select  $B = \tilde{m}$ . This observation is formalized by the following theorem.

*Theorem 3.4.* Let  $\mathbf{P} = \mathbf{U}_P \mathbf{D}_P \mathbf{V}_P^H$  denote the singular value decomposition of a training matrix with  $B \geq \tilde{m}$ , where  $\tilde{m} = \text{rank}(\mathbf{P})$ . If  $\bar{\Sigma} = \mathbf{I}_{BM}$ , then an identical MSE is achieved by the  $\tilde{m}$ -dimensional training matrix  $\mathbf{P}' = \mathbf{U}_P [\mathbf{D}_P]_{1:\tilde{m}}$ . Here,  $[\cdot]_{k_1:k_2}$  denotes the minor matrix that contains column  $k_1$  to  $k_2$  of the given matrix (with  $k_1 \leq k_2$ ).

*Proof.* The proof is given in Appendix 3.A.10.  $\square$

The interpretation of Theorem 3.4 is that the optimal training sequence length in noise-limited systems is equal to the rank of  $\mathbf{P}$ . In this case, optimal means that it is the smallest  $B$  that can achieve the minimal MSE. In general, the rank of  $\mathbf{P}$  can only be calculated numerically. In certain Kronecker-structured systems, the rank can however be derived explicitly.

*Corollary 3.6.* In a Kronecker-structured system with  $\mathbf{R}_R = \bar{\Sigma}_R$ , the MSE-minimizing training matrix  $\mathbf{P} \in \mathbb{C}^{N \times B}$  will have rank  $m = \min(N, B)$  if

$$\varrho > \sum_{j=1}^{m-1} \frac{\sqrt{\sigma_j^{(Q)} \sigma_m^{(Q)}}}{\lambda_m^{(T)}} - \frac{\sigma_j^{(Q)}}{\lambda_j^{(T)}} \quad (3.29)$$

and otherwise have  $\text{rank}(\mathbf{P}) = \tilde{m} < m$  where  $\tilde{m}$  is the positive integer that fulfills

$$\sum_{j=1}^{\tilde{m}-1} \frac{\sqrt{\sigma_j^{(Q)} \sigma_{\tilde{m}}^{(Q)}}}{\lambda_{\tilde{m}}^{(T)}} - \frac{\sigma_j^{(Q)}}{\lambda_j^{(T)}} < \varrho \leq \sum_{j=1}^{\tilde{m}} \frac{\sqrt{\sigma_j^{(Q)} \sigma_{\tilde{m}+1}^{(Q)}}}{\lambda_{\tilde{m}+1}^{(T)}} - \frac{\sigma_j^{(Q)}}{\lambda_j^{(T)}}. \quad (3.30)$$

In addition, if  $\text{rank}(\mathbf{P}) = \tilde{m} < m$  and there exists an integer  $B''$  in  $\tilde{m} \leq B'' < B$  that factorizes  $\mathbf{V}_Q$  as

$$\mathbf{V}_Q = \begin{bmatrix} \mathbf{V}_Q^{(1)} & \mathbf{0} \\ \mathbf{0} & \mathbf{V}_Q^{(2)} \end{bmatrix} \quad (3.31)$$

for some  $\mathbf{V}_Q^{(1)} \in \mathbb{C}^{B'' \times B''}$  and  $\mathbf{V}_Q^{(2)} \in \mathbb{C}^{B-B'' \times B-B''}$ . Then, an identical MSE is achieved by the  $B''$ -dimensional training sequence  $\mathbf{P}'' = [\mathbf{P}]_{1:B''} = \mathbf{U}_T[\mathbf{D}]_{1:B''}(\mathbf{V}_Q^{(1)})^H \in \mathbb{C}^{N \times B''}$ .

*Proof.* The proof is given in Appendix 3.A.11.  $\square$

This corollary shows that  $\mathbf{P}$  is rank deficient in systems with pronounced spatial correlation and/or limited total training power  $\varrho$ . It therefore extends Theorem 3.4 by showing that the optimal  $B$  depends on  $\text{rank}(\mathbf{P})$  also under correlated disturbances. The condition in (3.31) is, for example, satisfied when  $\bar{\Sigma}_Q = \mathbf{I}_B$ .

It was shown in [HH03] that the optimal  $B$  for  $\mathbf{R} = \mathbf{I}_{NM}$  and  $\bar{\Sigma} = \mathbf{I}_{BM}$  is exactly equal to  $N$ . Theorem 3.4 and Corollary 3.6 generalize this result by showing that the optimal  $B$  can be smaller than  $N$  under spatial correlation. This result stands in contrast to the belief that the training sequence length needs to excite all channel directions also in correlated systems [KKT08].

Under general system statistics, one can expect that  $\mathbf{P}$  is rank deficient when the training power is limited and there is a strong eigenvalue spread in either  $\mathbf{R}$  or  $\bar{\Sigma}$ . Even when Theorem 3.4 cannot be applied, the training sequence length can sometimes be reduced towards  $\text{rank}(\mathbf{P})$  with only a slight MSE degradation and with an improved overall data throughput (since more time instants are available for data transmission). The optimal training sequence length under non-Kronecker conditions will be illustrated numerically in Section 3.5.

### 3.5 Numerical Examples

Next, the results of this chapter will be illustrated and evaluated numerically. The MMSE estimator of the channel matrix will be compared with

other recently proposed estimators and the potential gain of training sequence optimization is exemplified. We will also show how the optimal length of training sequence depends on the spatial correlation and available training power. Finally, the importance of direct estimation of functions of the channel matrix is illustrated.

The MSE performance of channel matrix estimation was thoroughly evaluated in [LWH07] for interference-limited Kronecker-structured systems. Therefore, we consider the opposite setting of noise-limited non-Kronecker-structured systems. The channel statistics is generated using the jointly-correlated model [WHOB06]; see Chapter 2.1.3. The channels are zero-mean to enable comparison of different estimators, but recall from Remark 3.2 that the performance of channel matrix estimation is unaffected by the mean component. In the jointly-correlated model, the channel matrix can be expressed as  $\mathbf{H} = \mathbf{U}_A \mathbf{H}_\Omega \mathbf{U}_B^H$ , where  $\mathbf{U}_A, \mathbf{U}_B$  are unitary matrices and  $\mathbf{H}_\Omega \in \mathbb{C}^{M \times N}$  has independent elements with variances given by the corresponding elements of the coupling matrix  $\Omega$ . The unitary matrices will not affect the MSE performance (with optimal training matrices) and are therefore selected as identity matrices. Without loss of generality, we scale the coupling matrices such as  $\|\Omega\|_1 = NM$ , which makes the average training SINR identical to the total training power:  $\text{SINR}_{\text{training}} = \rho \text{tr}(\mathbf{R}) / \text{tr}(\bar{\Sigma}) = \rho$ .

### 3.5.1 Comparison of Different Estimators

First, we will compare the MMSE estimator of the channel matrix in Lemma 3.1 with three other estimators:

1. The MVU/ML channel estimator<sup>7</sup>  $\hat{\mathbf{H}} = \mathbf{Y}\mathbf{P}^H(\mathbf{P}\mathbf{P}^H)^{-1}$  [BG06];
2. The one-sided linear estimator in [BG06,KKT07] that was incorrectly claimed to be the linear MMSE estimator;
3. The two-sided Bayesian linear estimator proposed in [KKT08].

The performance measure is the average normalized MSE, defined as  $\mathbb{E}\{\|\mathbf{H} - \hat{\mathbf{H}}_{\text{MMSE}}\|_F^2\} / \text{tr}(\mathbf{R})$ , over scenarios with different coupling matrices with  $N = B = 8$ ,  $M = 4$ , and independent  $\chi_2^2$ -distributed elements in  $\Omega$ . The results are shown in Figure 3.2, as a function of the total training power  $\rho$ . The MVU/ML estimator does not exploit channel statistics (i.e., non-Bayesian) and therefore provides suboptimal estimation performance, but has asymptotic optimality. The two-sided linear estimator is also suboptimal under the given premises, but can provide good performance in

---

<sup>7</sup>For this problem, the maximum likelihood (ML) estimator is equivalent to the MVU estimator [Kay93, Theorem 7.5].

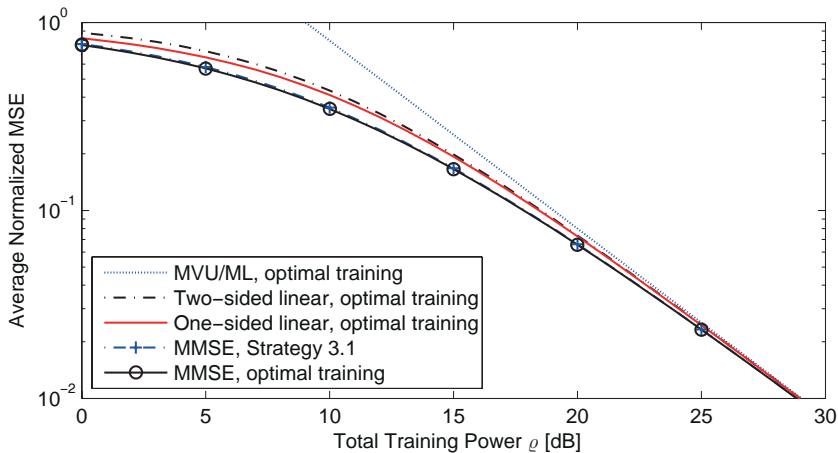


Figure 3.2: The average normalized MSEs of channel matrix estimation as a function of the total training power in a system with jointly-correlated statistics and  $\chi_2^2$ -distributed coupling matrices. The performance of four different estimators with MSE-minimizing training matrices is compared. The performance with the training matrix in Strategy 3.1 is also given.

certain special cases; see [KKT08]. The performance gap between the one-sided linear estimator and the MMSE estimator (which is also linear) is noticeable, while the difference is small between employing the optimal training matrix and our heuristic Strategy 3.1.

It should be pointed out that the use of independent  $\chi_2^2$ -distributed elements in the coupling matrix induces a spatially correlated environment with a few dominating paths. In less correlated scenarios, the difference between the estimators decreases, but the order of estimation quality is usually the same. The conclusion is that the MMSE estimator provides a clearly better MSE performance than other Bayesian estimators, while it clearly outperform non-Bayesian estimators at most training powers  $\rho$ .

### 3.5.2 Comparison of Training Sequences

Next, we illustrate the potential gain of training sequence optimization. To this end, we consider a difficult scattering environment proposed in [VLS05]

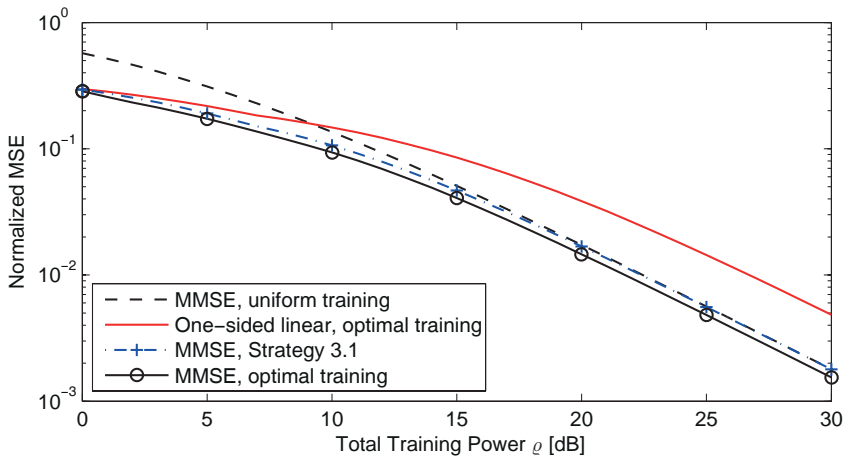


Figure 3.3: The normalized MSEs of channel matrix estimation as a function of the total training power in a system with jointly-correlated statistics and the coupling matrix in (3.32). The MMSE estimator with three different training matrices is compared with the one-sided linear estimator.

with  $N = M = B = 5$  and the coupling matrix

$$\mathbf{\Omega} = \frac{25}{5.7} \begin{bmatrix} 0.1 & 0 & 1 & 0 & 0 \\ 0 & 0.1 & 1 & 0 & 0 \\ 0 & 0 & 1 & 0 & 0 \\ 0 & 0 & 1 & 0.25 & 0 \\ 0 & 0 & 1 & 0 & 0.25 \end{bmatrix}. \quad (3.32)$$

This matrix describes an environment with two small scatterers, two big scatterers, and one large scattering cluster.

In Figure 3.3, the normalized MSE is given for MMSE estimation of the channel matrix. We consider the optimal training matrix, the simple training matrix in Strategy 3.1, and uniform training with  $\mathbf{P} = \sqrt{\frac{\rho}{N}} \mathbf{I}_N$ . The one-sided linear estimator is given as a reference. It is clear that the gain of employing an MSE-minimizing training sequence is substantial, although uniform training is asymptotically optimal at high training power. However, the proposed Strategy 3.1 captures most of this gain. Thus, our conclusion is that training optimization is important, but it is relatively easy to find well-performing heuristic sequences.

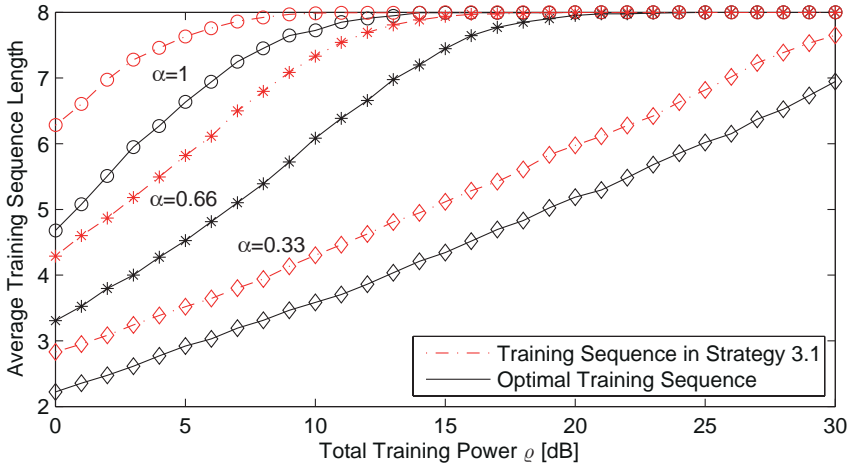


Figure 3.4: The average optimal training sequence length (smallest length that minimizes the MSE) as a function of the total training power  $\rho$ . The system statistics is jointly-correlated and the  $j$ th column of the coupling matrix has independent  $\chi_2^2$ -distributed elements scaled by  $\alpha^{j-1}$ , for different  $\alpha$ . Decreasing  $\alpha$  means increasing the spatial correlation.

### 3.5.3 Optimal Training Length

Next, we illustrate how the optimal length of the training sequence varies with the spatial correlation and training power. Recall that the optimal length is the smallest  $B$  that can achieve the minimal MSE. Theorem 3.4 proved that this is equal to the rank of  $\mathbf{P}$  (in noise-limited systems).

We consider jointly-correlated statistics with the system dimensions  $N = 8$ ,  $M = 4$ , and with coupling matrices with independent  $\chi_2^2$ -distributed elements. To induce random transmit-side correlation, the  $j$ th column of the coupling matrix is scaled by  $\alpha^{j-1}$  for different values on  $\alpha$ : 0.33, 0.66, and 1. The average optimal training sequence length (i.e., average rank of  $\mathbf{P}$ ) is shown in Figure 3.4 for both an MSE-minimizing training matrix and the matrix proposed in Strategy 3.1.

In the case of identically distributed elements of the coupling matrix ( $\alpha = 1$ ), there is sufficient spatial correlation to have  $\text{rank}(\mathbf{P}) < N$  at low training power. As the spatial correlation increases (i.e.,  $\alpha$  decreases), the optimal training length decreases and the convergence towards full rank becomes slower. The simulation shows that the heuristic Strategy 3.1 on average gives a slightly longer training sequence than necessary.

The simulation shows that the optimal  $B$  in general can be smaller than  $N$ , thus the results of [HH03] (i.e.,  $B = N$  in uncorrelated systems) does

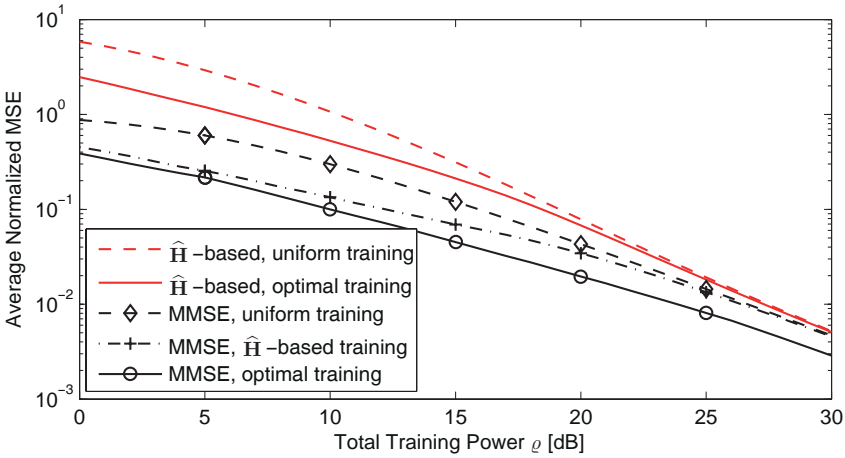


Figure 3.5: The normalized MSEs of channel squared norm estimation as a function of the total training power in a system with uncorrelated receive antennas and a transmit antenna correlation of 0.8. The MMSE estimator is compared with indirect estimation from an MMSE estimated channel matrix for different training matrices.

not hold in general. We conclude that careful system analysis is required to determine the optimal length under general statistics. Note that the loss in performance by employing an even shorter training sequence may be minor compared with the gain of having more time instants available for data transmission in each fading block.

### 3.5.4 Channel Norm Estimation

Finally, we will illustrate the importance of estimating functions  $h(\mathbf{H})$  directly, instead of indirectly as  $h(\hat{\mathbf{H}}_{\text{MMSE}})$ . We will use the squared Frobenius norm of the channel matrix as an example and its MMSE estimator was given in Lemma 3.2. Since the training sequence analysis is quite involved (see Section 3.3.3), we limit the simulations to Kronecker-structured systems (i.e., rank-one coupling matrices). We let the receive antennas be uncorrelated, while the correlation between adjacent transmit antennas is 0.8 (using the exponential correlation model in Chapter 2.1.3).

The normalized MSE is defined as  $\mathbb{E}\{\|\|\mathbf{H}\|_F^2 - \hat{\rho}\|^2\}/\text{tr}(\mathbf{R}\mathbf{R}^H)$  and is shown in Figure 3.5 as a function of the total training power. We compare the MMSE estimator with the  $\hat{\mathbf{H}}_{\text{MMSE}}$ -based indirect estimator  $\|\|\hat{\mathbf{H}}_{\text{MMSE}}\|_F^2$  and consider some different training matrices: uniform training and the optimal training matrix for each of the two estimators.

The first observation from Figure 3.5 is that the indirect approach yields poor performance at low training power (even worse than the purely statistical estimator  $\hat{\rho}_{\text{stat}} = \text{tr}(\mathbf{R})$ , which would give unit normalized MSE) and is not even asymptotically optimal at high power. The MSE performance can be considerably improved by proper training sequence design. A training sequence designed for  $\hat{\mathbf{H}}_{\text{MMSE}}$  will improve the performance over uniform training at low power, but they both share the same suboptimal asymptotic behavior. For the MMSE estimator, using a training matrix optimized for  $\hat{\mathbf{H}}_{\text{MMSE}}$  gives good performance, but with a non-vanishing gap to the optimal performance.

We conclude that it is crucial to estimate functions of the channel directly, especially if the training power is limited. MMSE estimators for different functions might have different optimal training sequences and different asymptotic properties. However, a given training matrix might work well for other estimators than it is optimized for. This is good news for practical applications, where the training sequence probably will be optimized for the channel matrix (or some receive filter) but also can be used to simultaneously estimate the squared norm or received SNR for the purpose of accurate feedback.

### 3.6 Summary

Training signaling can be used to estimate different types of channel information at the receiver and it is important to have a separate estimator for every application. Closed-form expressions for MMSE estimation of the channel matrix, its squared Frobenius norm, and the received SNR have been derived in this chapter under Rician channel and disturbance statistics. We have also shown how the training sequence can be designed to maximize the estimation performance. This optimization problem is convex under certain statistical conditions and can sometimes even have closed-form solutions. A heuristic training strategy was proposed based on these insights and it shows close-to-optimal performance and large potential improvements over uniform training. Finally, it was shown that both the optimal length of the training sequence and the estimation error reduces with the spatial correlation.

### 3.A Collection of Proofs

#### 3.A.1 Two Main Lemmas

First, we state and prove two lemmas that are essential in the proofs of the main mathematical results of this chapter. The first lemma provides the necessary structure of the training matrix when the weighted sum of  $n$  MSEs is minimized. It is basically a generalization of [LWH07, Corollary 5.1] where a single MSE was minimized (i.e.,  $n = 1$ ).

*Lemma 3.4.* Let  $a_1, \dots, a_n$  and  $b_1, \dots, b_n$  be positive scalar coefficients, and let  $\mathbf{\Lambda} \in \mathbb{R}^{N \times N}$  and  $\mathbf{\Upsilon} \in \mathbb{R}^{M \times M}$  be diagonal matrices with strictly positive elements ordered decreasingly and increasingly, respectively. Then, the optimization problem

$$\begin{aligned} & \underset{\bar{\mathbf{P}} \in \mathbb{C}^{N \times M}}{\text{minimize}} \quad \sum_{j=1}^n \text{tr} \left\{ (a_j \mathbf{\Lambda}^{-1} + b_j \bar{\mathbf{P}} \mathbf{\Upsilon}^{-1} \bar{\mathbf{P}}^H)^{-1} \right\} \\ & \text{subject to} \quad \text{tr}(\bar{\mathbf{P}}^H \bar{\mathbf{P}}) \leq \varrho \end{aligned} \quad (3.33)$$

is solved by  $\bar{\mathbf{P}} \in \mathbb{C}^{N \times M}$  being a rectangular diagonal matrix that satisfies  $\text{tr}(\bar{\mathbf{P}}^H \bar{\mathbf{P}}) = \varrho$  and gives decreasingly ordered diagonal elements of  $\bar{\mathbf{P}} \mathbf{\Upsilon}^{-1} \bar{\mathbf{P}}^H$  (i.e., the same order as for  $\mathbf{\Upsilon}^{-1}$  and  $\mathbf{\Lambda}$ ).

*Proof.* We will derive the structure of the optimal  $\bar{\mathbf{P}}$  by contradiction; that is, for every  $\bar{\mathbf{P}}$  that fulfills the constraint with equality we can find a solution that satisfy the given structure and achieves a smaller or identical function value. Observe that the function  $\text{tr}\{(\cdot)^{-1}\}$  is strictly convex in each eigenvalue of its argument. Therefore, if the constraint is not fulfilled with equality for a given  $\bar{\mathbf{P}}$ , we can always achieve a smaller function value by replacing it by  $\beta \bar{\mathbf{P}}$  for some  $\beta > 1$  and still satisfy the constraint.

For any given  $\bar{\mathbf{P}}$  that fulfills the constraint with equality, let its singular value decomposition be denoted  $\bar{\mathbf{P}} = \mathbf{U}_P \mathbf{D}_P \mathbf{V}_P^H$ . We will first show that  $\mathbf{V}_P$  can be removed if the diagonal elements of  $\mathbf{D}_P$  are reordered. For this purpose we introduce the notation  $\mathbf{W} = \bar{\mathbf{P}} \mathbf{\Upsilon}^{-1/2}$  and let its singular value decomposition be denoted  $\mathbf{W} = \mathbf{U}_W \mathbf{D}_W \mathbf{V}_W^H$ , where the singular values in  $\mathbf{D}_W$  are ordered decreasingly. Now, observe that  $\bar{\mathbf{P}}$  only appears in the cost function as  $\bar{\mathbf{P}} \mathbf{\Upsilon}^{-1} \bar{\mathbf{P}}^H = \mathbf{U}_W \mathbf{D}_W \mathbf{D}_W^H \mathbf{U}_W^H$  and thus we can modify  $\mathbf{V}_W$  without affecting the function value. Using the new notation, we can select  $\mathbf{W}$  arbitrarily as long as the following modified constraint is satisfied

$$\begin{aligned} \varrho &= \text{tr}(\bar{\mathbf{P}}^H \bar{\mathbf{P}}) = \text{tr}(\mathbf{W}^H \mathbf{W} \mathbf{\Upsilon}) \\ &\geq \sum_{i=1}^M \lambda_i(\mathbf{W}^H \mathbf{W}) \lambda_{M-i+1}(\mathbf{\Upsilon}) \end{aligned} \quad (3.34)$$

where  $\lambda_i(\cdot)$  denotes the  $i$ th largest eigenvalue. The inequality is given by [MO79, Theorem 20.A.4] and is fulfilled with equality if and only if  $\mathbf{W}^H \mathbf{W} = \mathbf{V}_W \mathbf{D}_W^H \mathbf{D}_W \mathbf{V}_W^H$  is diagonal and have elements in the opposite order of  $\mathbf{\Upsilon}$  (i.e., decreasingly ordered). This means that if  $\mathbf{V}_W \neq \mathbf{I}_M$ , we can set  $\mathbf{V}_W = \mathbf{I}_M$  and thereby reduce the power usage without affect the performance. The ideal structure  $\mathbf{V}_W = \mathbf{I}_M$  gives the following ideal structure on  $\bar{\mathbf{P}}$ :

$$\bar{\mathbf{P}} = \mathbf{W} \mathbf{\Upsilon}^{1/2} = \mathbf{U}_W \mathbf{D}_W \mathbf{\Upsilon}^{1/2}. \quad (3.35)$$

By comparing with the singular value decomposition of  $\bar{\mathbf{P}}$ , we see that we want  $\mathbf{V}_P = \mathbf{I}_M$  and the eigenvalues in  $\mathbf{D}_P$  to be ordered such that  $\mathbf{D}_P \mathbf{\Upsilon}^{-1/2}$  is in decreasing order. If this is not satisfied for the given  $\bar{\mathbf{P}}$ , we can find a better solution by first reordering the diagonal elements of  $\mathbf{D}_P$  and then setting  $\mathbf{V}_P = \mathbf{I}_M$ . This will give strict inequality in the constraint, thus a smaller function value can be achieved by scaling the new solution to use all power. The conclusion is that optimal solution must have the structure  $\bar{\mathbf{P}} = \mathbf{U}_P \mathbf{D}_P$  with  $\mathbf{D}_P$  having the prescribed ordering.

Finally, for a given solution of the type  $\bar{\mathbf{P}} = \mathbf{U}_P \mathbf{D}_P$ , we will show that we always can set  $\mathbf{U}_P = \mathbf{I}_N$  without increasing the function value. Let  $\mathbf{A}_j = a_j \mathbf{\Lambda}^{-1} + b_j \bar{\mathbf{P}} \mathbf{\Upsilon}^{-1} \bar{\mathbf{P}}^H$ , and observe that

$$\text{tr}\{\mathbf{A}_j^{-1}\} = \sum_{l=1}^N \frac{1}{\lambda_l(\mathbf{A}_j)}. \quad (3.36)$$

As mentioned in the beginning of the proof, each component of the sum is strictly convex in its eigenvalue. Thus, (3.36) is a Schur-convex function for all  $j$  [JB07, Proposition 2.7]. Recall that  $\mathbf{A}_j$  is a linear combination of  $\mathbf{\Lambda}^{-1}$  and  $\bar{\mathbf{P}} \mathbf{\Upsilon}^{-1} \bar{\mathbf{P}}^H$  with positive coefficients for each  $j$ . Therefore, we can use [JB07, Theorem 2.11] to show that each  $\text{tr}\{\mathbf{A}_j^{-1}\}$  is minimized when the eigenvalues of  $\mathbf{\Lambda}^{-1}$  and  $\bar{\mathbf{P}} \mathbf{\Upsilon}^{-1} \bar{\mathbf{P}}^H$  are added together in opposite order. If  $\mathbf{U}_P \neq \mathbf{I}_N$ , we can therefore decrease the function value by setting  $\mathbf{U}_P = \mathbf{I}_N$ , without affecting the power constraint.

To summarize, we have shown that for every given  $\bar{\mathbf{P}}$ , we can reduce the cost function by removing the unitary matrices of its singular value decomposition, reordering the diagonal elements, and scaling the remaining matrix to satisfy the constraint with equality. Thus, the optimal solution should be unaffected by these changes, which is only achieved for  $\bar{\mathbf{P}}$  with the structure given in the lemma.  $\square$

The next lemma provides a condition for when a function that originates from an optimal power allocation is Schur-convex or Schur-concave.

*Lemma 3.5.* Consider a continuous and twice continuously differentiable function  $f(\boldsymbol{\lambda}, \mathbf{p})$  of two non-negative vectors  $\boldsymbol{\lambda} = [\lambda_1, \dots, \lambda_N]^T$  and  $\mathbf{p} =$

$[p_1, \dots, p_m]^T$ . For every  $\boldsymbol{\lambda}$  such that  $f(\boldsymbol{\lambda}, \mathbf{p})$  is convex and the Hessian and all its square minors are non-singular with respect to  $\mathbf{p}$ , the solution to

$$g(\boldsymbol{\lambda}) = \min_{\mathbf{p}} f(\boldsymbol{\lambda}, \mathbf{p}) \quad \text{subject to} \quad \sum_{l=1}^m p_l = \varrho \quad \text{and} \quad p_l \geq 0 \quad (3.37)$$

is differentiable. The partial derivatives of the solution at the optimal power allocation  $\mathbf{p}_{\text{opt}}(\boldsymbol{\lambda})$  are

$$\frac{\partial g(\boldsymbol{\lambda})}{\partial \lambda_j} = f'_{\lambda_j}(\boldsymbol{\lambda}, \mathbf{p})|_{\mathbf{p}=\mathbf{p}_{\text{opt}}(\boldsymbol{\lambda})} \quad \forall j. \quad (3.38)$$

Then,  $g(\boldsymbol{\lambda})$  is Schur-convex with respect to  $\boldsymbol{\lambda}$  if and only if  $\frac{\partial g(\boldsymbol{\lambda})}{\partial \lambda_i} \geq \frac{\partial g(\boldsymbol{\lambda})}{\partial \lambda_j}$  for all  $\lambda_i \geq \lambda_j$ , and Schur-concave if and only if  $\frac{\partial g(\boldsymbol{\lambda})}{\partial \lambda_i} \leq \frac{\partial g(\boldsymbol{\lambda})}{\partial \lambda_j}$ .

*Proof.* Since the cost function is convex with respect to  $\mathbf{p}$  for every given  $\boldsymbol{\lambda}$  and the domain of  $\mathbf{p}$  is compact, the Karush-Kuhn-Tucker (KKT) conditions guarantee the existence of one or several solutions to (3.37) and these are given by the following system of stationarity equations

$$0 = f'_{p_l}(\boldsymbol{\lambda}, \mathbf{p}) - \alpha \quad (3.39)$$

for all  $p_l > 0$  (otherwise  $p_l = 0$ ), where the Lagrangian multiplier  $\alpha$  makes sure that  $\sum_{l=1}^m p_l = \varrho$  [BV04]. Let  $\mathcal{S}_p$  denote the index set of all  $p_l > 0$  and those  $p_l = 0$  for which the corresponding equation in (3.39) is also satisfied with equality (i.e., parameters that are on the boundary of becoming active). For the indices in  $\mathcal{S}_p$ , the Jacobian of the equation system in (3.39) will be identical to a minor of the Hessian of  $f(\boldsymbol{\lambda}, \mathbf{p})$  with respect to  $\mathbf{p}$ , and thus non-singular by assumption. If we denote the power allocation solution in (3.37) as a function  $\mathbf{p}_{\text{opt}} = \mathbf{p}_{\text{opt}}(\boldsymbol{\lambda})$ , we can then apply the Implicit function theorem in [Rud76, Theorem 9.28] to conclude all elements in  $\mathbf{p}_{\text{opt}}(\boldsymbol{\lambda})$  with indices in  $\mathcal{S}_p$  are differentiable with respect to  $\boldsymbol{\lambda}$ . For those  $p_l = 0$  with  $l \notin \mathcal{S}_p$ , this variable can be replaced with a zero in the optimization problem without affecting the solution, and thus its derivative can be defined as being zero.

We can now use that  $\mathbf{p}_{\text{opt}}(\boldsymbol{\lambda})$  is differentiable with respect to  $\boldsymbol{\lambda}$  to calculate the partial derivative of  $g(\boldsymbol{\lambda})$  with respect to  $\lambda_j$ :

$$\begin{aligned} \frac{\partial g(\boldsymbol{\lambda})}{\partial \lambda_j} &= \frac{\partial}{\partial \lambda_j} f(\boldsymbol{\lambda}, \mathbf{p}_{\text{opt}}(\boldsymbol{\lambda})) \\ &= f'_{\lambda_j}(\boldsymbol{\lambda}, \mathbf{p})|_{\mathbf{p}=\mathbf{p}_{\text{opt}}(\boldsymbol{\lambda})} + \sum_{l=0}^m f'_{p_l}(\boldsymbol{\lambda}, \mathbf{p})|_{\mathbf{p}=\mathbf{p}_{\text{opt}}(\boldsymbol{\lambda})} \frac{\partial p_l}{\partial \lambda_j} |_{\mathbf{p}=\mathbf{p}_{\text{opt}}(\boldsymbol{\lambda})}. \end{aligned} \quad (3.40)$$

Since  $f'_{p_l}(\boldsymbol{\lambda}, \mathbf{p})|_{\mathbf{p}=\mathbf{p}_{\text{opt}}(\boldsymbol{\lambda})} = \alpha$  for  $l \in \mathcal{S}_p$  and  $\frac{\partial p_l}{\partial \lambda_j}|_{\mathbf{p}=\mathbf{p}_{\text{opt}}(\boldsymbol{\lambda})} = 0$  for  $l \notin \mathcal{S}_p$ , we have that

$$\sum_{l=0}^m f'_{p_l}(\boldsymbol{\lambda}, \mathbf{p})|_{\mathbf{p}=\mathbf{p}_{\text{opt}}(\boldsymbol{\lambda})} \frac{\partial p_l}{\partial \lambda_j}|_{\mathbf{p}=\mathbf{p}_{\text{opt}}(\boldsymbol{\lambda})} = \alpha \sum_{l \in \mathcal{S}_p} \frac{\partial p_l}{\partial \lambda_j}|_{\mathbf{p}=\mathbf{p}_{\text{opt}}(\boldsymbol{\lambda})} = 0 \quad (3.41)$$

where the last equality follows from that  $\sum_{l \in \mathcal{S}_p} p_l = \varrho$  implies that  $\sum_{l \in \mathcal{S}_p} \frac{\partial p_l}{\partial \lambda_j} = 0$ . Thus, we have proved the differentiation procedure in (3.38). The last sentence of the lemma follows directly from Schur's condition in [MO79, Theorem 3.A.4], which states that  $g(\boldsymbol{\lambda})$  is Schur-convex if and only if

$$(\lambda_i - \lambda_j) \left( \frac{\partial g(\boldsymbol{\lambda})}{\partial \lambda_i} - \frac{\partial g(\boldsymbol{\lambda})}{\partial \lambda_j} \right) \geq 0 \quad (3.42)$$

for all  $i$  and  $j$ , and Schur-concave if the conditions are fulfilled with inverted inequalities.  $\square$

### 3.A.2 Proof of Lemma 3.2

For convenience, we use the notation  $\mathbf{h} = \text{vec}(\mathbf{H})$ . To calculate the MMSE estimate of  $\|\mathbf{H}\|_F^2$ , observe that

$$\|\mathbf{H}\|_F^2 = \mathbf{h}^H \mathbf{h} = \text{tr} \{ \mathbf{h} \mathbf{h}^H \}. \quad (3.43)$$

We then apply the posterior distribution  $\mathbf{h}|\mathbf{Y} \in \mathcal{CN}(\mathbf{m}, \mathbf{E})$  from (3.6) to achieve the MMSE estimate

$$\mathbb{E} \{ \text{tr} \{ \mathbf{h} \mathbf{h}^H \} | \mathbf{Y} \} = \text{tr} \{ \mathbf{m} \mathbf{m}^H + \mathbf{E} \} = \|\mathbf{m}\|_2^2 + \text{tr} \{ \mathbf{E} \} \quad (3.44)$$

using the last expression in (3.43). To find the corresponding MSE, we first need to calculate  $\mathbb{E} \{ \|\mathbf{H}\|_F^4 | \mathbf{Y} \}$ . We use the notation  $\tilde{\mathbf{h}} = \mathbf{h} - \mathbf{m}$  and observe that

$$\begin{aligned} \mathbb{E} \{ \|\mathbf{H}\|_F^4 | \mathbf{Y} \} &= \mathbb{E} \left\{ \|\tilde{\mathbf{h}} + \mathbf{m}\|_2^4 | \mathbf{Y} \right\} \\ &= \mathbb{E} \left\{ \|\tilde{\mathbf{h}}\|_2^4 | \mathbf{Y} \right\} + 2\mathbf{m}^H \mathbf{E} \mathbf{m} + 2\text{tr} \{ \mathbf{E} \} \|\mathbf{m}\|_2^2 + \|\mathbf{m}\|_2^4 \end{aligned} \quad (3.45)$$

where the second equality is achieved by expanding the norm, disregarding all terms that contain an odd number of  $\tilde{\mathbf{h}}$  (these are zero, see [HBO08a, Section IV.C]), and evaluating all the simple expectations. The remaining expectation,  $\mathbb{E} \{ \|\tilde{\mathbf{h}}\|_2^4 | \mathbf{Y} \}$ , can be viewed as the squared sum of exponentially distributed variables and is evaluated as

$$\mathbb{E} \{ \|\tilde{\mathbf{h}}\|_2^4 | \mathbf{Y} \} = \text{tr} \{ \mathbf{E} \mathbf{E} \} + (\text{tr} \{ \mathbf{E} \})^2. \quad (3.46)$$

Using (3.44), (3.45), and (3.46), the conditional variance of  $\|\mathbf{H}\|_F^2$  becomes

$$V_{\mathbf{m}, \mathbf{E}} = \mathbb{E}\{\|\mathbf{H}\|_F^4 | \mathbf{Y}\} - (\mathbb{E}\{\|\mathbf{H}\|_F^2 | \mathbf{Y}\})^2 = \text{tr}\{\mathbf{E}\mathbf{E}\} + 2\mathbf{m}^H \mathbf{E}\mathbf{m}. \quad (3.47)$$

Finally, we achieve the MSE by averaging the variance over  $\mathbf{m}$  (or  $\mathbf{Y}$ ):

$$\begin{aligned} \text{MSE}_{\hat{\rho}} &= \mathbb{E}\{V_{\mathbf{m}, \mathbf{E}}\} = \text{tr}\{\mathbf{E}\mathbf{E}\} + 2\text{tr}\{\mathbf{E}\mathbb{E}\{\mathbf{m}\mathbf{m}^H\}\} \\ &= \text{tr}\{\mathbf{E}\mathbf{E}\} + 2\text{tr}\{\mathbf{E}(\text{vec}(\bar{\mathbf{H}})\text{vec}(\bar{\mathbf{H}})^H + \mathbf{R} - \mathbf{E})\} \end{aligned} \quad (3.48)$$

where the expression for  $\mathbb{E}\{\mathbf{m}\mathbf{m}^H\}$  was calculated using (3.7) and then simplified using some algebra and the Woodbury identity (see [PP08]).

### 3.A.3 Proof of Theorem 3.1

First, we derive the structure of the MSE-minimizing training matrix. For Kronecker-structured systems, the MSE can be expressed as

$$\text{MSE} = \text{tr}\left\{\left(\mathbf{R}_T^{-T} \otimes \mathbf{R}_R^{-1} + (\mathbf{P}^* \bar{\Sigma}_Q^{-T} \mathbf{P}^T) \otimes \bar{\Sigma}_R^{-1}\right)^{-1}\right\}. \quad (3.49)$$

For analytical convenience, we would like to swap the order in the Kronecker products. This is achieved by taking the conjugate transpose of the training transmission model in (3.1) and then continue as in Section 3.2 to achieve an alternative expression for the MSE:

$$\begin{aligned} \text{MSE} &= \text{tr}\left\{\left(\mathbf{R}_R^{-T} \otimes \mathbf{R}_T^{-1} + \bar{\Sigma}_R^{-T} \otimes (\mathbf{P}\bar{\Sigma}_Q^{-1}\mathbf{P}^H)\right)^{-1}\right\} \\ &= \sum_{l=1}^M \text{tr}\left\{\left(\frac{1}{\lambda_l^{(R)}} \mathbf{\Lambda}_T^{-1} + \frac{1}{\sigma_l^{(R)}} \mathbf{U}_T^H \mathbf{P} \mathbf{V}_Q \mathbf{\Upsilon}_Q^{-1} \mathbf{V}_Q^H \mathbf{P}^H \mathbf{U}_T\right)^{-1}\right\} \end{aligned} \quad (3.50)$$

where the second equality follows from that  $\mathbf{R}_R$  and  $\bar{\Sigma}_R$  have identical eigenvectors and these are not affecting the trace. In addition, the trace of block matrices is equal to the sum of the traces for each block.

By setting  $a_j = 1/\lambda_j^{(R)}$ ,  $b_j = 1/\sigma_j^{(R)}$ , and  $\bar{\mathbf{P}} = \mathbf{U}_T^H \mathbf{P} \mathbf{V}_Q$ , we can apply Lemma 3.4 in Appendix 3.A.1 to conclude that the MSE-minimizing  $\bar{\mathbf{P}}$  should be rectangularly diagonal, fulfill the element ordering given in the theorem, and satisfy the power constraint with equality. With a training matrix of this type, the argument in the trace of (3.50) becomes diagonal, and the MSE can be expressed as

$$\text{MSE} = \sum_{j=1}^m \sum_{l=1}^M \frac{\lambda_j^{(T)} \lambda_l^{(R)}}{1 + p_j \frac{\lambda_j^{(T)} \lambda_l^{(R)}}{\sigma_j^{(Q)} \sigma_l^{(R)}}} + \text{tr}(\mathbf{R}_R) \sum_{j=m+1}^N \lambda_j^{(T)} \quad (3.51)$$

which is a convex function with respect to each  $p_j$  (since  $\frac{a}{1+bp_j}$  is a convex function for all  $a, b > 0$ ).

### 3.A.4 Proof of Corollary 3.1

The power allocation problem in (3.16) is convex and strictly feasible, thus the KKT conditions give necessary and sufficient condition for the optimal power allocation [BV04, Chapter 5.5]. The stationary condition is exactly the one given in (3.17). Next, we consider the two asymptotic cases. At high power, we approximate the MSE in (3.51) as

$$\begin{aligned} \text{MSE} &\approx \sum_{j=1}^m \sum_{l=1}^M \frac{\lambda_j^{(T)} \lambda_l^{(R)}}{p_j \frac{\lambda_j^{(T)} \lambda_l^{(R)}}{\sigma_j^{(Q)} \sigma_l^{(R)}}} + \text{tr}(\mathbf{R}_R) \sum_{j=m+1}^N \lambda_j^{(T)} \\ &= \text{tr}(\bar{\Sigma}_R) \sum_{j=1}^m \frac{\sigma_j^{(Q)}}{p_j} + \text{tr}(\mathbf{R}_R) \sum_{j=m+1}^N \lambda_j^{(T)} \end{aligned} \quad (3.52)$$

and straightforward Lagrangian methods show that it is minimized by (3.18). At low power, we approximate (3.51) as

$$\begin{aligned} \text{MSE} &\approx \sum_{j=1}^m \sum_{l=1}^M \lambda_j^{(T)} \lambda_l^{(R)} \left( 1 - \frac{p_j \lambda_j^{(T)} \lambda_l^{(R)}}{\sigma_j^{(Q)} \sigma_l^{(R)}} \right) + \text{tr}(\mathbf{R}_R) \sum_{j=m+1}^N \lambda_j^{(T)} \\ &= \text{tr}(\mathbf{R}_T) \text{tr}(\mathbf{R}_R) - \sum_{l=1}^M \frac{(\lambda_l^{(R)})^2}{\sigma_l^{(R)}} \sum_{j=1}^m \frac{p_j (\lambda_j^{(T)})^2}{\sigma_j^{(Q)}} \end{aligned} \quad (3.53)$$

using a first order Taylor polynomial. This expression is minimized by assigning all power in an arbitrary manner among the strongest term/terms of the second sum.

### 3.A.5 Proof of Theorem 3.2

First, we will show that the MSE expression in (3.9) can be rewritten as in (3.21) for training matrices with the assumed structure. To this end, we begin with the special case of  $N = M = B = 1$ . We let the received training signal be denoted  $y = \tilde{p}h + n$ , where  $\tilde{p}$  is the training signal,  $h \in \mathcal{CN}(\bar{h}, \lambda)$ , and  $n \in \mathcal{CN}(\bar{n}, \bar{\sigma})$ . We then get the conditional variance

$$\mathbf{E} = (\lambda^{-1} + |\tilde{p}|^2 \bar{\sigma}^{-1})^{-1} = \lambda \left( \frac{\lambda |\tilde{p}|^2}{\bar{\sigma}} + 1 \right)^{-1}. \quad (3.54)$$

Substituting this new notation into the MSE expression in (3.9) gives

$$\text{MSE}_{\hat{\rho}} = 2\lambda^2 \left( \frac{\lambda |\tilde{p}|^2}{\bar{\sigma}} + 1 \right)^{-1} - \lambda^2 \left( \frac{\lambda |\tilde{p}|^2}{\bar{\sigma}} + 1 \right)^{-2} + 2|\bar{h}|^2 \lambda \left( \frac{\lambda |\tilde{p}|^2}{\bar{\sigma}} + 1 \right)^{-1} \quad (3.55)$$

which is straightforward to rewrite into the MSE expression in (3.21).

In the MIMO case, observe that the elements of  $\mathbf{U}_R^H \mathbf{Y} \mathbf{V}_Q$  are statistically independent. Since the squared Frobenius norm is the sum of the squared magnitude of each element, we therefore have the sum of  $NM$  independent variables that can be estimated separately. We achieve the expression in (3.21) by summation over these dimensions (observe that  $p_j = 0$  for  $j > m$ ).

A function is convex if and only if its second derivative is non-negative. The second derivative of the MSE in (3.21) with respect to  $p_j$  is

$$\begin{aligned} \frac{\partial^2 \text{MSE}}{\partial p_j^2} = & \\ & \sum_{l=1}^M \frac{4p_j \frac{(\lambda_j^{(T)} \lambda_l^{(R)})^4}{(\sigma_j^{(Q)} \sigma_l^{(R)})^3} \left( \lambda_j^{(T)} \lambda_l^{(R)} + |\tilde{h}_{lj}|^2 \right) + 2 \frac{(\lambda_j^{(T)} \lambda_l^{(R)})^3}{(\sigma_j^{(Q)} \sigma_l^{(R)})^2} \left( 2|\tilde{h}_{lj}|^2 - \lambda_j^{(T)} \lambda_l^{(R)} \right)}{\left( p_j \frac{\lambda_j^{(T)} \lambda_l^{(R)}}{\sigma_j^{(Q)} \sigma_l^{(R)}} + 1 \right)^4} \end{aligned} \quad (3.56)$$

which can be negative in the neighborhood of  $p_j = 0$  and thus the MSE can be non-convex (for small values of  $p_j$ ). If the condition for convexity in the theorem is fulfilled, all terms in the second sum of (3.56) are positive at  $p_j = 0$  and thus the problem is convex. Even if the MSE is non-convex, the KKT conditions give necessary condition for the optimal power allocation [BV04, Chapter 5.5]. By a straightforward Lagrangian approach, the stationarity conditions for (3.21) can be expressed as in (3.22).

### 3.A.6 Proof of Corollary 3.3

At high training power, the necessary condition in (3.22) can be approximated and simplified as

$$\alpha \approx \sum_{l=1}^M \frac{2\sigma_j^{(Q)} \sigma_l^{(R)} (\lambda_j^{(T)} \lambda_l^{(R)} + |\tilde{h}_{lj}|^2)}{p_j^2} \quad (3.57)$$

which has the unique solution  $p_j = \varrho \sqrt{c_j} / \sum_i \sqrt{c_i}$  for all  $j$ .

At low training power, the MSE in (3.21) can be approximated as

$$\begin{aligned} \text{MSE} \approx & \sum_{l=1}^M \sum_{j=1}^N (\lambda_j^{(T)} \lambda_l^{(R)})^2 + 2|\tilde{h}_{lj}|^2 \lambda_j^{(T)} \lambda_l^{(R)} \\ & - \sum_{l=1}^M \sum_{j=1}^m \frac{p_j \lambda_j^{(T)} \lambda_l^{(R)}}{\sigma_j^{(Q)} \sigma_l^{(R)}} (\lambda_j^{(T)} \lambda_l^{(R)} + 2|\tilde{h}_{lj}|^2) \end{aligned} \quad (3.58)$$

by first disregarding the second term in the numerator and then use a first order Taylor polynomial of the remaining expression. Hence, the MSE is minimized by allocating all the power to the  $p_j$ -coefficient associated with the largest  $\sum_{l=1}^M \frac{\lambda_j^{(T)} \lambda_l^{(R)}}{\sigma_j^{(Q)} \sigma_l^{(R)}} (\lambda_j^{(T)} \lambda_l^{(R)} + 2|\tilde{h}_{lj}|^2)$ . If there is multiplicity in the largest value of this sum, the power can be allocated arbitrarily among these eigendirections.

### 3.A.7 Proof of Corollary 3.4

The condition  $\mathbf{R}_R = \bar{\Sigma}_R$  means that  $\lambda_l^{(R)} = \sigma_l^{(R)}$  for all  $l$ , and therefore we can remove the dependence on  $l$  in the denominator of (3.22). For all active training powers ( $p_j > 0$ ), the remaining expression in (3.22) can be formulated as a third degree polynomial equation in  $p_j$ :

$$2p_j b_j^2 \gamma_j + 2b_j \nu_j (p_j b_j + 1) = \alpha (p_j b_j + 1)^3, \quad (3.59)$$

using the notation  $b_j = \lambda_j^{(T)} / \sigma_j^{(Q)}$ . Its three solutions (for  $k = -1, 0, 1$ ) are

$$p_j = \left( \frac{b_j \gamma_j}{\alpha} \right)^{1/3} \frac{e^{i\frac{2\pi}{3}k}}{b_j} A_j + \frac{2(\gamma_j + \nu_j) b_j^{2/3}}{3\alpha^{2/3} \gamma_j^{1/3}} \frac{e^{-i\frac{2\pi}{3}k}}{b_j} \frac{1}{A_j} - \frac{1}{b_j} \quad (3.60)$$

where

$$A_j = \left( -1 + \sqrt{1 - \frac{8b_j(\gamma_j + \nu_j)^3}{27\gamma_j^2 \alpha}} \right)^{1/3}. \quad (3.61)$$

Observe that this expression has the form  $C_1 |A_j| e^{i(\arg(A_j) + \frac{2\pi}{3}k)} + \frac{C_2}{|A_j|} e^{-i(\arg(A_j) + \frac{2\pi}{3}k)} - C_3$ , where  $C_i$  are positive real-valued constants. Thus, in order for any of the solutions to be real-valued we need  $C_1 |A_j| = \frac{C_2}{|A_j|}$ .<sup>8</sup> If  $\alpha > \frac{8b_j(\gamma_j + \nu_j)^3}{27\gamma_j^2}$ , this condition can be expressed as

$$\left( -1 + \sqrt{1 - \frac{8b_j(\gamma_j + \nu_j)^3}{27\gamma_j^2 \alpha}} \right) = \frac{8b_j(\gamma_j + \nu_j)^3}{27\gamma_j^2 \alpha} \quad (3.62)$$

which has no solutions in the given  $\alpha$ -interval. For all  $0 < \alpha \leq \frac{8b_j(\gamma_j + \nu_j)^3}{27\gamma_j^2}$ , we observe that  $|A_j| = \left( \frac{8b_j(\gamma_j + \nu_j)^3}{27\gamma_j^2 \alpha} \right)^{1/6}$  which satisfies the condition

<sup>8</sup>We also get real-valued solutions when  $e^{i(\arg(A_j) + \frac{2\pi}{3}k)} = e^{-i(\arg(A_j) + \frac{2\pi}{3}k)} = 1$  but this will only happen for specific values on the Lagrange multiplier  $\alpha$  and will not be robust to small perturbations in the total training power. Since the power allocation is a continuous function of  $\rho$ , we disregard this special case.

$C_1|A_j| = \frac{C_2}{|A_j|}$ . Thus, for these  $\alpha$  we can rewrite (3.60) as

$$\begin{aligned} p_j &= 2\Re\left\{\left(\frac{b_j\gamma_j}{\alpha}\right)^{1/3} \frac{e^{i\frac{2\pi}{3}k}}{b_j} A_j\right\} - \frac{1}{b_j} \\ &= 2\sqrt{\frac{2(\gamma_j + \nu_j)}{3b_j\alpha}} \cos\left(\frac{\pi}{3}(1+2k) - \frac{\phi_j}{3}\right) - \frac{1}{b_j} \end{aligned} \quad (3.63)$$

where we used that  $\arg(A_j) = \frac{\pi - \phi_j}{3}$  with  $\phi_j$  defined as in the corollary. Since  $\phi_j \in [0, \frac{\pi}{2}]$ ,  $k = 1$  will only give negative solutions. For  $k = -1$  and  $k = 0$ , we see that the interval boundary  $\alpha = \frac{8b_j(\gamma_j + \nu_j)^3}{27\gamma_j^2}$  gives the coinciding solution  $p_j = \frac{\gamma_j - 2\nu_j}{2b_j(\gamma_j + \nu_j)}$ , while the limit  $\alpha \rightarrow 0$  gives  $p \rightarrow -\frac{1}{b_j}$  and  $p \rightarrow \infty$ , respectively. In order to show the intervals in (3.25) and (3.26), it remains to show that  $p_j$  is monotonically decreasing in  $\alpha$  for  $k = 0$  and increasing in  $\alpha$  for  $k = -1$ . The derivative of  $p_j$  with respect to  $\alpha$  can be expressed as

$$\begin{aligned} \frac{dp_j}{d\alpha} &= -\sqrt{\frac{2(\gamma_j + \nu_j)}{3^3b_j\alpha^3}} \frac{\cos\left(\frac{\pi}{3}(1+2k) - \frac{\phi}{3}\right)}{\sqrt{\frac{8b_j(\gamma_j + \nu_j)^3}{27\gamma_j^2\alpha} - 1}} \\ &\quad \times \left(\tan\left(\frac{\pi}{3}(1+2k) - \frac{\phi}{3}\right) + 3\sqrt{\frac{8b_j(\gamma_j + \nu_j)^3}{27\gamma_j^2\alpha} - 1}\right) \end{aligned} \quad (3.64)$$

where the multiplicative term outside the brackets is positive for all  $\alpha$  and  $k$ . The bracketed term can be expressed as

$$\begin{aligned} \tan\left(\frac{\pi}{3}(1+2k) - \frac{\arctan(x)}{3}\right) + \tan(\arctan(3x)) \\ \text{for } x = \sqrt{\frac{8b_j(\gamma_j + \nu_j)^3}{27\gamma_j^2\alpha} - 1}. \end{aligned} \quad (3.65)$$

Then, the intervals follow from the observation that  $\frac{\pi}{3} - \frac{\arctan(x)}{3} + \arctan(3x) > 0$  and  $-\frac{\pi}{3} - \frac{\arctan(x)}{3} + \arctan(3x) < 0$ .

### 3.A.8 Proof of Corollary 3.5

Observe that the second derivative of the MSE in (3.56) is positive if we limit ourself to  $p_j$  that satisfies

$$p_j \geq \frac{\sigma_j^{(Q)} \sigma_l^{(R)} (\lambda_j^{(T)} \lambda_l^{(R)} - 2|\tilde{h}_{lj}|^2)}{2\lambda_j^{(T)} \lambda_l^{(R)} (\lambda_j^{(T)} \lambda_l^{(R)} + |\tilde{h}_{lj}|^2)} \quad \forall l, \quad (3.66)$$

since then each term in the sum is positive. Thus, the MSE will be convex with respect to these  $p_j$  and the KKT conditions in (3.22) becomes necessary and sufficient.

In the special case  $\mathbf{R}_R = \bar{\Sigma}_R$ , we can strengthen the condition since the necessary KKT conditions only give a single feasible solution if

$$p_j \geq \frac{\sigma_j^{(Q)}(\gamma_j - 2\nu_j)}{2\lambda_j^{(T)}(\gamma_j + \nu_j)}. \quad (3.67)$$

In both the general and special case, these conditions need to be combined with the original constraint  $p_j \geq 0$ .

### 3.A.9 Proof of Theorem 3.3

First, we will prove that the MSE in (3.51) is Schur-concave with respect to the eigenvalues  $\lambda_1^{(T)}, \dots, \lambda_N^{(T)}$ . It is straightforward to show that the MSE is convex in the power allocation coefficients, differentiable with respect to  $\lambda_j^{(T)}$  and  $p_j$  for all  $j$ , and that the determinant of the Hessian is non-zero if the eigenvalues of  $\mathbf{R}_T$  and  $\mathbf{R}_R$  are distinct. Thus, we can apply Lemma 3.5 in Appendix 3.A.2. According to this lemma, Schur-concavity follows if  $\frac{\partial \text{MSE}}{\partial \lambda_i^{(T)}} \leq \frac{\partial \text{MSE}}{\partial \lambda_j^{(T)}}$  for all  $i, j$  such that  $\lambda_i^{(T)} \geq \lambda_j^{(T)}$ , where MSE denotes the pre-optimization MSE in (3.51) evaluated at the optimal power allocation  $p_1^*, \dots, p_m^*$ . Thus, we can calculate the partial derivatives of (3.51) as

$$\frac{\partial \text{MSE}}{\partial \lambda_j^{(T)}} = \sum_{l=1}^M \frac{\lambda_l^{(R)}}{\left(1 + p_j^* \frac{\lambda_j^{(T)} \lambda_l^{(R)}}{\sigma_j^{(Q)} \sigma_l^{(R)}}\right)^2} \quad \text{for } j = 1, \dots, m \quad (3.68)$$

and  $\frac{\partial \text{MSE}}{\partial \lambda_j^{(T)}} = \text{tr}(\mathbf{R}_R)$  for  $j = m+1, \dots, N$ . Observe that the derivatives are positive and that  $\lambda_j^{(T)}$  and  $p_j^*/\sigma_j^{(Q)}$  only appear in the denominators. From Corollary 3.1, we have that  $p_i^*/\sigma_i^{(Q)} \geq p_j^*/\sigma_j^{(Q)}$  whenever  $\lambda_i^{(T)} \geq \lambda_j^{(T)}$ . Hence, it follows that  $\frac{\partial \text{MSE}}{\partial \lambda_i^{(T)}} \leq \frac{\partial \text{MSE}}{\partial \lambda_j^{(T)}}$  and thus the MSE is Schur-concave.

Next, we have the case of  $\bar{\Sigma}_R = \mathbf{I}_M$  and then the MSE in (3.51) can be expressed as

$$\text{MSE} = \sum_{l=1}^M \left( \underbrace{\sum_{j=1}^m \frac{\lambda_j^{(T)}}{\lambda_l^{(R)} + p_j \frac{\lambda_j^{(T)}}{\sigma_j^{(Q)}}}}_{(a)} + \lambda_l^{(R)} \underbrace{\sum_{j=m+1}^N \lambda_j^{(T)}}_{(b)} \right) \quad (3.69)$$

which is a concave function in  $\lambda_l^{(R)}$  for all  $l$ . We apply [MO79, Proposition 3.C.1] to conclude that (a) and (b) are both Schur-concave with respect to  $\lambda_1^{(R)}, \dots, \lambda_M^{(R)}$ , and thus the MSE is Schur-concave.

### 3.A.10 Proof of Theorem 3.4

For  $\bar{\Sigma} = \mathbf{I}_{BM}$ , the MSE in (3.11) becomes

$$\begin{aligned} & \text{tr} \left\{ (\mathbf{R}^{-1} + (\mathbf{P}^T \otimes \mathbf{I}_M)^H \bar{\Sigma}^{-1} (\mathbf{P}^T \otimes \mathbf{I}_M))^{-1} \right\} \\ &= \text{tr} \left\{ (\mathbf{R}^{-1} + (\mathbf{U}_P \mathbf{D}_P \mathbf{D}_P \mathbf{U}_P^H \otimes \mathbf{I}_M)^T)^{-1} \right\}. \end{aligned} \quad (3.70)$$

The theorem follows from that (3.70) is independent of  $\mathbf{V}_P$  and that  $\mathbf{P}\mathbf{P}^H = \mathbf{U}_P \mathbf{D}_P \mathbf{D}_P \mathbf{U}_P^H = \mathbf{P}'(\mathbf{P}')^H$ .

### 3.A.11 Proof of Corollary 3.6

The rank of  $\mathbf{P}$  is equal to the number of active training powers  $p_j$ . Let  $\alpha$  be the optimal Lagrange multiplier. From Corollary 3.1, we know that the  $\tilde{m}$ th training power is active if and only if  $\alpha < (\lambda_{\tilde{m}}^{(T)})^2 / \sigma_{\tilde{m}}^{(Q)}$ . Suppose that we only have  $\tilde{m} - 1$  active training powers, then  $\alpha \geq (\lambda_{\tilde{m}}^{(T)})^2 / \sigma_{\tilde{m}}^{(Q)}$ . Substitution into the power constraint gives

$$\varrho = \sum_{j=1}^{\tilde{m}-1} \sqrt{\frac{\sigma_j^{(Q)}}{\alpha}} - \frac{\sigma_j^{(Q)}}{\lambda_j^{(T)}} \leq \sum_{j=1}^{\tilde{m}-1} \frac{\sqrt{\sigma_j^{(Q)} \sigma_{\tilde{m}}^{(Q)}}}{\lambda_{\tilde{m}}^{(T)}} - \frac{\sigma_j^{(Q)}}{\lambda_j^{(T)}} \quad (3.71)$$

for  $1 \leq \tilde{m} < m$ . All  $p_j$  will be active if and only if  $\varrho$  is larger than the constraint for  $\tilde{m} = m - 1$ .

Finally, if there exist a  $B''$  that fulfills the requirements, then  $\mathbf{Y} = \mathbf{H}\mathbf{P} + \mathbf{N}$  can be factorized as

$$[[\mathbf{Y}]_{1:B''} \quad [\mathbf{Y}]_{B''+1:B}] = [[\mathbf{H}\mathbf{P}]_{1:B''} \quad \mathbf{0}] + [[\mathbf{N}]_{1:B''} \quad [\mathbf{N}]_{B''+1:B}] \quad (3.72)$$

where  $[\mathbf{N}]_{1:B''}$  and  $[\mathbf{N}]_{B''+1:B}$  are independent. Thus,  $[\mathbf{Y}]_{B''+1:B}$  neither contains information of the channel matrix nor is correlated with previous disturbance in  $[\mathbf{N}]_{1:B''}$  and will therefore not affect the estimation. We can therefore use the shorter training sequence  $\mathbf{P}''$  without any loss in MSE performance.



## Chapter 4

# Fundamental Properties of Feedback Design

In this chapter, we consider some fundamental aspects in the design of multiuser MIMO systems with imperfect CSI: 1) Should one or multiple data streams be allocated to each scheduled multi-antenna user?; 2) What is the relative importance of feeding back directional and quality information?; 3) How is rate adaptation affected by having imperfect CSI?

Preliminaries on linear precoding under perfect and imperfect CSI are given in Section 4.1, including definitions of the well-known zero-forcing (with receive combining) and block-diagonalization precoding strategies. These strategies are exploited in Section 4.2 to analyze whether receive antennas should be used for receive combining (as with zero-forcing) or multistream multiplexing (as with block-diagonalization). The  $\epsilon$ -outage sum rate is defined in Section 4.3 as a better performance measure under imperfect CSI than the achievable sum rate. This measure is shown to achieve the full multiplexing gain using only directional feedback, only quality feedback, or neither—it all depends on the number of users, spatial correlation, and number of receive antennas. Finally, two low-complexity precoding strategies that exploit quantized CSI are outlined in Section 4.4 and extended to fit our system conditions: maximum estimated SINR Combiner (MES-C) strategy and norm-supported minimum-variance distortionless response (NS-MVDR) strategy. These are evaluated numerically, to clarify the tradeoff between feedback of directional and quality information under practical conditions.

### 4.1 Introduction to Linear Precoding

We consider the downlink system model introduced in Chapter 2.1, but make some assumptions that simplify the notation and analysis. All time

indices are dropped and we assume that all users have the same number of antennas  $M_k = M \forall k$ . The received signal  $\mathbf{y}_k \in \mathbb{C}^{M \times 1}$  at  $\text{MS}_k$  is

$$\mathbf{y}_k = \mathbf{H}_k \sum_{k=1}^{K_r} \mathbf{s}_k + \mathbf{n}_k. \quad (4.1)$$

The channel matrix  $\mathbf{H}_k \in \mathbb{C}^{M \times N}$  is assumed to satisfy the Kronecker model (see Chapter 2.1.3) with  $\mathbf{H}_k = \mathbf{R}_{R,k}^{1/2} \tilde{\mathbf{H}}_k \mathbf{R}_{T,k}^{1/2}$ , where  $\mathbf{R}_{T,k}$  and  $\mathbf{R}_{R,k}$  are the correlation matrices at the base station and user side, respectively, and  $\tilde{\mathbf{H}}_k$  has independent  $\mathcal{CN}(0, 1)$ -entries. The correlation matrices are typically different for each user, describing different spatial properties and directions. We let the noise  $\mathbf{n}_k \in \mathcal{CN}(\mathbf{0}_M, \mathbf{\Sigma}_k)$  be white with  $\mathbf{\Sigma}_k = \mathbf{I}_M$ , which can be achieved through prewhitening at the user without loss of generality.<sup>1</sup>

Under linear precoding, the data signal to  $\text{MS}_k$  can be factorized as

$$\mathbf{s}_k = \mathbf{V}_k \mathbf{d}_k \quad (4.2)$$

where  $\mathbf{V}_k \in \mathbb{C}^{N \times d_k}$  is the precoding matrix,  $\mathbf{d}_k \in \mathcal{CN}(\mathbf{0}, \mathbf{I}_{d_k})$  is the data vector signal, and  $d_k$  is the number of multiplexed data streams to user  $k$ . The achievable data rate of this user is (see the definition in (2.6))

$$g_k(q) = \log_2 \frac{\det \left( \mathbf{I}_M + \sum_{\bar{k}=1}^{K_r} \mathbf{H}_k \mathbf{V}_{\bar{k}} \mathbf{V}_{\bar{k}}^H \mathbf{H}_k^H \right)}{\det \left( \mathbf{I}_M + \sum_{\bar{k} \neq k} \mathbf{H}_k \mathbf{V}_{\bar{k}} \mathbf{V}_{\bar{k}}^H \mathbf{H}_k^H \right)} \quad (4.3)$$

and we assume a total power constraint (i.e.,  $L = 1$ )

$$\sum_{k=1}^{K_r} \text{tr}\{\mathbf{V}_k \mathbf{V}_k^H\} \leq q. \quad (4.4)$$

### 4.1.1 Two Simple Precoding Strategies

Two linear precoding strategies that are simple and have good asymptotic properties are: *block-diagonalization (BD)* [SSH04] and *zero-forcing with receive combining (ZFC)* [Jin08, TBH08]. Under perfect CSI, these strategies can be defined as follows.

*Definition 4.1. (Block-Diagonalization Precoding)* Let  $\mathcal{S}^{\text{BD}}$  be a scheduling set with at most  $\frac{N}{M}$  users. For each user  $k \in \mathcal{S}^{\text{BD}}$ , we set  $d_k = M$  and  $\mathbf{V}_k =$

---

<sup>1</sup>Noise prewhitening means multiplying the received signal vector with  $\mathbf{\Sigma}_k^{-1/2}$  and interpreting  $\mathbf{\Sigma}_k^{-1/2} \mathbf{H}_k$  as the actual channel.

$\mathbf{V}_k^{\text{BD}} \boldsymbol{\Upsilon}_k^{1/2}$ , where  $\mathbf{V}_k^{\text{BD}}$  is a semi-unitary matrix that satisfies  $\mathbf{V}_k^{\text{BD},H} \mathbf{V}_k^{\text{BD}} = \mathbf{I}_M$  and  $\mathbf{H}_k \mathbf{V}_k^{\text{BD}} = \mathbf{0}$  for all  $\bar{k} \in \mathcal{S}^{\text{BD}} \setminus \{k\}$ . The power allocation is given by the diagonal matrix  $\boldsymbol{\Upsilon}_k \succeq \mathbf{0}_M$ . The data rate becomes

$$g_k^{\text{BD}}(q) = \log_2 \det \left( \mathbf{I}_M + \mathbf{H}_k \mathbf{V}_k^{\text{BD}} \boldsymbol{\Upsilon}_k \mathbf{V}_k^{\text{BD},H} \mathbf{H}_k^H \right). \quad (4.5)$$

*Definition 4.2. (Zero-Forcing Precoding with Receive Combining)* Each user combines its antennas using some channel-dependent unit-norm vector  $\mathbf{r}_k \in \mathbb{C}^{M \times 1}$  (e.g., the dominating left singular vector of  $\mathbf{H}_k$ ). Based on the effective channels  $\mathbf{h}_k^H = \mathbf{r}_k^H \mathbf{H}_k \in \mathbb{C}^{1 \times N}$ , a scheduling set  $\mathcal{S}^{\text{ZFC}}$  with at most  $N$  users is selected. For each user  $k \in \mathcal{S}^{\text{ZFC}}$  we set  $d_k = 1$  and  $\mathbf{V}_k = \sqrt{p_k} \mathbf{v}_k^{\text{ZFC}}$ , where  $\mathbf{v}_k^{\text{ZFC}}$  is a unit-norm vector that satisfies  $\mathbf{h}_k^H \mathbf{v}_k^{\text{ZFC}} = 0$  for all  $\bar{k} \in \mathcal{S}^{\text{ZFC}} \setminus \{k\}$ . The power  $p_k \geq 0$  is allocated to user  $k$  and the data rate becomes

$$g_k^{\text{ZFC}}(q) = \log_2 \left( 1 + p_k |\mathbf{r}_k^H \mathbf{H}_k \mathbf{v}_k^{\text{ZFC}}|^2 \right). \quad (4.6)$$

For both BD and ZFC, the sum-rate maximizing power allocation is achieved through water-filling (see [SSH04]), but the asymptotic analysis in this chapter often assumes equal power allocation (i.e.,  $\boldsymbol{\Upsilon}_k = \frac{q}{M|\mathcal{S}^{\text{BD}}|} \mathbf{I}_M \forall k \in \mathcal{S}^{\text{BD}}$  and  $p_k = \frac{q}{|\mathcal{S}^{\text{ZFC}}|} \forall k \in \mathcal{S}^{\text{ZFC}}$ ) since this becomes optimal as  $q \rightarrow \infty$ .

Both BD and ZFC are designed to create zero co-user interference, but the difference is that ZFC only sends one data stream per scheduled user while BD selects fewer users but multiplexes  $M$  streams to each of them. BD and ZFC are identical when each user only has one antenna (i.e.,  $M = 1$ ), which is a special case that we call zero-forcing (ZF) precoding. However, this does *not* mean that BD is a generalization of ZFC, since there are many good reasons for applying ZFC when  $M > 1$ :

1. The base station only needs to acquire the effective channels  $\mathbf{h}_k$ ;
2. The effective channels  $\mathbf{h}_k$  have better properties and can be adapted for interference rejection (e.g., using only the strongest singular direction of  $\mathbf{H}_k$  or applying interference-aware combining);
3. User devices with simplified hardware that only decodes one stream.

The interference mitigation is, on the other hand, less restrictive under BD since fewer users and dimensions are involved. This provides more degrees of freedom for efficient precoding to the scheduled users [RJ08a]. We will compare the performance of ZFC and BD in Section 4.2.

Apart from zero-forcing with receive combining in Definition 4.2, another downlink zero-forcing strategy for multi-antenna users have been analyzed in prior work [YG06, LJ07]. That strategy views each receive antenna as a separate virtual user and sends a separate stream to each receive

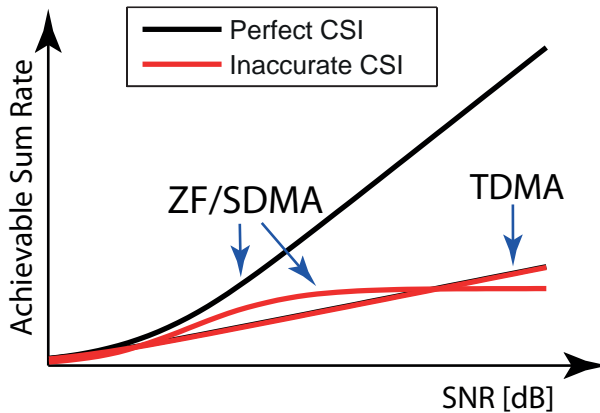


Figure 4.1: Illustration of the achievable sum rate performance with SDMA and TDMA, under perfect and inaccurate CSI. The potential performance gain of SDMA comes at the price of requiring accurate CSI.

antenna while creating zero inter-antenna interference. That approach is nothing else than BD with stricter interference mitigation and can never perform better than BD. The ZFC considered in this chapter exploits receive diversity and has therefore the potential of outperforming BD.

### 4.1.2 Imperfect Channel State Information

The current channel realizations,  $\mathbf{H}_k$ , represent the instantaneous channel state information (CSI) of the system. Practical systems can never achieve perfect CSI at the base station. If the base station acquires CSI through feedback from the users, the number of feedback bits will limit the CSI accuracy. If the base station exploits channel reciprocity and acquires CSI through reverse-link estimation (as in TDD systems), the CSI accuracy is limited by estimation errors. Hardware deficiencies and delays in CSI acquisition also impact the accuracy, but are neglected in this chapter.

An important factor in the design of multiuser MIMO systems is the CSI accuracy that can be achieved. Space division multiple access (SDMA) strategies, such as ZFC and BD precoding, can achieve the full multiplexing gain of  $N$  through simultaneous transmission to multiple users, but require high CSI accuracy to keep the co-user interference under control. The alternative of only transmitting to one user at a time, known as time division multiple access (TDMA), can only achieve a multiplexing gain of  $M \leq N$ , but is relatively robust to CSI deficiencies [GKH<sup>+</sup>07]. This fact is illustrated in Figure 4.1 in a scenario with  $N = 4$ ,  $M = 1$ , and either perfect CSI or a fixed CSI accuracy. In this scenario, ZF precoding can

achieve a high-SNR slope of 4 under perfect CSI (i.e., multiplexing gain 4), but the sum rate becomes interference-limited under inaccurate CSI. TDMA-based single-user transmission only achieves a high-SNR slope of 1, but the loss of having imperfect CSI is almost invisible. In other words, the gain of multi-user transmission comes at the price of requiring accurate CSI. The system should choose between SDMA and TDMA based on CSI accuracy [ZHKA09], but we should not forget that there are other factors that affect the position of the curves without affecting the high SNR-slopes (e.g., spatial correlation and user distribution [LTV05]). If the resources for CSI acquisition are fixed (e.g., fixed length of training sequence or fixed number of feedback bits), the question is how to utilize these resources to achieve high CSI accuracy. Channel estimation was considered in Chapter 3, while this chapter primarily considers quantized CSI feedback.

### 4.1.3 Preliminaries of Quantized Feedback

We consider a scenario where each user (or possibly a subset of users) feeds back  $B$  bits of CSI to the base station over an error-free uplink connection. These bits are divided into  $B_d$  bits of channel direction information (CDI) and  $B_q$  bits of channel quality information (CQI), where  $B = B_d + B_q$ .

The CDI feedback should be used to identify suitable transmit directions. For BD, this corresponds to the  $M_k$ -dimensional subspace spanned by the rows of  $\mathbf{H}_k$ , because this is the subspace where co-user interference is forbidden. Similarly, the one-dimensional direction of the effective channel  $\mathbf{h}_k$  should be fed back to enable ZFC.

The common approach to quantize a (linear) subspace of dimension  $\bar{M}$  (in an  $N$ -dimensional space) using  $B_d$  bits is to have a codebook  $\mathcal{C} = \{\mathbf{U}_1, \dots, \mathbf{U}_{2^{B_d}}\}$  with codewords  $\mathbf{U}_i \in \mathbb{C}^{N \times \bar{M}}$ ; see [LHS03, DLR08, RHS07, LHL<sup>+</sup>08, RJ08a]. Each codeword forms an orthonormal basis of an  $\bar{M}$ -dimensional subspace—that is,  $\mathbf{U}_i$  is a semi-unitary matrix satisfying  $\mathbf{U}_i^H \mathbf{U}_i = \mathbf{I}_{\bar{M}}$ . The codewords are selected from the (complex) *Grassmannian manifold*  $\mathcal{G}_{N, \bar{M}}$ , which is the set of all  $\bar{M}$ -dimensional linear subspaces (passing through the origin) in an  $N$ -dimensional space. Each user feeds back the index of the codeword that is closest to its channel, based on some distance metric. Herein, we consider the *chordal distance* [DHST08]

$$d(\mathbf{V}, \mathbf{U}_i) = \sqrt{\bar{M} - \text{tr}\{\mathbf{V}^H \mathbf{U}_i \mathbf{U}_i^H \mathbf{V}\}} \quad (4.7)$$

which is closely related to the leakage of signal power due to quantization and enables efficient codebook design [ZL06]. Different ways of construction the codebook  $\mathcal{C}$  will be exemplified later in this chapter.

The CQI is usually a positive scalar that depends on the channel gain and CDI quantization error [KdFG<sup>+</sup>07, dFS08]. It is often preferable to have a scalar metric in the form of an approximate SINR expres-

sion [YJG07]. The particular choice of CQI metric depends on the resource allocation strategy (i.e., the basis on which users are selected and how the precoding matrices are designed). For example, the CQI metric with BD and ZFC precoding should enable selection of spatially separated users that have strong channel gains and small CDI quantization errors.

The common approach to quantize a positive CQI scalar  $\nu_k$  using  $B_q$  bits is to divide its range  $[0, \infty)$  into  $2^{B_q}$  disjoint intervals; see [KdFG06, BO08c, YRT09, KY12]. Denote the interval boundaries by  $a_{k,0}, \dots, a_{k,2^{B_q}}$ . Each user  $k$  feeds back the index of the  $i$ th interval if  $\nu_k \in [a_{k,i-1}, a_{k,i})$ .

## 4.2 Receive Combining vs. Multistream Multiplexing

If only one user is selected for transmission at a time, the  $M$  receive antennas should be used to enable multiplexing [LJ10]. The situation is different under multiuser transmission, where only the number of transmit antennas limits the multiplexing gain (see Chapter 2.1.1). Without affecting the multiplexing gain and for any given number of data streams, the system has the choice between allocating these streams to many users or few users. This tradeoff is investigated in this section. The analysis is based on ZFC and BD precoding (see Section 4.1.1), which represent the two extremes. ZFC only sends one data stream per scheduled user, thus each user can combine the received signals on its antennas to achieve receive diversity and interference rejection (i.e., an effective channel with better properties). BD selects fewer users than ZFC but multiplexes  $M$  streams to each of them, which relaxes the interference mitigation and enables joint/iterative detection of each user's streams. In other words, ZFC exploits *receive combining* and BD exploits *multistream multiplexing*. The multimode switching technique in [CSAH08] is an example of a practical scheme that operates in between these extremes.

In this section, the tradeoff between receive combining and multistream multiplexing is analyzed using asymptotic analysis and performance bounds. The base station has either perfect CSI or imperfect CSI, and the results are confirmed with numerical examples. To achieve a fair comparison, we assume in this section that  $\frac{N}{M}$  is an integer so that BD can divide the  $N$  streams among the  $M$ -antenna users in a simple way.

Each user device is assumed to have a perfect estimate of its own channel matrix, to concentrate on the impact of imperfect CSI at the base station. It also enables coherent signal reception, making the data rate in (4.3) a measure of the highest achievable performance. The system performance will be measured by the achievable sum rate

$$f_{\text{sum}}(q) = \sum_{k=1}^{K_r} g_k(q). \quad (4.8)$$

### 4.2.1 Comparison of BD and ZFC under perfect CSI

If both the base station and the users have perfect CSI, the achievable sum rate in (4.8) asymptotically becomes (as  $q \rightarrow \infty$ ) [LJ07]

$$\begin{aligned} f_{\text{sum}}^{\text{BD}}(q) &\cong N \log_2 \left( \frac{q}{N} \right) + \sum_{k \in \mathcal{S}^{\text{BD}}} \log_2 \det(\mathbf{H}_k \mathbf{V}_k^{\text{BD}} \mathbf{V}_k^{\text{BD},H} \mathbf{H}_k^H), \\ f_{\text{sum}}^{\text{ZFC}}(q) &\cong N \log_2 \left( \frac{q}{N} \right) + \sum_{k \in \mathcal{S}^{\text{ZFC}}} \log_2 (|\mathbf{r}_k^H \mathbf{H}_k \mathbf{v}_k^{\text{ZFC}}|^2), \end{aligned} \quad (4.9)$$

for BD and ZFC, respectively. This result is based on having scheduling sets that satisfy  $|\mathcal{S}^{\text{BD}}| = \frac{N}{M}$  and  $|\mathcal{S}^{\text{ZFC}}| = N$  and equal power allocation (which is asymptotically optimal).

For both strategies, the asymptotic sum rate behaves as  $\mathcal{M}_\infty \log_2(q) + \mathcal{R}_\infty$ , where  $\mathcal{M}_\infty$  is the multiplexing gain and  $\mathcal{R}_\infty$  is the rate offset. Both BD and ZFC achieve a multiplexing gain of  $\mathcal{M}_\infty = N$ , which is the same high-SNR slope as the sum capacity achieves. We thus need to compare the rate offsets  $\mathcal{R}_\infty$  to conclude which strategy is preferable.

*Theorem 4.1.* Assume that the transmit antennas are uncorrelated (i.e.,  $\mathbf{R}_{T,k} = \mathbf{I}_N \forall k$ ), receive correlation matrices  $\mathbf{R}_{R,k}$  have eigenvalues  $\lambda_{k,M} \geq \dots \geq \lambda_{k,1} > 0$ , and random user selection with  $|\mathcal{S}^{\text{BD}}| = \frac{N}{M}$ ,  $|\mathcal{S}^{\text{ZFC}}| = N$ . The expected asymptotic difference between BD and ZFC is bounded as

$$\begin{aligned} \bar{\beta} &= \lim_{q \rightarrow \infty} \mathbb{E}\{f^{\text{BD}}(q) - f^{\text{ZFC}}(q)\} \\ &\leq N \frac{\log_2(e)}{M} \sum_{i=1}^{M-1} \frac{M-i}{i} + \log_2 \left( \frac{\prod_{k \in \mathcal{S}^{\text{BD}}} \prod_{m=1}^M \lambda_{k,m}}{\prod_{\bar{k} \in \mathcal{S}^{\text{ZFC}}} \lambda_{\bar{k},M}} \right). \end{aligned} \quad (4.10)$$

*Proof.* The proof is given in Appendix 4.A.1.  $\square$

The expected asymptotic difference in Theorem 4.1 consists of two terms. The first term is positive and is an upper bound on the expected gain of BD in an uncorrelated system (see [LJ07, Theorem 3]). The second term contains a ratio of eigenvalues. If all  $\mathbf{R}_{R,k}$  have the same eigenvalues  $\lambda_{k,m} = \lambda_m$ , it becomes  $N \log_2((\prod_{m=1}^M \lambda_m)^{1/M} / \lambda_M)$  which contains the geometric mean of all eigenvalues divided by the largest eigenvalue. This ratio is smaller than one (or equal in uncorrelated channels). As we take the logarithm of this quantity, the second term is negative and approaches  $-\infty$  as the eigenvalue spread increases. In other words, Theorem 4.1 shows that BD has a (bounded) advantage on uncorrelated channels, while ZFC becomes the best choice as the receive-side correlation grows. The explanation is that BD has less restrictive interference mitigation, but is more sensitive to poor channels since it uses all channel dimensions for transmission. Therefore, we can expect a similar impact of any channel property

that increases the eigenvalue spread in  $\mathbf{H}_k \mathbf{H}_k^H$  (on average or in some other way). This could for example be spatial correlation at the transmitter side or a strong (low-rank) line-of-sight component. Such properties are not included in analysis of this section as it both creates complicated mathematical structures and requires limiting assumptions on the user distribution geometry and fading environment.

Observe that this result was derived assuming random selection of the maximal number of users ( $\frac{N}{M}$  with BD and  $N$  with ZFC), although scheduling of spatially separated users is necessary to achieve the full potential of multiuser transmission [KKGK09]. We have assumed  $K_r \geq N$  users, meaning that only a subset of users are scheduled at each channel use. If the users are unevenly distributed in the cell, it could be beneficial to intentionally schedule fewer users than possible. Scheduling is also used to achieve user fairness and exploit multiuser diversity. The following theorem considers its impact on BD and ZFC.

*Theorem 4.2.* Assume that the transmit antennas are uncorrelated (i.e.,  $\mathbf{R}_{T,k} = \mathbf{I}_N \forall k$ ). For any given scheduling sets  $\mathcal{S}^{\text{BD}}, \mathcal{S}^{\text{ZFC}}$  (with  $|\mathcal{S}^{\text{BD}}| = \frac{N}{M}$  and  $|\mathcal{S}^{\text{ZFC}}| = N$ ) suppose that we replace one of the users in each set with the best one among  $K_r$  random users. If the best user is the one minimizing the expected asymptotic loss<sup>2</sup> compared with single-user transmission, these losses for BD and ZFC, respectively, can be lower bounded as

$$\begin{aligned} \mathbb{E}\{\text{Loss}_{\text{BD}}\} &\geq -M \log_2(1 - c_1 K_r^{-\frac{1}{M(N-M)}}) \\ \mathbb{E}\{\text{Loss}_{\text{ZFC}}\} &\geq -\log_2(1 - c_2 K_r^{-\frac{1}{N-M}}) \end{aligned} \quad (4.11)$$

when  $K_r$  is large ( $c_1, c_2$  are positive constants).

*Proof.* The proof is given in Appendix 4.A.2. □

This theorem indicates that it is easier to find users with near-orthogonal channels under ZFC than under BD, which is reasonable since the channels of BD users occupy  $M$  dimensions and should be compatible to the other users in all these dimensions, while ZFC users only have one dimension. If the scheduling also prioritizes strong users, recall from Theorem 4.1 that the performance of ZFC depends on the dominating eigenvalue, while BD depends on the geometric mean of the eigenvalues. The dominating eigenvalue among  $K_r$  users certainly scales faster than the geometric mean, thus ZFC should also be superior when it comes to exploiting strong channels (i.e., multiuser diversity).

To illustrate the results of Theorem 4.1 and Theorem 4.2, we adopt the exponential correlation model (ECM) from [Loy01] that was discussed in

---

<sup>2</sup>If  $\mathbf{B}_k = \text{span}(\mathbf{H}_k)$  is an orthonormal basis of the row space of  $\mathbf{H}_k$ , then the expected asymptotic loss becomes  $-\mathbb{E}\{\log_2 \det(\mathbf{B}_k \mathbf{V}_k \mathbf{V}_k^H \mathbf{B}_k^H)\}$ .

Chapter 2.1.3. In this model, the magnitude parameter  $|r|$  is the *correlation factor* between adjacent antennas, where  $|r| = 0$  means no spatial correlation and  $|r| = 1$  means full correlation. For simplicity, we assume that all users have the same path loss and correlation factor, but different uniformly distributed directions  $\angle r \in U[0, 2\pi)$ .

The dominating left singular vector of  $\mathbf{H}_k$  is used as a preliminary receive combiner  $\mathbf{r}_k$  for user  $k$  in the precoding design. This choice maximizes the channel gain and is known as *maximum ratio combining (MRC)*. Once the base station has fixed the precoding, user  $k$  can update its receive combining to balance between signal gain and interference rejection. For fixed  $\mathbf{v}_k^{\text{ZFC}} \forall k \in \mathcal{S}^{\text{ZFC}}$ , the SINR of user  $k \in \mathcal{S}^{\text{ZFC}}$  becomes

$$\text{SINR}_k = \frac{\mathbf{r}_k^H \left( p_k \mathbf{H}_k \mathbf{v}_k^{\text{ZFC}} \mathbf{v}_k^{\text{ZFC},H} \mathbf{H}_k^H \right) \mathbf{r}_k}{\mathbf{r}_k^H \left( \mathbf{I}_M + \sum_{\bar{k} \in \mathcal{S}^{\text{ZFC}} \setminus \{k\}} p_{\bar{k}} \mathbf{H}_{\bar{k}} \mathbf{v}_{\bar{k}}^{\text{ZFC}} \mathbf{v}_{\bar{k}}^{\text{ZFC},H} \mathbf{H}_{\bar{k}}^H \right) \mathbf{r}_k}. \quad (4.12)$$

The maximization of  $\text{SINR}_k$  is a generalized eigenvalue problem and is solved by the MMSE combiner [Win84]

$$\mathbf{r}_k^{\text{MMSE}} = \frac{\left( \mathbf{I}_M + \sum_{\bar{k} \in \mathcal{S}^{\text{ZFC}} \setminus \{k\}} p_{\bar{k}} \mathbf{H}_{\bar{k}} \mathbf{v}_{\bar{k}}^{\text{ZFC}} \mathbf{v}_{\bar{k}}^{\text{ZFC},H} \mathbf{H}_{\bar{k}}^H \right)^{-1} \mathbf{H}_k \mathbf{v}_k^{\text{ZFC}}}{\left\| \left( \mathbf{I}_M + \sum_{\bar{k} \in \mathcal{S}^{\text{ZFC}} \setminus \{k\}} p_{\bar{k}} \mathbf{H}_{\bar{k}} \mathbf{v}_{\bar{k}}^{\text{ZFC}} \mathbf{v}_{\bar{k}}^{\text{ZFC},H} \mathbf{H}_{\bar{k}}^H \right)^{-1} \mathbf{H}_k \mathbf{v}_k^{\text{ZFC}} \right\|_2}. \quad (4.13)$$

This update can have a major impact on the performance and can be achieved with limited overhead, since the precoded channels already have to be estimated to enable coherent reception [TBH08]. Observe that this update is supported by the system operation in Chapter 2.2, where the second training sequence is used to estimate the precoded channels.

The expected asymptotic difference between BD and ZFC is shown in Figure 4.2 and as a function of the correlation factor, using  $N = 8$  transmit antennas and  $M = 2$  receive antennas. This simulation confirms that BD is advantageous in uncorrelated systems, while ZFC becomes beneficial as the correlation increases ( $|r| > 0.4$  under receive-side correlation,  $|r| > 0.7$  under transmit-side correlation, and  $|r| > 0.25$  when both sides are correlated). The bound in Theorem 4.1 is only tight at high correlation. Note that  $|r|$  impacts the perceived spatial correlation non-linearly; typical spatially correlated environments correspond to  $|r| \approx 0.9$  [BHO09].

To exemplify the impact of user selection, we consider the *capacity-based suboptimal user selection algorithm* in [SCA<sup>+</sup>06]. This is a greedy algorithm that adds one user at the time based on the achievable sum rate performance. It remembers the performance in each iteration and selects

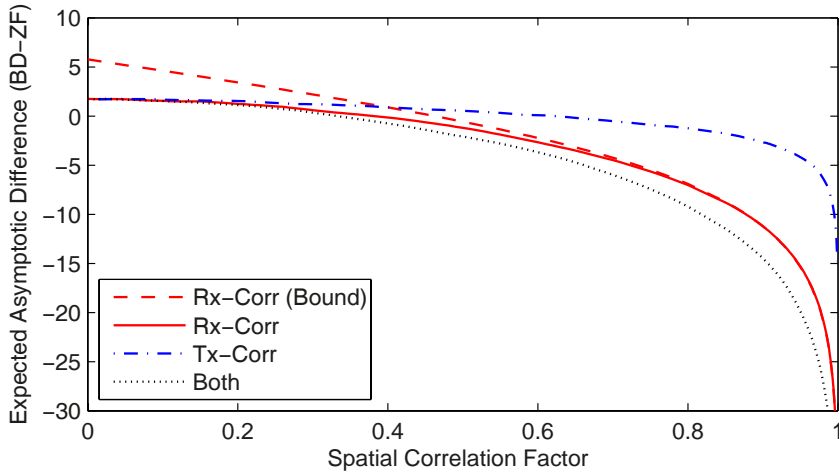


Figure 4.2: The expected asymptotic difference between BD and ZFC in a system with  $N = 8$  transmit antennas,  $M = 2$  receive antennas per user, and random user selection. The impact of spatial correlation at the receiving users, transmitting base station, and both sides is shown (using the exponential correlation model from [Loy01]).

the user constellation with the highest performance, which might include fewer than  $N$  data streams. The average achievable sum rate is shown in Figure 4.3 in a scenario with  $N = 8$  transmit antennas,  $M = 2$  or  $M = 4$  receive antennas, and a total transmit power of  $q = 10$  dB or  $q = 20$  dB. Since the system is spatially uncorrelated, it is remarkable that the inclusion of user selection makes ZFC superior to BD. Fewer than  $N$  streams are used when the number of users is small, while the number of active streams increases with  $K_r$ . ZFC clearly benefits more from scheduling than BD, which also confirms Theorem 4.2.

The conclusion is that ZFC is the method of choice in multiuser MIMO systems with perfect CSI. Although it is possible to find scenarios when BD is better than ZFC, these disregard spatial correlation and user selection.

#### 4.2.2 Comparison of BD and ZFC under Quantized CSI

Next, we analyze the impact of having quantized CSI at the base station. The codebooks are based on random vector quantization (RVQ) [SH04,AYL07,Jin08,RJ08a], meaning that we average over codebooks with random codewords from the Grassmannian manifold. As any judicious codebook design is better than RVQ, the upper bounds on the performance loss that we will derive are valid for any reasonable codebook. We assume

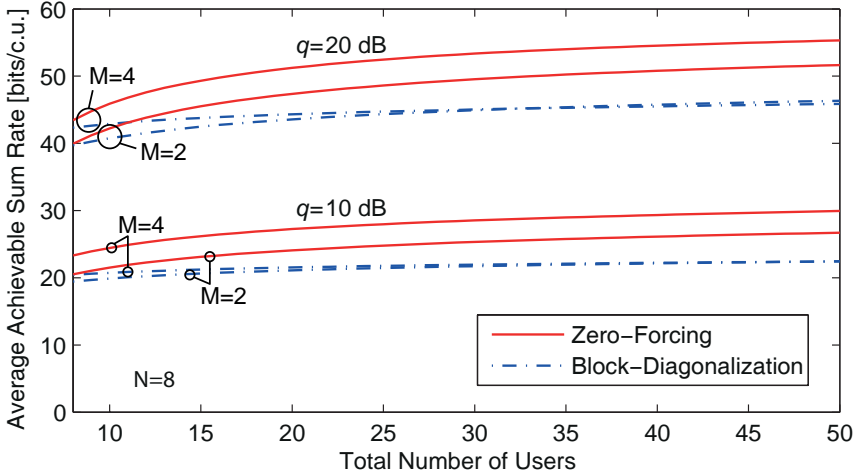


Figure 4.3: The average achievable sum rate with BD and ZFC in a system with  $N = 8$  transmit antennas and different number of receive antennas. A low-complexity user selection algorithm from [SCA<sup>+</sup>06] is used.

error-free feedback and perfect CSI at each user for analytical simplicity, but the conclusions are expected to hold true under imperfect feedback and imperfect receive-side CSI [CJKR10].

### Block-Diagonalization Precoding

Under BD precoding, the CDI quantization codebook for user  $k$  is denoted  $\mathcal{C}_k^{\text{BD}} \subset \mathcal{G}_{N,M}$  and the best codeword is selected as

$$\bar{\mathbf{H}}_k = \arg \min_{\mathbf{U} \in \mathcal{C}_k^{\text{BD}}} d(\text{span}\{\mathbf{H}_k\}, \mathbf{U}) \quad (4.14)$$

where  $\text{span}\{\mathbf{H}_k\}$  gives an orthonormal basis of the row space of  $\mathbf{H}_k$ . When only the quantized subspaces  $\bar{\mathbf{H}}_k$  are known at the base station, zero co-user interference cannot be achieved. There is a variety of ways to handle the channel uncertainty, but a simple approach is to treat  $\bar{\mathbf{H}}_1, \dots, \bar{\mathbf{H}}_{K_r}$  as being the true channels [RJ08a] and calculate approximate BD precoding matrices  $\bar{\mathbf{V}}_k^{\text{BD}} \forall k \in \mathcal{S}^{\text{BD}}$  as in Definition 4.1. This results in a lower bound on the performance and the data rate of user  $k \in \mathcal{S}^{\text{BD}}$  (under equal power allocation) is

$$g_k^{\text{BD-QUANT}}(q) = \log_2 \frac{\det\left(\mathbf{I}_M + \frac{q}{M|\mathcal{S}^{\text{BD}}|} \sum_{\bar{k} \in \mathcal{S}^{\text{BD}}} \mathbf{H}_k \bar{\mathbf{V}}_{\bar{k}}^{\text{BD}} \bar{\mathbf{V}}_{\bar{k}}^{\text{BD},H} \mathbf{H}_k^H\right)}{\det\left(\mathbf{I}_M + \frac{q}{M|\mathcal{S}^{\text{BD}}|} \sum_{\bar{k} \in \mathcal{S}^{\text{BD}} \setminus \{k\}} \mathbf{H}_k \bar{\mathbf{V}}_{\bar{k}}^{\text{BD}} \bar{\mathbf{V}}_{\bar{k}}^{\text{BD},H} \mathbf{H}_k^H\right)}. \quad (4.15)$$

The following theorem provides an upper bound on the performance loss of having quantized CSI.

*Theorem 4.3.* Assume that the transmit antennas are uncorrelated (i.e.,  $\mathbf{R}_{T,k} = \mathbf{I}_N \forall k$ ), that  $\mathbf{R}_{R,k}$  has arbitrary correlation, and that  $\frac{N}{M}$  users are scheduled randomly. The average rate loss for user  $k \in \mathcal{S}^{\text{BD}}$  due to CSI quantization is upper bounded as

$$\begin{aligned} \Delta^{\text{BD-QUANT}} &= \mathbb{E}\{g_k^{\text{BD}}(q) - g_k^{\text{BD-QUANT}}(q)\} \\ &\leq \log_2 \det \left( \mathbf{I}_M + \frac{q}{M} D^{\text{BD}} \mathbf{R}_{R,k} \right) \end{aligned} \quad (4.16)$$

where the average quantization distortion is

$$\begin{aligned} D^{\text{BD}} &= \mathbb{E}\{d^2(\mathbf{H}_k, \hat{\mathbf{H}}_k)\} \\ &\approx \frac{\Gamma\left(\frac{1}{M(N-M)}\right)}{M(N-M)} \left( \frac{2^{-B_d}}{(M(N-M))!} \prod_{m=1}^M \frac{(N-i)!}{(M-i)!} \right)^{-\frac{1}{M(N-M)}} \end{aligned} \quad (4.17)$$

*Proof.* The proof is given in Appendix 4.A.3.  $\square$

This theorem will be compared with the corresponding result for ZFC.

### Zero-Forcing Precoding with Receive Combining

Under ZFC precoding, the CDI quantization codebook for user  $k$  is denoted  $\mathcal{C}_k^{\text{ZFC}} \subset \mathcal{G}_{N,1}$ . The best codeword depends on the effective channel  $\mathbf{h}_k^H = \mathbf{r}_k^H \mathbf{H}_k$ , which is a function of the receive combining vector  $\mathbf{r}_k$ . There are primarily two factors to consider when selecting the receive combiner: the gain of the effective channel  $\|\mathbf{h}_k\|_2^2$  and the quantization distortion of  $\mathbf{h}_k$ . The results of [KdFG06, RJ08b] indicate that the top priority in multiuser MIMO systems is to achieve small quantization errors. The error can be minimized by the *quantization-based combining* (QBC) approach in [Jin08], where we select the codeword and the receive combiner jointly as

$$(\mathbf{r}_k^{\text{QBC}}, \bar{\mathbf{h}}_k) = \arg \max_{\substack{\mathbf{r}: \|\mathbf{r}\|_2=1 \\ \mathbf{u} \in \mathcal{C}_k^{\text{ZFC}}}} d \left( \frac{\mathbf{H}_k^H \mathbf{r}}{\|\mathbf{H}_k^H \mathbf{r}\|_2}, \mathbf{u} \right). \quad (4.18)$$

This can be solved by finding the error-minimizing receive combiner for every codeword and check which combination that gives the smallest error; the exact details are available in [Jin08]. The alternative *maximum expected SINR combiner (MESIC)* in [TBH08] achieves better practical performance by maximizing an approximate SINR expression, but is asymptotically equal to QBC at high SNR. Since this is the regime of interest in this section, we will exploit the analytical simplicity of QBC. Observe

that QBC (and MESOC) is only used for improved feedback accuracy; the MMSE combiner in (4.13) should be used to maximize the performance during transmission (this was not included in the original QBC framework in [Jin08]).

If the quantized effective channels  $\bar{\mathbf{h}}_1, \dots, \bar{\mathbf{h}}_{K_r}$  are treated as the true channels, we can apply Definition 4.2 to calculate approximate ZFC precoding vectors  $\bar{\mathbf{v}}_k^{\text{ZFC}}$ . This results in a lower bound on the performance and the data rate of user  $k \in \mathcal{S}^{\text{ZFC}}$  (under equal power allocation) is

$$g_k^{\text{ZFC-QUANT}}(q) = \log_2 \left( 1 + \frac{\frac{q}{|\mathcal{S}^{\text{ZFC}}|} |\mathbf{r}_k^H \mathbf{H}_k \bar{\mathbf{v}}_k^{\text{ZFC}}|^2}{1 + \frac{q}{|\mathcal{S}^{\text{ZFC}}|} \sum_{k \in \mathcal{S}^{\text{ZFC}} \setminus \{k\}} |\mathbf{r}_k^H \mathbf{H}_k \bar{\mathbf{v}}_k^{\text{ZFC}}|^2} \right) \quad \forall k \in \mathcal{S}^{\text{ZFC}}. \quad (4.19)$$

The following theorem provides an upper bound on the performance loss under quantized CSI.

*Theorem 4.4.* Assume that the transmit antennas are uncorrelated (i.e.,  $\mathbf{R}_{T,k} = \mathbf{I}_N \quad \forall k$ ), that  $\mathbf{R}_{R,k}$  has eigenvalues  $\lambda_{k,M} > \dots > \lambda_{k,1} > 0$ , and that  $N$  users are selected randomly. The average rate loss for ZFC (using the same  $\mathbf{r}_k^{\text{QBC}}$ ) due to quantized CSI can be upper bounded as

$$\begin{aligned} \Delta^{\text{ZFC-QUANT}} &= \mathbb{E}\{g_k^{\text{ZFC}}(q) - g_k^{\text{ZFC-QUANT}}(q)\} \\ &\leq \log_2 \left( 1 + \frac{q}{N} D^{\text{QBC}} G \right) \end{aligned} \quad (4.20)$$

where the average quantization distortion is

$$D^{\text{QBC}} = \mathbb{E}\{d^2(\mathbf{h}_k, \bar{\mathbf{h}}_k)\} \approx 2^{-\frac{B_d}{N-M}} \binom{N-1}{M-1}^{-\frac{1}{N-M}} \quad (4.21)$$

and average channel gain  $G$  with QBC is (where  $\mu_n = 1/\lambda_{k,n}$ )

$$\begin{aligned} G &= \sum_{m=1}^{M-1} \sum_{n=1}^m \sum_{l=m+1}^M \frac{(N-M+1)A_{m,n,l}}{(\mu_n - \mu_l) \prod_{i=1, i \neq n}^m (\mu_n - \mu_i) \prod_{j=1, j \neq l}^m (\mu_j - \mu_l)}, \\ A_{m,n,l} &= \log_e \left( \frac{\mu_{m+1}}{\mu_m} \right) \mu_n^{m-1} (-\mu_l)^{M-m-2} (m\mu_l + \mu_n(M-m-1)) \\ &\quad + \sum_{s=0}^{m-1} \sum_{r=0}^{M-m-1} \binom{m}{s} \binom{M-m-1}{r} \frac{(-1)^s \mu_n^{m-s} (-\mu_l)^{M-m-1-r}}{1+s+r} \\ &\quad \times \left( \frac{m-s}{\mu_n} + \frac{M-m-1-r}{\mu_l} \right) (\mu_m^{r+s} - \mu_{m+1}^{r+s}). \end{aligned} \quad (4.22)$$

*Proof.* The proof is given in Appendix 4.A.4.  $\square$

### Asymptotic Comparison under Quantized CSI

The rate loss expressions in Theorem 4.5 and Theorem 4.6 indicate the impact of spatial correlation (at the receiver side) and CSI quantization on the performance, but are certainly not easy to quantify. However, the important result is that spatial correlation will not have any large effect on the required number of feedback bits; the sufficient number of CDI feedback bits to achieve the full multiplexing gain has the same scaling as for uncorrelated channels in [RJ08a].

*Corollary 4.1.* To achieve the full multiplexing gain with BD or ZFC under quantized CSI and arbitrary receive correlation, it is sufficient to scale the total number of CDI feedback bits for the scheduled users as

$$B_{d,\text{tot}} \approx N(N - M) \log_2(q) + \mathcal{O}(1). \quad (4.23)$$

While this corollary only provides a sufficient condition, we can expect the scaling law in (4.23) to also be necessary.<sup>3</sup> It might seem unreasonable that the number of feedback bits should approach infinity with increasing SNR, but if we can achieve the full multiplexing gain in the downlink it is natural to assume that it is also achievable in the uplink [CJKR10]. Therefore, the uplink sum rate behaves as  $N \log_2(q) + \mathcal{O}(1)$  and it is sufficient to allocate (approximately)  $N - M$  channel uses for CSI feedback.

Observe that this result is based on random user selection among users with homogenous channel conditions. To achieve multiuser diversity, both CDI and CQI feedback from additional users is required. As BD requires  $M$  times more bits per user, ZFC can typically achieve feedback from  $M$  times more users. We therefore expect ZFC to be better than BD at exploiting multiuser diversity, just as in the case of perfect CSI. In addition, spatial correlation at the transmitter-side (and other factors that make the channel matrices ill-conditioned) will inflict larger performance losses to BD than ZFC, just as in the case of perfect CSI.

### 4.2.3 Comparison of BD and ZFC under Estimated CSI

Next, we assume that the base station acquires CSI through imperfect CSI estimation. The primary focus will be on TDD systems, where channel estimates are obtained through training signaling on the uplink (assuming perfect channel reciprocity). But it is worth noting that this approach is similar to having analog CSI feedback in FDD systems, where the unquantized channel coefficients are sent on an uplink subcarrier (to avoid the codebook complexity) [RJ08a, CJKR10].<sup>4</sup>

<sup>3</sup>The necessary scaling can be proved for ZFC with QBC using a technique from [Jin06, Theorem 4], while simulations in [RJ08a] shows that quantized ZFC and BD has the same scaling in the necessary number of bits.

<sup>4</sup>Digital/quantized feedback can offer substantial performance improvements over analog/unquantized feedback. But if very accurate CSI is required, Corollary 4.1 shows

The reciprocal uplink counterpart to the channel in (4.1) is

$$\tilde{\mathbf{y}}_k = \mathbf{H}_k^T \tilde{\mathbf{x}}_k + \tilde{\mathbf{n}}_k \quad (4.24)$$

where  $\tilde{\mathbf{y}}_k \in \mathbb{C}^{N \times 1}$  is the received uplink signal,  $\tilde{\mathbf{x}}_k \in \mathbb{C}^{M \times 1}$  is the transmitted uplink signal, and  $\tilde{\mathbf{n}}_k \in \mathcal{CN}(\mathbf{0}, \sigma^2 \mathbf{I}_N)$  is the noise vector.<sup>5</sup>

As in Chapter 3, user  $k$  sends an MSE-minimizing training matrix  $\mathbf{P}_k \in \mathbb{C}^{M \times M}$  over  $M$  uplink channel uses to estimate the channel  $\mathbf{H}_k$ . The MMSE estimate of  $\mathbf{H}_k$  and its error covariance matrix  $\mathbf{E}_k$  are given by Lemma 3.1 and become

$$\begin{aligned} \text{vec}(\hat{\mathbf{H}}_k^T) &= \frac{1}{\sigma^2} \mathbf{E}_k \tilde{\mathbf{P}}_k^H \text{vec}(\mathbf{Y}_k), \\ \mathbf{E}_k &= \left( (\mathbf{R}_{R,k} \otimes \mathbf{R}_{T,k}^T)^{-1} + \frac{1}{\sigma^2} \tilde{\mathbf{P}}_k^H \tilde{\mathbf{P}}_k \right)^{-1} \end{aligned} \quad (4.25)$$

where  $\tilde{\mathbf{P}}_k = (\mathbf{P}_k^T \otimes \mathbf{I}_M)$  and  $\mathbf{Y}_k$  is the received signal from training signaling. The training matrix  $\mathbf{P}_k$  has a total power constraint  $\text{tr}\{\mathbf{P}_k^H \mathbf{P}_k\} = \varrho$ .

### Block-Diagonalization Precoding

As under quantized CSI, we calculate the approximate BD precoding  $\hat{\mathbf{V}}_k^{\text{BD}} \forall k \in \mathcal{S}^{\text{BD}}$  by treating  $\hat{\mathbf{H}}_1, \dots, \hat{\mathbf{H}}_{K_r}$  as the true channels [RJ08a]. This results in a lower bound on the performance and the data rate of user  $k \in \mathcal{S}^{\text{BD}}$  is

$$g_k^{\text{BD-EST}}(q) = \log_2 \frac{\det\left(\mathbf{I}_M + \frac{q}{M|\mathcal{S}^{\text{BD}}|} \sum_{k \in \mathcal{S}^{\text{BD}}} \mathbf{H}_k \hat{\mathbf{V}}_k^{\text{BD}} \hat{\mathbf{V}}_k^{\text{BD},H} \mathbf{H}_k^H\right)}{\det\left(\mathbf{I}_M + \frac{q}{M|\mathcal{S}^{\text{BD}}|} \sum_{k \in \mathcal{S}^{\text{BD}} \setminus \{k\}} \mathbf{H}_k \hat{\mathbf{V}}_k^{\text{BD}} \hat{\mathbf{V}}_k^{\text{BD},H} \mathbf{H}_k^H\right)}. \quad (4.26)$$

The following theorem provides an upper bound on the performance loss due to imperfect CSI estimation.

*Theorem 4.5.* Assume that the transmit antennas are uncorrelated (i.e.,  $\mathbf{R}_{T,k} = \mathbf{I}_N \forall k$ ), that  $\mathbf{R}_{R,k}$  has arbitrary correlation, and that  $\frac{N}{M}$  users are scheduled randomly. The average rate loss for user  $k \in \mathcal{S}^{\text{BD}}$  due to CSI estimation is upper bounded as

$$\begin{aligned} \Delta^{\text{BD}} &= \mathbb{E}\{g_k^{\text{BD}}(q) - g_k^{\text{BD-EST}}(q)\} \\ &\leq \log_2 \det \left( \mathbf{I}_M + \frac{q(N-M)}{N} \left( \mathbf{R}_{R,k}^{-T} + \frac{\mathbf{P}_k^H \mathbf{P}_k}{\sigma^2} \right)^{-1} \right). \end{aligned} \quad (4.27)$$

---

that the quantization codebooks grow very large and thus the search for the best code-word becomes computationally infeasible.

<sup>5</sup>The downlink noise vector was normalized towards the channel matrix. To account for a different noise level at the base station,  $\sigma^2$  is the (relative) uplink noise variance.

*Proof.* The proof is given in Appendix 4.A.5.  $\square$

This theorem will be compared with the corresponding result for ZFC.

### Zero-Forcing Precoding with Receive Combining

When users are unaware of the channels of other active users, MRC is a reasonable combining strategy as it maximizes the effective channel gain. ZFC precoding is very similar to applying BD precoding to the effective channels  $\mathbf{h}_k^H = \mathbf{r}_k^H \mathbf{H}_k$ , but an important difference is that the effective channels are not Rayleigh fading (since  $\mathbf{r}_k$  is based on the current channel realization). This makes it difficult to derive the MMSE estimator of  $\mathbf{h}_k$ , but fortunately the linear MMSE (LMMSE) estimator is given by Lemma 3.1 (as discussed in Chapter 3.2). To apply this LMMSE estimator, we need the statistics of  $\mathbf{h}_k$ .

*Lemma 4.1.* Assume that the transmit antennas are uncorrelated (i.e.,  $\mathbf{R}_T = \mathbf{I}_N$ ) and that  $\mathbf{R}_R$  has eigenvalues  $\lambda_M > \dots > \lambda_1 > 0$ , where the user indices were dropped for convenience. If  $\mathbf{r}$  is the dominating left singular vector of  $\mathbf{H}$ , it holds that

- the direction  $\mathbf{h}/\|\mathbf{h}\|_2$  is isotropically distributed on the unit sphere;
- the gain  $\|\mathbf{h}\|_2^2$  is independent of the direction and

$$\begin{aligned} \mathbb{E}\{\|\mathbf{h}\|_2^2\} &= \sum_{l=1}^M \sum_{\zeta \in \mathcal{A}_M} \frac{\prod_{\bar{k}=1}^M \lambda_{\zeta_{\bar{k}}}^{N-\bar{k}+1} \prod_{\bar{k}=N-M+1}^N (\bar{k}-1)!}{(-1)^{\text{per}(\zeta)+l+1} \det(\mathbf{\Delta})} \\ &\times \sum_{\beta \in \mathcal{B}_{l,M}} \sum_{\bar{k}=0}^{K_l(\beta)} \sum_{\tilde{k} \in \tilde{\Omega}_{\bar{k}}^{(l)}} \frac{\bar{k}!}{\tilde{k}_1! \cdots \tilde{k}_l!} \frac{(\sum_{i=1}^l \lambda_{\zeta_{\beta_i}}^{-1})^{-(\bar{k}+1)}}{\prod_{i=1}^l \lambda_{\zeta_{\beta_i}}^{\tilde{k}_i}}, \end{aligned} \quad (4.28)$$

where the  $ij$ th element of  $\mathbf{\Delta} \in \mathbb{R}^{M \times M}$  is given by

$$[\mathbf{\Delta}]_{ij} = \lambda_j^{N-i+1} (N-i)!. \quad (4.29)$$

In (4.28), the set of all permutations of  $\{1, \dots, M\}$  is denoted  $\mathcal{A}_M$ . The sign of a given permutation  $\zeta = \{\zeta_1, \dots, \zeta_M\} \in \mathcal{A}_M$  is denoted  $(-1)^{\text{per}(\zeta)}$ , where  $\text{per}(\cdot)$  is the number of inversions<sup>6</sup> in the permuted sequence. Next,  $\mathcal{B}_{l,M}$  is the collection of all subsets of  $\mathcal{A}_M$  with cardinality  $l$  and increasing elements (i.e.,  $\beta_1 < \dots < \beta_l$  for  $\beta = \{\beta_1, \dots, \beta_l\} \in \mathcal{B}_{l,M}$ ). The upper bound in the summation over  $\bar{k}$  is  $K_l(\beta) = \sum_{i=1}^l (N - \beta_i)$ . Finally,  $\tilde{\Omega}_{\bar{k}}^{(l)}$  is

<sup>6</sup>An inversion in a sequence is a pair of numbers that are in incorrect order (i.e., not in ascending order).

the set of all  $l$ -length partitions  $\{\tilde{k}_1, \dots, \tilde{k}_l\}$  of  $\bar{k}$  (i.e.,  $\sum_{i=1}^l \tilde{k}_i = \bar{k}$ ) that satisfy  $0 \leq \tilde{k}_i \leq N - \beta_i$ :

$$\tilde{\Omega}_k^{(l)} = \left\{ \{\tilde{k}_1, \dots, \tilde{k}_l\} : \sum_{j=1}^l \tilde{k}_j = \bar{k}, 0 \leq \tilde{k}_j \leq N - \beta_j \forall j \right\}. \quad (4.30)$$

*Proof.* The proof is given in Appendix 4.A.6.  $\square$

As for BD precoding, we treat  $\hat{\mathbf{h}}_1, \dots, \hat{\mathbf{h}}_{K_r}$  as being the true channels and the resulting data rate of user  $k \in \mathcal{S}^{\text{ZFC}}$  is

$$g_k^{\text{ZFC-EST}}(q) = \log_2 \left( 1 + \frac{\frac{q}{|\mathcal{S}^{\text{ZFC}}|} |\mathbf{r}_k^H \mathbf{H}_k \hat{\mathbf{v}}_k^{\text{ZFC}}|^2}{1 + \frac{q}{|\mathcal{S}^{\text{ZFC}}|} \sum_{\bar{k} \in \mathcal{S}^{\text{ZFC}} \setminus \{k\}} |\mathbf{r}_k^H \mathbf{H}_k \hat{\mathbf{v}}_k^{\text{ZFC}}|^2} \right). \quad (4.31)$$

Once the base station has fixed the precoding  $\hat{\mathbf{v}}_k^{\text{ZFC}}$ , user  $k$  can maximize the performance by applying the MMSE combiner in (4.13). The following theorem upper bounds the performance loss due to CSI estimation.

*Theorem 4.6.* Assume that the transmit antennas are uncorrelated (i.e.,  $\mathbf{R}_{T,k} = \mathbf{I}_N \forall k$ ), that  $N$  users are scheduled randomly, and that  $\mathbf{r}_k$  is selected as in Lemma 4.1. The average rate loss for user  $k \in \mathcal{S}^{\text{ZFC}}$  due to CSI estimation is upper bounded as

$$\begin{aligned} \Delta^{\text{ZFC-EST}} &= \mathbb{E}\{g_k^{\text{ZFC}}(q) - g_k^{\text{ZFC-EST}}(q)\} \\ &\leq \log_2 \left( 1 + \frac{q(N-1)}{N} \frac{1}{\mathbb{E}\{\|\mathbf{h}_k\|_2^2\}^{-1} + \varrho/\sigma^2} \right). \end{aligned} \quad (4.32)$$

*Proof.* The proof is given in Appendix 4.A.7.  $\square$

### Asymptotic Comparison under Estimated CSI

The rate loss expressions in Theorem 4.5 and Theorem 4.6 indicate the impact of spatial correlation and channel estimation on the performance. BD is slightly more resilient to channel uncertainty, since the BD expression contains  $(N - M)$  where the ZFC expression has  $(N - 1)$ . But observe that the performance losses are calculated against the same precoding strategy with perfect CSI; we know from Section 4.2.1 that ZFC often has better performance than BD under perfect CSI, making it hard to analytically conclude which strategy to use under imperfect CSI estimation. However, the important result is the following extension of [CJKR10] to correlated scenarios with  $M \geq 1$ .

*Corollary 4.2.* To achieve the full multiplexing gain with BD or ZFC precoding under imperfect CSI estimation and arbitrary receive correlation, it is sufficient to scale the training power  $\varrho$  as

$$q/\varrho \rightarrow \text{constant} < \infty \quad \text{when } q \rightarrow \infty. \quad (4.33)$$

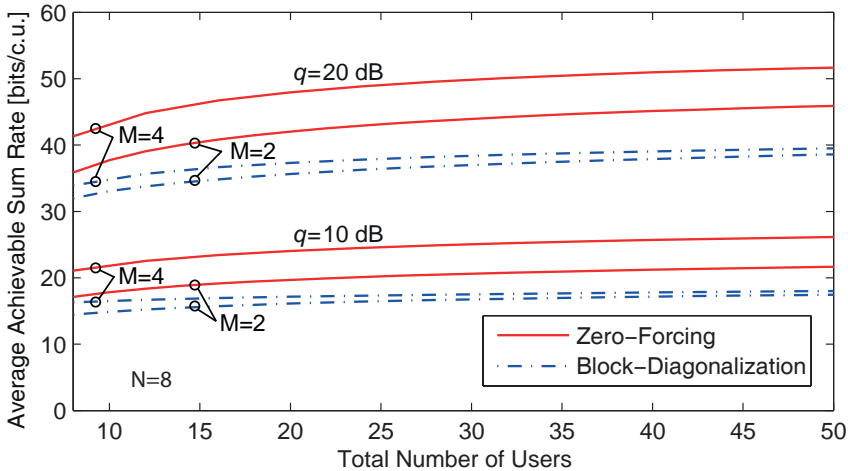


Figure 4.4: The average achievable sum rate with BD and ZFC under imperfect CSI estimation and using a (modified) low-complexity user selection algorithm from [SCA<sup>+</sup>06].

This corollary says that the training power should increase linearly with the transmit power to achieve the optimal sum rate scaling. This is for example satisfied by setting the total training power to  $\varrho = q$  under ZFC and  $\varrho = Mq$  under BD, which corresponds to the reasonable assumption of having the same average SNR in the downlink and in the uplink.<sup>7</sup> The demands for higher CSI accuracy with increasing SNR is therefore automatically fulfilled by the reduced estimation errors. Observe that one uplink channel use is consumed per user antenna dimension that is estimated, thus creating a practical bound on how many user channels that can be estimated in block fading systems [CJKR10]. As ZFC only has one effective antenna per user, it can accommodate  $M$  times more users than BD on the same estimation overhead.

#### 4.2.4 Numerical Examples under Imperfect CSI

First, we compare BD and ZFC by repeating the simulation in Figure 4.3 for the case of imperfect CSI estimation. The approximate BD and ZFC precoding are implemented as described earlier in this chapter. We use a training power of  $q$  per channel dimension and the capacity-based schedul-

<sup>7</sup>Battery-powered user devices might operate at lower power than the base station, but Corollary 4.2 is satisfied as long as  $q$  and  $\varrho$  exhibit the same scaling. In practical scenarios, the path loss is the main source of SNR variations and affects the downlink and uplink equally.

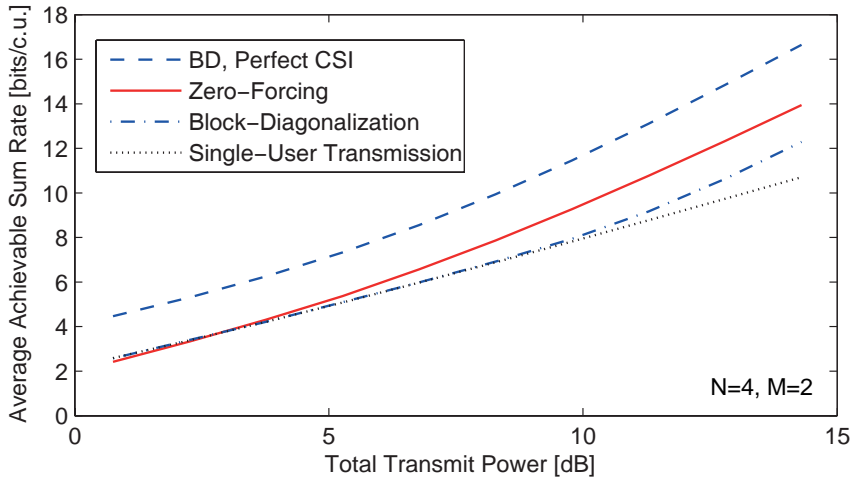


Figure 4.5: The average achievable sum rate with BD and ZFC under quantized CSI and using a (modified) low-complexity user selection algorithm from [SCA<sup>+</sup>06]. The number of feedback bits is scaled with the transmit power according to Corollary 4.1.

ing algorithm in [SCA<sup>+</sup>06] is modified<sup>8</sup> to include the average interference due to CSI estimation errors. The average achievable sum rate is shown in Figure 4.4 as a function of the number of users that we obtain CSI estimates for using ZFC (while BD only obtains channel estimates for  $1/M$  of them). We consider  $N = 8$  transmit antennas,  $M = 2$  or  $M = 4$  receive antennas, and a total transmit power of  $q = 10$  dB or  $q = 20$  dB. The performance loss compared with having perfect CSI is about 10%, but the conclusions are otherwise the same: ZFC outperforms BD both in terms of performance with few users and in exploiting multiuser diversity.

Next, we consider quantized CSI and let the number of feedback bits (per channel dimension) be scaled as  $(N - M) \log_2(q) - \text{constant}$ , where the constant is selected as in [RJ08a, Eq. (17)] to maintain a 3 dB gap between BD with perfect and quantized CSI. We consider  $N = 4$  transmit antennas,  $M = 2$  receive antennas, random vector quantization (RVQ), and modify<sup>9</sup> the capacity-based scheduling algorithm in [SCA<sup>+</sup>06] to include the average interference due to quantization. We compare BD precoding (having either quantized or perfect CSI) with quantized ZFC precoding

<sup>8</sup>Estimation errors contribute with an average interference of  $q(|S| - 1)/|S|\mathbf{E}_{\text{est}}$ , where  $\mathbf{E}_{\text{est}} = (\mathbf{R}_{R,k}^{-T} + \mathbf{P}_k^H \mathbf{P}_k / \sigma^2)^{-1}$  for BD and  $\mathbf{E}_{\text{est}} = (1/\mathbb{E}\{\|\mathbf{h}_k\|_2^2\} + q/\sigma^2)^{-1}$  for ZFC.

<sup>9</sup>Quantization errors contribute with an average interference of  $q(|S| - 1)/|S|\mathbf{E}_{\text{quant}}$ , where  $\mathbf{E}_{\text{quant}} = N/(M(N - M))D^{\text{BD}}\mathbf{R}_{R,k}$  for BD and  $\mathbf{E}_{\text{quant}} = D^{\text{QBC}}G/(N - 1)$  for ZFC. In these formulas, BD uses  $M$  times more feedback bits per user than ZFC.

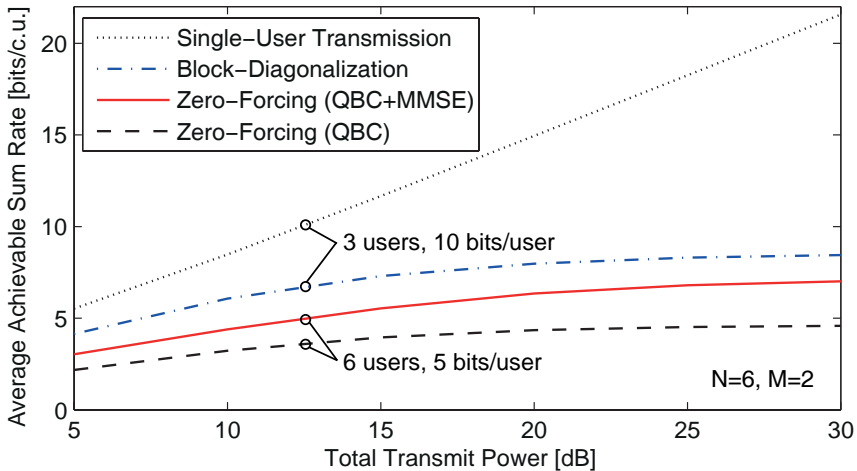


Figure 4.6: Comparison of single-user transmission, BD, and different forms of ZFC under quantized CSI feedback. The scenario is the same as in [RJ08a, Fig. 6], where the superior single-user strategy was not included.

based on MESC-MMSE [TBH08] and with single-user SVD-based transmission (to a randomly selected user). The quantized effective channels are obtained from 8 users under ZFC, while the quantized complete channels are acquired from 4 users under BD. The average achievable sum rate is shown in Figure 4.5 as a function of the transmit power  $q$ . At low SNR, quantized BD precoding only selects one user and performs similarly to single-user transmission. As two data streams are transmitted to the selected user, both strategies are slightly better than ZFC in this regime. But quantized ZFC precoding quickly improves with  $q$  and becomes the method of choice at practical SNRs. The simulation was stopped at  $q = 14.3$  dB where BD requires feedback of 22 bits per user, meaning that the best codeword should be selected in a codebook with over a million entries.<sup>10</sup> BD is therefore suboptimal both in terms of sum rate and computational complexity.

This conclusion stands in contrast to the numerical results in [RJ08a], where BD clearly beats ZFC under quantized CSI. To explain the difference, we repeat the simulation in [RJ08a, Fig. 6] with  $N = 6$  transmit antennas and  $M = 2$  receive antennas. In this simulation, the quantization codebooks contain 10 bits/user under BD and 5 bits/user under ZFC. The achievable sum rate is shown in Figure 4.6 for the quantized BD approach

<sup>10</sup>An approach to emulate the quantization procedure for very large random codebooks was proposed in [RJ08a], but this will not change the fact that the quantization complexity becomes infeasible much faster under BD precoding than under ZFC.

in [RJ08a] and the ZF-QBC approach in [Jin08]. We have also included: 1) an improved version of ZF-QBC where the MMSE combiner in (4.13) is applied during transmission; and 2) single-user SVD-based transmission to a randomly selected user. Our simulation confirms that BD is better than ZFC in this scenario, but the difference becomes much smaller when the MMSE combiner is applied. However, none of these strategies should be used in this scenario since single-user transmission is vastly superior.

To summarize, ZFC achieves better performance than BD if the CSI accuracy is sufficient to support multiuser transmission. If the transmitting base station has inaccurate CSI (compared with the transmit power), single-user transmission should be used instead of BD and ZFC.

### 4.2.5 Conclusion: Receive Combining vs. Multistream Multiplexing

There are two modes in multiuser MIMO systems: single-user and multi-user transmission. When the base station has relatively accurate CSI, multi-user transmission is beneficial as it can achieve the full multiplexing gain. In this scenario, we have analyzed whether the receive antennas at each user should be combined for achieving receive diversity (as with ZFC) or for multistream multiplexing (as with BD). The unexpected conclusion is that receive combining is the favorable choice, since ZFC is better at exploiting spatial correlation and multiuser diversity than BD. This result has positive implications for the design of multiuser systems as it reduces the hardware constraints, especially in terms of processing at the user devices and the required CSI accuracy per user. When only inaccurate CSI can be achieved, the performance is limited by co-user interference making single-user transmission advantageous over multi-user transmission strategies such as BD and ZFC. In this regime, BD is certainly better than ZFC since it creates less co-user interference, but this observation has no further implications since single-user transmission is the method of choice.

## 4.3 $\epsilon$ -Outage Sum Rate and Feedback Design

The analysis so far in this chapter has considered the (average) achievable sum rate, which provides an achievable upper bound on the information throughput with a given precoding strategy. To achieve this throughput with zero probability of error, the transmitting base station needs to know the highest achievable rate of each user and apply channel coding over a block-length of data that grows without bound [CT91]. This is not feasible under the system operation of this thesis (see Chapter 2.2), where the resource allocation is updated rapidly (at least once per the coherence time of the channel) to exploit multiuser diversity and achieve small delays. In

addition, each user only knows its own channel, while the base station has imperfect CSI of the user channels. If the precoding and user selection cannot be based on perfect CSI, it is unreasonable that the base station can select optimal data rates that are only computable using perfect CSI. In principle, the achievable rate can be estimated at each user during data reception and then fed back to the base station, but this is not possible in the considered system operation. Instead, the supported data rates in a block fading system need to be estimated at the base station under CSI uncertainty, leading to a probability of outage due to overestimation.

The maximum coding rate at a given outage probability and block-length is still an open research problem, although recent work provides close approximations [PPV10]. For simplicity, we assume that the coherence time of the channel is sufficient to neglect the effect of having an insufficient coding block-length. Instead, we concentrate on the effect of imperfect rate adaptation. Based on the analysis in Section 4.2, we let the effective channel of user  $k$  be  $\mathbf{h}_k \in \mathbb{C}^{N \times 1}$ . To enable analysis, we model it as Rayleigh fading with  $\mathbf{h}_k \in \mathcal{CN}(\mathbf{0}, \mathbf{R}_{T,k})$ , where the transmit-side correlation  $\mathbf{R}_{T,k}$  might have a different scaling than it had for the original channel (as an effect of receive combining). If  $M > 1$ , the analysis basically considers a lower bound on the performance (corresponding to a fixed suboptimal receive combining that only exploits statistical CSI and thereby maintains the Rayleigh fading distribution), which is fine since we will only consider the achievability of the different asymptotic properties.

If  $\mathcal{S}$  is the set of scheduled users, then the instantaneous SINR of user  $k \in \mathcal{S}$  becomes

$$\text{SINR}_k = \frac{|\mathbf{h}_k^H \mathbf{v}_k|^2}{1 + \sum_{\bar{k} \in \mathcal{S} \setminus \{k\}} |\mathbf{h}_k^H \mathbf{v}_{\bar{k}}|^2} \quad (4.34)$$

where  $\mathbf{v}_k \in \mathbb{C}^{N \times 1}$  denotes some precoding vector. Let  $F_{\text{SINR}_k}(\cdot)$  be the CDF of  $\text{SINR}_k$ , based on the CSI available at the base station. Then, having an acceptable outage probability of  $\epsilon > 0$  means that

$$\Pr\{\log_2(1 + \text{SINR}_k) < R_{k,\text{out}}\} = F_{\text{SINR}_k}(2^{R_{k,\text{out}}} - 1) = \epsilon. \quad (4.35)$$

To satisfy this probability, we thus transmit at the  $\epsilon$ -outage rate  $R_{k,\text{out}} = \log_2(1 + F_{\text{SINR}_k}^{-1}(\epsilon))$  to user  $k \in \mathcal{S}$ . The  $\epsilon$ -outage sum rate is

$$R_{\text{sum}}(q, \epsilon) = \sum_{k \in \mathcal{S}} R_{k,\text{out}} = \sum_{k \in \mathcal{S}} \log_2(1 + F_{\text{SINR}_k}^{-1}(\epsilon)). \quad (4.36)$$

Data sent in outage is not lost, but can be handled by an HARQ protocol at the expense of some additional transmission delay. To achieve a good tradeoff between high throughput and short delays, [WJ09b] shows that a good value on the outage probability is  $\epsilon = 0.1$ .

### 4.3.1 Tradeoff between CDI and CQI feedback

In a limited feedback system, the  $\epsilon$ -outage sum rate depends on the feedback accuracy. This raises the question of how the  $B$  feedback bits that are available per user should be split between CDI and CQI. While CDI provides good beamforming directions, CQI shows which users that have strong channels. Both quantities impact the transmitter's ability to estimate the instantaneous SINR. Next, we will analyze this tradeoff in the high SNR regime, where the multiplexing gain of the  $\epsilon$ -outage sum rate is defined as

$$\lim_{q \rightarrow \infty} \frac{R_{\text{sum}}(q, \epsilon)}{\log_2(q)} = \mathcal{M}_\infty. \quad (4.37)$$

To achieve the full multiplexing gain of  $N$ , each interference term  $\sum_{\bar{k} \in \mathcal{S} \setminus \{k\}} |\mathbf{h}_k^H \mathbf{v}_{\bar{k}}|^2$  in (4.34) needs to be bounded by a constant as  $q \rightarrow \infty$ .

As proved in Corollary 4.1 (and in [Jin06] for uncorrelated channels), the achievable sum rate achieves the full multiplexing gain if ZF precoding is applied under sufficiently accurate CDI (and without any CQI feedback). The following theorem provides a similar result for the  $\epsilon$ -outage sum rate:

*Theorem 4.7.* For any selection of  $N$  users, let the channel directions  $\bar{\mathbf{h}}_k = \frac{\mathbf{h}_k}{\|\mathbf{h}_k\|_2}$  be known to the transmitter while the channels gains  $\|\mathbf{h}_k\|_2^2$  are unknown. With probability one, ZF precoding makes the  $\epsilon$ -outage sum rate achieve the full multiplexing gain of  $N$ .

*Proof.* The proof is given in Appendix 4.A.8. □

Based on this theorem, one might believe that CDI feedback is of dominating importance in multiuser MIMO systems. But apart from the multiplexing gain, the high SNR performance is also characterized by the constant rate offset. This parameter depends on CQI feedback and might have great impact at practical SNRs. In addition, Theorem 4.7 is not saying whether the full multiplexing gain is achievable under other conditions, for instance, using only CQI feedback. Remarkably, it can be achieved if a set of random beamforming directions are used and the number of users is large [SH05], such that each random beamformer closely models the channel of some user. The long-term average sum rate was considered in [SH05], based on feedback of the index of the best beamforming vector and the corresponding channel quality. The next theorem shows a similar result for the  $\epsilon$ -outage sum rate using only CQI feedback and beamforming based on the dominating eigenvector  $\mathbf{u}_k$  of each  $\mathbf{R}_{T,k}$ .

*Theorem 4.8.* Assume that the transmitter knows the quality indicator

$$\gamma_k = \frac{q |\mathbf{h}_k^H \mathbf{u}_k|^2}{1 + q (\|\mathbf{h}_k\|_2^2 - |\mathbf{h}_k^H \mathbf{u}_k|^2)} \quad (4.38)$$

for all  $k = 1, \dots, K_r$ , while the channel directions  $\frac{\mathbf{h}_k}{\|\mathbf{h}_k\|_2}$  are unknown. If all  $\mathbf{R}_{T,k}$  have the same distinct dominating eigenvalue  $\lambda_N > 0$  but different eigenvectors<sup>11</sup>, then precoding exploiting only statistics can (with probability one) make the  $\epsilon$ -outage sum rate achieve the full multiplexing gain of  $N$  if  $K_r \rightarrow \infty$  such that  $\frac{q}{\log(K_r)} \rightarrow c < \infty$ .

*Proof.* The proof is given in Appendix 4.A.9. □

Some scepticism is in order when interpreting Theorem 4.8; the number of users should scale exponentially fast to find users that are sufficiently aligned with their dominating eigendirection (i.e.,  $\frac{\mathbf{h}_k}{\|\mathbf{h}_k\|_2} \approx \mathbf{u}_k$ ) to achieve the full multiplexing gain. Then, a multiuser diversity gain also appears since the strongest channel gain approaches infinity [SH05], which violates the law of energy conservation (i.e., more power cannot be received than was transmitted) and basically is a modeling artifact of Rayleigh fading channels [DHL<sup>+</sup>11, GK11]. To the best of our knowledge, the scaling of the strongest channel gain in a set of randomly located users has not been investigated by measurements. However, it is reasonable to believe that increasing the number of users can suppress interference by making the selected user channels near-orthogonal.<sup>12</sup>

Despite these observations, the performance under pure CQI feedback might be good at practical SNRs and number of users. When quantization is considered, one should keep in mind that the one-dimensional CQI is easier to quantize accurately than the  $(N - 1)$ -dimensional CDI.

Other important factors are spatial correlation and the number of receive antennas; the channel direction is more or less given by the covariance matrix in strongly correlated environments, while receive antennas can create effective MISO channels with predefined properties. The next theorem shows that the full multiplexing gain can be achieved without any feedback if the correlation is strong or  $M$  is sufficiently large.

*Theorem 4.9.* Assume that the transmitter only has statistical CSI and has selected  $|\mathcal{S}| = N$  users such that  $\mathbf{R}_{T,k}$  have different dominating eigenvectors  $\mathbf{u}_k$  for each  $k \in \mathcal{S}$ . In addition, let each user have  $M \leq N$  uncorrelated receive antennas.

If  $\lambda_{k,N} > \lambda_{k,N-1} \geq \dots \geq \lambda_{k,1}$  denotes the eigenvalues of  $\mathbf{R}_{T,k}$ , then precoding that only exploits statistics can achieve the full multiplexing gain of  $N$  if  $\frac{\lambda_{k,N}}{\lambda_{k,N-M}} \rightarrow \infty$  such that  $\frac{q}{\lambda_{k,N}/\lambda_{k,N-M}} \rightarrow c_k < \infty$  for all  $k \in \mathcal{S}$ .

*Proof.* The proof is given in Appendix 4.A.10. □

<sup>11</sup>This is satisfied by the exponential model in [Loy01] with equal antenna correlation and random user directions [BHO09], but is merely assumed to simplify the derivation.

<sup>12</sup>In multicell systems, increasing the number of users also enhances the probability of finding users where the intercell interference is carried by weak channel realizations.

If  $M = 1$ , this theorem says that statistical precoding will satisfy the full multiplexing gain if the spatial correlation is sufficiently strong. This effect can be amplified by employing multiple antennas at each user and use these to cancel out certain eigendirections. In the special case of  $M = N$ , we let  $\lambda_{k,0} = 0$  for notational convenience. The condition  $\frac{\lambda_{k,N}}{\lambda_{k,N-M}} \rightarrow \infty$  is therefore always satisfied, meaning that the full multiplexing gain can be achieved without any constraints on the spatial correlation. This is quite expected, given that single-user transmission can achieve the full multiplexing gain without having instantaneous CSI when  $M = N$  [GKH<sup>+</sup>07].

The bottom line of this section is that asymptotic analysis can provide very diverse answers to feedback design questions in multiuser MIMO systems. The actual performance depends on the relationship between transmission strategy, SNR, number of users, number of receive antennas, spatial correlation, and feedback design. This dependence will be evaluated numerically in the next section.

## 4.4 Low-Complexity Feedback Quantization

Next, we evaluate the performance of two practical precoding strategies that try to maximize the  $\epsilon$ -outage sum rate under quantized CSI feedback. The first scheme builds upon the *maximum estimated SINR combiner (MESOC)* strategy of [TBH08] and is expected to work well in spatially uncorrelated systems. The second scheme is an extension of the *norm-supported minimum-variance distortionless response (NS-MVDR)* strategy of [HBO08a,HBO08b] that only needs CQI feedback as it exploits the CDI provided by the channel statistics in spatially correlated systems. By comparing these strategies using low-complexity quantization codebooks, the tradeoff between CDI and CQI feedback will be studied numerically.

### 4.4.1 Scheme 1: Maximum Estimated SINR Combiner (MESOC) Strategy

The MESOC strategy of [TBH08] is basically an adaptation of ZFC precoding for the case of quantized CSI. We will outline this technique, including its main feature of joint selection of receive combining and CDI codewords. Based on the system model, users cannot predict the co-user interference at the point of feedback. Therefore, the quantization in MESOC is based on an (approximative) lower bound on the SINR:

$$\text{SINR}_k \gtrsim |\mathbf{u}_k^H \mathbf{v}_k|^2 \underbrace{\frac{\frac{q}{N} |\mathbf{r}_k^H \mathbf{H}_k \mathbf{u}_k|^2}{1 + \frac{q}{N} \|\mathbf{r}_k^H \mathbf{H}_k - (\mathbf{r}_k^H \mathbf{H}_k \mathbf{u}_k) \mathbf{u}_k^H\|_2^2}}_{\gamma_k^{\text{bound}}} \quad (4.39)$$

where  $\mathbf{v}_k$  is the unit-norm precoding vector used for transmission and  $\mathbf{u}_k \in \mathcal{C}_k$  is a quantization of effective channel direction  $\mathbf{H}_k^H \mathbf{r}_k / \|\mathbf{H}_k^H \mathbf{r}_k\|_2$ . The approximate SINR expression is achieved by assuming equal power allocation, a scheduling set  $\mathcal{S}$  with  $|\mathcal{S}| = N$ , and that interference is equally spread in the space orthogonal to  $\mathbf{u}_k$  [YJG07, TBT07].

The SINR approximation in (4.39) consists of two parts. The first term,  $|\mathbf{u}_k^H \mathbf{v}_k|^2$ , is the signal loss due to the precoding strategy (i.e., the price of avoiding interference with ZFC) and cannot be optimized at the user as the co-user interference is unknown at this point. The second part,  $\gamma_k^{\text{bound}}$ , can however be maximized by joint selection of  $\mathbf{r}_k$  and the codeword  $\mathbf{u}_k$ :

$$(\mathbf{r}_k^{\text{MESC}}, \mathbf{u}_k) = \arg \max_{\substack{\mathbf{r}: \|\mathbf{r}\|_2=1 \\ \mathbf{u} \in \mathcal{C}_k}} \frac{\mathbf{r}^H (\frac{q}{N} \mathbf{H}_k \mathbf{u} \mathbf{u}^H \mathbf{H}_k^H) \mathbf{r}}{1 + \mathbf{r}^H (\frac{q}{N} \mathbf{H}_k (\mathbf{I}_N - \mathbf{u} \mathbf{u}^H) \mathbf{H}_k^H) \mathbf{r}}. \quad (4.40)$$

For every codeword, the optimal receive combining can be achieved in closed form by solving (4.40) as a generalized eigenvalue problem [TBH08]. Thus, the joint selection in (4.40) can be performed by finding the best receive combiner for every codeword and check which combination that gives the largest approximate SINR.

In the MESC strategy, each user feeds back the CDI codeword  $\mathbf{u}_k$  from (4.40) along with CQI feedback of the corresponding value of  $\gamma_k^{\text{bound}}$ . The base station uses some greedy scheduling algorithm to select the user set  $\mathcal{S}$  to maximize the approximate sum rate

$$\sum_{k \in \mathcal{S}} \log_2(1 + |\mathbf{u}_k^H \bar{\mathbf{v}}_k^{\text{ZFC}}|^2 \bar{\gamma}_k^{\text{bound}}), \quad (4.41)$$

where  $\bar{\gamma}_k^{\text{bound}}$  is the quantization of  $\gamma_k^{\text{bound}}$  and  $\bar{\mathbf{v}}_k^{\text{ZFC}}$  is the approximate ZFC vector achieved by treating  $\{\mathbf{u}_k\}_{k \in \mathcal{S}}$  as the true channels.

Finally, the base station selects a transmission rate based on the pessimistic SINR estimate

$$\widehat{\text{SINR}}_k = \zeta_k |\mathbf{u}_k^H \bar{\mathbf{v}}_k^{\text{ZFC}}|^2 \bar{\gamma}_k^{\text{bound}} \quad (4.42)$$

where  $\zeta_k$  is a fade-margin (or back-off factor) selected numerically to make  $\Pr\{\log_2(1 + \text{SINR}_k) < \log_2(1 + \widehat{\text{SINR}}_k)\} = \epsilon$  [HBO08a]. At the point of reception, each selected user replaces its preliminary receive combiner from (4.40) with the MMSE combiner in (4.13).

#### 4.4.2 Scheme 2: Norm-Supported Minimum-Variance Distortionless Response (NS-MVDR) Strategy

In spatially correlated environments, the long-term statistics provide directional channel information. If the statistics are combined with CQI

feedback of the instantaneous channel norm  $\|\mathbf{h}_k\|_2^2$ , this information is sufficient to perform efficient user selection and precoding (without any instantaneous CDI feedback) [HBO08b]. A particular feature of this approach is its ability to estimate the instantaneous SINR for any set of precoding vectors, which enables efficient rate adaptation [HBO08a]. This stands in contrast to the CQI feedback in MESC and similar strategies [TBT07, KdFG<sup>+</sup>07, YJG07, dFS08], which try to predict the SINRs at each user (although users are uninformed about co-user locations).

Prior works on the NS-MVDR strategy have thoroughly analyzed both user selection and precoding design, but assumed perfect/unquantized CQI feedback and single-antenna users [HBO08a, HBO08b]. In this section, we show how efficient receive combining can be achieved while maintaining the nice statistical structure and how to improve the SINR estimation.

### Receive Combining and Quantization

As discussed in Section 4.2, each user can apply a preliminary receive combiner that simplifies the precoding design and replace it with the MMSE combiner in (4.13) during reception. Since only CQI is fed back (i.e.,  $B_q = B$ ), the preliminary receive combiner  $\mathbf{r}_k^{\text{prel}}$  should be designed such that the statistics of the effective channel  $\mathbf{h}_k = \mathbf{H}_k^H \mathbf{r}_k^{\text{prel}}$  are deterministic at both the user and the base station. At first sight, this seems to require that  $\mathbf{r}_k^{\text{prel}}$  is independent of the current channel realization  $\mathbf{H}_k$ , but we can actually do better than that.

For ease of exposition, we drop the user indices and assume a Kronecker-structured system with uncorrelated receive antennas (i.e.,  $\mathbf{R}_R = \mathbf{I}_M$ ). Let the eigen decomposition (with  $\lambda_N \geq \dots \geq \lambda_1$ ) of the transmit-side correlation matrix be partitioned as

$$\begin{aligned} \mathbf{R}_T &= \mathbf{U} \mathbf{\Lambda} \mathbf{U}^H \\ &= [\mathbf{u}^{(D)} \mathbf{U}^{(I)} \mathbf{U}^{(0)}] \text{diag}(\lambda_N, \dots, \lambda_1) [\mathbf{u}^{(D)} \mathbf{U}^{(I)} \mathbf{U}^{(0)}]^H \end{aligned} \quad (4.43)$$

where  $\mathbf{u}^{(D)} \in \mathbb{C}^{N \times 1}$  is the *dominating* eigenvector and is suitable for transmission. Similarly,  $\mathbf{U}^{(I)} \in \mathbb{C}^{N \times M-1}$  spans the subspace associated with the  $M - 1$  following eigenvalues. The user will be sensitive to *interference* in this subspace. Finally,  $\mathbf{U}^{(0)} \in \mathbb{C}^{N \times N-M}$  spans the subspace of the remaining eigendirections. Under high spatial correlation (and  $M > 1$ ), these eigenvalues are close to *zero*, meaning that the interference from these eigendirections is small. In other words, the main interference is expected from  $\mathbf{U}^{(I)}$ . We therefore select  $\mathbf{r}^{\text{prel}}$  to completely cancel out the interference in these directions:

$$\mathbf{r}^{\text{prel}} = \text{null}((\mathbf{H}\mathbf{U}^{(I)})^H) \quad (4.44)$$

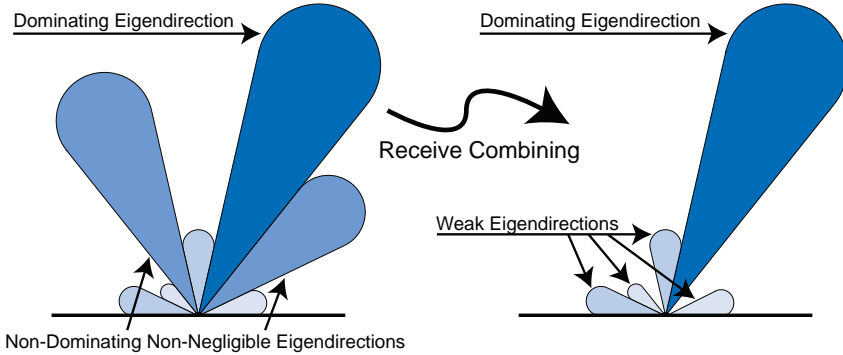


Figure 4.7: Illustration of the average transmit power carried by different eigendirections. Each beam represents an eigendirection and its size describes the corresponding eigenvalue. The eigenvalue spread is large in highly correlated scenarios. The proposed receive combining cancels out the strongest non-dominating eigendirections, which leaves one strong eigenvalue and a few very small ones. This essentially makes the effective channel aligned with the dominating eigendirection, which is already known to the transmitter.

where  $\text{null}(\cdot)$  gives an orthonormal basis to the right null space. Although this receive combining exploits instantaneous CSI to cancel out certain eigendirections, the base station knows that the effective channel  $\mathbf{h} = \mathbf{H}^H \mathbf{r}$  will be Rayleigh fading with covariance matrix

$$\tilde{\mathbf{R}}_T = \mathbf{U} \text{diag}(\lambda_N, 0, \dots, 0, \lambda_{N-M}, \dots, \lambda_1) \mathbf{U}^H. \quad (4.45)$$

In other words, the base station does not need to know *how* the eigendirections of  $\mathbf{U}^{(T)}$  were nulled, but only that the corresponding eigenvalues will be zero. If  $M$  is sufficiently large (compared with the spatial correlation), this receive combining transforms the MIMO channel into a Rayleigh fading MISO channel with a covariance matrix that essentially has rank one and is aligned with  $\mathbf{u}^{(D)}$ . Thus, accurate instantaneous CDI is achieved without explicit CDI feedback. This is illustrated in Figure 4.7.

### Estimation of the SINR

Efficient user selection and precoding can be achieved by combining the quantized norm feedback with the statistics of the effective channels. A greedy user-selection algorithm and precoding based on the MVDR crite-

tion<sup>13</sup> was proposed in [HBO08b]. In this section, we simply assume that the user selection  $\mathcal{S}$  and the precoding vectors  $\mathbf{v}_k \forall k \in \mathcal{S}$  are given.

If the CQI feedback says that  $a \leq \|\mathbf{h}_k\|_2^2 < b$  for some quantization boundaries  $a$  and  $b$ , we estimate the SINR pessimistically as<sup>14</sup>

$$\widehat{\text{SINR}}_k = \max \left( 0, \frac{\mathbb{E}\{\|\mathbf{B}_{1,k}\mathbf{h}_k\|_2^2|a, b\} - \zeta \sqrt{\text{MSE}\{\|\mathbf{B}_{1,k}\mathbf{h}_k\|_2^2|a, b\}}}{\mathbb{E}\{\|\mathbf{B}_{2,k}\mathbf{h}_k\|_2^2|a, b\} + \zeta \sqrt{\text{MSE}\{\|\mathbf{B}_{2,k}\mathbf{h}_k\|_2^2|a, b\}} + 1} \right) \quad (4.46)$$

where  $\mathbf{B}_{1,k} = \mathbf{v}_k^H$  is the precoding vector to user  $k$  and  $\mathbf{B}_{2,k} = [\mathbf{v}_{\tilde{\mathcal{S}}(1)} \dots \mathbf{v}_{\tilde{\mathcal{S}}(|\tilde{\mathcal{S}}|)}]^H$  contains the precoding vectors to the co-users in  $\tilde{\mathcal{S}} = \mathcal{S} \setminus \{k\}$ . The back-off parameter  $\zeta$  is selected numerically (and adaptively) to satisfy a given outage probability [HBO08a]. To calculate the estimates  $\mathbb{E}\{\|\mathbf{B}\mathbf{h}_k\|_2^2|a, b\}$  and the corresponding  $\text{MSE}\{\|\mathbf{B}\mathbf{h}_k\|_2^2|a, b\} = \mathbb{E}\{\|\mathbf{B}\mathbf{h}_k\|_2^4|a, b\} - \mathbb{E}\{\|\mathbf{B}\mathbf{h}_k\|_2^2|a, b\}^2$ , we first need the following theorem.

*Theorem 4.10.* Let  $\mathbf{v} = [v_1, \dots, v_N]^T \in \mathcal{CN}(\mathbf{0}, \text{diag}(\mu_1, \dots, \mu_N))$ , where the eigenvalues  $\mu_i$  are distinct and strictly positive. If it is known that  $a \leq \|\mathbf{h}\|_2^2 < b$ , the  $p$ th order conditional moment of  $|v_i|^2$  and  $(p_i, p_j)$ th order conditional cross-moment between  $|v_i|^2$  and  $|v_j|^2$  ( $i \neq j$ ) are

$$\begin{aligned} \mathbb{E}\{|v_i|^{2p}|a, b\} &= \frac{1}{C_{\text{prob}}} \sum_{\substack{k=1 \\ k \neq i}}^N \frac{G_{p,0,i,k}^{(1)}(a, b)}{\mu_k \prod_{l \notin \{i,k\}} (1 - \frac{\mu_l}{\mu_k})}, \\ \mathbb{E}\{|v_i|^{2p_i}|v_j|^{2p_j}|a, b\} &= \frac{1}{C_{\text{prob}}} \begin{cases} \sum_{k=1}^N \frac{G_{p_i,p_j,i,j,k}^{(2)}(a, b)}{\mu_k \prod_{l \notin \{i,j,k\}} (1 - \frac{\mu_l}{\mu_k})}, & N > 2, \\ (-1)^{p_j} G_{p_i,p_j,i,j}^{(1)}(a, b), & N = 2, \end{cases} \end{aligned} \quad (4.47)$$

where  $C_{\text{prob}} = \sum_{k=1}^N (e^{-\frac{a}{\mu_k}} - e^{-\frac{b}{\mu_k}}) / (\prod_{i \neq k} (1 - \frac{\mu_i}{\mu_k}))$  and we have

$$\begin{aligned} G_{N,M,i,j}^{(1)}(a, b) &= \sum_{k=0}^M \binom{M}{k} \frac{(N+k)! (-1)^{M-k}}{(\frac{1}{\mu_i} - \frac{1}{\mu_j})^{N+k+1}} \\ &\quad \times \left( G_{M-k,j}^{(3)}(a, b) - \sum_{m=0}^{N+k} \frac{G_{M+m-k,i}^{(3)}(a, b)}{m! (\frac{1}{\mu_i} - \frac{1}{\mu_j})^{-m}} \right), \end{aligned} \quad (4.48)$$

<sup>13</sup>MVDR is a classic criterion where the beamforming direction is selected to minimize the expected received interference subject to a fixed received signal power. Only the expected signal power along the dominating eigendirection is counted in the NS-MVDR approach of [HBO08b].

<sup>14</sup>A similar estimator was used in [HBO08b, HBO08a], but these papers estimate each interference term separately which increases the estimation error.

$$G_{N,M,i,j,m}^{(2)}(a,b) = M! \left( \frac{G_{N,0,i,m}^{(1)}(a,b)}{\left(\frac{1}{\mu_j} - \frac{1}{\mu_m}\right)^{M+1}} - \sum_{l=0}^M \frac{G_{N,l,i,j}^{(1)}(a,b)}{(-1)^l l! \left(\frac{1}{\mu_j} - \frac{1}{\mu_m}\right)^{M-l+1}} \right), \quad (4.49)$$

$$G_{N,i}^{(3)}(a,b) = \frac{N!}{\left(\frac{1}{\mu_i}\right)^{N+1}} \sum_{m=0}^N \frac{\left(\frac{a}{\mu_i}\right)^m e^{-\frac{a}{\mu_i}} - \left(\frac{b}{\mu_i}\right)^m e^{-\frac{b}{\mu_i}}}{m!}. \quad (4.50)$$

*Proof.* The proof is given in Appendix 4.A.11.  $\square$

Observe that this theorem considers quantized norm feedback, while the case of perfect feedback was considered in [HBO08a]. Theorem 4.10 is limited to channel covariance matrices where all eigenvalues are distinct. Eigenvalues that are measured in practice are naturally distinct, but clustering of those that are close-to-identical may be necessary to achieve numerical stability. The general case with multiple sets of repeated eigenvalues is not included in the thesis for brevity, but is available in [BHO09]. This extension builds upon results in [Sch88, AM97].

Using Theorem 4.10, the following corollary shows how to calculate  $\mathbb{E}\{\|\mathbf{B}\mathbf{h}\|_2^2|a,b\}$  and  $\mathbb{E}\{\|\mathbf{B}\mathbf{h}\|_2^4|a,b\}$  in the SINR expression of (4.46). The special case of  $N_B = 1$  was given in [HBO08a] (for exact norm feedback).

*Corollary 4.3.* Let  $\mathbf{h} \in \mathcal{CN}(\mathbf{0}, \mathbf{R})$ , where  $\mathbf{R} = \mathbf{U}\mathbf{\Lambda}\mathbf{U}^H$  is the eigen decomposition of the covariance matrix with  $\mathbf{\Lambda} = \text{diag}(\lambda_1, \dots, \lambda_N)$ . For any fixed  $\mathbf{B} \in \mathbb{C}^{N_B \times N}$ , we have

$$\begin{aligned} \mathbb{E}\{\|\mathbf{B}\mathbf{h}\|_2^2|a,b\} &= \mathbf{1}^T \mathbf{A}_{|\cdot|^2} \widehat{\mathbf{\Lambda}} \mathbf{1}, \\ \mathbb{E}\{\|\mathbf{B}\mathbf{h}\|_2^4|a,b\} &= \frac{1}{2} \mathbf{p}^T \mathbf{T} \mathbf{p} + \frac{1}{2} \sum_{k_1=1}^{N_B} \sum_{k_2=1}^{N_B} \tilde{\mathbf{p}}_{k_1 k_2}^H \mathbf{T} \tilde{\mathbf{p}}_{k_1 k_2}, \end{aligned} \quad (4.51)$$

where  $\mathbf{A} = \mathbf{B}\mathbf{U}$ ,  $[\mathbf{A}_{|\cdot|^2}]_{ij} = |a_{ij}|^2$ ,  $\mathbf{1} = [1, \dots, 1]^T$ ,  $\mathbf{p} = \mathbf{A}_{|\cdot|^2}^T \mathbf{1}$ ,  $\tilde{\mathbf{p}}_{k_1 k_2} = [a_{k_1 1} a_{k_2 1}^*, \dots, a_{k_1 N} a_{k_2 N}^*]^T$ , and

$$\begin{aligned} [\widehat{\mathbf{\Lambda}}]_{ij} &= \begin{cases} \mathbb{E}\{|v_i|^2|a,b\}, & i=j, \\ 0, & i \neq j, \end{cases} \\ [\mathbf{T}]_{ij} &= \begin{cases} \mathbb{E}\{|v_i|^4|a,b\}, & i=j, \\ 2\mathbb{E}\{|v_i|^2|v_j|^2|a,b\}, & i \neq j. \end{cases} \end{aligned} \quad (4.52)$$

For all  $i$  with  $\lambda_i = 0$ ,  $\mathbb{E}\{|v_i|^2|a,b\} = \mathbb{E}\{|v_i|^4|a,b\} = \mathbb{E}\{|v_i|^2|v_j|^2|a,b\} = 0$ . The remaining conditional moments in (4.52) are achieved by Theorem 4.10 (by only considering non-zero eigenvalues).

*Proof.* The proof is given in Appendix 4.A.12.  $\square$

To summarize, the combination of norm feedback and long-term statistics enables estimation of the SINR for any set of precoding vectors. The estimation quality increases with the spatial correlation, and the proposed receive combining increases the effective correlation by nulling the  $M - 1$  strongest non-dominating eigendirections. During the transmission, the MMSE combiner in (4.13) will be used to enhance performance.

### 4.4.3 Numerical Evaluation

Next, we will evaluate the performance of the described low-complexity strategies: MESC and NS-MVDR. As an upper bound, we consider ZFC with perfect CSI (using MRC in the capacity-based suboptimal user selection algorithm of [SCA<sup>+</sup>06] and the MMSE combiner during transmission). We also consider the random beamforming strategy of [SH05] (with MMSE combining if  $M > 1$ ), which selects a set of  $N$  random beamforming directions and let each user feed back the preferred direction (using  $\log_2(N)$  bits) and the corresponding quantized SINR. This strategy is presumably good at exploiting multiuser diversity, but has rather mediocre performance at practical number of users [YG06, HBO08b, KGS08] and can thus be viewed as a lower bound on the performance.

A Grassmannian codebook<sup>15</sup>  $\mathcal{C}^{\text{grass}} = \{\mathbf{g}_1, \dots, \mathbf{g}_{2^{B_d}}\}$  is used for CDI feedback in the MESC strategy [LHS03, DHST08]. To account for spatial correlation, the codebook is rotated according to each user's channel statistics:  $\mathcal{C}_k^{\text{corr-grass}} = \{\mathbf{u}_{k,1}, \dots, \mathbf{u}_{k,2^{B_d}}\}$  with  $\mathbf{u}_{k,n} = \mathbf{R}_{T,k}^{1/2} \mathbf{g}_n / \|\mathbf{R}_{T,k}^{1/2} \mathbf{g}_n\|_2 \forall n$  [LH06]. All CQI codebooks are generated such that every codeword is equally probable to be fed back [BO08c, YRT09].

To concentrate on the tradeoff between CDI and CQI feedback, we consider a simple setup where the users are equally spaced on a circle around a base station with  $N = 4$  antennas. Hence, users have identical average SNRs, which becomes  $q \cdot \text{tr}(\mathbf{R}_{T,k})$  under single-user transmission. Based on [WJ09b], the outage probability is fixed at 10% (i.e.,  $\epsilon = 0.1$ ).

In Figure 4.8, we consider an uncorrelated scenario with a total transmit power of  $q = 15$  dB,  $M = 1$  antennas per user, and different numbers of feedback bits. The performance increases with the number of users, but the highest  $\epsilon$ -outage sum rate is always achieved with MESC by allocating 2 bits for CQI feedback and the remaining bits for CDI feedback. The MESC strategy provides much better performance than random beamforming, but the number of feedback bits is only sufficient to achieve half the optimal ZF performance. Random beamforming performs rather poorly, which indicates that the optimal asymptotic behavior proved in [SH05]

<sup>15</sup>The Grassmannian codebook maximizes the minimal angle between the codeword vectors  $\mathbf{g}_i$ . We generated the codebooks using the algorithm in [DHST08].

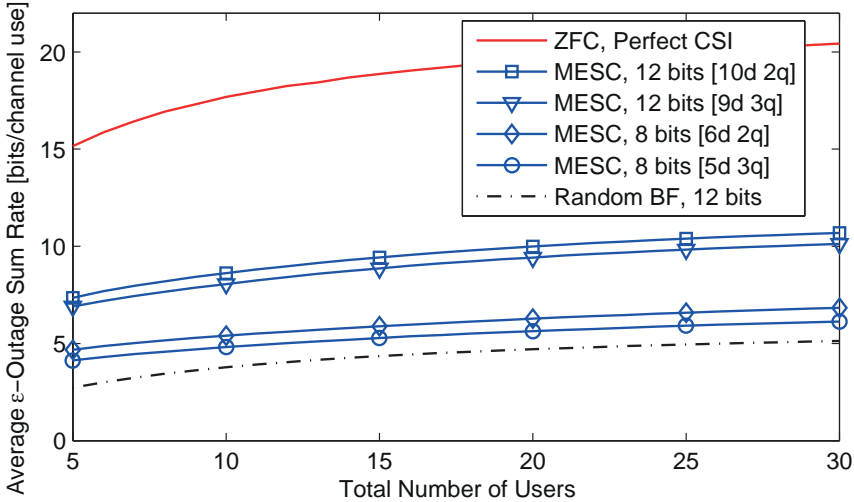


Figure 4.8: Average  $\epsilon$ -outage sum rate as a function of the number of users at a total transmit power of  $q = 15$  dB. Different transmission strategies and uses of feedback bits are compared.

(and similarly in Theorem 4.8) has little impact on the performance at practical  $K_r$ .

The same setup is considered in Figure 4.9, but the number of users is fixed at  $K_r = 15$  and the number of receive antennas  $M$  is varied. Apparently, there is a large gain of employing additional antennas for receive combining; adding an extra antenna per user increases the throughput with 50% without affecting the number of feedback bits. The gap towards perfect CSI continues to decrease rapidly with the number of antennas. CQI feedback also becomes increasingly important, explained by the improved CDI accuracy achieved through receive combining. In addition, MESC increases faster with the number of antennas than random beamforming. This indicates that the more accurate CSI we have, the more important it is to design beamforming directions based on it.

Next, we consider an outdoor scenario where the transmit-side correlation is generated using the local scattering model (see Chapter 2.1.3) with an UCA and half a wavelength antenna separation. The performance is shown in Figure 4.10 as a function of the angular spread (as seen from the base station)—small spread means high spatial correlation. The total transmit power is  $q = 15$  dB, there are  $K_r = 20$  users,  $M = 1$  antennas per user, and  $B = 8$  feedback bits are available per user. In highly correlated scenarios, we observe a higher importance of CQI feedback than in the uncorrelated case. This is mainly since the covariance matrix  $\mathbf{R}_{T,k}$

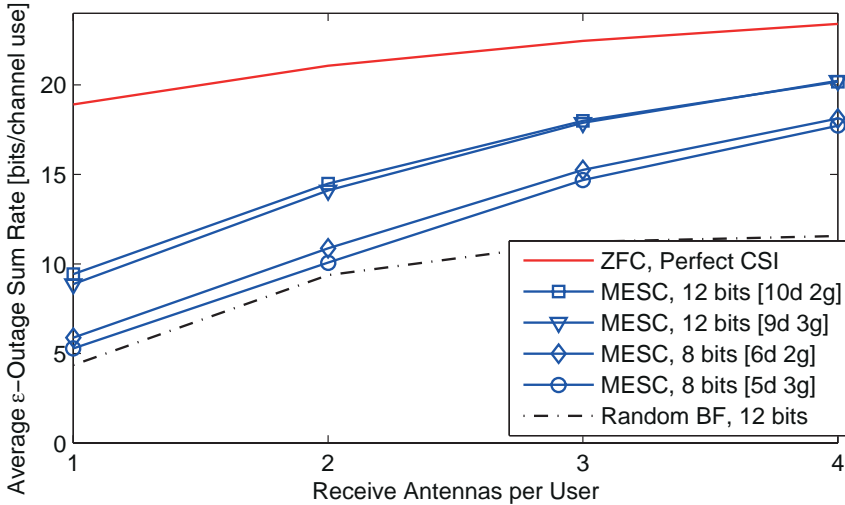


Figure 4.9: Average  $\epsilon$ -outage sum rate as a function of the number of antennas per user at a total transmit power of  $q = 15$  dB and  $K_r = 15$  users. Different transmission strategies are compared.

already provides much CDI [HBO08a]. NS-MVDR demonstrates that good performance is achievable in highly correlated systems using only CQI feedback. As the angular spread increases, additional CDI feedback is necessary to pertain high performance, which explains why the performance of NS-MVDR drops rather quickly. The different feedback divisions for MESC confirms that CQI is increasingly important under high correlation, but the differences are on the other hand quite small. Random beamforming ignores the correlation and is therefore almost unaffected by it.

As the NS-MVDR strategy only exploits CQI feedback, it can operate under very low feedback load per user.<sup>16</sup> This is illustrated in Figure 4.11 with a total transmit power of  $q = 15$  dB,  $K_r = 20$  users,  $M = 2$  antennas per user, and only  $B = 3$  feedback bits per user. In this scenario, NS-MVDR clearly outperforms MESC.

To summarize, recall from Section 4.3.1 that the full multiplexing gain can be achieved with only CDI feedback, only CQI feedback, or without any feedback (if the number of receive antennas or spatial correlation is large). The numerical evaluation shows that it is often sufficient to allocate 2 – 3 bits for CQI feedback while the remaining bits should be used for CDI feedback. The importance of CQI increases with the spatial correlation

<sup>16</sup>If the total number of feedback bits is fixed, there is a tradeoff between achieving accurate CSI from a few users and coarse CSI from many users (to exploit multiuser diversity) [RJ08b]. In the latter case, the number of bits per user can be very small.

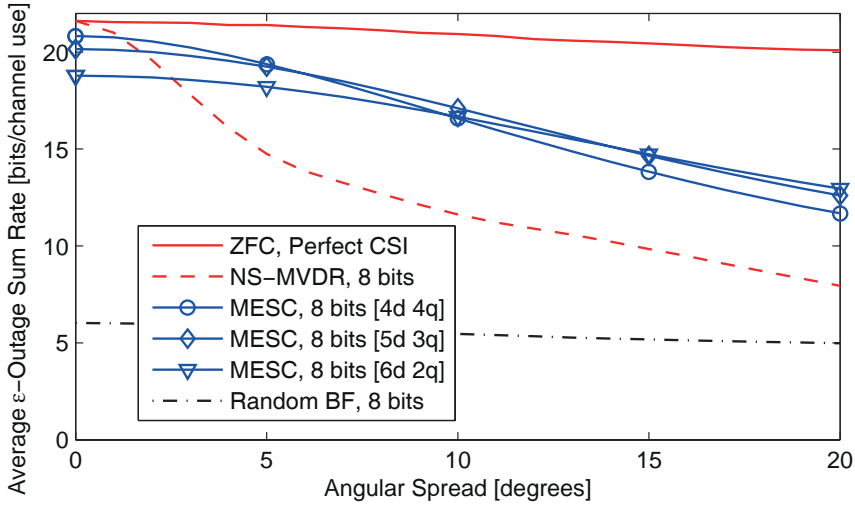


Figure 4.10: Average  $\epsilon$ -outage sum rate as a function of the angular spread at a total transmit power of  $q = 15$  dB. The spatial correlation is based on the local scattering model in Chapter 2.1.3.

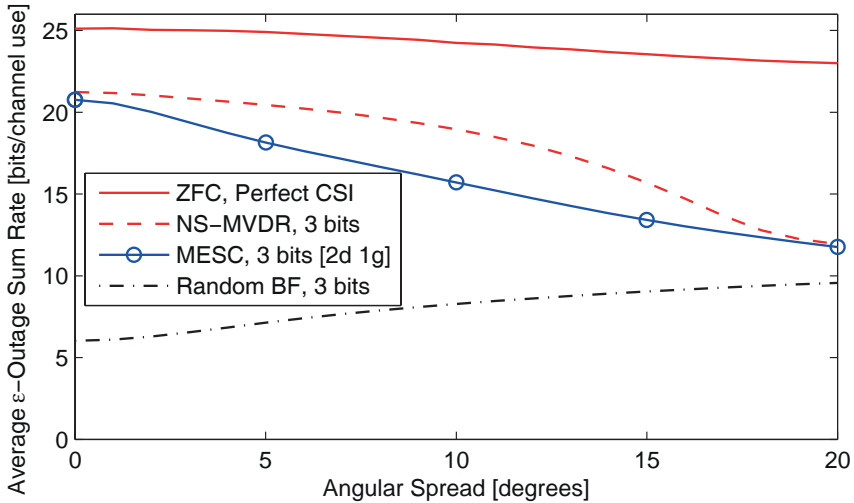


Figure 4.11: Average  $\epsilon$ -outage sum rate as a function of the angular spread at a total transmit power of  $q = 15$  dB. Different transmission strategies are compared when  $B$  is very small.

and overall CSI accuracy, but it is fair to say that CDI feedback is of dominating importance under practical non-asymptotic conditions. This conclusion is in line with Theorem 4.7 and with the prior work in [KdFG06, RJ08b], where achieving accurate CDI is shown to be essential for multiuser transmission while the exploitation of multiuser diversity is of secondary importance.<sup>17</sup> Employing additional receive antennas to enable receive combining has a large impact on the performance and can be viewed as an alternative to increasing the feedback load.

## 4.5 Summary

Practical multiuser MIMO systems operate under imperfect CSI, but can still achieve the full multiplexing gain if sufficient resources are allocated for CSI acquisition (i.e., training-signaling and CSI feedback). This chapter has shown that if such sufficient resources are available, only one data stream should be allocated per scheduled user (and users should use their antennas for receive combining). This is explained by more efficient scheduling, exploitation of multiuser diversity, and greater resilience towards ill-conditioned channels. It also has positive implications for the hardware design of user devices. Our result stands in contrast to prior work that shows a benefit of allocating multiple streams per user when the CSI accuracy is insufficient. But we have shown that prior results are misleading since single-user transmission is the best choice in these scenarios.

In addition, we have proved that depending on the number of users, number of receive antennas, and the spatial correlation, the full multiplexing gain can be achieved with only CDI feedback, only CQI feedback, or without any feedback at all. Thus, asymptotic analysis provides very diverse answers to the tradeoff between CDI and CQI feedback in practical systems. To clarify this tradeoff, we considered different low-complexity precoding strategies that utilize quantized CSI. These were adapted to maximize the  $\epsilon$ -outage sum rate, which is entirely based on the CSI available at the transmitter and thus is a better measure of the practical performance in block-fading systems than the achievable sum rate. The numerical evaluation reveals that 2-3 bits of CQI feedback is often sufficient, while the remaining bits should be used for CDI feedback. The importance of CQI increases with the spatial correlation and number of receive antennas, while it is well-known that the CDI accuracy needs to increase with the SNR.

---

<sup>17</sup>For a fixed number of bits *per user*, CDI feedback is essential when there are few users. It becomes less important as the number of users increases [KdFG06]. When the *total* feedback load is limited, it is beneficial to acquire very accurate CSI from a few users rather than dividing the bits among many users to exploit multiuser diversity [RJ08b].

## 4.A Collection of Proofs

### 4.A.1 Proof of Theorem 4.1

Using (4.9), the asymptotic difference can be expressed as

$$\beta = \log_2 \left( \frac{\prod_{k \in \mathcal{S}^{\text{BD}}} \det(\mathbf{H}_k \mathbf{V}_k^{\text{BD}} \mathbf{V}_k^{\text{BD},H} \mathbf{H}_k^H)}{\prod_{k \in \mathcal{S}^{\text{ZFC}}} |\mathbf{r}_k^H \mathbf{H}_k \mathbf{v}_k^{\text{ZFC}}|^2} \right). \quad (4.53)$$

Assume that  $\mathbf{r}_k$  is selected suboptimally as the dominating eigenvector of  $\mathbf{R}_{R,k}$ . This is a lower bound because every judicious selection based on perfect CSI (e.g., MRC or MMSE combining) achieves better performance, but it is convenient since  $\mathbf{r}_k^H \mathbf{H}_k = \sqrt{\lambda_{k,M}} \tilde{\mathbf{h}}_k^H$  with  $\tilde{\mathbf{h}}_k \in \mathcal{CN}(\mathbf{0}, \mathbf{I}_N)$ . The asymptotic difference can thus be upper bounded as

$$\begin{aligned} \beta &\leq \log_2 \left( \frac{\prod_{k \in \mathcal{S}^{\text{BD}}} \det(\tilde{\mathbf{H}}_k \mathbf{V}_k^{\text{BD}} \mathbf{V}_k^{\text{BD},H} \tilde{\mathbf{H}}_k^H)}{\prod_{k \in \mathcal{S}^{\text{ZFC}}} |\tilde{\mathbf{h}}_k^H \mathbf{v}_k^{\text{ZFC}}|^2} \right) \\ &\quad + \sum_{k \in \mathcal{S}^{\text{BD}}} \log_2 \det(\mathbf{R}_{R,k}) - \sum_{k \in \mathcal{S}^{\text{ZFC}}} \log_2(\lambda_{k,M}). \end{aligned} \quad (4.54)$$

The expectation of the first term can be rewritten as the first term in (4.10) by applying [LJ07, Theorem 3]. The cited theorem is valid for uncorrelated channels, but can be applied since  $\mathbf{V}_k^{\text{BD}}$  is the same regardless of  $\mathbf{R}_{R,\bar{k}}$  for all  $\bar{k} \in \mathcal{S}^{\text{ZFC}}$ . This is understood by the following lemma which shows that receive correlation will not affect the row space of channels, which are the spaces where co-user interference are canceled.

*Lemma 4.2.* Let  $\mathbf{A} \succ \mathbf{0}_M$  be any Hermitian positive-definite matrix and let  $\tilde{\mathbf{H}} \in \mathbb{C}^{M \times N}$  be an arbitrary matrix. Then,  $\text{span}(\tilde{\mathbf{H}}) = \text{span}(\mathbf{A}\tilde{\mathbf{H}})$ , where  $\text{span}(\cdot)$  denotes the row space.

*Proof.* Let  $\mathbf{A} = \mathbf{U}_A \mathbf{\Lambda}_A \mathbf{U}_A^H$  be an eigen decomposition of  $\mathbf{A}$ . The lemma follows by observing that  $\mathbf{U}_A$  only rotates the basis vectors of the row space and  $\mathbf{\Lambda}_A$  scales the rows without affecting their span.  $\square$

Finally, observe that the last two terms of (4.54) are deterministic and correspond to the second term in (4.10).

### 4.A.2 Proof of Theorem 4.2

The expected asymptotic loss (compared with single-user transmission) is defined for BD precoding as

$$\begin{aligned} \mathbb{E}\{\text{Loss}_{\text{BD}}\} &= \mathbb{E}\{\log_2 \det(\mathbf{H}_k \mathbf{H}_k^H) - \log_2 \det(\mathbf{H}_k \mathbf{V}_k^{\text{BD}} \mathbf{V}_k^{\text{BD},H} \mathbf{H}_k^H)\} \\ &= -\mathbb{E}\{\log_2 \det(\mathbf{B}_k \mathbf{V}_k^{\text{BD}} \mathbf{V}_k^{\text{BD},H} \mathbf{B}_k^H)\} \end{aligned} \quad (4.55)$$

where  $\mathbf{B}_k = \text{span}(\mathbf{H}_k) \in \mathbb{C}^{M \times N}$  is an orthonormal basis of the row space of  $\mathbf{H}_k$ . Assume that there are  $K_r$  candidates to become the new user  $k$ ,  $\mathcal{K} = \{1, \dots, K_r\}$ , while the other users in  $\mathcal{S}^{\text{BD}}$  are fixed. Since  $|\mathcal{S}^{\text{BD}}| = \frac{N}{M}$ , all available degrees of freedom are consumed by the interference cancellation. The precoding matrix  $\mathbf{V}_k^{\text{BD}}$  is therefore completely determined by the common null space of the co-users' channels and fixed in this proof.

Minimizing (4.55) corresponds to finding the user  $\bar{k} \in \mathcal{K}$  with a row space of  $\mathbf{H}_{\bar{k}}$  that is at most compatible with  $\mathbf{V}_k^{\text{BD}}$ . Observe that (4.55) for user candidate  $\bar{k}$  can be lower bounded as

$$\begin{aligned}
& -\mathbb{E}\{\log_2 \det(\mathbf{B}_{\bar{k}} \mathbf{V}_k^{\text{BD}} \mathbf{V}_k^{\text{BD},H} \mathbf{B}_{\bar{k}}^H)\} \\
&= -M\mathbb{E}\{\log_2(\det(\mathbf{B}_{\bar{k}} \mathbf{V}_k^{\text{BD}} \mathbf{V}_k^{\text{BD},H} \mathbf{B}_{\bar{k}}^H)^{1/M})\} \\
&\geq -M\mathbb{E}\left\{\log_2\left(\frac{\text{tr}\{\mathbf{B}_{\bar{k}} \mathbf{V}_k^{\text{BD}} \mathbf{V}_k^{\text{BD},H} \mathbf{B}_{\bar{k}}^H\}}{M}\right)\right\} \\
&\geq -M\log_2\left(\frac{\mathbb{E}\{\text{tr}\{\mathbf{B}_{\bar{k}} \mathbf{V}_k^{\text{BD}} \mathbf{V}_k^{\text{BD},H} \mathbf{B}_{\bar{k}}^H\}\}}{M}\right) \\
&= -M\log_2\left(1 + \frac{\mathbb{E}\{\text{tr}\{\mathbf{B}_{\bar{k}} \mathbf{V}_k^{\text{BD}} \mathbf{V}_k^{\text{BD},H} \mathbf{B}_{\bar{k}}^H\} - M\}}{M}\right).
\end{aligned} \tag{4.56}$$

The first inequality is the classic inequality of arithmetic and geometric means, while the second inequality follows from applying Jensen's inequality to the convex function  $-\log_2 \det(\cdot)$ . The final expression in (4.56) contains  $M - \text{tr}\{\mathbf{B}_{\bar{k}} \mathbf{V}_k^{\text{BD}} \mathbf{V}_k^{\text{BD},H} \mathbf{B}_{\bar{k}}^H\}$ , which is the squared chordal distance between  $\mathbf{B}_{\bar{k}}$  and  $\mathbf{V}_k^{\text{BD}}$ .

Since the matrices  $\mathbf{B}_{\bar{k}}$ , for  $\bar{k} \in \mathcal{K}$ , are independent and isotropically distributed on the Grassmannian manifold  $\mathcal{G}_{N,M}$  (see Lemma 4.2 and its preceding discussion), we can bring in results from quantization of Grassmannian manifolds using  $K_r$  random codewords [DLR08]. From [DLR08, Theorem 4], we have the following lower bound on the average squared chordal distance (for sufficiently large  $K_r$ ):

$$\begin{aligned}
& \min_{\bar{k} \in \mathcal{K}} \mathbb{E}\left\{M - \text{tr}\{\mathbf{B}_{\bar{k}} \mathbf{V}_k^{\text{BD}} \mathbf{V}_k^{\text{BD},H} \mathbf{B}_{\bar{k}}^H\}\right\} \\
&\geq \frac{M(N-M)}{M(N-M)+1} c_{N,M,M,2}^{-\frac{1}{M(N-M)}} K_r^{-\frac{1}{M(N-M)}}
\end{aligned} \tag{4.57}$$

where  $c_{N,M,M,2}$  is a positive constant defined in [DLR08, Eq. (8)]. Plugging (4.57) into (4.56) yields the lower bound for BD precoding in the theorem.

A similar approach can be taken under ZFC precoding (by setting  $M = 1$  in the derivation), but the receive antennas provide degrees of freedom to select the effective channel as the vector in the row space of  $\mathbf{H}_{\bar{k}}$  that

minimizes the chordal distance to  $\mathbf{v}_k^{\text{ZFC}}$ . This is achieved by the quantized-based-combining (QBC) approach in [Jin08], which was derived for uncorrelated channels but can be applied under receive correlation due to Lemma 4.2. We apply [Jin08, Lemma 1], which says that the minimal chordal distance is the minimum of  $K_r$  independent  $\beta(N-M, M)$ -distributed random variables. This quantity can be lower bounded by taking the minimum of  $K_r$  independent  $\beta(N-M, 1)$  and further lower bounded by applying the quantization bound in [DLR08, Theorem 4]:

$$\min_{\tilde{\mathbf{h}}_k \in \mathcal{K}} \mathbb{E} \left\{ 1 - \left| \frac{\mathbf{h}_k^H}{\|\tilde{\mathbf{h}}_k\|_2} \mathbf{v}_k^{\text{ZFC}} \right|^2 \right\} \geq \frac{(N-M)}{(N-M)+1} c_{N-M+1,1,1,2}^{-\frac{1}{(N-M)}} K_r^{-\frac{1}{(N-M)}} \quad (4.58)$$

where  $c_{N-M+1,1,1,2}$  is a positive constant defined in [DLR08, Eq. (8)]. Plugging (4.58) into (4.56) (with  $M=1$ ) yields the lower bound for ZFC precoding in the theorem.

### 4.A.3 Proof of Theorem 4.3

Using Lemma 4.2, we observe that the row space of the correlated channel  $\mathbf{H}_k = \mathbf{R}_{R,k}^{1/2} \tilde{\mathbf{H}}_k$  is the same as for the uncorrelated channel  $\tilde{\mathbf{H}}_k$ . Consequently, the BD precoding matrices  $\tilde{\mathbf{V}}_k^{\text{BD}}$  are the same as for uncorrelated channels, which enables us to reuse the approach in the proof of [RJ08a, Theorem 1]. The average rate under perfect CSI is smaller or equal to the numerator of (4.15), thus both terms can be removed to achieve an upper bound. Therefore, the loss is upper bounded by the denominator of (4.15). Using Jensen's inequality, we achieve a new upper bound by moving the expectation inside  $\log \det(\cdot)$ . Next, observe that

$$\begin{aligned} & \mathbb{E} \{ \mathbf{H}_k \tilde{\mathbf{V}}_k^{\text{BD}} \tilde{\mathbf{V}}_k^{\text{BD},H} \mathbf{H}_k^H \} \\ &= \mathbf{R}_{R,k}^{1/2} \mathbb{E} \{ \mathbf{L}_k \mathbf{Q}_k \tilde{\mathbf{V}}_k^{\text{BD}} \tilde{\mathbf{V}}_k^{\text{BD},H} \mathbf{Q}_k^H \mathbf{L}_k^H \} \mathbf{R}_{R,k}^{1/2,H} \end{aligned} \quad (4.59)$$

using that  $\mathbf{H}_k = \mathbf{R}_{R,k}^{1/2} \tilde{\mathbf{H}}_k = \mathbf{R}_{R,k}^{1/2} \mathbf{L}_k \mathbf{Q}_k$ , where  $\mathbf{L}_k \in \mathbb{C}^{M \times M}$  is the lower triangular matrix and  $\mathbf{Q}_k \in \mathbb{C}^{M \times N}$  is the semi-unitary matrix of an LQ decomposition of  $\tilde{\mathbf{H}}_k$ . Observe that  $\mathbf{L}_k$  and  $\mathbf{Q}_k$  are independent, thus we can calculate their expectations sequentially as

$$\begin{aligned} & \mathbb{E} \{ \mathbf{L}_k \mathbf{Q}_k \tilde{\mathbf{V}}_k^{\text{BD}} \tilde{\mathbf{V}}_k^{\text{BD},H} \mathbf{Q}_k^H \mathbf{L}_k^H \} \\ &= \frac{D^{\text{BD}}}{N-M} \mathbb{E} \{ \mathbf{L}_k \mathbf{I}_M \mathbf{L}_k^H \} = \frac{ND^{\text{BD}}}{N-M} \mathbf{I}_M. \end{aligned} \quad (4.60)$$

The first equality follows from [RJ08a, Eq. (43)-(45)], while the second is based on  $\mathbb{E} \{ \mathbf{L}_k \mathbf{L}_k^H \} = N \mathbf{I}_M$  (since  $\mathbb{E} \{ \tilde{\mathbf{H}}_k \tilde{\mathbf{H}}_k^H \} = N \mathbf{I}_M$ ). Plugging (4.60)

into [RJ08a, Eq. (40)] yields

$$\Delta^{\text{BD}} \leq \log_2 \det \left( \mathbf{I}_M + \frac{q}{N} \left( \frac{N}{M} - 1 \right) \frac{ND^{\text{BD}}}{N-M} \mathbf{R}_{R,k} \right) \quad (4.61)$$

from which (4.16) follows directly. The approximate expression for  $D^{\text{BD}}$  is given in [RJ08a, Eq. (26)].

#### 4.A.4 Proof of Theorem 4.4

The proof follows along the lines of [Jin08, Theorem 1], with the difference that 1) we include spatial correlation at the receiver side; and 2) we use QBC also under perfect CSI. Using Lemma 4.2, we observe that the row space of the correlated channel  $\mathbf{H}_k = \mathbf{R}_{R,k}^{1/2} \tilde{\mathbf{H}}_k$  is the same as for the uncorrelated channel  $\tilde{\mathbf{H}}_k$ . Since the gain of the effective channel is ignored in (4.18), the error-minimizing codeword is the same as for uncorrelated channels and we can still apply [Jin08, Lemma 2] to conclude that the direction of the effective channel is isotropically distributed. The only difference compared with [Jin08] is the distribution of the norm of the effective channel, which will affect the bound. Let  $\mathbf{r}_k^{\text{QBC}}$  be the QBC for the correlated channel  $\mathbf{H}_k$  and let  $\mathbf{r}_k^{\text{UNCORR}}$  be the QBC for the uncorrelated channel  $\tilde{\mathbf{H}}_k$ , then

$$\mathbf{r}_k^{\text{QBC}} = \frac{\mathbf{R}_{R,k}^{-1/2} \mathbf{r}_k^{\text{UNCORR}}}{\|\mathbf{R}_{R,k}^{-1/2} \mathbf{r}_k^{\text{UNCORR}}\|_2}. \quad (4.62)$$

We can therefore express the effective channel as

$$\mathbf{h}_k = \mathbf{H}_k^H \mathbf{r}_k^{\text{QBC}} = \mathbf{H}_k^H \frac{\mathbf{R}_{R,k}^{-1/2} \mathbf{r}_k^{\text{UNCORR}}}{\|\mathbf{R}_{R,k}^{-1/2} \mathbf{r}_k^{\text{UNCORR}}\|_2} = \frac{\tilde{\mathbf{H}}_k^H \mathbf{r}_k^{\text{UNCORR}}}{\|\mathbf{R}_{R,k}^{-1/2} \mathbf{r}_k^{\text{UNCORR}}\|_2} \quad (4.63)$$

and its squared norm will be

$$\|\mathbf{h}_k\|_2^2 = \|\tilde{\mathbf{H}}_k^H \mathbf{r}_k^{\text{UNCORR}}\|_2^2 \frac{1}{\mathbf{r}_k^{\text{UNCORR},H} \mathbf{R}_{R,k}^{-1} \mathbf{r}_k^{\text{UNCORR}}}. \quad (4.64)$$

The first part is the same as under uncorrelated fading and has the mean value  $N - M + 1$  (see [Jin08, Lemma 4]), while the second part depends on  $\mathbf{R}_{R,k}$ . Since both the quantization codebook and  $\tilde{\mathbf{H}}_k$  are isotropically distributed,  $\mathbf{r}_k^{\text{UNCORR}}$  is also isotropic and the two terms in (4.64) are independent. To characterize the second term, observe that  $\mathbf{r}_k^{\text{UNCORR}}$  can be viewed as a normalized uncorrelated complex Gaussian vector. By exploiting that the eigenvectors of  $\mathbf{R}_{R,k}$  will not affect the distribution and that squared

magnitudes of  $\mathcal{CN}(0, 1)$ -variables are exponentially distributed [HBO08a], we conclude that the second term of (4.64) has the same distribution as

$$\frac{\sum_{i=1}^M \xi_i}{\sum_{i=1}^M \xi_i / \lambda_{k,i}} \quad (4.65)$$

for independent exponentially distributed variables  $\xi_i \in \text{Exp}(1)$ . For any  $a$  in the interval  $\lambda_{k,m} \leq a \leq \lambda_{k,m+1}$ , we can write the CDF as

$$\begin{aligned} & \Pr \left\{ \frac{\sum_{i=1}^M \xi_i}{\sum_{i=1}^M \xi_i / \lambda_{k,i}} \leq a \right\} \\ &= \Pr \left\{ \underbrace{\sum_{i=1}^m \left( \frac{a}{\lambda_{k,i}} - 1 \right) \xi_i}_{\geq 0} - \sum_{i=m+1}^M \underbrace{\left( 1 - \frac{a}{\lambda_{k,i}} \right) \xi_i}_{\geq 0} \geq 0 \right\}. \end{aligned} \quad (4.66)$$

This is the difference of two sums of exponentially distributed variables (with distinct positive variances). The PDF of each sum is characterized by [HBO08a, Theorem 4] and by calculating their convolution and integrate over all positive values, we achieve the CDF

$$\begin{aligned} & \Pr \left\{ \frac{\sum_{i=1}^M \xi_i}{\sum_{i=1}^M \xi_i / \lambda_{k,i}} \leq a \right\} \\ &= \sum_{n=1}^m \sum_{l=m+1}^M \frac{(\mu_n - a^{-1})^m (a^{-1} - \mu_l)^{M-m-1}}{(\mu_n - \mu_l) \prod_{i=1, i \neq n}^m (\mu_n - \mu_i) \prod_{j=1, j \neq l}^m (\mu_j - \mu_l)} \end{aligned} \quad (4.67)$$

where we use the simplifying notation  $\mu_n = \frac{1}{\lambda_{k,n}}$ . The corresponding mean value can be achieved from this CDF by simply taking the derivative and sum up the mean values over each  $a$ -interval. By multiplying the achieved mean value expression with  $N - M + 1$  (i.e., the contribution of the first part in (4.64)), we achieve the expression for  $G$  in the theorem.

#### 4.A.5 Proof of Theorem 4.5

The proof follows along the lines of [RJ08a, Proof of Theorem 1], with the difference that we consider CSI estimation errors (instead of quantization errors) and include spatial correlation. First, observe that both  $\mathbf{V}_k^{\text{BD}}$  and  $\widehat{\mathbf{V}}_k^{\text{BD}}$  are isotropically distributed on the Grassmannian manifold  $\mathcal{G}_{N,M}$  (since receive-side correlation is not affecting the row space of  $\mathbf{H}_k$  and  $\widehat{\mathbf{H}}_k$ ;

see Lemma 4.2). The average rate loss can therefore be bounded as

$$\begin{aligned} \Delta^{\text{BD-EST}} &\stackrel{\text{(a)}}{\leq} \mathbb{E} \left\{ \log_2 \det \left( \mathbf{I}_M + \frac{q}{N} \sum_{\bar{k} \in \mathcal{S}^{\text{BD}} \setminus \{k\}} \mathbf{H}_k \widehat{\mathbf{V}}_{\bar{k}}^{\text{BD}} \widehat{\mathbf{V}}_{\bar{k}}^{\text{BD},H} \mathbf{H}_k^H \right) \right\} \\ &\stackrel{\text{(b)}}{\leq} \log_2 \det \left( \mathbf{I}_M + \frac{q}{N} \sum_{\bar{k} \in \mathcal{S}^{\text{BD}} \setminus \{k\}} \mathbb{E} \{ \mathbf{H}_k \widehat{\mathbf{V}}_{\bar{k}}^{\text{BD}} \widehat{\mathbf{V}}_{\bar{k}}^{\text{BD},H} \mathbf{H}_k^H \} \right), \end{aligned} \quad (4.68)$$

where (a) follows from removing the term

$$\begin{aligned} &\log_2 \det \left( \mathbf{I}_M + \frac{q}{N} \mathbf{H}_k \mathbf{V}_k^{\text{BD}} \mathbf{V}_k^{\text{BD},H} \mathbf{H}_k^H \right) \\ &\quad - \log_2 \det \left( \mathbf{I}_M + \frac{q}{N} \sum_{\bar{k} \in \mathcal{S}^{\text{BD}}} \mathbf{H}_k \widehat{\mathbf{V}}_{\bar{k}}^{\text{BD}} \widehat{\mathbf{V}}_{\bar{k}}^{\text{BD},H} \mathbf{H}_k^H \right) \end{aligned} \quad (4.69)$$

which is negative since  $\mathbf{H}_k \mathbf{V}_k^{\text{BD}} \mathbf{V}_k^{\text{BD},H} \mathbf{H}_k^H$  has the same distribution as  $\mathbf{H}_k \widehat{\mathbf{V}}_{\bar{k}}^{\text{BD}} \widehat{\mathbf{V}}_{\bar{k}}^{\text{BD},H} \mathbf{H}_k^H$  (and the second term contains additional positive semi-definite matrices). The inequality (b) follows from applying Jensen's inequality on the concave function  $\log_2 \det(\cdot)$ . From (4.25) we have

$$\mathbf{H}_k = \widehat{\mathbf{H}}_k + \left( \mathbf{R}_{R,k}^{-T} + \frac{\mathbf{P}_k^H \mathbf{P}_k}{\sigma^2} \right)^{-\frac{1}{2}} \widetilde{\mathbf{E}}_k \quad (4.70)$$

where the second term is the estimation error and  $\widetilde{\mathbf{E}}_k$  has  $\mathcal{CN}(0, 1)$ -entries. By exploiting that  $\widehat{\mathbf{H}}_k \widehat{\mathbf{V}}_{\bar{k}}^{\text{BD}} = \mathbf{0}$  for  $\bar{k} \neq k$ , we achieve

$$\begin{aligned} &\mathbb{E} \{ \mathbf{H}_k \widehat{\mathbf{V}}_{\bar{k}}^{\text{BD}} \widehat{\mathbf{V}}_{\bar{k}}^{\text{BD},H} \mathbf{H}_k^H \} \\ &= \left( \mathbf{R}_{R,k}^{-T} + \frac{\mathbf{P}_k^H \mathbf{P}_k}{\sigma^2} \right)^{-\frac{1}{2}} \mathbb{E} \{ \widetilde{\mathbf{E}}_k \widehat{\mathbf{V}}_{\bar{k}}^{\text{BD}} \widehat{\mathbf{V}}_{\bar{k}}^{\text{BD},H} \widetilde{\mathbf{E}}_k^H \} \left( \mathbf{R}_{R,k}^{-T} + \frac{\mathbf{P}_k^H \mathbf{P}_k}{\sigma^2} \right)^{-\frac{1}{2}}. \end{aligned} \quad (4.71)$$

Observe that  $\mathbb{E} \{ \widetilde{\mathbf{E}}_k \widehat{\mathbf{V}}_{\bar{k}}^{\text{BD}} \widehat{\mathbf{V}}_{\bar{k}}^{\text{BD},H} \widetilde{\mathbf{E}}_k^H \} = M \mathbf{I}_M$  since  $\widetilde{\mathbf{E}}_k$  is complex Gaussian and independent of  $\widehat{\mathbf{V}}_{\bar{k}}^{\text{BD}}$ . The final expression is achieved by plugging this into (4.68) and observing that each of the  $(\frac{N}{M} - 1)$  interference terms becomes  $M(\mathbf{R}_{R,k}^{-T} + \mathbf{P}_k^H \mathbf{P}_k / \sigma^2)^{-1}$ .

#### 4.A.6 Proof of Lemma 4.1

Observe that  $\mathbf{H} = \mathbf{R}_R^{1/2} \widetilde{\mathbf{H}}$  has the same distribution as  $\mathbf{H}\mathbf{U}$  for any unitary matrix  $\mathbf{U}$ . Thus, we can rotate  $\mathbf{h}$  arbitrarily without changing the statistics, meaning that  $\mathbf{h} / \|\mathbf{h}\|_2$  must be isotropically distributed. Next,

note that  $\|\mathbf{h}\|_2^2 = \|\mathbf{r}^H \mathbf{H} \mathbf{U}\|_2^2 = \|\mathbf{r}^H \mathbf{H}\|_2^2$ , thus unitary rotations will not affect the effective channel gain and thus the direction and the channel gain are statistically independent.  $\|\mathbf{h}\|_2^2$  is the dominating eigenvalue of the correlated complex Wishart matrix  $\mathbf{H} \mathbf{H}^H \in \mathcal{W}_M(N, \mathbf{R}_R)$ . The mean value expression in (4.28) can be achieved directly from [BO08c, Theorem 3] or by using the moment generating function in [MCS06] (which gives an equivalent expression that looks slightly different).

#### 4.A.7 Proof of Theorem 4.6

This theorem is proved in the same way as Theorem 4.5. The only notable difference is that we use the effective channel  $\mathbf{h}_k$ , which has a single effective receive antenna, instead of the original channel  $\mathbf{H}_k$ . The effective channel is zero-mean and has an average channel gain  $\mathbb{E}\{\|\mathbf{h}_k\|_2^2\}$  given by (4.28). Thus, the effective channel and its channel estimate is related as  $\mathbf{h}_k^H = \hat{\mathbf{h}}_k^H + (1/\mathbb{E}\{\|\mathbf{h}_k\|_2^2\} + \varrho/\sigma^2)^{-1/2} \tilde{\mathbf{e}}_k^H$ , where  $\tilde{\mathbf{e}}_k \in \mathcal{CN}(\mathbf{0}, \mathbf{I}_N)$ .

#### 4.A.8 Proof of Theorem 4.7

With probability one, the random channel directions are different:  $|\bar{\mathbf{h}}_k^H \bar{\mathbf{h}}_k| < 1 \forall k \neq k$ . Thus, ZF precoding exists and can be used to cancel out all co-user interference. Let  $\mathbf{v}_k^{(\text{ZF})}$  denote the ZF vector of user  $k \in \mathcal{S}$  and let  $qp_k$  be the corresponding power allocation, for some fixed  $p_k > 0$ . The conditional CDF of  $\text{SINR}_k$  becomes

$$\begin{aligned} F_{\text{SINR}_k | \bar{\mathbf{h}}_k}(x) &= \Pr \left\{ qp_k \|\mathbf{h}_k\|_2^2 |\bar{\mathbf{h}}_k^H \mathbf{v}_k^{(\text{ZF})}|^2 \leq x \right\} \\ &= F_{\|\mathbf{h}_k\|_2^2 | \bar{\mathbf{h}}_k} \left( \frac{x}{qp_k |\bar{\mathbf{h}}_k^H \mathbf{v}_k^{(\text{ZF})}|^2} \right) = \epsilon. \end{aligned} \quad (4.72)$$

The second equality follows from using the (conditional) CDF of  $\|\mathbf{h}_k\|_2^2$ , which is the only random variable when  $\bar{\mathbf{h}}_k$  is given. This CDF can be derived using Bayes' theorem and by rewriting the PDF of a complex Gaussian vector in a similar manner as in [HBO08a]:

$$F_{\|\mathbf{h}_k\|_2^2 | \bar{\mathbf{h}}_k}(x) = 1 - e^{-x \bar{\mathbf{h}}_k^H \mathbf{R}_{T,k}^{-1} \bar{\mathbf{h}}_k} \sum_{m=0}^{N-1} \frac{(x \bar{\mathbf{h}}_k^H \mathbf{R}_{T,k}^{-1} \bar{\mathbf{h}}_k)^m}{m!}. \quad (4.73)$$

Using this expression, we can evaluate the  $\epsilon$ -outage rate expression (defined in (4.35) and (4.36)) by inverting the CDF expression in (4.72):

$$\begin{aligned} R_{k,\text{out}} &= \log_2 \left( 1 + F_{\text{SINR}_k | \bar{\mathbf{h}}_k}^{-1}(\epsilon) \right) \\ &= \log_2 \left( 1 + qp_k |\bar{\mathbf{h}}_k^H \mathbf{v}_k^{(\text{ZF})}|^2 F_{\|\mathbf{h}_k\|_2^2 | \bar{\mathbf{h}}_k}^{-1}(\epsilon) \right). \end{aligned} \quad (4.74)$$

For any  $\epsilon > 0$ ,  $F_{\|\mathbf{h}_k\|_2^2|\bar{\mathbf{h}}_k}^{-1}(\epsilon)$  has a strictly positive and constant value. Thus,  $R_{k,\text{out}}$  behaves as  $\log_2(q) + \text{constant}$  at high  $q$ . By repeating this for all the  $N$  selected users, we conclude that the  $\epsilon$ -outage sum rate achieves the full multiplexing gain of  $N$ .

#### 4.A.9 Proof of Theorem 4.8

For any user selection with  $|\mathcal{S}| = N$ , the dominating eigenvectors  $\{\mathbf{u}_k\}_{k \in \mathcal{S}}$  satisfy  $|\mathbf{u}_k^H \mathbf{u}_{\bar{k}}| < 1 \forall \bar{k} \in \mathcal{S} \setminus \{k\}$ . Thus, there exist ZF-like vectors  $\{\tilde{\mathbf{w}}_k\}_{k \in \mathcal{S}}$  such that  $\mathbf{u}_k^H \tilde{\mathbf{w}}_{\bar{k}} = 0$  for  $\bar{k} \neq k$ . Assuming power allocation  $qp_k$  for some fixed  $p_k > 0$ , the SINR of user  $k$  can be lower bounded as

$$\begin{aligned} \frac{qp_k |\mathbf{h}_k^H \tilde{\mathbf{w}}_k|^2}{1 + \sum_{\bar{k} \in \mathcal{S} \setminus \{k\}} qp_{\bar{k}} |\mathbf{h}_k^H \tilde{\mathbf{w}}_{\bar{k}}|^2} &\geq \frac{qp_k \beta_k |\mathbf{h}_k^H \mathbf{u}_k|^2}{1 + q(\|\mathbf{h}_k\|_2^2 - |\mathbf{h}_k^H \mathbf{u}_k|^2)} \\ &= p_k \beta_k \gamma_k > 0 \end{aligned} \quad (4.75)$$

for some  $\beta_k > 0$  that satisfy  $|\mathbf{h}_k^H \tilde{\mathbf{w}}_k|^2 \geq \beta_k |\mathbf{h}_k^H \mathbf{u}_k|^2$  (with probability one). The bound is achieved by pretending that all co-user transmissions create maximal interference (i.e.,  $|\mathbf{h}_k^H \tilde{\mathbf{w}}_{\bar{k}}|^2$  is replaced by  $\|\mathbf{h}_k\|_2^2 - |\mathbf{h}_k^H \mathbf{u}_k|^2$ ) and by identifying the quality indicator  $\gamma_k$  in (4.38) which is known to the transmitter. If we can show that  $\gamma_k$  scales linearly with  $q$  at high  $q$  (and large  $K_r$ ), we have proved the multiplexing gain.

For notational convenience, assume there are  $NK_r$  users, which are divided into  $N$  equally large groups. In each group, we schedule the user with the largest  $\gamma_k$ . We will show that

$$\begin{aligned} \Pr\left\{ \max_{1 \leq k \leq K_r} \gamma_k \geq q\lambda_N \log(K_r) - qN\lambda_N \log(q \log(K_r)) + \mathcal{O}(1) \right\} \\ \geq 1 - \mathcal{O}\left(\frac{1}{K_r^q}\right) \end{aligned} \quad (4.76)$$

by applying the results from extreme value theory that are summarized in [SH05, Theorem A.2]. First, observe that for any  $c \geq 0$  we have

$$\Pr\left\{ \max_{1 \leq k \leq K_r} \gamma_k \geq c \right\} \geq \Pr\left\{ \max_{1 \leq k \leq K_r} \tilde{\gamma}_k \geq c \right\} \quad (4.77)$$

where  $\tilde{\gamma}_k$  is achieved by replacing the covariance matrix  $\mathbf{R}_{T,k}$  with  $\lambda_N \mathbf{I}_N$  for all  $k$  (i.e., increasing the non-dominating eigenvalues and thereby increasing the interference). From [SH05, Eq. (14)-(15)], we then have that the PDF and CDF of  $\tilde{\gamma}_k$  are

$$\begin{aligned} f_{\tilde{\gamma}_k}(x) &= \frac{e^{-x/(q\lambda_N)}}{(1+x)^N} \left( \frac{1+x}{q\lambda_N} + N - 1 \right) \quad x \geq 0, \\ F_{\tilde{\gamma}_k}(x) &= 1 - \frac{e^{-x/(q\lambda_N)}}{(1+x)^{N-1}} \quad x \geq 0. \end{aligned} \quad (4.78)$$

In addition, it follows from [SH05, Eq. (20)] that

$$g(x) = \frac{1 - F_{\tilde{\gamma}_k}(x)}{f_{\tilde{\gamma}_k}(x)} = q\lambda_N - \frac{q\lambda_N(N-1)}{(1+x)/(q\lambda_N) + (N-1)}. \quad (4.79)$$

To apply [SH05, Theorem A.2], we need to check that  $\lim_{x \rightarrow \infty} g(x) = q\lambda_N$  is strictly positive, which is satisfied. Next, we need to find the unique value  $u_{K_r}$  that solves the equation  $1 - F_{\tilde{\gamma}_k}(u_{K_r}) = 1/K_r$ :

$$\frac{e^{-u_{K_r}/(q\lambda_N)}}{(1+u_{K_r})^{N-1}} = \frac{1}{K_r} \Rightarrow \quad (4.80)$$

$$\begin{aligned} u_{K_r} &= q\lambda_N \log(K_r) - (N-1)q\lambda_N \log(1+u_{K_r}) \\ &= q\lambda_N \log(K_r) - (N-1)q\lambda_N \log(q\lambda_N \log(K_r)) + \mathcal{O}(1) \end{aligned} \quad (4.81)$$

where  $\mathcal{O}(1)$  is bounded when  $K_r, q \rightarrow \infty$  such that  $\frac{q}{\log(K_r)} \rightarrow c < \infty$ .

Let  $u = -\log(q\lambda_N \log(K_r))$ , then [SH05, Theorem A.2] says that

$$\begin{aligned} F_{\tilde{\gamma}_k}^{K_r}(u_{K_r} + ug(u_{K_r})) &= e^{-e^{-u - u^2 g'(u_{K_r})/2! + \dots + \mathcal{O}(\frac{e^{-u + \mathcal{O}(u^2 g'(u_{K_r}))}}{K_r})}} \\ &= e^{-e^{\log(q \log(K_r)) + \mathcal{O}(1)}} = e^{-\log(K_r^q) \cdot \mathcal{O}(1)} \\ &= \mathcal{O}\left(\frac{1}{K_r^q}\right). \end{aligned} \quad (4.82)$$

To achieve the final expression, we exploited that  $u^{l+1}g^{(l)}(u_{K_r}) = \log^2(q\lambda_N \log(K_r))\mathcal{O}(1/(q \log(K_r))^{l+1}) \rightarrow 0$  when  $K_r, q \rightarrow \infty$  as prescribed. Finally, we interpret (4.82) as

$$\begin{aligned} 1 - \mathcal{O}\left(\frac{1}{K_r^q}\right) &= 1 - F_{\tilde{\gamma}_k}^{K_r}(u_{K_r} + ug(u_{K_r})) \\ &= \Pr\left\{\max_{1 \leq k \leq K_r} \tilde{\gamma}_k \geq u_k - \log(q\lambda_N \log(K_r))g(u_{K_r})\right\} \\ &\leq \Pr\left\{\max_{1 \leq k \leq K_r} \gamma_k \geq u_k - \log(q\lambda_N \log(K_r))g(u_{K_r})\right\} \\ &= \Pr\left\{\max_{1 \leq k \leq K_r} \gamma_k \geq u_k - q\lambda_N \log(q\lambda_N \log(K_r)) + \mathcal{O}(1)\right\} \end{aligned} \quad (4.83)$$

where the inequality follows from (4.77) and the last equality from that  $g(u_{K_r}) = q\lambda_N - \mathcal{O}(1/(q \log(K_r)))$ . Substituting (4.81) into (4.83) gives (4.76). Based on (4.76), observe  $q \log(K_r) - qN \log(q \log(K_r))$  is dominated by  $q \log(K_r)$  when  $\frac{q}{\log(K_r)} \rightarrow c < \infty$ . For sufficiently large  $K_r$  and  $q$ , the rate of the user with the largest  $\gamma_k$  scales as  $\log_2(q \log(K_r))$  with a probability larger than  $1 - \epsilon$ . This holds for the user with the largest  $\gamma_k$  in each of the  $N$  groups, yielding a total multiplexing gain of  $N$ .

#### 4.A.10 Proof of Theorem 4.9

The channel matrix of user  $k \in \mathcal{S}$  is  $\mathbf{H}_k = \tilde{\mathbf{H}}_k \mathbf{R}_{T,k}^{1/2}$ , where  $\mathbf{R}_{T,k} = \mathbf{U}_k \text{diag}(\lambda_{k,N}, \dots, \lambda_{k,1}) \mathbf{U}_k^H$  can be partitioned as in (4.43). The dominating eigenvectors  $\mathbf{u}_k$  are different for each selected user (by assumption). We achieve an effective channel  $\mathbf{h}_k \in \mathcal{CN}(\mathbf{0}, \tilde{\mathbf{R}}_{T,k})$  with  $\tilde{\mathbf{R}}_{T,k} = \mathbf{U}_k \text{diag}(\lambda_{k,N}, 0, \dots, \lambda_{k,N-M}, \dots, \lambda_{k,1}) \mathbf{U}_k^H$  by selecting the receive combiner  $\mathbf{r}_k$  in the left null space of  $\mathbf{H}_k \mathbf{U}_k^{(I)}$ .

Using this receive combiner, there exist ZF-like precoding vectors  $\{\tilde{\mathbf{w}}_k\}_{k \in \mathcal{S}}$  such that  $\mathbf{u}_k^H \tilde{\mathbf{w}}_{\bar{k}} = 0$  for  $\bar{k} \neq k$ . Thus, the signal term in  $\text{SINR}_k$  scales like  $q\lambda_{k,N}$  while the interference term scales as  $q\lambda_{k,N-M}$  (i.e., the second largest eigenvalue of  $\tilde{\mathbf{R}}_{T,k}$ ). If  $\frac{q}{\lambda_{k,N}/\lambda_{k,N-M}} \rightarrow c_k < \infty$ , then the signal term goes to infinity with  $q$  while the interference term is bounded. Therefore, the full multiplexing gain is achieved.

#### 4.A.11 Proof of Theorem 4.10

If all non-zero eigenvalues are distinct, the CDF of  $\rho = \|\mathbf{h}\|_2^2$  is well-known in the field of renewal theory [Sch88] and was derived for communications purposes in [HBO08a]:

$$F_{\|\mathbf{h}\|_2^2}(\rho) = \left(1 - \sum_{k=1}^N \frac{e^{-\frac{\rho}{\mu_k}}}{\prod_{i \neq k} (1 - \frac{\mu_i}{\mu_k})}\right) H_0(\rho), \quad (4.84)$$

where  $H_0(\rho) = 1$  for  $\rho \geq 0$  and zero otherwise. The conditional moments can be expressed as

$$\mathbb{E}\{|v_i|^{2p} | a, b\} = \int_a^b \mathbb{E}\{|v_i|^{2p} | \rho\} f_{\|\mathbf{h}\|_2^2 | a, b}(\rho | a, b) d\rho = \frac{\int_a^b \mathbb{E}\{|v_i|^{2p} | \rho\} f_{\|\mathbf{h}\|_2^2}(\rho) d\rho}{\int_a^b f_{\|\mathbf{h}\|_2^2}(\rho) d\rho} \quad (4.85)$$

where  $\rho$  represents the exact value of  $\|\mathbf{h}\|_2^2$ . The conditional moment  $\mathbb{E}\{|v_i|^{2p} | \rho\}$  was given in [HBO08a, Corollary 5-6] for  $p = 1, 2$  and in [BHO09, Theorem 1] for arbitrary  $p$ . The integral in the numerator of (4.85) can be solved through straightforward integration, while the integral in the denominator is  $F_{\|\mathbf{h}\|_2^2}(b) - F_{\|\mathbf{h}\|_2^2}(a)$ . The conditional cross-moments are derived using the same approach.

#### 4.A.12 Proof of Corollary 4.3

Let  $\tilde{\mathbf{h}} = \mathbf{U}^H \mathbf{h}$  and observe that  $\tilde{\mathbf{h}} \in \mathcal{CN}(\mathbf{0}, \mathbf{\Lambda})$ . The corollary follows from straightforward and tedious expansion of  $\|\mathbf{Bh}\|_2^2 = \|\mathbf{A}\tilde{\mathbf{h}}\|_2^2 = \sum_{k=1}^{N_B} |\sum_{l=1}^N a_{kl} v_l|^2$  and  $\|\mathbf{A}\tilde{\mathbf{h}}\|_2^4 = (\|\mathbf{A}\tilde{\mathbf{h}}\|_2^2)^2$ . The expectations are evaluated using Theorem 4.10.



## Chapter 5

# Framework for General Multicell Coordination

In this chapter, we propose a general framework for modeling multicell systems and measuring their performance. This framework resolves some feasibility issues of previous models and enables unified analysis of everything from interference channels to ideal network MIMO systems.

The motivation behind our new system model is given in Section 5.1, along with the theoretical details of the proposed dynamic cooperation clusters. A general way of measuring performance is proposed in Section 5.2, where the user performance is represented by arbitrary increasing functions of the SINRs (e.g., representing data rates, error rates, or mean square errors) while the system performance function combines the user performance using a criterion (e.g., sum performance, proportional fairness, or max-min fairness). The performance region is defined as a concept that ties the user and system performance together and basic properties of the region are derived. Finally, Section 5.3 shows that the optimal solution to our general multicell resource allocation problem applies single-stream beamforming and satisfies some constraints with equality.

### 5.1 Extending Multiuser MIMO to Multicell MIMO

If reliable CSI can be achieved at the transmitter and receivers, multiuser MIMO transmission is a promising way of enhancing the throughput of wireless systems with one base station and many users; a survey on this immense research area is provided in [GKH<sup>+</sup>07]. The main idea is to employ multiple transmit antennas to exploit the spatial dimension and serve multiple users on a given frequency band. As a single base station is in charge in multiuser MIMO, it can make autonomous resource allocation

decisions and be sure that no uncoordinated interference appears within the cell.

A different story emerges in multicell MIMO systems, where many base stations are employed to serve many users simultaneously using the same frequency resources. The counterpart of multiuser MIMO in cellular networks have been given many names, including *network MIMO* and *coordinated multi-point* (CoMP) transmission. It is based on the same idea of exploiting the spatial dimension for serving multiple users in parallel while still controlling the interference. The initial work on network MIMO in [SZ01, ZD04, KJV06] assumed perfect co-processing at the base stations and modeled the whole network as one large multiuser MIMO system where the transmit antennas happen to be distributed over a large area; the multicell characteristics were basically reduced to just constraining the transmit power per transmitter array or antenna, instead of the total transmit power. While mathematically convenient, this approach leads to several implicit assumptions that are hard to justify in practice. Firstly, global CSI is required, which puts huge demands on the channel estimation, feedback links, and backhaul networks [MF08]. Secondly, coherent multicell transmission requires very accurate synchronization (see Chapter 8) and increases the delay-spread [ZMM<sup>+</sup>08], potentially turning flat-fading channels into frequency-selective. Thirdly, the complexity of centralized scheduling and precoding algorithms is infeasible in terms of computations, delays and scalability.

Various alternative models have been proposed to capture multicell-specific characteristics. The CSI requirements were reduced in [JTS<sup>+</sup>08, NEHA08] by using the one-dimensional Wyner model where interference only comes from immediate neighboring cells. The base stations in [MF08, HTH<sup>+</sup>09, ZCA<sup>+</sup>09] are divided into *static disjoint cooperation clusters*, where each cluster basically is operated as a multiuser MIMO system. If the clusters are sufficiently small, this approach enables practical channel acquisition and coordination within each cluster. Networks with static clusters will unfortunately provide poor spectral efficiency when the user distribution is heterogeneous [MBG<sup>+</sup>11] and will still suffer from out-of-cluster interference. The impact of these drawbacks can be reduced by having different static disjoint cooperation clusters on different subcarriers [MF11], by increasing the cluster size and serve each user by a subset of its base stations [BTO<sup>+</sup>11], by having fractional frequency reuse in the cell edge areas [LZX<sup>+</sup>10], and by changing the disjoint clusters over time [PGH08, MBG<sup>+</sup>11]. But since the clustering in these approaches is built on a base station-perspective, the consequence is that there will be strict boundaries between the clusters where uncoordinated interference arises. Steps toward more dynamic and flexible multicell coordination were taken in [TCJ08, KK10] by creating clusters from a user-centric perspective. This means that each base station has its own set of users to serve.

For each user, the base station coordinates with those base stations that also serve this user. However, global CSI and interference coordination was assumed in these works, which is not feasible in large networks.

### 5.1.1 Dynamic Cooperation Clusters

Next, we extend the downlink single-cell system model in Chapter 2.1 to a multicell environment with  $K_t$  base stations, where the  $j$ th base station is denoted  $\text{BS}_j$  and is equipped with  $N_j$  antennas. The total number of transmit antennas is still denoted  $N = \sum_{j=1}^{K_t} N_j$ . Our general multicell system model will acknowledge the following observations:

- Each user is jointly served by a subset of all base stations;
- Some base stations and users are very far apart, making it impractical to estimate and separate the interference on these channels from the background noise.

Based on these observations, we propose a coordination structure:

*Definition 5.1. Dynamic cooperation clusters* means that  $\text{BS}_j$

- has channel estimates to users in  $\mathcal{C}_j \subseteq \{1, \dots, K_r\}$ , while interference generated to users  $\bar{k} \notin \mathcal{C}_j$  is negligible and can be treated as part of the background noise;
- serves the users in  $\mathcal{D}_j \subseteq \mathcal{C}_j$  with data.

This coordination framework is characterized by the sets  $\mathcal{C}_j, \mathcal{D}_j \forall j$ , which are illustrated in Figure 5.1. The mnemonic rule is that  $\mathcal{D}_j$  describes *data* from  $\text{BS}_j$ , while  $\mathcal{C}_j$  describes *coordination* from  $\text{BS}_j$ . The membership of users to these sets changes dynamically during operation (e.g., based on individual user locations and the user density in different areas), such that the system only accepts the overhead involved in interference coordination and joint transmission if the expected performance gains are substantial. How to select these sets efficiently is a very interesting and important problem, but the solution depends on the system architecture and is beyond the scope of this thesis (see [ZL04, FGH06, PDF<sup>+</sup>08, XCL10, BTO<sup>+</sup>11, MBG<sup>+</sup>11]). However, a simple scheme would be to include  $\text{MS}_k$  in  $\mathcal{C}_j$  if the (current) average channel gain from  $\text{BS}_j$  is above a certain threshold. If the gain is also above a second (larger) threshold, the user is also included in  $\mathcal{D}_j$ . Observe that although  $\mathcal{C}_j, \mathcal{D}_j$  can be selected decentralized at  $\text{BS}_j$  and varies relatively slowly (e.g., with the long-term statistics), the network needs to know if it should route a certain user's data to the base station and some rapid coordination mechanism between adjacent base stations is required during

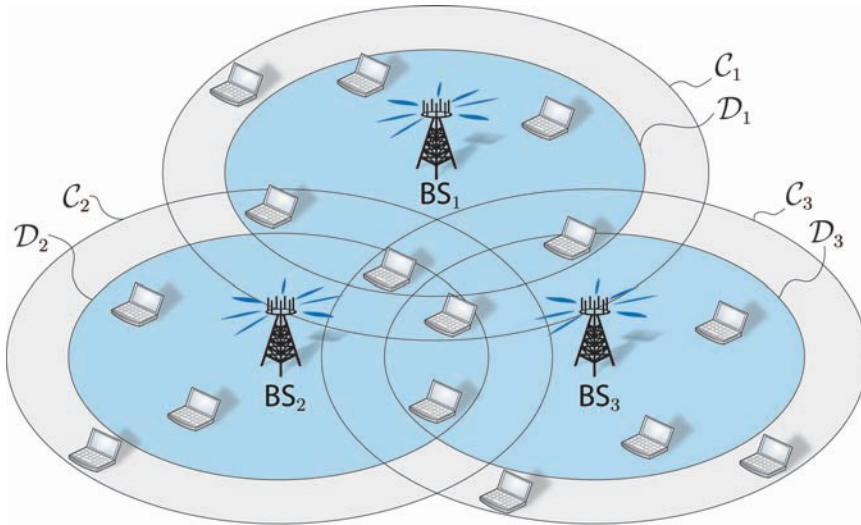


Figure 5.1: Schematic intersection of three cells.  $BS_j$  serves users in the inner circle ( $\mathcal{D}_j$ ), while coordinating interference to users in the outer circle ( $\mathcal{C}_j$ ). Ideally, negligible interference is caused to users outside both circles.

each resource allocation decision. This can be achieved through local message passing [NEHA08] and imperfections can be handled by decentralized decision making [ZG10b].

The intention of our coordination framework is two-fold. Firstly, it enables joint analysis of different levels of multicell coordination (including everything from interference channels to ideal network MIMO systems). Secondly, it resolves some of the issues that appear when multicell MIMO is viewed as a multiuser MIMO system with distributed power constraints. In our framework,  $BS_j$  only needs to know its own channel to users that receive non-negligible interference from it—a natural assumption since these are the users for which  $BS_j$  can achieve reliable channel estimates.<sup>1</sup> In addition, only neighboring base stations need to be phase synchronized and only a limited increase in delay-spread will occur (which is easy to handle in OFDM systems by increasing the cyclic prefix [ZMM<sup>+</sup>08]).

<sup>1</sup>In TDD systems, multiple base stations can exploit the same uplink training sequence to estimate their respective channels. The CSI acquisition is more demanding in FDD systems, since more resources are required for CSI feedback to the additional base stations (and possibly some extra backhaul signaling).

### 5.1.2 General Multicell System Model

Motivated by the analysis in Chapter 4.2 and for analytical convenience, we assume that each user only has one effective antenna.<sup>2</sup> The channel from all base stations to  $\text{MS}_k$  is denoted  $\mathbf{h}_k = [\mathbf{h}_{1k}^T \dots \mathbf{h}_{K_t k}^T]^T \in \mathbb{C}^{N \times 1}$ , where  $\mathbf{h}_{jk} \in \mathbb{C}^{N_j \times 1}$  is the channel from  $\text{BS}_j$ . Based on the coordination framework in Definition 5.1, only certain channel elements in  $\mathbf{h}_k$  will carry data and/or non-negligible interference. These can be selected by the diagonal matrices  $\mathbf{D}_k \in \mathbb{C}^{N \times N}$  and  $\mathbf{C}_k \in \mathbb{C}^{N \times N}$ , which are defined as

$$\mathbf{D}_k = \begin{bmatrix} \mathbf{D}_{1k} & & \mathbf{0} \\ & \ddots & \\ \mathbf{0} & & \mathbf{D}_{K_t k} \end{bmatrix} \quad \text{where} \quad \mathbf{D}_{jk} = \begin{cases} \mathbf{I}_{N_j}, & \text{if } k \in \mathcal{D}_j, \\ \mathbf{0}_{N_j}, & \text{otherwise,} \end{cases} \quad (5.1)$$

$$\mathbf{C}_k = \begin{bmatrix} \mathbf{C}_{1k} & & \mathbf{0} \\ & \ddots & \\ \mathbf{0} & & \mathbf{C}_{K_t k} \end{bmatrix} \quad \text{where} \quad \mathbf{C}_{jk} = \begin{cases} \mathbf{I}_{N_j}, & \text{if } k \in \mathcal{C}_j, \\ \mathbf{0}_{N_j}, & \text{otherwise.} \end{cases} \quad (5.2)$$

Thus,  $\mathbf{h}_k^H \mathbf{D}_k$  is the channel that carries data to  $\text{MS}_k$  and  $\mathbf{h}_k^H \mathbf{C}_k$  is the channel that carries non-negligible interference. It is necessary to have both  $\mathbf{D}_k$  and  $\mathbf{C}_k$ , to make sure that only the correct base stations transmit to  $\text{MS}_k$  when solving a resource allocation problem.

Extending the single-cell input-output model in (2.1), the symbol-sampled complex-baseband received signal at  $\text{MS}_k$  is  $y_k \in \mathbb{C}$  and is given by

$$y_k = \mathbf{h}_k^H \mathbf{C}_k \sum_{\bar{k}=1}^{K_r} \mathbf{D}_{\bar{k}} \bar{\mathbf{s}}_{\bar{k}} + n_k, \quad (5.3)$$

where the time instant has been removed for notational convenience. The additive term  $n_k$  is assumed to be zero-mean, to have variance  $\sigma_k^2$ , and to model both noise and weak interference from all  $\text{BS}_j$  with  $k \notin \mathcal{C}_j$  (see Definition 5.1). This assumption limits the amount of CSI required to analyze the transmission and is reasonable if base stations coordinate interference to all cell edge users of adjacent cells. When nothing else is said,  $\text{BS}_j$  is assumed to know the channels  $\mathbf{h}_{jk}$  perfectly to all users  $k \in \mathcal{C}_j$ .

Just as in the single-cell scenario, the transmission is limited by the  $L_p$  linear power constraints in (2.4) and each user  $k$  has the  $L_k$  soft-shaping constraints in (2.5). Each power constraint in multicell systems will typically only affect one base station, but the analysis in this and succeeding chapters can be applied to any set of linear constraints. As mentioned briefly in Chapter 2, the matrices  $\mathbf{D}_k$  can be viewed as being soft-shaping constraints with  $\mathbf{T}_{1k} = \mathbf{I}_N - \mathbf{D}_k$ , which forbid all  $\text{BS}_j$  with  $k \notin \mathcal{D}_j$  from transmitting to  $\text{MS}_k$ .

---

<sup>2</sup>This model applies to low-complexity multi-antenna users that fix a receive combining prior to transmission optimization to achieve good channel conditions and accurate CSI feedback; see Chapter 4.2.

### 5.1.3 Examples: Two Simple Multicell Scenarios

We conclude this section by illustrating that the proposed dynamic cooperation clusters can describe a variety of multicell scenarios. We provide two simple examples: ideal network MIMO systems [KFV06] (where all base stations serve all users) and interference channels [SCP11] (with only one unique user per base station).

*Example 5.1 (Ideal Network MIMO System).* All base stations serve and coordinate interference to all users, thus  $\mathbf{D}_k = \mathbf{C}_k = \mathbf{I}_N$  for all  $k$ . If a total power constraint is used, then  $L = 1$  and  $\mathbf{Q}_1 = \mathbf{I}_N$ . If per-antenna constraints are used, then  $L = N$  and  $\mathbf{Q}_l$  is only non-zero on the  $l$ th diagonal element. If per-transmitter constraints are used, then  $L = K_t$  and  $\mathbf{Q}_l$  is block-diagonal and only the  $l$ th block is non-zero.

*Example 5.2 (Two-user MISO Interference Channel).* Let  $\text{BS}_k$  serve  $\text{MS}_k$  and coordinate interference to the other user. Then,  $\mathbf{D}_1 = \begin{bmatrix} \mathbf{I}_{N_1} & \mathbf{0} \\ \mathbf{0} & \mathbf{0} \end{bmatrix}$  and  $\mathbf{D}_2 = \begin{bmatrix} \mathbf{0} & \mathbf{0} \\ \mathbf{0} & \mathbf{I}_{N_2} \end{bmatrix}$ , while  $\mathbf{C}_1 = \mathbf{C}_2 = \mathbf{I}_N$ . If each base station has its own total power constraint, then  $L = 2$  and  $\mathbf{Q}_l = \mathbf{D}_l$  for  $l = 1, 2$ .

## 5.2 Multicell Performance Measures

In this section, we propose a general way of measuring the performance in multicell systems. It is instructive to separate the performance into two parts: 1) the performance that each user experiences; and 2) a system-level criterion that determines if the resources are allocated among the users in a good way. These two parts are considered in the following subsections.

### 5.2.1 User Performance

Recall that we assumed the use of single user detection in Chapter 2.1 to achieve simple and practical user devices. Under this assumption, the signal-to-interference-and-noise ratio (SINR) for  $\text{MS}_k$  is

$$\begin{aligned} \text{SINR}_k(\mathbf{S}_1, \dots, \mathbf{S}_{K_r}) &= \frac{\mathbf{h}_k^H \mathbf{C}_k \mathbf{D}_k \mathbf{S}_k \mathbf{D}_k^H \mathbf{C}_k^H \mathbf{h}_k}{\sigma_k^2 + \mathbf{h}_k^H \mathbf{C}_k \left( \sum_{\bar{k} \neq k} \mathbf{D}_{\bar{k}} \mathbf{S}_{\bar{k}} \mathbf{D}_{\bar{k}}^H \right) \mathbf{C}_k^H \mathbf{h}_k} \\ &= \frac{\mathbf{h}_k^H \mathbf{D}_k \mathbf{S}_k \mathbf{D}_k^H \mathbf{h}_k}{\sigma_k^2 + \mathbf{h}_k^H \mathbf{C}_k \left( \sum_{\bar{k} \in \mathcal{I}_k} \mathbf{D}_{\bar{k}} \mathbf{S}_{\bar{k}} \mathbf{D}_{\bar{k}}^H \right) \mathbf{C}_k^H \mathbf{h}_k} \end{aligned} \quad (5.4)$$

where  $\mathbf{S}_k = \mathbb{E}\{\mathbf{s}_k \mathbf{s}_k^H\}$  is the signal correlation matrix to  $\text{MS}_k$  and the second equality follows from  $\mathbf{C}_k \mathbf{D}_k = \mathbf{D}_k$  and  $\mathbf{C}_k \mathbf{D}_{\bar{k}} \neq \mathbf{0}$  only for users  $\bar{k}$  in

$$\mathcal{I}_k = \bigcup_{\{j \in \mathcal{J}; k \in \mathcal{C}_j\}} \mathcal{D}_j \setminus \{k\}. \quad (5.5)$$

This is the set of co-users being served by the same base stations that serve  $\text{MS}_k$ . For brevity, we will write  $\text{SINR}_k$  instead of  $\text{SINR}_k(\mathbf{S}_1, \dots, \mathbf{S}_{K_r})$ .

The achievable performance of a user can be measured in different ways, for example the data rate, mean squared error (MSE), and bit/symbol error rate (BER/SER) [PCL03]. Each quality measure has its merits and demerits. The data rate has a simple and marketable interpretation, but builds on idealized coding and complexity assumptions. The MSE often gives simple expressions, but is only vaguely connected to the user-experienced service quality. The BER/SER (at a given signal constellation) is self-explaining, but typically has complicated expressions. Fortunately, most common quality measures (including those mentioned above) are monotonic functions of the SINR and therefore we describe the performance of  $\text{MS}_k$  by an arbitrary continuous function  $g_k(\text{SINR}_k)$  of the SINR that is *strictly monotonically increasing* and satisfies  $g_k(0) = 0$  (for notational convenience). Good user performance thus means large positive values of  $g_k(\text{SINR}_k)$ .<sup>3</sup>

The user performance is limited by the power and soft-shaping constraints in (2.4) and (2.5), respectively, but also by co-user interference. The SINR in (5.4) improves if the interference is decreased, but this will on the other hand degrade the SINRs for other users. This relationship is characterized by the performance region:

*Definition 5.2.* The achievable *performance region*  $\mathcal{R} \subset \mathbb{R}_+^{K_r}$  is

$$\mathcal{R} = \left\{ (g_1(\text{SINR}_1), \dots, g_{K_r}(\text{SINR}_{K_r})) : (\mathbf{S}_1, \dots, \mathbf{S}_{K_r}) \in \mathbb{S} \right\} \quad (5.6)$$

where  $\mathbb{S}$  is the set of feasible transmit strategies:

$$\mathbb{S} = \left\{ (\mathbf{S}_1, \dots, \mathbf{S}_{K_r}) : \mathbf{S}_k \succeq \mathbf{0}_N, \sum_{k=1}^{K_r} \text{tr}\{\mathbf{Q}_l \mathbf{S}_k\} \leq q_l \quad \forall l, \text{tr}\{\mathbf{T}_{ik} \mathbf{S}_k\} \leq \tau_{ik} \quad \forall i, k \right\}. \quad (5.7)$$

This region describes the performance that can be guaranteed to be simultaneously achieved by the users. The shape of the  $K_r$ -dimensional performance region depends strongly on the effective channels, constraints, and dynamic cooperation clusters. In general, it is a non-convex set, but it can be characterized as being normal [Tuy00]:

*Definition 5.3.* A set  $\mathcal{T} \subset \mathbb{R}_+^n$  is called *normal* if for any point  $\mathbf{x} \in \mathcal{T}$ , all  $\mathbf{x}' \in \mathbb{R}_+^n$  with  $\mathbf{x}' \leq \mathbf{x}$  also satisfy  $\mathbf{x}' \in \mathcal{T}$  (with componentwise inequality).

*Lemma 5.1.* The performance region  $\mathcal{R}$  is a compact and normal set.

---

<sup>3</sup>We use the convention that the performance measure is a function to be maximized. Thus, if the problem is to minimize the error (e.g., MSE, BER, or SER), we maximize either its inverse or the error with a negative sign.

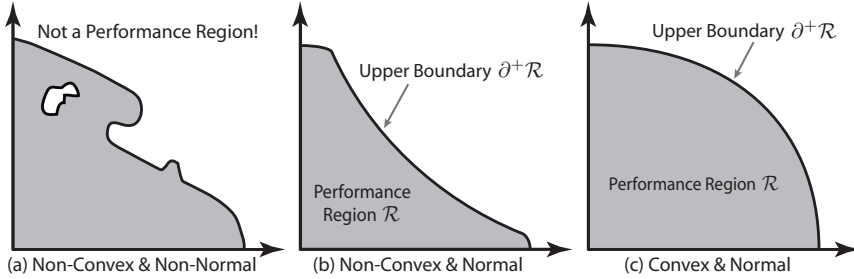


Figure 5.2: Examples of three compact regions with different shapes. Only (b) and (c) are normal and can thus be performance regions.

*Proof.* The proof is given in Appendix 5.A.1.  $\square$

This means that for any point  $\mathbf{x} \in \mathcal{R}$ , all points that give weaker performance than  $\mathbf{x}$  are also in  $\mathcal{R}$ . This property is very natural and rational. In fact, if a region is not normal it looks very unnatural; see the illustrations in Figure 5.2 where only (b) and (c) are possible shapes for a performance region, while (a) is not a simply-connected set (i.e., contains holes) and has a strange boundary. Knowing that  $\mathcal{R}$  is a normal and compact set simplifies the search for performance-optimizing points in  $\mathcal{R}$ ; they all lie on the upper boundary  $\partial^+ \mathcal{R}$  and this boundary is easy to identify since  $\mathcal{R}$  is simply-connected (i.e., contains no holes).

*Definition 5.4.* A point  $\mathbf{y}$  is an *upper boundary point* of a compact normal set  $\mathcal{T}$ , if  $\mathbf{y} \in \mathcal{T}$  while  $\{\mathbf{y}' \in \mathbb{R}_+^n : \mathbf{y}' > \mathbf{y}\} \cap \mathcal{T} = \emptyset$ . The set of all upper boundary points is called the *upper boundary of  $\mathcal{T}$*  and is denoted  $\partial^+ \mathcal{T}$ .

To determine which point on  $\partial^+ \mathcal{R}$  that is preferable, we need a system performance perspective.

### 5.2.2 System Performance

While the achievable user performance is given by the multi-dimensional performance region  $\mathcal{R}$ , the system performance is represented by a function  $f : \mathcal{R} \rightarrow \mathbb{R}$  that takes a point in  $\mathcal{R}$  as input and produces a scalar value. For a given point  $\mathbf{g} = (g_1, \dots, g_{K_r}) \in \mathcal{R}$ , typical examples are

- Sum performance:  $f(\mathbf{g}) = \sum_k g_k$ ;
- Proportional fairness:  $f(\mathbf{g}) = \prod_k g_k^{1/K_r}$  (i.e., geometric mean);
- Harmonic mean:  $f(\mathbf{g}) = K_r (\sum_k g_k^{-1})^{-1}$ ;
- Max-min fairness:  $f(\mathbf{g}) = \min_k g_k$ .

Weights can be included in all these examples to compensate for heterogeneous channel conditions, handle delay constraints, etc. A typical example is the weighted sum performance  $f(\mathbf{g}) = \sum_k w_k g_k$  with weights  $w_k \geq 0 \forall k$ .

The system performance function  $f(g_1(\text{SINR}_1), \dots, g_{K_r}(\text{SINR}_{K_r}))$  is assumed to be Lipschitz continuous and *strictly increasing*<sup>4</sup>. This is satisfied by the aforementioned examples, and by all reasonable system performance measures.<sup>5</sup> The resulting system-wide resource allocation problem can either be expressed as

$$\underset{\mathbf{g} \in \mathcal{R}}{\text{maximize}} \quad f(\mathbf{g}) \quad (5.8)$$

or identically in the following extensive way that includes all constraints:

$$\begin{aligned} & \underset{\mathbf{s}_1 \succeq \mathbf{0}_N, \dots, \mathbf{s}_{K_r} \succeq \mathbf{0}_N}{\text{maximize}} \quad f(g_1(\text{SINR}_1), \dots, g_{K_r}(\text{SINR}_{K_r})) \\ & \text{subject to} \quad \sum_{k=1}^{K_r} \text{tr}\{\mathbf{Q}_l \mathbf{s}_k\} \leq q_l \quad \forall l, \\ & \quad \quad \quad \text{tr}\{\mathbf{T}_{ik} \mathbf{s}_k\} \leq \tau_{ik} \quad \forall i, k. \end{aligned} \quad (5.9)$$

By exploiting the fact that the performance region  $\mathcal{R}$  is compact and normal, we have the following important result.

*Lemma 5.2.* If  $f(\cdot)$  is a strictly increasing function and  $\mathcal{R}$  is a compact and normal set, the global optimum (if it exists) to (5.8) and (5.9) is attained on  $\partial^+ \mathcal{R}$ . In addition, for any  $\tilde{\mathbf{g}} \in \partial^+ \mathcal{R}$  there exists a strictly increasing  $f(\cdot)$  with  $\tilde{\mathbf{g}}$  as global optimum.

*Proof.* The proof is given in Appendix 5.A.2. □

Based on this lemma, we only need to search the upper boundary of  $\mathcal{R}$  to solve any system performance optimization problem (5.9). Unfortunately, this is not as simple as it seems; [LZ08] showed that sum performance maximization is NP-hard for any number of transmit antennas, while [LDL11] showed NP-hardness for the harmonic mean and proportional fairness if  $N_j > 1$ . A main characteristic of NP-hard problems is that there are no known algorithms that solve them in polynomial time, and it is widely believed that there exist no such algorithms. The analysis in Chapter 6 reveals that the user dimension,  $K_r$ , is the limiting factor in multicell resource allocation. Although the computational complexity is exponential

<sup>4</sup>A function  $f : \mathbb{R}_+^n \rightarrow \mathbb{R}$  is *strictly increasing* if for any  $\mathbf{x}, \mathbf{x}', \mathbf{x}'' \in \mathbb{R}_+^n$  such that  $\mathbf{x} \geq \mathbf{x}'$  and  $\mathbf{x} > \mathbf{x}''$ , it follows  $f(\mathbf{x}) \geq f(\mathbf{x}')$  and  $f(\mathbf{x}) > f(\mathbf{x}'')$ .

<sup>5</sup>Every continuously differentiable function is locally Lipschitz continuous, but some functions are not globally Lipschitz since the first derivative becomes infinite in the origin. The geometric mean  $\prod_k g_k^{1/K_r}$  has such problems, but these can be resolved by optimizing  $\prod_k g_k$  instead. The harmonic mean also needs additional treatment.

in  $K_r$ , it is actually polynomial in the number of antennas  $N$  and in the number of constraints  $L$ .

Based on the results of [LZ08, LDL11] it is fair to say that the system performance optimization problem in (5.9) is generally NP-hard. However, there is a useful problem that can be solved efficiently (i.e., in polynomial time), namely the max-min fairness optimization (defined above) [LDL11]. It belongs to a larger category of problems, *fairness-profile optimization* (FPO), that we introduce in Chapter 6. It is also an essential subproblem of the *branch-reduce-and-bound* (BRB) algorithm that we propose in Chapter 6 for solving (5.9) in a systematic way that guarantees finding the solution in finitely many iterations. The BRB algorithm therefore provides an ideal performance bound for practical resource allocation strategies, although the NP-hardness makes the convergence of the BRB algorithm unsuitable for real-time implementation.

### 5.3 Basic Properties of Optimal Strategies

In this section, we derive two properties of the optimal solutions to (5.9):

- Optimality of single-stream beamforming;
- Conditions for full power usage.

Taking these optimality properties into account when solving (5.9) will greatly reduce the search space for optimal solutions. We will exploit the derived properties for improved resource allocation in Chapters 6 and 7.

#### 5.3.1 Optimality of Single-Stream Beamforming

The first property is the sufficiency of considering signal correlation matrices  $\mathbf{S}_k$  that are rank one. This might seem intuitive when each user only has a single effective antenna and is often assumed without discussion (see [YL07, DY10, TCJ08, ZWN08b, TPK09, VPW10]). However, the following toy example shows that it is actually not a necessary condition under general system performance functions and power constraints (i.e., high-rank solutions can give the same performance, but never better, than the rank-one solutions).

*Example 5.3.* Consider a point-to-point system ( $K_t = K_r = 1$ ) with two transmit antennas, the channel vector  $\mathbf{h}_1 = [1 \ 0]^T$ , and the per-antenna power constraints  $\text{tr} \left\{ \begin{bmatrix} 1 & 0 \\ 0 & 0 \end{bmatrix} \mathbf{S}_1 \right\} \leq 1$  and  $\text{tr} \left\{ \begin{bmatrix} 0 & 0 \\ 0 & 1 \end{bmatrix} \mathbf{S}_1 \right\} \leq 1$ . Under these conditions, (5.2) is solved optimally by both the rank-one single correlation matrix  $\mathbf{S}_1 = \begin{bmatrix} 1 & 0 \\ 0 & 0 \end{bmatrix}$  and by the rank-two matrix  $\mathbf{S}_1 = \begin{bmatrix} 1 & 0 \\ 0 & 1 \end{bmatrix}$ .

To prove the sufficiency of rank-one signal correlation matrices, we start with a lemma from [WES08].

*Lemma 5.3.* The convex optimization problem

$$\begin{aligned} & \underset{\mathbf{X} \succeq 0}{\text{maximize}} && \mathbf{a}^H \mathbf{X} \mathbf{a} \\ & \text{subject to} && \text{tr}\{\mathbf{B}_i \mathbf{X}\} \leq b_i \quad \text{for } i = 1, \dots, M, \end{aligned} \quad (5.10)$$

with arbitrary Hermitian matrices  $\mathbf{B}_i \succeq 0$  and scalars  $b_i \geq 0 \forall i$ , has optimal solutions with  $\text{rank}(\mathbf{X}) \leq 1$ .

*Proof.* The proof is given in [WES08, Appendix III].  $\square$

By applying this lemma, we achieve the following main result.

*Theorem 5.1.* If there exist feasible solutions to (5.9), there exist optimal solutions that apply single-stream beamforming (i.e.,  $\text{rank}(\mathbf{S}_k) \leq 1 \forall k$ ).

*Proof.* The proof is given in Appendix 5.A.3.  $\square$

The optimality of single-stream beamforming both decreases the search space for optimal solutions and makes the solution easier to implement in practice (since vector coding or successive interference cancelation are required if  $\text{rank}(\mathbf{S}_k) > 1$  [GJJV03]). Observe that  $\text{rank}(\mathbf{S}_k) \leq 1$  in Theorem 5.1 implies that the rank might be zero, which corresponds to  $\mathbf{S}_k = \mathbf{0}_N$  (i.e., no transmission to  $\text{MS}_k$  at the current time instant).

Recently, similar optimality results for single-stream beamforming have been derived for a few special multicell scenarios. The MISO interference channel was considered in [SCP11] and a certain class of multicell systems was considered in [MJ11a] under per-transmitter power constraints. Theorem 5.1 generalizes these results by considering arbitrary linear constraints and our general multicell framework.

### 5.3.2 Conditions for Full Power Usage

If only the total power usage over all base station is constrained, it is trivial to prove that the optimal solution to (5.9) will use all available power. Under general linear power and soft-shaping constraints, it may be better to not use full power at each transmitter or antenna; there is a balance between increasing signal gains and limiting the interference. This is illustrated by the following toy example:

*Example 5.4.* Consider a two-user interference channel with single-antenna base stations ( $K_t = K_r = 2$ ,  $N_1 = N_2 = 1$ ) and the channel vectors  $\mathbf{h}_1 = [1 \ \sqrt{1/10}]^T$  and  $\mathbf{h}_2 = [\sqrt{1/2} \ 1]^T$ .  $\text{BS}_j$  transmits to  $\text{MS}_j$  and coordinates interference to both users, meaning that  $\mathbf{D}_1 = \begin{bmatrix} 1 & 0 \\ 0 & 0 \end{bmatrix}$ ,  $\mathbf{D}_2 = \begin{bmatrix} 0 & 0 \\ 0 & 1 \end{bmatrix}$ , and  $\mathbf{C}_1 = \mathbf{C}_2 = \mathbf{I}_2$ . The per-transmitter power is constrained as  $\text{tr}\{\mathbf{D}_j \mathbf{S}_j\} \leq 20 \forall j$ .

Under max-min data rate optimization with  $f(\mathbf{S}_1, \mathbf{S}_2) = \min_k \log_2(1 + \text{SINR}_k)$ , the optimal transmit strategy for (5.9) is  $\mathbf{S}_1 = 10\mathbf{D}_1$  and  $\mathbf{S}_2 =$

20D<sub>2</sub>. This strategy gives  $\text{SINR}_1 = \text{SINR}_2 = 10/3$ , and observe that only BS<sub>2</sub> uses full power. If BS<sub>1</sub> would increase its power usage, then  $\text{SINR}_2$  would decrease and thus the performance would be degraded.

In principle, knowing that a certain constraint is active removes one dimension from the optimization problem. The following theorem provides conditions for when full power should be used in general multicell systems.

*Theorem 5.2.* For the resource allocation problem in (5.9) it holds that

- There exist optimal strategies that satisfy at least one constraint with equality.
- If only the total power per transmitter is constrained, BS<sub>*j*</sub> should use full power if  $|\mathcal{C}_j| \leq N_j$ .

*Proof.* The proof is given in Appendix 5.A.4. □

The interpretation is that at least one constraint should be active in the optimal solution. In addition, the fewer users that a base station coordinates interference to, the more power can be used at this base station. BS<sub>*j*</sub> should use full power if there are fewer than  $N_j$  users in  $\mathcal{C}_j$ , which can be relaxed by only considering those users in  $\mathcal{C}_j$  that are actually scheduled (i.e., receive non-zero signal power).

## 5.4 Summary

There are many similarities between multiuser MIMO and multicell MIMO, but also important differences that need to be managed when multiuser MIMO techniques are extended to multicell systems. In this chapter, we proposed a novel and flexible multicell framework that can describe everything from interference channels to ideal network MIMO systems. In particular, we suggest that intercell interference is managed by having *dynamic cooperation clusters* where each base station coordinates interference to exactly those users that it causes non-negligible interference to, while only sending data to a subset of them. In addition, we have proposed a general way of measuring the performance in such multicell systems. The user performance was based on arbitrary monotonic increasing functions of the SINRs, while the system performance criterion is an increasing function of each user's performance. The performance region is a concept that ties the user and system performance together. This region is in general non-convex, but we have shown that it satisfies the properties of being compact and normal. Finally, we proved that the optimal system performance can be achieved using single-stream beamforming and derived conditions on the use of full transmit power.

## 5.A Collection of Proofs

### 5.A.1 Proof of Lemma 5.1

To prove that the set is normal, take  $\mathbf{x} = (x_1, \dots, x_{K_r}) \in \mathcal{R}$  and assume that  $\mathbf{S}_1^*, \dots, \mathbf{S}_{K_r}^*$  is a feasible strategy that attains this point. We want show that any given  $\mathbf{x}' = (x'_1, \dots, x'_{K_r}) \in \mathbb{R}_+^{K_r}$  with  $\mathbf{x}' \leq \mathbf{x}$  also belongs to  $\mathcal{R}$ . To this end, we consider the transmit strategy  $p_1 \mathbf{S}_1^*, \dots, p_{K_r} \mathbf{S}_{K_r}^*$ , where  $p_1, \dots, p_{K_r}$  is a set of power allocation coefficients that should belong to

$$\mathcal{P} = \left\{ (p_1, \dots, p_{K_r}) : \sum_{k=1}^{K_r} p_k \text{tr}\{\mathbf{Q}_l \mathbf{S}_k^*\} \leq q_l \quad \forall l, \quad p_k \text{tr}\{\mathbf{T}_{ik} \mathbf{S}_k^*\} \leq \tau_{ik} \quad \forall i, k \right\} \quad (5.11)$$

to make the strategy feasible. Obviously, the point  $\mathbf{x}$  is achieved by selecting  $\mathbf{p}^* = [p_1^*, \dots, p_{K_r}^*]^T = \mathbf{1}_N$ . To prove that the given  $\mathbf{x}'$  belongs to  $\mathcal{R}$ , we need to find  $(p_1, \dots, p_{K_r}) \in \mathcal{P}$  that gives the SINRs

$$\gamma'_k = g_k^{-1}(x'_k) = \frac{p_k \mathbf{h}_k^H \mathbf{C}_k \mathbf{D}_k \mathbf{S}_k^* \mathbf{D}_k^H \mathbf{C}_k^H \mathbf{h}_k}{\sigma_k^2 + \mathbf{h}_k^H \mathbf{C}_k \left( \sum_{\bar{k} \neq k} \mathbf{D}_{\bar{k}} p_{\bar{k}} \mathbf{S}_{\bar{k}}^* \mathbf{D}_{\bar{k}}^H \right) \mathbf{C}_k^H \mathbf{h}_k} = \frac{p_k}{b_k + \sum_{\bar{k} \neq k} p_{\bar{k}} a_{k\bar{k}}} \quad (5.12)$$

for all  $k$ , where we introduced the notation<sup>6</sup>

$$a_{k\bar{k}} = \frac{\mathbf{h}_k^H \mathbf{C}_k \mathbf{D}_{\bar{k}} \mathbf{S}_{\bar{k}}^* \mathbf{D}_{\bar{k}}^H \mathbf{C}_k^H \mathbf{h}_k}{\mathbf{h}_k^H \mathbf{C}_k \mathbf{D}_k \mathbf{S}_k^* \mathbf{D}_k^H \mathbf{C}_k^H \mathbf{h}_k}, \quad (5.13)$$

$$b_k = \frac{\sigma_k^2}{\mathbf{h}_k^H \mathbf{C}_k \mathbf{D}_k \mathbf{S}_k^* \mathbf{D}_k^H \mathbf{C}_k^H \mathbf{h}_k}.$$

In matrix form, we can summarize (5.12) as

$$\underbrace{\begin{bmatrix} \gamma'_1 & 0 & 0 \\ 0 & \ddots & 0 \\ 0 & 0 & \gamma'_{K_r} \end{bmatrix}}_{=\mathbf{\Gamma}'^*} \left( \underbrace{\begin{bmatrix} 0 & a_{12} & \dots \\ a_{21} & \ddots & \vdots \\ a_{K_r 1} & \dots & 0 \end{bmatrix}}_{=\mathbf{A}} \underbrace{\begin{bmatrix} p_1 \\ \vdots \\ p_{K_r} \end{bmatrix}}_{=\mathbf{p}} + \underbrace{\begin{bmatrix} b_1 \\ \vdots \\ b_{K_r} \end{bmatrix}}_{=\mathbf{b}} \right) = \underbrace{\begin{bmatrix} p_1 \\ \vdots \\ p_{K_r} \end{bmatrix}}_{=\mathbf{p}} \quad (5.14)$$

or equally

$$(\mathbf{I}_N - \mathbf{\Gamma}'^* \mathbf{A}) \mathbf{p} = \mathbf{\Gamma}'^* \mathbf{b}. \quad (5.15)$$

As noted in [PSC05], the necessary and sufficient condition for (5.15) to have a positive solution  $\mathbf{p}$  for every  $\mathbf{b} \geq \mathbf{0}_{K_r \times 1}$  is that the spectral radius

<sup>6</sup>If  $\mathbf{S}_k^* = \mathbf{0}_N$  for some user  $k$ , meaning that  $x_k = x'_k = 0$ , we should remove these users from the analysis to make  $a_{k\bar{k}}$  and  $b_k$  well-defined.

of  $\Gamma' \mathbf{A}$  is strictly bounded by unity. Assume for a moment that this holds true, then we can find a power allocation that attains  $\mathbf{x}'$  by solving (5.15) as

$$\mathbf{p} = (\mathbf{I}_N - \Gamma' \mathbf{A})^{-1} \Gamma' \mathbf{b} = \left( \mathbf{I} + \sum_{n=1}^{\infty} (\Gamma' \mathbf{A})^n \right) \Gamma' \mathbf{b}. \quad (5.16)$$

The second equality follows from a Taylor expansion of  $(\mathbf{I}_N - \Gamma' \mathbf{A})^{-1}$  and shows that each  $p_k$  is given by a polynomial in  $\gamma'_1, \dots, \gamma'_{K_r}$  with positive coefficients. Thus, any increase in  $\gamma'_k$  will increase at least one of the power allocation coefficients. This means that  $\mathbf{p} \leq \mathbf{p}^*$  since  $\gamma'_k \leq \gamma_k = g_k^{-1}(x_k)$  for all  $k$ . In other words,  $\mathbf{p} \in \mathcal{P}$  since each user requires less power than with the feasible strategy that attained  $\mathbf{x}$ .

We have now given a constructive proof of that any  $\mathbf{x}' \in \mathbb{R}_+^{K_r}$  (with  $\mathbf{x}' \leq \mathbf{x}$ ) belongs to  $\mathcal{R}$ , if only  $\text{radius}\{\Gamma' \mathbf{A}\} < 1$ . To show that  $\text{radius}\{\Gamma' \mathbf{A}\} < 1$  is satisfied, we bring in [SB05, Theorem 3.5] from the theory of interference functions, which basically says that

$$\begin{aligned} \text{radius}\{\Gamma' \mathbf{A}\} &= \min_{\mathbf{p} > \mathbf{0}_N: \|\mathbf{p}\|_1 = N} \left( \max_{1 \leq k \leq K_r} \frac{\gamma'_k \sum_{\bar{k} \neq k} p_{\bar{k}} a_{k\bar{k}}}{p_k} \right) \\ &< \max_{1 \leq k \leq K_r} \underbrace{\gamma_k \left( \frac{b_k + \sum_{\bar{k} \neq k} p_{\bar{k}}^* a_{k\bar{k}}}{p_k} \right)}_{=1/\gamma_k} = 1. \end{aligned} \quad (5.17)$$

The inequality follows from plugging in the power allocation  $\mathbf{p} = \mathbf{1}_{K_r}$  (which might not minimize the expression), replacing  $\gamma'_k$  with  $\gamma_k$  and adding  $b_k > 0$  to the numerators. We observe that this strict upper bound is nothing else than  $\gamma_k/\gamma_k = 1$  and thus the spectral norm is strictly bounded by unity.

Finally, we should prove that  $\mathcal{R}$  is a compact set. First, observe that the set of feasible transmit strategies  $\mathbb{S}$  in (5.7) is compact. Next, observe that  $\text{SINR}_k(\mathbf{S}_1, \dots, \mathbf{S}_{K_r})$  is a continuous function and that the user performance functions  $g_k(\text{SINR}_k)$  are continuous by definition. Finally, we invoke [Rud76, Theorem 4.14], which says that the continuous mapping of a compact set is also a compact set. Since  $\mathcal{R}$  is the image of a continuous mapping from  $\mathbb{S}$ , the performance region is compact.

### 5.A.2 Proof of Lemma 5.2

The first statement is proved in [Tuy00, Proposition 7]. The second statement is proved using the strictly increasing function  $f(\mathbf{g}) = \min_k g_k/\tilde{g}_k$  for the given  $\tilde{\mathbf{g}} = (\tilde{g}_1, \dots, \tilde{g}_{K_r}) \in \partial^+ \mathcal{R}$ . Obviously,  $\max_{\mathbf{g} \in \mathcal{R}} f(\mathbf{g}) \geq f(\tilde{\mathbf{g}}) = 1$

and assume for the purpose of contradiction that there exists  $\mathbf{g}^* \in \mathcal{R}$  that achieves strict inequality. This means that  $\mathbf{g}^* > \tilde{\mathbf{g}}$  and thus  $\tilde{\mathbf{g}}$  cannot be an upper boundary point since that would require  $\{\mathbf{y}' \in \mathbb{R}_+^n : \mathbf{y}' > \tilde{\mathbf{g}}\} \cap \mathcal{R} \neq \emptyset$  (according to Definition 5.4). This contradiction yields  $\max_{\mathbf{g} \in \mathcal{R}} f(\mathbf{g}) = f(\tilde{\mathbf{g}})$  and thus  $\tilde{\mathbf{g}}$  is the (non-unique) global optimum.

### 5.A.3 Proof of Theorem 5.1

Let  $\mathbf{S}_1^*, \dots, \mathbf{S}_{K_r}^*$  be an optimal solution to (5.9). For each such optimal signal correlation matrix  $\mathbf{S}_k^*$ , we can create the problem

$$\begin{aligned} & \underset{\mathbf{S}_k \succeq \mathbf{0}}{\text{maximize}} && \mathbf{h}_k^H \mathbf{D}_k \mathbf{S}_k \mathbf{D}_k^H \mathbf{h}_k \\ & \text{subject to} && \mathbf{h}_k^H \mathbf{C}_{\bar{k}} \mathbf{D}_k \mathbf{S}_k \mathbf{D}_k^H \mathbf{C}_{\bar{k}}^H \mathbf{h}_{\bar{k}} \leq z_{k\bar{k}}^2 \forall \bar{k} \neq k, \\ & && \text{tr}\{\mathbf{Q}_l \mathbf{S}_k\} \leq \tilde{q}_{lk} \quad \forall l, \\ & && \text{tr}\{\mathbf{T}_{ik} \mathbf{S}_k\} \leq \tilde{\tau}_{ik} \quad \forall i, \end{aligned} \quad (5.18)$$

where  $z_{k\bar{k}}^2 = \mathbf{h}_k^H \mathbf{C}_{\bar{k}} \mathbf{D}_k \mathbf{S}_k^* \mathbf{D}_k^H \mathbf{C}_{\bar{k}}^H \mathbf{h}_{\bar{k}}$ ,  $\tilde{q}_{lk} = \text{tr}\{\mathbf{Q}_l \mathbf{S}_k^*\}$ , and  $\tilde{\tau}_{ik} = \text{tr}\{\mathbf{T}_{ik} \mathbf{S}_k^*\}$ . This problem tries to maximize the signal gain under the constraint that neither more interference is caused nor more transmit power is used than with  $\mathbf{S}_k^*$ . Obviously,  $\mathbf{S}_k^*$  is an optimal solution to (5.18) (if strictly better solutions would have existed, these could have been used to improve the performance in (5.9), which is a contradiction).

Now, observe that (5.18) has the structure of (5.10) in Lemma 5.3 (since  $\mathbf{h}_k^H \mathbf{C}_{\bar{k}} \mathbf{D}_k \mathbf{S}_k \mathbf{D}_k^H \mathbf{C}_{\bar{k}}^H \mathbf{h}_{\bar{k}} = \text{tr}\{\mathbf{D}_k^H \mathbf{C}_{\bar{k}}^H \mathbf{h}_{\bar{k}} \mathbf{h}_k^H \mathbf{C}_{\bar{k}} \mathbf{D}_k \mathbf{S}_k\}$ ). Thus, if  $\mathbf{S}_k^*$  has rank greater than one, Lemma 5.3 shows that there exist an alternative solution  $\mathbf{S}_k^{**}$  with  $\text{rank}(\mathbf{S}_k^{**}) \leq 1$ . This solution can be used instead of  $\mathbf{S}_k^*$  without decreasing the performance.

### 5.A.4 Proof of Theorem 5.2

If  $\tau_{ik} = 0$  for some  $i, k$  or  $q_l = 0$  for some  $l$ , the first part of the theorem is always satisfied. Now assume that  $\tau_{ik} > 0 \forall i, k$  and  $q_l > 0 \forall l$ . Let  $\mathbf{S}_1^*, \dots, \mathbf{S}_{K_r}^*$  be a given optimal strategy and assume that all power constraints in (2.4) and all soft-shaping constraints in (2.5) are inactive. We define

$$\zeta = \max \left( \max_l \sum_k \text{tr}\{\mathbf{Q}_l \mathbf{S}_k^*\} / q_l, \max_{k,i} \text{tr}\{\mathbf{T}_{ik} \mathbf{S}_k^*\} / \tau_{ik} \right) \quad (5.19)$$

and note that  $\zeta > 1$  since all constraints are inactive. The alternative strategy  $\zeta \mathbf{S}_1^*, \dots, \zeta \mathbf{S}_{K_r}^*$  will satisfy all constraints and at least one of them will be active. The performance is not decreased since the factor  $\zeta$  can be seen as decreasing the relative noise power in each SINR in (5.4). Thus, there always exist a solution that satisfies at least one active constraint.

The second part is proved by contradiction. For a given optimal strategy  $\tilde{\mathbf{S}}_1, \dots, \tilde{\mathbf{S}}_{K_r}$ , suppose that BS<sub>*j*</sub> is not using full power; that is,

$$\sum_k \text{tr} \left\{ \mathbf{Q}_j^{\text{per-BS}} \tilde{\mathbf{S}}_k \right\} < q_j \quad (5.20)$$

where  $\mathbf{Q}_j^{\text{per-BS}} = \text{diag}(\mathbf{0}_{N_1}, \dots, \mathbf{0}_{N_{j-1}}, \mathbf{1}_{N_j}, \mathbf{0}_{N_{j+1}}, \dots, \mathbf{0}_{N_{K_t}})$ .

We require the existence of a  $k \in \mathcal{D}_j$  with

$$\mathbf{h}_{jk} \notin \text{span} \left( \bigcup_{\bar{k} \in \mathcal{C}_j \setminus \{k\}} \{\mathbf{h}_{j\bar{k}}\} \right). \quad (5.21)$$

This is a very mild requirement when  $|\mathcal{C}_j| \leq N_j$  (e.g., it is satisfied with probability one when the channel realizations are drawn stochastically from a distribution with non-singular covariance matrices).

Since  $\mathbf{h}_{jk} \notin \text{span}(\bigcup_{\bar{k} \in \mathcal{C}_j \setminus \{k\}} \{\mathbf{h}_{j\bar{k}}\})$ , it exists a unit-norm ZF vector  $\mathbf{v} \neq \mathbf{0}_{N_j \times 1}$  such that  $\mathbf{h}_{jk}^H \mathbf{v} \neq 0$  and  $\mathbf{h}_{j\bar{k}}^H \mathbf{v} = 0$  for all  $\bar{k} \in \mathcal{C}_j \setminus \{k\}$ . Then, the alternative signal correlation matrix  $\mathbf{S}_k = \tilde{\mathbf{S}}_k + \tilde{\mathbf{v}}\tilde{\mathbf{v}}^H$  with

$$\tilde{\mathbf{v}} = \left[ \mathbf{0}_{1 \times N_1} \dots \mathbf{0}_{1 \times N_{j-1}} \sqrt{q_j - \sum_k \text{tr}\{\mathbf{Q}_j^{\text{per-BS}} \tilde{\mathbf{S}}_k\}} \mathbf{v}^T \mathbf{0}_{1 \times N_{j+1}} \dots \mathbf{0}_{1 \times N_{K_t}} \right]^T \quad (5.22)$$

will strictly increase the signal power and will cause exactly the same co-user interference as  $\tilde{\mathbf{S}}_k$ . This contradiction to the optimality of  $\tilde{\mathbf{S}}_k$  means that BS<sub>*j*</sub> must use full transmit power if  $|\mathcal{C}_j| \leq N_j$ .

## Chapter 6

# Optimal Solutions to Multicell Resource Allocation

In this chapter, we consider the general multicell resource allocation problem that was defined in Chapter 5. We show that a certain instance of this problem, which we call *fairness-profile optimization (FPO)*, is quasi-convex and can be solved efficiently. This stands in contrast to the general resource allocation problem which is NP-hard and thus has exponential complexity. Solving this difficult problem is still important, as a benchmark, to enable evaluation of suboptimal strategies. To this end, this chapter proposes an algorithm for solving the general problem to global optimality. Our results are applicable under both perfect and uncertain CSI.

The considered multicell resource allocation problem is given in Section 6.1. The special case of FPO, which generalizes classic max-min optimization, is solved efficiently in Section 6.2. The FPO problem turns out to be an essential subproblem of the *branch-reduce-and-bound (BRB) algorithm* in Section 6.3, which solves any multicell resource allocation problem optimally. Section 6.4 shows that the BRB algorithm can be applied whenever the performance region is compact and normal and the FPO problem can be solved efficiently. In particular, we provide the details for applying it under worst-case robustness towards CSI uncertainty. Finally, some properties of the proposed algorithms and of performance regions in general are illustrated numerically in Section 6.5.

### 6.1 Multicell Resource Allocation

In this chapter, we consider a general multicell resource allocation problem based on the dynamic cooperation clusters introduced in Chapter 5. By exploiting the optimality of using (single-stream) beamforming vectors  $\mathbf{v}_k \in \mathbb{C}^{N \times 1}$  (proved in Theorem 5.1), the general resource allocation prob-

lem in (5.9) can be rewritten as

$$\begin{aligned}
& \underset{\mathbf{v}_1, \dots, \mathbf{v}_{K_r}}{\text{maximize}} && f(g_1(\text{SINR}_1), \dots, g_{K_r}(\text{SINR}_{K_r})) \\
& \text{subject to} && \text{SINR}_k = \frac{|\mathbf{h}_k^H \mathbf{C}_k \mathbf{D}_k \mathbf{v}_k|^2}{\sigma_k^2 + \sum_{\bar{k} \neq k} |\mathbf{h}_k^H \mathbf{C}_k \mathbf{D}_{\bar{k}} \mathbf{v}_{\bar{k}}|^2} \quad \forall k, \\
& && \sum_{k=1}^{K_r} \mathbf{v}_k^H \mathbf{Q}_l \mathbf{v}_k \leq q_l \quad \forall l, \\
& && \mathbf{v}_k^H \mathbf{T}_{ik} \mathbf{v}_k \leq \tau_{ik} \quad \forall i, k.
\end{aligned} \tag{6.1}$$

Recall that the user performance functions  $g_k(\cdot)$  are continuous and strictly monotonic increasing, while the system performance function  $f(\cdot)$  is Lipschitz continuous and strictly monotonic increasing. Based on these properties, (6.1) belongs to the category of monotonic optimization problems [Tuy00, TAKT05].

This resource allocation problem will be solved to global optimality in this chapter. In general, (6.1) is a non-convex and NP-hard problem [LZ08, LDL11], which calls for the use of systematic but computationally costly algorithms from global/monotonic optimization theory to guarantee global convergence [Tuy00, TAKT05]. In preparation for this, the next section considers a particular  $f(\cdot)$  that makes (6.1) solvable in polynomial time and is an essential subproblem of our general algorithm.

## 6.2 Fairness-Profile Optimization

In this section, we consider a particular  $f(\cdot)$  for which we will see that (6.1) can be solved efficiently:<sup>1</sup>

$$\begin{aligned}
& \underset{\mathbf{v}_1, \dots, \mathbf{v}_{K_r}}{\text{maximize}} && \min_k \frac{g_k(\text{SINR}_k) - a_k}{\alpha_k}, \\
& \text{subject to} && g_k(\text{SINR}_k) \geq a_k \quad \forall k, \\
& && \sum_{k=1}^{K_r} \mathbf{v}_k^H \mathbf{Q}_l \mathbf{v}_k \leq q_l \quad \forall l, \\
& && \mathbf{v}_k^H \mathbf{T}_{ik} \mathbf{v}_k \leq \tau_{ik} \quad \forall i, k.
\end{aligned} \tag{6.2}$$

---

<sup>1</sup> Using the standard convention that supremum of the empty set is  $-\infty$ , fairness-profile optimization corresponds to the system performance function

$$f(\mathbf{g}) = \begin{cases} \min_k (g_k - a_k) / \alpha_k, & \text{if } \min_k g_k / a_k \geq 1, \\ -\infty, & \text{otherwise.} \end{cases}$$

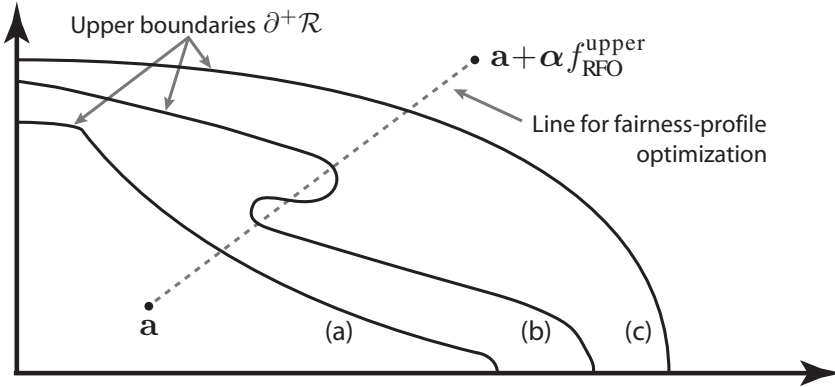


Figure 6.1: Examples of performance regions with different shapes: (a) is normal but non-convex, (b) is neither normal nor convex, and (c) is both normal and convex. Simple bisection along a fairness-profile is not guaranteed to find the upper boundary of non-normal regions.

This problem can be seen as a generalization of classic max-min optimization (see e.g., [WES06]) where two fairness constraints have been added:

1. Each user has a lowest acceptable level  $g_k(\text{SINR}_k) \geq a_k$ ;
2. The total performance above this level is divided such that each user gets a predefined portion  $\alpha_k \geq 0$ .

The first constraint is represented by  $\mathbf{a} = [a_1, \dots, a_{K_r}]^T \geq \mathbf{0}_{K_r \times 1}$ . The second constraint is called a *fairness-profile*<sup>2</sup> and is symbolized by a vector  $\boldsymbol{\alpha} = [\alpha_1, \dots, \alpha_{K_r}]^T$  that satisfies  $\sum_{k=1}^{K_r} \alpha_k = 1$  (without loss of generality).

We call (6.2) a *fairness-profile optimization (FPO)* problem and observe that it has a simple geometric interpretation in terms of the performance region  $\mathcal{R}$  (see Definition 5.2); we start in  $\mathbf{a} \in \mathcal{R}$  and follow a ray in the direction of  $\boldsymbol{\alpha}$  until a point on the upper boundary  $\partial^+ \mathcal{R}$  is found.<sup>3</sup> In general search regions, the ray might leave the region and come back again which makes the search very complicated. Fortunately, Lemma 5.2 proved that  $\mathcal{R}$  is a compact and normal set and thus the ray intersects the upper boundary in a unique point. This is illustrated in Figure 6.1, where (a)

<sup>2</sup>The terminology *rate-profile* has been used for similar problems in prior work [ZH10, KL10, MZC06], but herein we extend these works by having arbitrary performance measures and general multicell scenarios.

<sup>3</sup>This geometric approach finds an optimal solution to (6.2) where  $(g_k(\text{SINR}_k) - a_k)/\alpha_k$  is the same for all  $\text{MS}_k$ . In certain special cases (e.g., when the upper boundary is flat in some dimension), there also exist solutions where a few users get higher performance than this worst-case level. This discussed in [MAMK09].

and (c) are normal sets while (b) is non-normal and thus some rays from within the set cross the upper boundary multiple times.

If we can find an upper bound  $f_{\text{FPO}}^{\text{upper}}$  on the optimal value of (6.2), we know geometrically that the optimum lies on the line-segment between  $\mathbf{a}$  and  $\mathbf{a} + \alpha f_{\text{FPO}}^{\text{upper}}$ ; see the illustration in Figure 6.1. Hoping to simplify the FPO problem, we rewrite (6.2) as a bisection over this line-segment.

*Lemma 6.1.* For fixed  $\mathbf{a}, \alpha$  and a given upper bound  $f_{\text{FPO}}^{\text{upper}}$  on the optimal value of (6.2), the problem can be solved by bisection over the range  $\mathcal{F} = [0, f_{\text{FPO}}^{\text{upper}}]$ . For a given  $f_{\text{FPO}}^{\text{candidate}} \in \mathcal{F}$ , the feasibility problem

$$\begin{aligned} & \text{find } \mathbf{v}_1, \dots, \mathbf{v}_{K_r} \\ & \text{subject to } \text{SINR}_k \geq \gamma_k \quad \forall k, \\ & \sum_{k=1}^{K_r} \mathbf{v}_k^H \mathbf{Q}_l \mathbf{v}_k \leq q_l \quad \forall l, \\ & \mathbf{v}_k^H \mathbf{T}_{ik} \mathbf{v}_k \leq \tau_{ik} \quad \forall i, k, \end{aligned} \tag{6.3}$$

is solved for  $\gamma_k = g_k^{-1}(a_k + \alpha_k f_{\text{FPO}}^{\text{candidate}})$ . If the problem is feasible, all  $\tilde{f} \in \mathcal{F}$  with  $\tilde{f} < f_{\text{FPO}}^{\text{candidate}}$  are removed. Otherwise, all  $\tilde{f} \in \mathcal{F}$  with  $\tilde{f} \geq f_{\text{FPO}}^{\text{candidate}}$  are removed. The initial feasibility of (6.2) is checked by solving (6.3) for  $f_{\text{FPO}}^{\text{candidate}} = 0$ .

*Proof.* The proof is given in Appendix 6.A.1. □

Obviously, the FPO problem is infeasible if  $\mathbf{a}$  is outside of  $\mathcal{R}$ , which can be checked as described in the lemma. A successful bisection also requires an initial selection of  $f_{\text{FPO}}^{\text{upper}}$  such that  $\mathbf{a} + \alpha f_{\text{FPO}}^{\text{upper}}$  is outside  $\mathcal{R}$ . If not given in advance,  $f_{\text{FPO}}^{\text{upper}}$  can be achieved in different ways:

- $f_{\text{FPO}}^{\text{upper}} = K_r \sup_k \lim_{p \rightarrow \infty} (g_k(p) - a_k)$ . Cannot be used if  $g_k(p) \rightarrow \infty$  as  $p \rightarrow \infty$ .
- $f_{\text{FPO}}^{\text{upper}} = \sum_k g_k(\sigma_k^2 / (\kappa_k \|\mathbf{D}_k^H \mathbf{h}_k\|_2^2 + \sigma_k^2)) - a_k$ , where  $\kappa_k$  is a bound on the transmit power and is calculated as the smallest positive eigenvalue of  $\frac{\mathbf{D}_k^H \mathbf{Q}_l \mathbf{D}_k}{q_l \text{tr}(\mathbf{D}_k)}$  among all  $l$ .
- $f_{\text{FPO}}^{\text{upper}} = \sum_k g_k(\text{SINR}_{\text{su},k}) - a_k$ , where  $\text{SINR}_{\text{su},k}$  is the optimal SINR if  $\text{MS}_k$  is the only active user.

The first one is the simplest and ignores the power and soft-shaping constraints, while the second one ignores co-user interference and assumes that the highest power available in some spatial direction can be used in any direction. The third one takes the SINRs achieved in a single-user system. This requires that these problems are solved (which is simple under some power constraints), but achieves the tightest value on  $f_{\text{FPO}}^{\text{upper}}$ .

### 6.2.1 Convexity of Feasibility Subproblems

Solving the FPO problem using bisection, as suggested in Lemma 6.1, is appealing as the range is halved in each iteration; thus, the number of iterations scales only logarithmically with the desired accuracy  $\delta$  of the solution, also known as linear convergence. To be precise, the lemma will solve  $\lceil \log_2(f_{\text{FPO}}^{\text{upper}}/\delta) \rceil$  feasibility problems to achieve the desired accuracy. As this variable is bounded by a constant, the computational complexity of the FPO problem is just a constant times the complexity of the feasibility problem (6.3) solved in each iteration. Next, we will see that (6.3) can be solved efficiently using an approach from [WES06, YL07].

*Lemma 6.2.* The feasibility problem in (6.3) can be rewritten into the following convex feasibility problem:

$$\begin{aligned}
 & \text{find } \mathbf{v}_1, \dots, \mathbf{v}_{K_r} \\
 & \text{subject to } \left\| \begin{array}{c} \mathbf{h}_k^H \mathbf{C}_k \mathbf{D}_1 \mathbf{v}_1 \\ \vdots \\ \mathbf{h}_k^H \mathbf{C}_k \mathbf{D}_{K_r} \mathbf{v}_{K_r} \\ \sigma_k \end{array} \right\| \leq \sqrt{\frac{1 + \gamma_k}{\gamma_k}} (\mathbf{h}_k^H \mathbf{C}_k \mathbf{D}_k \mathbf{v}_k) \quad \forall k, \\
 & \Im\{\mathbf{h}_k^H \mathbf{C}_k \mathbf{D}_k \mathbf{v}_k\} = 0 \quad \forall k, \\
 & \sum_{k=1}^{K_r} \mathbf{v}_k^H \mathbf{Q}_l \mathbf{v}_k \leq q_l \quad \forall l, \\
 & \mathbf{v}_k^H \mathbf{T}_{ik} \mathbf{v}_k \leq \tau_{ik} \quad \forall i, k.
 \end{aligned} \tag{6.4}$$

*Proof.* The proof is given in Appendix 6.A.2.  $\square$

Knowing that each subproblem of the bisection algorithm in Lemma 6.1 is convex, we conclude that fairness-profile optimization is a quasi-convex problem [BV04]. Thus, the computational complexity of both the feasibility problem and the FPO problem (for a fixed  $\delta$ ) is polynomial in the number of antennas  $N$ , users  $K_r$ , and power constraints  $L$  [BTN01, Chapter 6]. The exact complexity depends both on current systems conditions and the choice of solver algorithm (e.g., interior-point methods [TTT03]), but we illustrate the complexity in Section 6.5. For example, faster practical convergence can be achieved by fixed point algorithms under total power constraints [SB05], while such algorithms need to be combined with outer optimization procedures under general power constraints [YL07]. The polynomial complexity is quite affordable, making the FPO problem a reasonable candidate for resource allocation in practical systems. To put it differently, the system designer basically has the choice between solving an FPO problem optimally or solving some other NP-hard resource allocation problem in (6.1) suboptimally.

The bisection algorithm for solving (6.2) is given in Algorithm 6.1.

**Algorithm 6.1** Centralized Fairness-Profile Optimization

---

```

1: input starting-point  $\mathbf{a}$  and fairness-profile  $\boldsymbol{\alpha}$ 
2: input accuracy  $\delta$ ,  $f_{\text{FPO}}^{\text{lower}} = 0$ , and  $f_{\text{FPO}}^{\text{upper}}$  (see suggestions)
3: while  $f_{\text{FPO}}^{\text{upper}} - f_{\text{FPO}}^{\text{lower}} > \delta$ 
4:   set  $f_{\text{FPO}}^{\text{candidate}} = (f_{\text{FPO}}^{\text{lower}} + f_{\text{FPO}}^{\text{upper}})/2$ 
5:   set  $\gamma_k = g_k^{-1}(a_k + \alpha_k f_{\text{FPO}}^{\text{candidate}}) \quad \forall k$ 
6:   if problem (6.3) is feasible for these  $\gamma_k$ : set  $f_{\text{FPO}}^{\text{lower}} = f_{\text{FPO}}^{\text{candidate}}$ 
7:   else: set  $f_{\text{FPO}}^{\text{upper}} = f_{\text{FPO}}^{\text{candidate}}$    end
8: end
9: return  $[f_{\text{FPO}}^{\text{lower}}, f_{\text{FPO}}^{\text{upper}}]$  and last feasible solution to (6.3) from step 6

```

---

**6.2.2 Distributed Implementation**

Algorithm 6.1 is centralized in the sense that each feasibility problem requires full CSI. In practice, backhaul signaling is constrained and thus it might be worthwhile to decompose the centralized optimization into distributed subproblems only requiring local CSI, which in this section means channels that can be estimated at the base station in a TDD system. The transmission to each user will be optimized separately, and if multiple base stations serve a given user they will have to pool their local CSI.

Using dual decomposition theory [PC06], CSI signaling between base stations can be replaced by iterative interference control signaling. As a first step, the feasibility problem in (6.3) is rewritten as

$$\begin{aligned}
& \text{find } \{\mathbf{v}_k\}_{\forall k}, \{I_{\bar{k}k}\}_{\forall k, \bar{k}}, \{\tilde{I}_{\bar{k}k}\}_{\forall k, \bar{k}}, \{q_{lk}\}_{\forall l, k} \\
& \text{subject to } \frac{|\mathbf{h}_k^H \mathbf{C}_k \mathbf{D}_k \mathbf{v}_k|^2}{\sigma_k^2 + \sum_{\bar{k} \neq k} \tilde{I}_{\bar{k}k}} \geq \gamma_k \quad \forall k, \\
& |\mathbf{h}_k^H \mathbf{C}_k \mathbf{D}_{\bar{k}} \mathbf{v}_{\bar{k}}|^2 \leq I_{\bar{k}k}, \quad I_{\bar{k}k} \leq \tilde{I}_{\bar{k}k} \quad \forall k, \bar{k}, k \neq \bar{k}, \quad (6.5) \\
& \mathbf{v}_k^H \mathbf{Q}_l \mathbf{v}_k \leq q_{lk}, \quad \sum_{\bar{k}=1}^{K_r} q_{l\bar{k}} \leq q_l \quad \forall l, k, \\
& \mathbf{v}_k^H \mathbf{T}_{ik} \mathbf{v}_k \leq \tau_{ik} \quad \forall i, k.
\end{aligned}$$

Here,  $I_{\bar{k}k}$  is the actual interference generated at  $\text{MS}_k$  by transmissions to  $\text{MS}_{\bar{k}}$ , while  $\tilde{I}_{\bar{k}k}$  is its believed value in the transmission optimization for  $\text{MS}_k$ . Similarly, the power constraints are separated between users by using the variables  $q_{lk}$ . To perform dual decomposition, a partial Lagrangian is formed for the consistency constraints  $I_{\bar{k}k} \leq \tilde{I}_{\bar{k}k}$  and  $\sum_{\bar{k}=1}^{K_r} q_{l\bar{k}} \leq q_l$ . If the corresponding Lagrange multipliers are denoted  $x_{\bar{k}k}$  and  $z_l$ , (6.5) can be

decomposed into  $K_r$  subproblems where the  $k$ th is

$$\begin{aligned}
& \underset{\mathbf{v}_k, \{I_{k\bar{k}}\}_{\forall \bar{k}}, \{\tilde{I}_{\bar{k}k}\}_{\forall \bar{k}}, \{q_{lk}\}_{\forall l}}{\text{minimize}} && \sum_{\bar{k} \neq k} \left( x_{k\bar{k}} I_{k\bar{k}} - x_{\bar{k}k} \tilde{I}_{\bar{k}k} \right) + \sum_{l=1}^{L_p} z_l q_{lk} \\
& \text{subject to} && \frac{|\mathbf{h}_k^H \mathbf{C}_k \mathbf{D}_k \mathbf{v}_k|^2}{\sigma_k^2 + \sum_{\bar{k} \neq k} \tilde{I}_{\bar{k}k}} \geq \gamma_k \quad \forall k, \\
& && \mathbf{v}_k^H \mathbf{Q}_l \mathbf{v}_k \leq q_{lk}, \quad q_{lk} \leq q_l \quad \forall l, \\
& && |\mathbf{h}_{\bar{k}}^H \mathbf{C}_{\bar{k}} \mathbf{D}_k \mathbf{v}_k|^2 \leq I_{k\bar{k}} \quad \bar{k} \neq k, \\
& && \mathbf{v}_k^H \mathbf{T}_{ik} \mathbf{v}_k \leq \tau_{ik} \quad \forall i,
\end{aligned} \tag{6.6}$$

and a master dual problem

$$\underset{\{x_{\bar{k}k}\}_{\forall k, \bar{k}}, \{z_l\}_{\forall l}}{\text{maximize}} \sum_k \sum_{\bar{k} \neq k} x_{\bar{k}k} \left( I_{k\bar{k}}^* - \tilde{I}_{\bar{k}k}^* \right) + \sum_l z_l \left( \sum_k q_{lk}^* - q_l \right) \tag{6.7}$$

where  $I_{\bar{k}k}^*, \tilde{I}_{\bar{k}k}^*, q_{lk}^*, \mathbf{v}_k^*$  are the subproblem solutions. We assume that it exists a central station that updates the master problem, while the subproblems are solved distributively.

The resulting algorithm is summarized in Algorithm 6.2 on the next page, where we for notational convenience have assumed that  $q_l > 0 \forall l$  and that there are no soft-shaping constraints.

This distributed algorithm requires the decomposition step length  $\xi > 0$  and the search step length  $\nu > 0$  to be selected appropriately (they could either be fixed or updated iteratively). In addition, some stopping criterion is required (e.g., on  $|f_{\text{FPO}}^{\text{step}}|$  or on the number of iterations).

In comparison with Algorithm 6.1, this modified algorithm is distributed. In each iteration, the subproblem for  $\text{MS}_k$  only requires local CSI (i.e.,  $\mathbf{h}_{j\bar{k}} \forall \bar{k} \in \mathcal{C}_j$ ) for all base stations  $j$  with  $k \in \mathcal{D}_j$  (typically, one or a few adjacent base stations) and is solved at one of these base stations. The solutions (i.e.,  $I_{k\bar{k}}^*, \tilde{I}_{\bar{k}k}^*, q_{lk}^*, \beta_k$ ) are sent to a central station that constructs a solution with feasible power usage. If it is better than previous solutions, the search parameters are updated. If the improvement is small, the Lagrange multipliers  $x_{k\bar{k}}, z_l$  are updated and their new values are sent to the distributed solvers. The convergence is validated in Section 6.5.

### 6.3 Multicell Monotonic Optimization

In this section, we aim at solving the monotonic optimization problem in (6.1) for any system performance function  $f(\cdot)$ . Recall from Lemma 5.2 that the optimum lies on the upper boundary. Hence, we can in principle look for an approximate solution in a large set of boundary points of  $\mathcal{R}$

**Algorithm 6.2** Distributed Fairness-Profile Optimization

- 
- 1: **input** starting-point  $\mathbf{a}$  and fairness-profile  $\boldsymbol{\alpha}$
  - 2: **input**  $f_{\text{FPO}}^{\text{lower}} = 0$ , and  $f_{\text{FPO}}^{\text{step}} = f_{\text{FPO}}^{\text{upper}}$  (see suggestions)
  - 3: set  $x_{\bar{k}k} = 0$  and  $z_l = 0 \forall k, \bar{k} \neq k, l$
  - 4: **while** stopping criterion is not satisfied
  - 5:   set  $\gamma_k = g_k^{-1}(a_k + \alpha_k(f_{\text{FPO}}^{\text{lower}} + \nu f_{\text{FPO}}^{\text{step}})) \forall k$
  - 6:   send  $\gamma_k$  to distributed solvers, which solve (6.6) for each  $k$
  - 7:   send  $I_{\bar{k}k}^*, \tilde{I}_{\bar{k}k}^*, q_{lk}^*$ , and  $\beta_k = |\mathbf{h}_k^H \mathbf{C}_k \mathbf{D}_k \mathbf{v}_k^*|^2$  to central station
  - 8:   set  $c = \max(\max_l \sum_k \frac{q_{lk}^*}{q_l}, 1)$
  - 9:   set  $\psi_k = (g_k(\frac{\beta_k}{c\sigma_k^2 + \sum_{\bar{k} \neq k} I_{\bar{k}k}^*}) - a_k) / \alpha_k \forall k$
  - 10: **if**  $\min_k \psi_k < f_{\text{FPO}}^{\text{lower}} + \nu f_{\text{FPO}}^{\text{step}}$ :
  - 11:   set  $x_{\bar{k}k} = x_{\bar{k}k} - \xi(\tilde{I}_{\bar{k}k}^* - I_{\bar{k}k}^*)$  and  $z_l = z_l - \xi(q_l - \sum_k q_{lk}^*)$
  - 12: **if**  $\min_k \psi_k > f_{\text{FPO}}^{\text{lower}}$ :
  - 13:   set  $f_{\text{FPO}}^{\text{lower}} = \min_k \psi_k$  and  $f_{\text{FPO}}^{\text{step}} = (\max_k \psi_k - \min_k \psi_k)$
  - 14:   send updated parameters to distributed solvers **end while**
  - 15: **return**  $f_{\text{FPO}}^{\text{lower}}$  and last solution satisfying the condition in Step 12
- 

achieved by solving the FPO problem in Section 6.2 for a very fine grid of fairness-profiles  $\boldsymbol{\alpha}$ . However, this naive approach has huge computational complexity, which calls for a more systematic approach that concentrates on the boundary in *good* directions.

Next, we propose a branch-reduce-and-bound (BRB) algorithm for solving (6.1) systematically and with global convergence. It can be seen as an adaptation of the generic BRB algorithm in [TAKT05] to general multicell resource allocation.

The algorithm maintains a set  $\mathcal{N}$  with non-overlapping hyperrectangles that surely covers the parts of the performance region  $\mathcal{R}$  where the optimal solutions lie (the solution might be non-unique). Iteratively, we split certain hyperrectangles and try to improve a lower bound  $f_{\min}$  and an upper bound  $f_{\max}$  on the optimal value of (6.1). To aid this process, a local upper bound  $\beta(\mathcal{M})$  is also stored for each  $\mathcal{M} \in \mathcal{N}$ . The algorithm proceeds until  $f_{\max} - f_{\min} < \varepsilon$ , for a predefined solution accuracy  $\varepsilon$ .

In what follows, hyperrectangles are called *boxes*:

*Definition 6.1.* For given  $\mathbf{a}, \mathbf{b} \in \mathbb{R}_+^{K_r}$  with  $\mathbf{a} \leq \mathbf{b}$ , the set of all  $\mathbf{x}$  such that  $\mathbf{a} \leq \mathbf{x} \leq \mathbf{b}$  is called a *box* and is denoted  $[\mathbf{a}, \mathbf{b}]$ .

Initially,  $\mathcal{N} = \{\mathcal{M}_0\}$  for a box  $\mathcal{M}_0 = [\mathbf{0}, \mathbf{b}_0] \subset \mathbb{R}_+^{K_r}$  where  $\mathbf{b}_0$  is based on some suitable upper bound that guarantees  $\mathcal{R} \subseteq \mathcal{M}_0$  (see suggestions in Section 6.2). The initial lower and upper bounds can be taken as  $f_{\min} =$

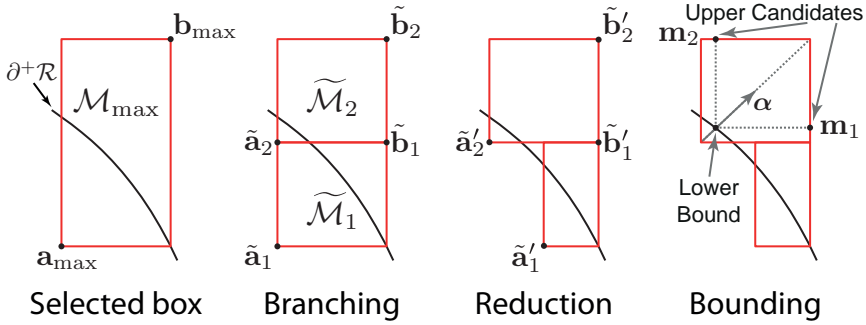


Figure 6.2: An iteration of the BRB algorithm: A box is selected and branched into two new boxes. These are reduced based on the current bounds on the optimal value. Finally, line search between the lower and upper bounds on the outmost box is applied to improve the bounds.

$f(\mathbf{0}) = 0$  and  $f_{\max} = f(\mathbf{b}_0)$ , but some low-complexity resource allocation strategy can be used to obtain a better lower bound.

Each iteration of the BRB algorithm consists of three steps:

1. Branch: Divide a box from  $\mathcal{N}$  into two new boxes.
2. Reduce: Remove parts of these new boxes that cannot contain optimal solutions.
3. Bound: Search for a feasible solution in one of the new boxes and use it to improve  $f_{\min}$ ,  $f_{\max}$ , and  $\beta(\cdot)$ .

These steps are illustrated in Figure 6.2 and the details are explained in the next subsections. The final algorithm is given in Section 6.3.4. For notational convenience, the  $k$ th element of any vector  $\mathbf{x}$  is denoted  $x_k$ .

### 6.3.1 Branching

Each iteration begins with selecting a box  $\mathcal{M}_{\max} = [\mathbf{a}_{\max}, \mathbf{b}_{\max}]$  that contains the current upper bound  $f_{\max}$ :

$$\mathcal{M}_{\max} = \arg \max_{\mathcal{M} \in \mathcal{N}} \beta(\mathcal{M}). \quad (6.8)$$

The intention is to improve the upper bound by partitioning  $\mathcal{M}_{\max}$  into two new boxes  $\tilde{\mathcal{M}}_1, \tilde{\mathcal{M}}_2$ . New boxes of equal size are achieved by bisecting  $\mathcal{M}_{\max}$  along its longest side (see Figure 6.2). The index of this side is

$\dim = \operatorname{argmax}_k (b_{\max,k} - a_{\max,k})$  and the new boxes are

$$\begin{aligned}\widetilde{\mathcal{M}}_1 &= [\mathbf{a}_{\max}, \mathbf{b}_{\max} - s\mathbf{e}_{\dim}], \\ \widetilde{\mathcal{M}}_2 &= [\mathbf{a}_{\max} + s\mathbf{e}_{\dim}, \mathbf{b}_{\max}],\end{aligned}\tag{6.9}$$

where  $s = (b_{\max,\dim} - a_{\max,\dim})/2$  and  $\mathbf{e}_k$  is the  $k$ th column of a  $K_r$ -dimensional identity matrix  $\mathbf{I}_{K_r}$ . The (local) upper bounds over these new boxes are also based on  $\mathcal{M}_{\max}$ :

$$\begin{aligned}\beta(\widetilde{\mathcal{M}}_1) &= \min(\beta(\mathcal{M}_{\max}), f(\mathbf{b}_{\max} - s\mathbf{e}_{\dim})), \\ \beta(\widetilde{\mathcal{M}}_2) &= \beta(\mathcal{M}_{\max}).\end{aligned}\tag{6.10}$$

Finally, the set  $\mathcal{M}_{\max}$  is replaced with  $\widetilde{\mathcal{M}}_1$  and  $\widetilde{\mathcal{M}}_2$  in  $\mathcal{N}$ .

### 6.3.2 Reduction

In this step, the new boxes  $\widetilde{\mathcal{M}}_l = [\tilde{\mathbf{a}}_l, \tilde{\mathbf{b}}_l]$ , for  $l = 1, 2$ , are reduced by cutting off parts that cannot achieve function values between the lower bound  $f_{\min}$  and (local) upper bound  $\beta(\widetilde{\mathcal{M}}_l)$ . If  $\beta(\widetilde{\mathcal{M}}_l) < f_{\min}$ , the whole box is removed from  $\mathcal{N}$ . Otherwise, it is replaced by a (potentially) smaller box  $[\tilde{\mathbf{a}}'_l, \tilde{\mathbf{b}}'_l]$  based on the following lemma.

*Lemma 6.3.* If  $f_{\min} \leq \beta(\widetilde{\mathcal{M}}_l)$ , all points  $\mathbf{g} \in [\tilde{\mathbf{a}}_l, \tilde{\mathbf{b}}_l]$  satisfying  $f_{\min} \leq f(\mathbf{g}) \leq \beta(\widetilde{\mathcal{M}}_l)$  are also contained in  $[\tilde{\mathbf{a}}'_l, \tilde{\mathbf{b}}'_l] \subseteq [\tilde{\mathbf{a}}_l, \tilde{\mathbf{b}}_l]$ , where

$$\tilde{\mathbf{a}}'_l = \tilde{\mathbf{b}}_l - \sum_{k=1}^{K_r} \nu_k (\tilde{b}_{l,k} - \tilde{a}_{l,k}) \mathbf{e}_k\tag{6.11}$$

$$\tilde{\mathbf{b}}'_l = \tilde{\mathbf{a}}_l + \sum_{k=1}^{K_r} \mu_k (\tilde{b}_{l,k} - \tilde{a}'_{l,k}) \mathbf{e}_k\tag{6.12}$$

with  $\nu_k$  and  $\mu_k$  (for  $k = 1, \dots, K_r$ ) calculated as

$$\begin{aligned}\nu_k &= \max \left\{ \nu; 0 \leq \nu \leq 1, f(\tilde{\mathbf{b}}_l - \nu(\tilde{b}_{l,k} - \tilde{a}_{l,k})\mathbf{e}_k) \geq f_{\min} \right\} \\ \mu_k &= \max \left\{ \mu; 0 \leq \mu \leq 1, f(\tilde{\mathbf{a}}_l + \mu(\tilde{b}_{l,k} - \tilde{a}'_{l,k})\mathbf{e}_k) \leq \beta(\widetilde{\mathcal{M}}_l) \right\}.\end{aligned}\tag{6.13}$$

*Proof.* The proof is given in Appendix 6.A.3. □

The reduction procedure in Lemma 6.3 is illustrated in Figure 6.2 and observe that it needs to be implemented sequentially; first, the lower point  $\tilde{\mathbf{a}}_l$  is updated using (6.11) and then it is used to update the upper point  $\tilde{\mathbf{b}}_l$  using (6.12). Each reduction requires calculation of the parameters  $\nu_k, \mu_k$  in (6.13), generally solved by standard line search procedures. However, closed

form expressions can be attained in many cases. For example, weighted sum performance with  $f(\mathbf{g}) = \sum_{k=1}^{K_r} w_k g_k$  (with weights  $w_k > 0$ ) gives

$$\begin{aligned} \nu_k &= \min \left( \frac{\sum_{\bar{k}=1}^{K_r} w_{\bar{k}} \tilde{b}_{l,k} - f_{\min}}{w_k (\tilde{b}_{l,k} - \tilde{a}_{l,k})}, 1 \right), \\ \mu_k &= \min \left( \frac{\beta(\widetilde{\mathcal{M}}_l) - \sum_{\bar{k}=1}^{K_r} w_{\bar{k}} \tilde{a}'_{l,k}}{w_k (\tilde{b}_{l,k} - \tilde{a}'_{l,k})}, 1 \right) \end{aligned} \quad (6.14)$$

where the min-operator makes sure that  $\nu_k, \mu_k \leq 1$ .

### 6.3.3 Bounding

Each iteration ends with a bounding step where we search for feasible solutions in  $\widetilde{\mathcal{M}}_2 = [\tilde{\mathbf{a}}'_2, \tilde{\mathbf{b}}'_2]$ , which is the new box with the largest (local) upper bound (i.e.,  $\beta(\widetilde{\mathcal{M}}_2) \geq \beta(\widetilde{\mathcal{M}}_1)$ ). These solutions are used to improve  $f_{\min}$ ,  $f_{\max}$ , and  $\beta(\widetilde{\mathcal{M}}_2)$ .

First, the feasibility of the lower corner  $\tilde{\mathbf{a}}'_2$  is checked by solving (6.3) with  $\gamma_k = g_k^{-1}(\tilde{a}'_{2,k}) \forall k$ . If this problem is infeasible, then  $\widetilde{\mathcal{M}}_2$  contains no feasible solutions and is removed from  $\mathcal{N}$ . If the problem is feasible, the following lemma is used to find lower and upper bounds on the feasible performance in  $\widetilde{\mathcal{M}}_2$  by solving a single FPO problem:

*Lemma 6.4.* Consider a box  $\mathcal{M} = [\mathbf{a}, \mathbf{b}] \subset \mathbb{R}_+^{K_r}$  such that  $\mathcal{M} \cap \mathcal{R} \neq \emptyset$ . If  $\mathcal{R}$  is compact and normal, the highest feasible performance in  $\mathcal{M}$  can be bounded as  $[\bar{f}_{\min}, \bar{f}_{\max}]$  for

$$\begin{aligned} \bar{f}_{\min} &= f(\mathbf{a} + \boldsymbol{\alpha} f_{\text{FPO}}^{\min}) \\ \bar{f}_{\max} &= \max_k f(\mathbf{b} - (b_k - n_k) \mathbf{e}_k) \end{aligned} \quad (6.15)$$

where  $\mathbf{n} = [n_1, \dots, n_{K_r}]^T = \mathbf{a} + \boldsymbol{\alpha} f_{\text{FPO}}^{\max}$ ,  $\boldsymbol{\alpha} = (\mathbf{b} - \mathbf{a}) / \|\mathbf{b} - \mathbf{a}\|_1$ , and  $\mathbf{e}_k$  denotes the  $k$ th column of  $\mathbf{I}_{K_r}$ . The variables  $f_{\text{FPO}}^{\min}$ ,  $f_{\text{FPO}}^{\max}$  are the interval endpoints achieved by Algorithm 6.1 with starting-point  $\mathbf{a}$ , fairness-profile  $\boldsymbol{\alpha}$ ,  $f_{\text{FPO}}^{\text{upper}} = \|\mathbf{b} - \mathbf{a}\|_1$ , and some given line-search accuracy  $\delta$ .

*Proof.* The proof is given in Appendix 6.A.4. □

The lemma is illustrated in Figure 6.2, where a line-search is performed between the lower and upper corner of the box. The best feasible point on this line provides a local lower bound  $\bar{f}_{\min}$  on the feasible performance. Since the region is normal, the outer points  $\mathbf{m}_k = \tilde{\mathbf{b}}'_2 - (\tilde{b}'_{2,k} - n_k) \mathbf{e}_k$  are candidates for giving a new upper bound on the feasible performance in the box. Observe that if the size of the box  $\|\tilde{\mathbf{b}}'_2 - \tilde{\mathbf{a}}'_2\|_1$  is smaller than the line-search accuracy  $\delta$ , then no line-search is performed. This will not affect the convergence, as proved in the next subsection.

The local lower bound  $\bar{f}_{\min}$  from Lemma 6.4 replaces the global lower bound  $f_{\min}$  if  $\bar{f}_{\min} \geq f_{\min}$ . Similarly, we set  $\beta(\widetilde{\mathcal{M}}_2) = \bar{f}_{\max}$  if  $\bar{f}_{\max} < \beta(\widetilde{\mathcal{M}}_2)$ . Finally, we update  $f_{\max}$  with the largest upper bound  $\max_{\mathcal{M} \in \mathcal{N}} \beta(\mathcal{M})$  among the remaining boxes. The stopping criterion  $f_{\max} - f_{\min} < \varepsilon$  is checked before a new iteration is started.

### 6.3.4 Final BRB Algorithm

The BRB algorithm that solves the general monotonic optimization problem in (6.1) is summarized in Algorithm 6.3.

---

**Algorithm 6.3** Branch-Reduce-and-Bound (BRB) for Resource Allocation

---

- 1: **input**  $\mathcal{M}_0 = [\mathbf{0}, g_{\max} \mathbf{1}_{K_r}]$ , accuracy  $\varepsilon$ , line-search accuracy  $\delta$
  - 2: set  $f_{\min}, f_{\max}$  based on the available prior knowledge.
  - 3: set  $\mathcal{N} = \{\mathcal{M}_0\}$  and  $\beta(\mathcal{M}_0) = f_{\max}$
  - 4: **while**  $f_{\max} - f_{\min} > \varepsilon$
  - 5:   set  $\mathcal{M}_{\max} = \operatorname{argmax}_{\mathcal{M} \in \mathcal{N}} \beta(\mathcal{M})$
  - 6:   **for**  $l = 1, 2$ :
  - 7:     create new box  $\widetilde{\mathcal{M}}_l$  using (6.9) and set  $\beta(\widetilde{\mathcal{M}}_l)$  using (6.10)
  - 8:     **if**  $f_{\min} \leq \beta(\widetilde{\mathcal{M}}_l)$ : reduce  $\widetilde{\mathcal{M}}_l$  using Lemma 6.3
  - 9:     **else**: set  $\widetilde{\mathcal{M}}_l = \emptyset$    **end**
  - 10:   **end**
  - 11:   Check feasibility of  $\tilde{\mathbf{a}}'_2$  by solving (6.3) for  $\gamma_k = g_k^{-1}(\tilde{a}'_{2,k})$
  - 12:   **if** feasible:
  - 13:     Calculate bounds  $\bar{f}_{\min}, \bar{f}_{\max}$  for  $\widetilde{\mathcal{M}}_2$  using Lemma 6.4
  - 14:     set  $f_{\min} = \max(f_{\min}, \bar{f}_{\min})$
  - 15:     set  $\beta(\widetilde{\mathcal{M}}_2) = \min(\beta(\widetilde{\mathcal{M}}_2), \bar{f}_{\max})$
  - 16:   **else**: set  $\widetilde{\mathcal{M}}_2 = \emptyset$    **end**
  - 17:   set  $\mathcal{N} = (\mathcal{N} \setminus \mathcal{M}_{\max}) \cup \{\widetilde{\mathcal{M}}_1, \widetilde{\mathcal{M}}_2\}$
  - 18:   set  $f_{\max} = \max_{\mathcal{M} \in \mathcal{N}} \beta(\mathcal{M})$
  - 19: **end**
  - 20: **return**  $[f_{\min}, f_{\max}]$  and a feasible solution that achieved  $f_{\min}$
- 

The global convergence of the BRB algorithm is established by the following theorem.

*Theorem 6.1.* For any given accuracy  $\varepsilon > 0$ , the BRB algorithm finds an interval  $[f_{\min}, f_{\max}]$  for the optimal value of (6.1) that satisfies  $f_{\max} - f_{\min} \leq \varepsilon$ , in a finite number of iterations. The line-search accuracy  $\delta > 0$  can be selected arbitrarily.

*Proof.* The proof is given in Appendix 6.A.5. □

In other words, the BRB algorithm converges to the global optimum  $f_{\text{opt}}$  of (6.1) in the sense that an  $\varepsilon$ -approximate interval  $f_{\text{opt}} \in [f_{\text{min}}, f_{\text{max}}]$ , with  $f_{\text{max}} - f_{\text{min}} \leq \varepsilon$ , is achieved in finitely many iterations for any  $\varepsilon > 0$ . Observe that the line-search accuracy  $\delta$  is used (and can be varied) in the bounding step to improve convergence speed, but there are no constraints on it to achieve convergence.

Although the algorithm converges, the worst-case convergence speed is generally exponential in the number of users  $K_r$  because the general problem is NP-hard. On the other hand,  $N$  and  $L$  are not affecting the convergence scaling of the BRB algorithm. The main computational complexity lies in the feasibility problem (6.3), which is solved individually in Step 11 and as part of Lemma 6.4 (an FPO problem) in Step 13. A convex formulation was given in Lemma 6.2 making it solvable in polynomial time, but as the BRB algorithm solves a long sequence of convex subproblems the total complexity makes it unsuitable for real-time applications. However, we show numerically in Section 6.5 that the proposed BRB algorithm has better convergence behavior than the outer polyblock approximation in [BU09, JL10, BU10].

*Remark 6.1.* The BRB algorithm in Table 6.3 is formulated to be applicable to any monotonic optimization problem. If only a certain type of user and system performance functions is of interest, this knowledge can be used to improve convergence. In particular, the bounding step should exploit any additional structure added to the problem. Instead of searching for feasible solutions on a straight line through the box (as the FPO does), the search can take place along any continuously componentwise-increasing curve between the lower and upper corner. The special case of weighted sum rate optimization was recently considered in [ESV<sup>+</sup>10] and [WCLaE10]. Under a total power constraint, [ESV<sup>+</sup>10] formulated the search in a box as an approximate convex problem, which greatly improves the bounding step. With single-antenna transmitters, [WCLaE10] showed that the feasibility problems can be solved by simply checking the spectral radius of a matrix. The special case when  $f(\cdot)$  is a (jointly) concave function and  $g_k(\text{SINR}_k) = \text{SINR}_k$  was considered in [RTSH11]. This structure enables convex bounding operations based on interference-temperature levels.

The BRB algorithm can also be applied to more general problems, for example, including CSI uncertainty. This is considered in the next section.

## 6.4 Extensions to the System Model

The proposed BRB algorithm in Section 6.3 relies on two basic properties:

- The performance region  $\mathcal{R}$  is compact and normal;
- The fairness-profile optimization problem can be solved efficiently.

It is therefore possible to extend the multicell system model, as long as these conditions are still satisfied. The compactness of  $\mathcal{R}$  is natural, given that the power constraints and soft-shaping constraints are compact (and the user performance functions are continuous). It might be more difficult to prove that  $\mathcal{R}$  is normal, although it is hard to imagine a scenario where this property is not satisfied. The FPO problem can be solved efficiently if the feasibility problem in (6.4) is solvable in polynomial time (e.g., if the feasibility problem is convex).

Two straightforward extensions are to add non-linear precoding (e.g., Tomlinson-Harashima precoding [SD09]) and multiple subcarriers (by viewing the signal received at each subcarrier as a separate user [BJBO11]). It is more challenging to relax the CSI accuracy at the base stations from being perfect to include some uncertainty. However, this is an important extension since practical transmitters have uncertain CSI. The uncertainty originates from a variety of sources, including channel estimation, feedback quantization, hardware deficiencies, and delays in CSI acquisition on fading channels. It is common to assume an additive error model [BTGN09, ZWN08a, VB09, VBS09, SD09, TPW11, CSCG07, SD08, WCWKM11] with

$$\mathbf{h}_k = \widehat{\mathbf{h}}_k + \boldsymbol{\epsilon}_k \quad \forall k \quad (6.16)$$

where  $\widehat{\mathbf{h}}_k = [\widehat{\mathbf{h}}_{1k}^T \dots \widehat{\mathbf{h}}_{K_t k}^T]^T \in \mathbb{C}^{N \times 1}$  is the uncertain CSI of the combined channel vector  $\mathbf{h}_k$  and  $\boldsymbol{\epsilon}_k \in \mathbb{C}^{N \times 1}$  is the combined error vector. This model can, for instance, be motivated by viewing channel estimation as the main source of uncertainty [BO10].<sup>4</sup> Observe that both the channel estimate and the error should be set to zero for all  $\mathbf{h}_{jk}$  with  $k \notin \mathcal{C}_j$ .

The stochastic distribution for  $\boldsymbol{\epsilon}_k$  is unbounded,<sup>5</sup> thus communication cannot be robust towards any error. This is usually handled by only considering a subset of error vectors, *the uncertainty set*, that has high probability [BTGN09, ZWN08a, VB09, VBS09, SD09, TPW11, CSCG07, SD08, WCWKM11]. If the design of this set is included in the resource allocation (i.e., optimization with acceptable outage probabilities), conservative approximations of each user's performance are required to achieve tractable problem formulations [CSCG07, SD08, WCWKM11]. The alternative of having fixed uncertainty sets and maximizing the worst-case performance over this set is more convenient as it can provide convex problem formulations [SD09, VBS09, TPW11]. This section will therefore concentrate on this case and show that the properties for applying the BRB algorithm

<sup>4</sup>Under the training-based MMSE channel estimation in Chapter 3, the error takes the form of (6.16). The stochastic error vector is  $\boldsymbol{\epsilon}_k \in (\mathbf{0}, \mathbf{E}_k)$  under Rayleigh fading. If the channel from each base station to user  $k$  is estimated separately, then the estimation error covariance matrix  $\mathbf{E}_k$  becomes block-diagonal.

<sup>5</sup>This holds for Rayleigh fading channels, while practical estimation errors of course are bounded but can be very large.

are satisfied. It should be noted that having fixed uncertainty sets often is accused of giving conservative performance results [GSS<sup>+</sup>10], although this is the result of using ill-structured sets and can be avoided by proper selection of them.<sup>6</sup>

#### 6.4.1 Worst-case Robustness to CSI Uncertainty

For analytical convenience and motivated by channel estimation<sup>7</sup> [VBS09, SD09, TPW11], we consider (compact) ellipsoidal channel uncertainty sets

$$\mathcal{U}_k(\widehat{\mathbf{h}}_k, \mathbf{B}_k) = \left\{ \mathbf{h}_k : \mathbf{h}_k = \widehat{\mathbf{h}}_k + \mathbf{B}_k \tilde{\boldsymbol{\epsilon}}_k, \|\tilde{\boldsymbol{\epsilon}}_k\|_2 \leq 1 \right\} \quad (6.17)$$

where  $\mathbf{B}_k \in \mathbb{C}^{N \times N}$  defines the shape of the ellipsoid. Since many uncertainty sources are independent between base stations (e.g., estimation and quantization are done separately),  $\mathbf{B}_k$  is typically block-diagonal in multicell systems. However, the analysis herein is not limited to such  $\mathbf{B}_k$ .

The user performance under CSI uncertainty will be based on the MSE instead of the SINR, to enable exact analysis.  $\text{MS}_k$  is assumed to use an equalizing coefficient  $r_k$  to achieve an estimate  $\hat{s}_k = r_k y_k$  of the transmitted data signal  $s_k$ . Thus, the MSE in the data estimation at  $\text{MS}_k$  is  $\text{MSE}_k = \mathbb{E}\{|\hat{s}_k - s_k|^2\}$  and becomes

$$\begin{aligned} \text{MSE}_k &= \|r_k \mathbf{h}_k^H \mathbf{C}_k [\mathbf{D}_1 \mathbf{v}_1 \dots \mathbf{D}_{K_r} \mathbf{v}_{K_r}] - \mathbf{e}_k^T\|_2^2 + |r_k|^2 \sigma_k^2 \\ &= \underbrace{|r_k \mathbf{h}_k^H \mathbf{C}_k \mathbf{D}_k \mathbf{v}_k - 1|^2}_{\text{signal distortion}} + \underbrace{\sum_{\bar{k} \neq k} |r_k \mathbf{h}_k^H \mathbf{C}_k \mathbf{D}_{\bar{k}} \mathbf{v}_{\bar{k}}|^2}_{\text{co-user interference}} + \underbrace{|r_k|^2 \sigma_k^2}_{\text{noise}} \end{aligned} \quad (6.18)$$

where  $\mathbf{e}_k$  denotes the  $k$ th column of  $\mathbf{I}_{K_r}$ . For MSE optimization, it suffices to consider real-valued  $r_k \geq 0$  as any complex phase can be included in the beamforming vector  $\mathbf{v}_k$  without affecting the MSE in (6.18). A block diagram of this extended system model is shown in Figure 6.3.

While  $\mathcal{U}_1, \dots, \mathcal{U}_{K_r}$  represents the CSI at the transmitter side, each  $\text{MS}_k$  is assumed to only have a local estimate of  $\mathbf{h}_k$ . Thus, the users are unaware

<sup>6</sup>In the probabilistic approach, the guaranteed performance is maximized under a given outage probability. Using an optimal precoding solution, one can create a set  $\mathcal{U}$  of all error vectors that gives exactly the optimal guaranteed performance (or better). If  $\mathcal{U}$  is used as the uncertainty set in the worst-case approach, it will provide the same optimal precoding solution.

<sup>7</sup>Continuing the estimation example in a previous footnote, recall that  $\boldsymbol{\epsilon}_k \in \mathcal{CN}(\mathbf{0}, \mathbf{A}_k)$ . Thus,  $\boldsymbol{\epsilon}_k$  belongs with probability  $\rho$  to the ellipsoidal set  $\{\boldsymbol{\epsilon}_k : 2\boldsymbol{\epsilon}_k^H \mathbf{E}_k^{-1} \boldsymbol{\epsilon}_k \leq \chi_\rho^2(2N)\}$ , where  $\chi_\rho^2(n)$  is the  $\rho$ -percentile of the  $\chi^2(n)$ -distribution. If we limit the robustness to this set, the channel uncertainty is given by (6.17) using  $\mathbf{B}_k = \sqrt{\chi_\rho^2(2N)/2\mathbf{E}_k^{1/2}}$ . To enforce higher or lower robustness to errors on channels from some base stations, one can use different weights on the diagonal blocks of  $\mathbf{B}_k$ .

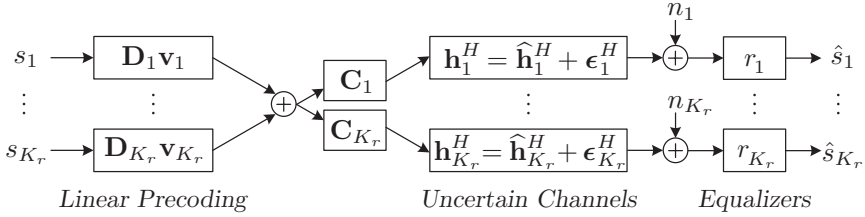


Figure 6.3: Block diagram of the extended multicell system under channel uncertainty. Linear precoding is applied to each data stream and  $\mathbf{D}_k$  decides which antennas that can transmit to user  $k$ . The channel uncertainty is modeled by additive errors  $\epsilon_k$ , while  $\mathbf{C}_k$  removes negligible channels that are included in the additive noise  $n_k$ . User  $k$  applies the equalizing coefficient  $r_k$  to estimate its data signal.

of co-user interference and precoding vectors, and are therefore assumed to be optimized by the base stations and told how to process their received signals. Observe that the actual performance can be improved by, for example, estimating the optimal equalizing coefficient at each user based on the precoded channels; see the system operation in Chapter 2.2.

Since the MSE is the average squared distance between  $s_k$  and its estimate  $\hat{s}_k$ , it should be small. The range of reasonable<sup>8</sup> MSE values is

$$0 < \text{MSE}_k \leq \mathbb{E}\{|s_k|^2\} = 1 \quad (6.19)$$

where the lower bound assumes negligible noise and interference, while the upper bound is the original signal variance. By following our convention that good performance corresponds to large positive values, the user performance under CSI uncertainty is measured by a continuous and *strictly decreasing*<sup>9</sup> function  $\tilde{g}_k(\text{MSE}_k)$  that satisfies  $\tilde{g}_k(1) = 0$ . The following lemma from [SD09] clarifies the relationship between having user performance functions based on MSEs and SINRs.

*Lemma 6.5.* If a given transmit strategy achieves  $\text{MSE}_k = \tilde{\gamma}_k$  for user  $k$ , this user is also guaranteed to achieve  $\text{SINR}_k \geq \frac{1}{\tilde{\gamma}_k} - 1$ .

MSE-based user performance functions therefore provide lower bounds on the SINR-based performance, such that  $g_k(\text{SINR}_k) \geq g_k(\frac{1}{\tilde{\gamma}_k} - 1)$ . Equality is only achieved if the optimal equalizing coefficient is found (which requires perfect CSI at each user).

The robust counterpart to performance region in Definition 5.2 is:

<sup>8</sup>We can always disregard the received signal at user  $k$  by setting  $r_k = 0$  and achieve  $\text{MSE}_k = 1$ , thus  $\text{MSE}_k > 1$  is always suboptimal.

<sup>9</sup>A function  $\tilde{g} : \mathbb{R}_+ \rightarrow \mathbb{R}$  is *strictly decreasing* if for any  $x, x' \in \mathbb{R}_+$  such that  $x > x'$  it follows that  $\tilde{g}(x) < \tilde{g}(x')$ .

*Definition 6.2.* The robust performance region  $\tilde{\mathcal{R}} \subset \mathbb{R}_+^{K_r}$  is

$$\tilde{\mathcal{R}} = \left\{ (g_1(\widetilde{\text{MSE}}_1), \dots, g_{K_r}(\widetilde{\text{MSE}}_{K_r})) : (\mathbf{v}_1, \dots, \mathbf{v}_{K_r}) \in \mathcal{V}, \quad r_k \geq 0 \quad \forall k \right\} \quad (6.20)$$

where the worst-case MSE is denoted

$$\widetilde{\text{MSE}}_k = \min \left( \max_{\mathbf{h}_k \in \mathcal{U}_k} \text{MSE}_k, 1 \right) \quad (6.21)$$

and  $\mathcal{V}$  is the set of feasible transmit strategies:

$$\mathcal{V} = \left\{ (\mathbf{v}_1, \dots, \mathbf{v}_{K_r}) : \sum_{k=1}^{K_r} \mathbf{v}_k^H \mathbf{Q}_l \mathbf{v}_k \leq q_l \quad \forall l, \quad \mathbf{v}_k^H \mathbf{T}_{ik} \mathbf{v}_k \leq \tau_{ik} \quad \forall i, k \right\}. \quad (6.22)$$

This region describes the performance that can be *guaranteed* to be simultaneously achievable by the users. The shape and size of this  $K_r$ -dimensional region depends on the uncertainty sets, but the region is always compact and normal (even if the sets are non-ellipsoidal):

*Lemma 6.6.* The robust performance region  $\tilde{\mathcal{R}}$  with compact uncertainty sets  $\mathcal{U}_1, \dots, \mathcal{U}_{K_r}$  is a compact and normal set.

*Proof.* The proof is given in Appendix 6.A.6. □

This lemma proves the first of the two basic properties that are required to apply the BRB algorithm. In other words, the robust resource allocation problem

$$\underset{\tilde{\mathbf{g}} \in \tilde{\mathcal{R}}}{\text{maximize}} \quad f(\tilde{\mathbf{g}}), \quad (6.23)$$

where the system performance function  $f(\cdot)$  is the same as under perfect CSI (i.e., Lipschitz continuous and strictly increasing), has an optimal solution on the upper boundary  $\partial^+ \tilde{\mathcal{R}}$  of the robust performance region.

The robust counterpart to the FPO problem is

$$\begin{aligned} & \underset{\substack{\mathbf{v}_1, \dots, \mathbf{v}_{K_r} \\ r_1, \dots, r_{K_r}}}{\text{maximize}} \quad \min_k \frac{\tilde{g}_k(\widetilde{\text{MSE}}_k) - a_k}{\alpha_k}, \\ & \text{subject to} \quad \tilde{g}_k(\widetilde{\text{MSE}}_k) \geq a_k \quad \forall k, \\ & \quad \sum_{k=1}^{K_r} \mathbf{v}_k^H \mathbf{Q}_l \mathbf{v}_k \leq q_l \quad \forall l, \\ & \quad \mathbf{v}_k^H \mathbf{T}_{ik} \mathbf{v}_k \leq \tau_{ik} \quad \forall i, k. \end{aligned} \quad (6.24)$$

This problem seems difficult to solve since there are infinitely many MSE constraints (one for each  $\mathbf{h}_k \in \mathcal{U}_k$ ). Fortunately, the following theorem

shows that the problem still can be solved by bisection, by exploiting well-known results from robust optimization [BTGN09].

*Theorem 6.2.* Consider (6.24) under the compact uncertainty sets in (6.17) for fixed  $\mathbf{a}, \boldsymbol{\alpha}$  and a given upper bound  $f_{\text{FPO}}^{\text{upper}}$  on the optimal value. This problem can be solved by bisection over the range  $\mathcal{F} = [0, f_{\text{FPO}}^{\text{upper}}]$ . For a given  $f_{\text{FPO}}^{\text{candidate}} \in \mathcal{F}$ , the convex feasibility problem

$$\begin{aligned} & \text{find } \mathbf{v}_1, \dots, \mathbf{v}_{K_r}, \tilde{r}_1, \dots, \tilde{r}_{K_r}, \lambda_1, \dots, \lambda_{K_r} \\ & \text{subject to } \mathbf{A}_k \succeq \mathbf{0}_{N+K_r+2} \quad \forall k, \\ & \sum_{k=1}^{K_r} \mathbf{v}_k^H \mathbf{Q}_l \mathbf{v}_k \leq q_l \quad \forall l, \\ & \mathbf{v}_k^H \mathbf{T}_{ik} \mathbf{v}_k \leq \tau_{ik} \quad \forall i, k, \\ & \tilde{r}_k \geq 0, \lambda_k \geq 0 \quad \forall k, \end{aligned} \quad (6.25)$$

where  $\bar{\mathbf{V}} = [\mathbf{D}_1 \mathbf{v}_1 \dots \mathbf{D}_{K_r} \mathbf{v}_{K_r}]$  and

$$\mathbf{A}_k = \begin{bmatrix} \sqrt{\tilde{\gamma}_k \tilde{r}_k} - \lambda_k & \hat{\mathbf{h}}_k^H \mathbf{C}_k \bar{\mathbf{V}} - \tilde{r}_k \mathbf{e}_k^T & \sigma_k & \mathbf{0} \\ \bar{\mathbf{V}}^H \mathbf{C}_k^H \hat{\mathbf{h}}_k - \tilde{r}_k \mathbf{e}_k & \sqrt{\tilde{\gamma}_k \tilde{r}_k} \mathbf{I}_{K_r} & \mathbf{0} & -\bar{\mathbf{V}}^H \mathbf{C}_k^H \mathbf{B}_k \\ \sigma_k & \mathbf{0} & \sqrt{\tilde{\gamma}_k \tilde{r}_k} & \mathbf{0} \\ \mathbf{0} & -\mathbf{B}_k^H \mathbf{C}_k \bar{\mathbf{V}} & \mathbf{0} & \lambda_k \mathbf{I}_N \end{bmatrix} \quad (6.26)$$

is solved for  $\tilde{\gamma}_k = \tilde{g}_k^{-1}(a_k + \alpha_k f_{\text{FPO}}^{\text{candidate}})$  as part of the bisection.

*Proof.* The proof is given in Appendix 6.A.7.  $\square$

This theorem only has one (linear) semi-definite constraint per user and has replaced the uncertainty set  $\mathcal{U}_k$  by a variable  $\lambda_k$  that indirectly represents the worst channel; if we can find  $\lambda_k \geq 0$  that satisfies the constraint, then  $\text{MSE}_k \leq \tilde{\gamma}_k$  for all  $\mathbf{h}_k \in \mathcal{U}_k$ . Having CSI uncertainty naturally increases the computational complexity, compared with the case of perfect CSI in Lemma 6.1. The number of constraints are the same, but there are more variables under CSI uncertainty and the user performance constraints have larger dimension. However, the robust FPO problem is still convex, thus the computational complexity is polynomial in the number of antennas  $N$ , users  $K_r$ , and power constraints  $L$  [BTN01, Chapter 6]. In addition, CSI uncertainty reduces the performance region  $\tilde{\mathcal{R}}$ , thus fewer feasibility problems need to be solved to attain a given accuracy  $\delta$ .

Single-cell counterparts to the convex feasibility problem in Theorem (6.2) have recently been derived in [ZWN08a, VB09, SD09], while the multicell generalization is novel. In the special case of  $\tilde{g}_k(\text{MSE}_k) = \text{MSE}_k^{-1} - 1$  and  $\mathbf{a} = \mathbf{0}$ , the robust FPO problem is equivalent to minimization of the (weighted) worst MSE among the users and can be posed as a generalized

eigenvalue problem [BG93, WES06, SD09], which improves the computational complexity.

To summarize, Lemma 6.6 showed that the robust performance region  $\tilde{\mathcal{R}}$  is compact and normal, while Theorem 6.2 showed that the fairness-profile optimization can be solved efficiently. Thus, the BRB algorithm in Section 6.3 can be applied under worst-case robustness to find the solution to (6.23). The only difference compared with Algorithm 6.3 is that the feasibility problems (in Steps 11 and 13) are solved using Theorem 6.2.

Finding the optimal resource allocation strategy is very important as a benchmark for suboptimal transmission strategies under CSI uncertainty. To evaluate some given precoding vectors  $\mathbf{v}_1, \dots, \mathbf{v}_{K_r}$  and equalizing coefficients  $r_1, \dots, r_{K_r}$ , we need to know the worst-case robust MSE  $\tilde{\gamma}_k = \max_{\mathbf{h}_k \in \mathcal{U}_k} \text{MSE}_k$  that each MS $_k$  achieves. With the notation  $\tilde{\gamma}_k = \sqrt{\tilde{\gamma}_k}$ , the robust MSE  $\tilde{\gamma}_k$  is easily obtained by solving

$$\begin{aligned} & \underset{\tilde{\gamma}_k \geq 0, \lambda_k \geq 0}{\text{minimize}} && \tilde{\gamma}_k \\ & \text{subject to} && \mathbf{A}_k \succeq \mathbf{0}_{N+K_r+2} \end{aligned} \quad (6.27)$$

which is a convex problem in  $\tilde{\gamma}_k$  and  $\lambda_k$ . The matrix  $\mathbf{A}_k$  is given in (6.26) using  $\tilde{r}_k = r_k^{-1}$  and  $\tilde{\gamma} = \sqrt{\tilde{\gamma}_k}$ .

## 6.5 Numerical Illustrations

Some properties of our framework for optimal resource allocation will be illustrated numerically in this section, under both perfect and uncertain CSI. The implementation is based on the YALMIP toolbox of [Löf04] and the numerical convex optimization solver SDPT3 from [TTT03]. First, the concepts of performance regions and system performance functions are illustrated. Then, the computational complexity of solving FPO problems is exemplified and the convergence of the BRB algorithm is compared with the outer polyblock approximation algorithm. The BRB algorithm is applied for benchmarking in realistic multicell systems in Chapter 8.

### 6.5.1 Performance Regions

To illustrate the shape of the (robust) performance regions, we consider a simple network MIMO scenario with  $K_r = 2$  users. The total number of transmit antennas is  $N = 3$ , all channels are Rayleigh fading and spatially uncorrelated, and we use per-antenna constraints with  $q_l = 10$  (i.e., 10 dB). The average SNR  $\mathbb{E}\{\|\mathbf{h}_k\|_2^2\}/\sigma_k^2$  is  $N$  for user 1 and  $N/4$  for user 2, creating an asymmetry that will highlight properties of different system performance functions. Spherical uncertainty sets  $\mathcal{U}_k(\hat{\mathbf{h}}_k, \mathbf{B}_k)$  are assumed with  $\mathbf{B}_k = \sqrt{\xi} \mathbf{I}_N$  in (6.17), where the parameter  $\sqrt{\xi}$  is the radius of the

sphere. If one standard deviation of the channel estimation error is used as uncertainty set, then  $\xi$  equals the estimation error variance.

Figure 6.4 shows the robust performance regions for a random channel realization and different  $\xi$ , including perfect CSI ( $\xi = 0$ ). In Figure 6.4a, the inverse MSE is considered (i.e.,  $\tilde{g}_k(\text{MSE}_k) = \text{MSE}_k^{-1} - 1$  to make  $\tilde{g}_k(1) = 0$ , or  $g_k(\text{SINR}_k) = \text{SINR}_k$  under perfect CSI), but the figure axes show MSEs to enhance viewing. The guaranteed data rate (i.e.,  $\tilde{g}_k(\text{MSE}_k) = \log_2(\text{MSE}_k^{-1})$  or  $g_k(\text{SINR}_k) = \log_2(1 + \text{SINR}_k)$  under perfect CSI) is the user performance measure in Figure 6.4b. In both figures, the optimal system performance points are shown for the four functions exemplified in Chapter 5.2.2: sum performance, proportional fairness, harmonic mean, and max-min fairness.

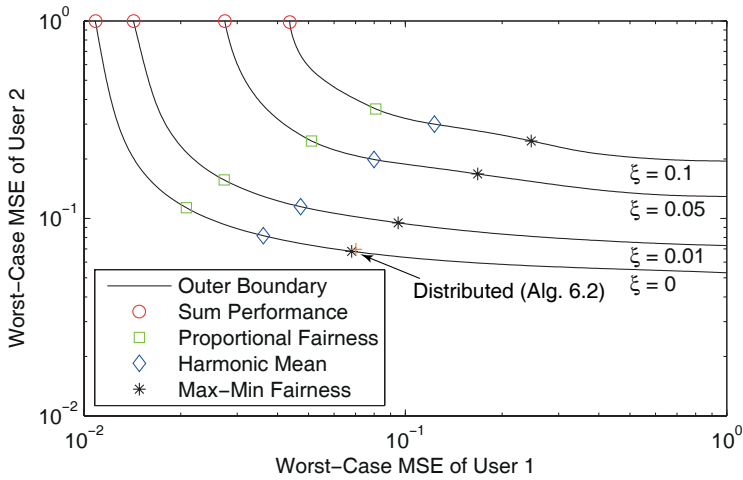
Robustness towards channel uncertainty decreases the size of the performance regions, but without affecting the general shape (in this scenario). The optimal points with the four system performance functions are all on the upper boundaries (confirming Lemma 5.2), but at quite different places. By introducing user weights in the system functions, the optimal points can be moved around on the upper boundary; in fact, the upper boundaries in Figure 6.4 were generated by solving (weighted) max-min fairness optimization problems for a large set of weights (i.e., Algorithm 6.1 with  $\mathbf{a} = \mathbf{0}_{K_r \times 1}$  and different  $\boldsymbol{\alpha}$ ).

Figure 6.4 also shows the approximate max-min fairness point obtained by the distributed FPO approach (Algorithm 6.2). Using 30 iterations as stopping criterion and the parameter values  $\xi = 1$  and  $\nu = 1/3$ , the distributed algorithm achieves a point corresponding to 99% of the optimal max-min data rate. Increasing the number of iterations will only result in slight improvements, which indicates that  $\xi$  and  $\nu$  should be varied to achieve exact convergence.

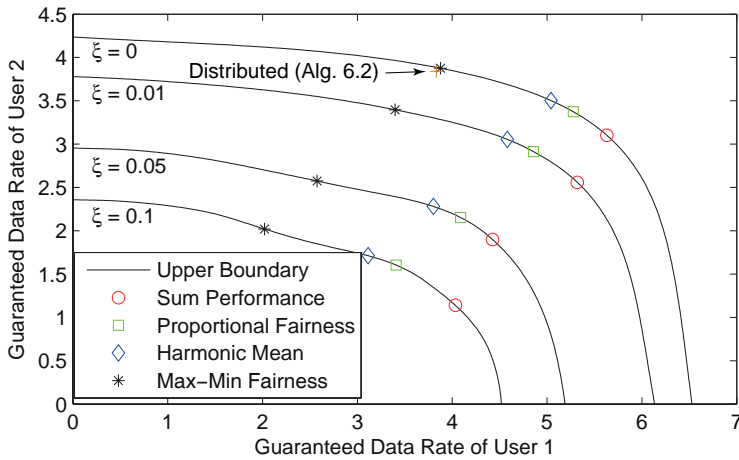
## 6.5.2 Computational Complexity

Next, the computational complexity of the fairness-profile optimization problem is evaluated. We consider the same multicell scenario as in the previous subsection, but we fix the transmit power per base station at 10 dB and vary the number of users  $K_r \in \{4, 8, 12, 16, 20\}$  and the number of transmit antennas  $N_1 = N_2 \in \{4, 8, 12\}$ . Recall that the FPO problem is solved by iterating the feasibility problem in (6.3) or (6.25) until a given line-search accuracy is achieved (10-15 iterations usually give a good accuracy, but it depends on the user performance functions). Therefore, Figure 6.5 shows the average computational time for solving this subproblem. The simulation was performed at a standard PC running Linux/Ubuntu with an Intel Core2Duo Q8400 at 2.66 GHz using all four cores.

Figure 6.5 shows how the computational time increases with both the number of users and total number of antennas. It is clear that the com-



(a) User Performance Measure: Inverse Worst-Case MSE.



(b) User Performance Measure: Guaranteed Data rate.

Figure 6.4: Robust performance regions with different squared radius  $\xi$  of the channel uncertainty sets. The user performance measure is either (a) the inverse MSE or (b) the guaranteed data rate. The optimal points with different system performance functions are shown.

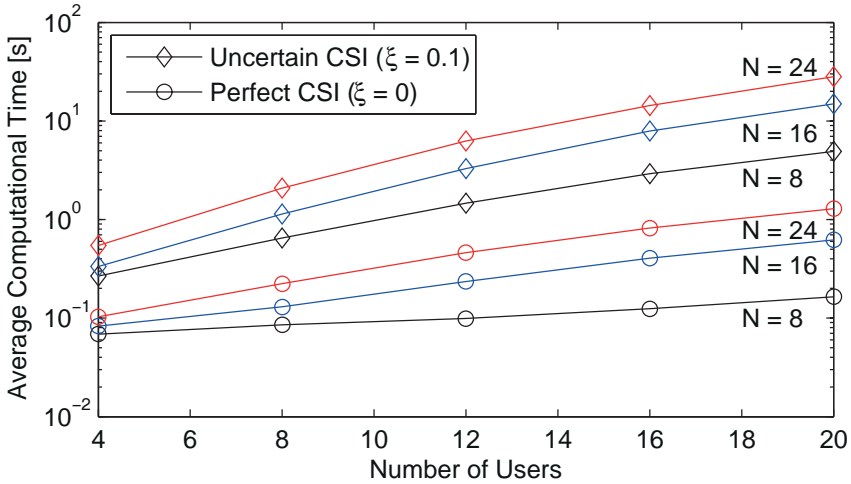


Figure 6.5: Example of the average computational time of solving the feasibility problems in (6.3) and (6.25) with perfect and uncertain CSI, respectively. Different number of users and total number of antennas are considered.

plexity under channel uncertainty ( $\xi = 0.1$ ) is several times higher and has a steeper slope than under perfect CSI. This was expected from the discussion in Section 6.4. Comparing all the scenarios, it is clear that the computational time spans from a fraction of a second to a fraction of a minute; thus, the FPO problem can be solved quite efficiently (even at a standard PC with a general-purpose numerical solver) and is applicable for future real-time applications.

### 6.5.3 Convergence Comparison

Finally, the convergence of the proposed BRB algorithm is compared with the outer polyblock approximation in [BU10]. As these algorithms are rather different, it is not meaningful to compare the number of iterations. Instead, we consider the performance as a function of the number of feasibility evaluations of the type in (6.3). This convex subproblem is the main source of complexity in both algorithms.

We only consider perfect CSI, which is the case in [BU09, JL10, BU10]. We consider a multicell scenario with  $K_t = 2$  base stations with  $N_1 = N_2 = 3$  antennas. Each base station serves two unique users (i.e.,  $K_r = 4$ ), while coordinating interference to all users. The average SNR  $\mathbb{E}\{\|\mathbf{h}_{jk}\|_2^2\}/\sigma_k^2$  is  $N_j$  if user  $k \in \mathcal{D}_j$  and  $N_j/2$  if  $k \notin \mathcal{D}_j$ . Each base station has its own total

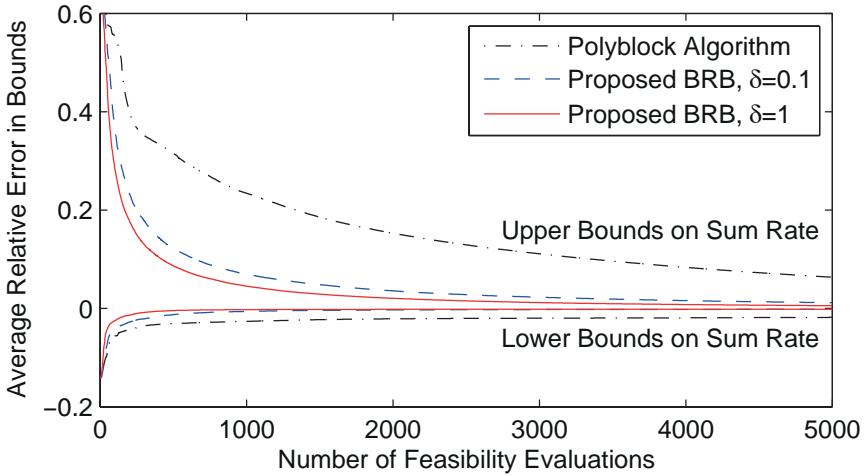


Figure 6.6: Relative error of lower and upper bounds on the sum rate as a function of the number of feasibility evaluations.

power constraint with  $q_j = 10$  (i.e., 10 dB for single-user transmission) and the sum rate is used as performance measure.

Figure 6.6 shows the average relative deviations<sup>10</sup> (over 250 channel realizations) of the lower and upper bounds on the sum rate as a function of the number of feasibility evaluations. The BRB algorithm is used with a line-search accuracy  $\delta$  of either 0.1 or 1, while  $\delta = 0.1$  was used for the polyblock algorithm. Both algorithms quickly find feasible solutions within a few percent from the optimal value, but many evaluations are required to achieve a tight upper bound. However, the proposed BRB algorithm shows much faster convergence in both the lower and the upper bound; after 5000 feasibility evaluations, the polyblock algorithm has still not reached the accuracy that the BRB algorithm achieved with 1000 evaluations. This is consistent with observations in [TAKT05], where the difference is also claimed to increase with the number of users. Thus, in terms of achieving an  $\varepsilon$ -approximation on the optimal performance, the proposed BRB algorithm shows much faster convergence. For the BRB algorithm,  $\delta = 1$  gives faster convergence than  $\delta = 0.1$ , indicating that having many BRB iterations with loose line-search bounds could be more efficient than having few BRB iterations with tight bounds.

<sup>10</sup>If  $f_{\text{opt}}$  is the optimal solution, the relative deviations of the lower and upper bound are  $(f_{\text{min}} - f_{\text{opt}})/f_{\text{opt}}$  and  $(f_{\text{max}} - f_{\text{opt}})/f_{\text{opt}}$ , respectively.

## 6.6 Summary

Resource allocation in multicell systems is generally a non-convex problem and even NP-hard. An important exception is the category of fairness-profile optimization problems (a novel generalization of max-min optimization), which we have shown to be quasi-convex under both perfect CSI and worst-case robustness to CSI uncertainty. The explanation for its polynomial complexity is that the general problem only has exponential complexity in the number of users, and the FPO problem avoids this by searching on a one-dimensional curve in the multi-dimensional performance region. Whenever the FPO problem can be solved efficiently (and the performance region is compact and normal), we can apply our proposed BRB algorithm to solve any multicell resource allocation problem. The computational complexity will certainly be high (since exponential complexity is expected from NP-hard problems), but the BRB algorithm has guaranteed convergence and is suitable for evaluating suboptimal strategies toward the optimal solution. The BRB algorithm was shown to provide far better convergence than the previously known outer polyblock approximation algorithm, and its benchmarking capability is exemplified in Chapter 8.

## 6.A Collection of Proofs

### 6.A.1 Proof of Lemma 6.1

From Lemma 5.1,  $\mathcal{R}$  is a compact and normal set. For such sets, a ray from a point within the region (in a positive direction) meets  $\partial^+\mathcal{R}$  in a unique point (see [Tuy00, Proposition 6]). This point is the optimum of (6.2), since the optimum must be on  $\partial^+\mathcal{R}$  (as proved in Lemma 5.2). As the ray only meets the upper boundary once, it can be divided into two parts: one part is inside of  $\mathcal{R}$  and one part is outside. The intersection can be found (to any accuracy) by a line search (e.g., bisection) that iteratively checks if a point  $\mathbf{a} + \alpha f_{\text{FP0}}^{\text{candidate}}$  is inside  $\mathcal{R}$  by solving (6.3).

### 6.A.2 Proof of Lemma 6.2

Since the power and soft-shaping constraints in (6.3) are semi-definite, only the SINR constraints need reformulation. Following the approach in [YL07], observe that we can select the phase of  $\mathbf{v}_k$  in an arbitrary way and thus can decide that  $\mathbf{h}_k^H \mathbf{C}_k \mathbf{D}_k \mathbf{v}_k > 0$  (making the square root of  $|\mathbf{h}_k^H \mathbf{C}_k \mathbf{D}_k \mathbf{v}_k|^2$  well-defined). By moving around in the SINR constraints, it is straightforward to achieve the convex second-order cone form given in (6.4).

### 6.A.3 Proof of Lemma 6.3

First, consider the reduction of the box from  $[\tilde{\mathbf{a}}_l, \tilde{\mathbf{b}}_l]$  to  $[\tilde{\mathbf{a}}'_l, \tilde{\mathbf{b}}'_l]$  (i.e, from below). If the boxes are identical, no solutions are lost and we are finished. Otherwise,  $\tilde{\mathbf{a}}_l \leq \tilde{\mathbf{a}}'_l$  with strict inequality in at least one element. For elements with strict inequality we have  $\nu_k < 1$ , while  $\nu_k = 1$  holds for all other elements. There exist  $\mathbf{g} \in [\tilde{\mathbf{a}}_l, \tilde{\mathbf{b}}_l]$  such that  $\mathbf{g} \notin [\tilde{\mathbf{a}}'_l, \tilde{\mathbf{b}}'_l]$ . For any such  $\mathbf{g}$  there is one dimension  $k$  such that  $g_k < \tilde{a}'_{l,k}$  and  $\nu_k < 1$ . Thus,  $\mathbf{g} \leq \tilde{\mathbf{b}}_l - \tilde{\nu}(\tilde{b}_{l,k} - \tilde{a}_{l,k})\mathbf{e}_k$  for some  $\tilde{\nu}$  with  $\nu_k < \tilde{\nu} \leq 1$ . For the (strictly increasing) system performance functions, we have

$$\begin{aligned} f(\mathbf{g}) &\leq f(\tilde{\mathbf{b}}_l - \tilde{\nu}(\tilde{b}_{l,k} - \tilde{a}_{l,k})\mathbf{e}_k) \\ &< f(\tilde{\mathbf{b}}_l - \nu_k(\tilde{b}_{l,k} - \tilde{a}_{l,k})\mathbf{e}_k) = f_{\min}. \end{aligned} \tag{6.28}$$

The strict inequality follows since  $\nu_k$  is selected to be the largest value that gives equality in the set defined in (6.13). From (6.28) it is clear that any  $\mathbf{g}$  removed in the reduction (from below) has a function value strictly below  $f_{\min}$ . The reduction from above is proved analogously. Finally, observe that  $[\tilde{\mathbf{a}}'_l, \tilde{\mathbf{b}}'_l] \subseteq [\tilde{\mathbf{a}}_l, \tilde{\mathbf{b}}_l]$  since each element in  $\tilde{\mathbf{a}}'_l$  and  $\tilde{\mathbf{b}}'_l$  are calculated as convex combinations of  $\tilde{\mathbf{a}}_l$  and  $\tilde{\mathbf{b}}_l$ .

#### 6.A.4 Proof of Lemma 6.4

The line-search procedure in Algorithm 6.1 finds the best feasible solution (with accuracy  $\delta$ ) on the line segment between  $\mathbf{a}$  and  $\mathbf{b}$ . Thus,  $\mathbf{a} + \alpha f_{\text{FPO}}^{\min}$  is feasible and can be used for a lower bound on the performance. Similarly,  $\mathbf{n}$  is either on the upper boundary or infeasible. Since  $\mathcal{R}$  is normal, there are no feasible points  $\mathbf{x} \in \mathcal{M}$  with  $\mathbf{x} > \mathbf{n}$ . The corner points where all elements but one are larger than in  $\mathbf{n}$  are  $\mathbf{b} - (b_k - n_k)\mathbf{e}_k$  for  $k = 1, \dots, K_r$ . These can be used to calculate an upper bound on the performance.

#### 6.A.5 Proof of Theorem 6.1

The convergence of the algorithm in Table 6.3 can be studied as a standard branch-and-bound algorithm, treating the reduction step (which does not remove the solution) as part of the bounding step. In the appendix of [BBB91], two sufficient conditions are given for achieving an  $\varepsilon$ -approximate solution in a finite number of iterations: 1) The bounding step truly calculates lower and upper bounds on the optimal value; 2) The difference  $f_{\max} - f_{\min}$  converges (uniformly) to zero. The first condition was proved in Lemma 6.4, while the second condition follows from the exhaustiveness of bisection and the Lipschitz continuity of  $f$  (i.e.,  $\|\mathbf{b} - \mathbf{a}\| \leq \text{constant}_1$  means that  $f(\mathbf{b}) - f(\mathbf{a}) \leq \text{constant}_2$ ). Finally, observe that bounding the performance in a box using only the lower and upper corners satisfies these conditions; thus, any  $\delta > 0$  can be used.

#### 6.A.6 Proof of Lemma 6.6

To prove that the set is normal, take  $\mathbf{x} = (x_1, \dots, x_{K_r}) \in \tilde{\mathcal{R}}$  and assume that  $\{r_k^*\}_{k=1}^{K_r}$  and  $\{\mathbf{v}_k^*\}_{k=1}^{K_r}$  is a feasible strategy that attains this point. We want to show that any  $\mathbf{x}' = (x'_1, \dots, x'_{K_r}) \in \mathbb{R}_+^{K_r}$  with  $\mathbf{x}' \leq \mathbf{x}$  also belongs to  $\tilde{\mathcal{R}}$ . To this end, we fix the precoding vectors at  $\{\mathbf{v}_k^*\}_{k=1}^{K_r}$  and search for equalizing coefficients  $\{r_{\mathbf{x}',k}\}_{k=1}^{K_r}$  that gives  $\widetilde{\text{MSE}}_k = \tilde{\gamma}'_k$  for all  $k$ , where  $\tilde{\gamma}'_k = \tilde{g}_k^{-1}(x'_k)$ . For a given channel realization  $\mathbf{h}_k$ , denote the MSE in (6.18) as  $\text{MSE}_k(r_k, \mathbf{h}_k)$ . Observe that  $\text{MSE}_k(r_k, \mathbf{h}_k)$  is a second-order polynomial in  $r_k$  that has a unique minimum and then approaches infinity continuously as  $r_k \rightarrow \infty$ . Thus, we can solve the second-order equation  $\text{MSE}_k(r_k, \mathbf{h}_k) = \tilde{\gamma}'_k$  to derive the largest root

$$r'_k(\mathbf{h}_k) = \frac{a_k + \sqrt{a_k^2 - (1 - \tilde{\gamma}'_k)b_k}}{b_k} \quad (6.29)$$

where  $a_k = \Re(\mathbf{h}_k^H \mathbf{C}_k \mathbf{D}_k \mathbf{v}_k)$  and  $b_k = \|\mathbf{h}_k^H \mathbf{C}_k [\mathbf{D}_1 \mathbf{v}_1 \dots \mathbf{D}_{K_r} \mathbf{v}_{K_r}]\|_2^2 + \sigma_k^2$ . This solution will be real-valued, because it is real-valued for  $\mathbf{x}' = \mathbf{x}$  and increases with  $\tilde{\gamma}'_k$ . Since we consider the largest root,  $\text{MSE}_k(r_k, \mathbf{h}_k) > \tilde{\gamma}'_k$

for all  $r_k > r'_k(\mathbf{h}_k)$ . By selecting

$$r_{\mathbf{x}',k} = \min_{\mathbf{h}_k \in \mathcal{U}_k} r'_k(\mathbf{h}_k) \quad \forall k \quad (6.30)$$

we can make sure that  $\tilde{g}_k(\widetilde{\text{MSE}}_k) = x'_k$  and thus that  $\mathbf{x}' \in \widetilde{\mathcal{R}}$ .

Next, we prove that  $\widetilde{\mathcal{R}}$  is a compact set. First, observe that the set of feasible precoding vectors,  $\mathcal{V}$ , in (6.22) is compact. Next, observe that it is sufficient to search for equalizing coefficients  $r_k$  in the compact set  $\mathcal{E}_k = [0, 1/\sigma_k]$ , since greater values make the noise part of the MSE in (6.18) larger than one (and thus,  $\text{MSE}_k \geq 1$ ). The MSEs are continuous functions of the precoding and equalizing coefficients, and the performance functions  $\tilde{g}_k(\widetilde{\text{MSE}}_k)$  are continuous by definition. Therefore,  $\tilde{g}_k(\min(\max_{\mathbf{h}_k \in \mathcal{U}_k} \text{MSE}_k, 1))$  is continuous for any compact set  $\mathcal{U}_k$ . Finally, we invoke [Rud76, Theorem 4.14], which says that the continuous mapping of a compact set is also a compact set. Since  $\widetilde{\mathcal{R}}$  is the image of a continuous mapping from  $\mathcal{V}$  and  $\mathcal{E}_k$ , the robust performance region is compact.

### 6.A.7 Proof of Theorem 6.2

Since the robust performance region  $\widetilde{\mathcal{R}}$  is compact and robust (see Lemma 6.6), the robust fairness-profile optimization problem in (6.24) can be solved using the bisection approach in Lemma 6.1. The only exception is that the feasibility problems are replaced by

$$\begin{aligned} & \text{find } \mathbf{v}_1, \dots, \mathbf{v}_{K_r}, r_1 \geq 0, \dots, r_{K_r} \geq 0 \\ & \text{subject to } \widetilde{\text{MSE}}_k \leq \tilde{\gamma}_k \quad \forall k, \\ & \sum_{k=1}^{K_r} \mathbf{v}_k^H \mathbf{Q}_l \mathbf{v}_k \leq q_l \quad \forall l, \\ & \mathbf{v}_k^H \mathbf{T}_{ik} \mathbf{v}_k \leq \tau_{ik} \quad \forall i, k. \end{aligned} \quad (6.31)$$

To see that this problem is convex, we need to reformulate the MSE constraints into a convex form. To this end, we use the following well-known result in robust worst-case optimization theory:

*Lemma 6.7.* Given  $\mathbf{A}, \mathbf{P}, \mathbf{Q}$ , with  $\mathbf{A} = \mathbf{A}^H$ , the expression

$$\mathbf{A} \succeq \mathbf{P}^H \mathbf{Z} \mathbf{Q} + \mathbf{Q}^H \mathbf{Z}^H \mathbf{P} \quad \forall \mathbf{Z} : \|\mathbf{Z}\|_2 \leq \bar{\varrho} \quad (6.32)$$

holds if and only if

$$\exists \lambda \in \mathbb{R}_+ \quad \text{s.t.} \quad \begin{bmatrix} \mathbf{A} - \lambda \mathbf{Q}^H \mathbf{Q} & -\bar{\varrho} \mathbf{P}^H \\ -\bar{\varrho} \mathbf{P} & \lambda \mathbf{I} \end{bmatrix} \succeq \mathbf{0}. \quad (6.33)$$

*Proof.* The proof is given in [EM04, Proposition 2].  $\square$

Lemma 6.7 can be used to reformulate each MSE constraint

$$\max_{\mathbf{h}_k \in \mathcal{U}_k} \text{MSE}_k \leq \tilde{\gamma}_k \quad (6.34)$$

into a (linear) semi-definite constraint. First, we replace  $\mathbf{h}_k$  with  $\hat{\mathbf{h}}_k + \mathbf{B}_k \tilde{\boldsymbol{\epsilon}}_k$  in the MSE expression of (6.18). Next, we apply Schur complement lemma [Zha05, Theorem 1.12] to rewrite (6.34) as

$$\begin{aligned} & \begin{bmatrix} \sqrt{\tilde{\gamma}_k} r_k^{-1} & \hat{\mathbf{h}}_k^H \mathbf{C}_k \bar{\mathbf{V}} - r_k^{-1} \mathbf{e}_k^T & \sigma_k \\ \bar{\mathbf{V}}^H \mathbf{C}_k^H \hat{\mathbf{h}}_k - r_k^{-1} \mathbf{e}_k & \sqrt{\tilde{\gamma}_k} r_k^{-1} \mathbf{I}_{K_r} & \mathbf{0} \\ \sigma_k & \mathbf{0} & \sqrt{\tilde{\gamma}_k} r_k^{-1} \end{bmatrix} \\ & + \begin{bmatrix} 0 & \tilde{\boldsymbol{\epsilon}}_k^H \mathbf{B}_k^H \mathbf{C}_k \bar{\mathbf{V}} 0 \\ \bar{\mathbf{V}}^H \mathbf{C}_k^H \mathbf{B}_k \tilde{\boldsymbol{\epsilon}}_k & \mathbf{0}_{K_r} & \mathbf{0} \\ 0 & \mathbf{0} & 0 \end{bmatrix} \succeq \mathbf{0} \quad \forall \tilde{\boldsymbol{\epsilon}}_k : \|\tilde{\boldsymbol{\epsilon}}\|_2 \leq 1. \end{aligned} \quad (6.35)$$

Finally, we apply Lemma 6.7 with  $\mathbf{A}$  being the first matrix in (6.35),  $\mathbf{P} = [\mathbf{0} \ \mathbf{B}_k^H \mathbf{C}_k \bar{\mathbf{V}} \ \mathbf{0}]$ ,  $\mathbf{Q} = [-1 \ \mathbf{0} \ 0]$ ,  $\mathbf{Z} = \tilde{\boldsymbol{\epsilon}}_k$ , and  $\tilde{\rho} = 1$ . The obtained reformulation of (6.35) is the constraint in (6.25). By optimizing over  $\tilde{r}_k = r_k^{-1}$  instead of  $r_k$ , we observe that this constraint is linear in  $\mathbf{v}_1, \dots, \mathbf{v}_{K_r}, \tilde{r}_k$ . Thus, the reformulated feasibility problem is convex. Further details are available in similar proofs (under different system assumptions) in for instance [BTGN09, ZWN08a, VB09, SD09].

## Chapter 7

# Practical Solutions to Multicell Resource Allocation

In this chapter, we analyze the general multicell resource allocation problem that was defined in Chapter 5. Solving this problem optimally is not feasible in large cellular networks with tight delay constraints, limited backhaul capacity, and limited computational power. To gain some intuition on the optimal solution structure, we derive two precoding characterizations. The first one shows that the optimal precoding vector for a base station belongs to a subspace defined using only local CSI; thus, the difficulty of multicell coordination is not the lack of CSI but the need for coordinated decision making. The second one gives an explicit expression for the optimal resource allocation strategy, which is parameterized using  $K_r + L - 1$  numbers between zero and one. Finding the optimal parameters is difficult, but we propose two low-complexity strategies that exploit this structure. The CVSINR strategy is centralized and provides close-to-optimal performance, while the distributed DVSINR strategy only requires limited backhaul signaling of scheduling decisions.

The considered multicell resource allocation problem is given in Section 7.1. In Section 7.2, the optimal precoding vectors are shown to be linear combinations of maximum ratio transmission and zero-forcing vectors. In addition, the optimal strategy is parameterized and it is shown how this provides a characterization of the Pareto boundary of the performance region. These results are exploited in Section 7.3 to propose low-complexity strategies that are either centralized or distributed. Their performance is evaluated in Chapter 8. Many of the results of this chapter can easily be extended for systems with multiple subchannels; see [BJBO11] for details.

## 7.1 Multicell Resource Allocation

This chapter considers the multicell resource allocation problem

$$\begin{aligned}
 & \underset{\mathbf{v}_1, \dots, \mathbf{v}_{K_r}}{\text{maximize}} && f(g_1(\text{SINR}_1), \dots, g_{K_r}(\text{SINR}_{K_r})) \\
 & \text{subject to} && \text{SINR}_k = \frac{|\mathbf{h}_k^H \mathbf{C}_k \mathbf{D}_k \mathbf{v}_k|^2}{\sigma_k^2 + \sum_{\bar{k} \neq k} |\mathbf{h}_k^H \mathbf{C}_k \mathbf{D}_{\bar{k}} \mathbf{v}_{\bar{k}}|^2} \quad \forall k, \\
 & && \sum_{k=1}^{K_r} \mathbf{v}_k^H \mathbf{Q}_l \mathbf{v}_k \leq q_l \quad \forall l, \\
 & && \mathbf{v}_k^H \mathbf{T}_{ik} \mathbf{v}_k \leq \tau_{ik} \quad \forall i, k,
 \end{aligned} \tag{7.1}$$

which is the same problem as in Chapter 6 and is based on the dynamic cooperation clusters introduced in Chapter 5. The optimal solution to (7.1) was derived in Chapter 6, but since the problem is generally NP-hard we cannot operate at the optimum in practice [LZ08, LDL11]. The search-space for optimal resource allocation strategies consists of all  $K_r$  vectors  $\mathbf{v}_k \in \mathbb{C}^{N \times 1}$  that satisfy the constraints in (7.1). Next section shows how this search-space can be greatly reduced without removing the optimum.

## 7.2 Characterization of Optimal Resource Allocation

In this section, we analyze the multicell resource allocation problem in (7.1) and show: 1) Optimal precoding vectors belong to sets that are defined using only local CSI; 2) Optimal precoding vectors can be characterized using  $K_r + L - 1$  parameters from zero to one. We also show that this parametrization can be used to characterize the Pareto boundary of the performance region  $\mathcal{R}$ .

### 7.2.1 Precoding Parametrization Based on Local CSI

The collective precoding vectors can be decomposed as  $\mathbf{v}_k = [\mathbf{v}_{1k}^T \dots \mathbf{v}_{K_r k}^T]^T$ , where  $\mathbf{v}_{jk} \in \mathbb{C}^{N_j \times 1}$  is the precoding vector from BS <sub>$j$</sub>  to MS <sub>$k$</sub> . Two classic ways of selecting these vectors are *maximum ratio transmission (MRT)* and *zero-forcing (ZF)*, which maximizes the received signal power and minimizes the co-user interference, respectively. In the special case of  $K_r = 2$ , these precoding vectors are aligned with  $\mathbf{h}_{jk}$  and  $\mathbf{\Pi}_{\mathbf{h}_{j\bar{k}}}^\perp \mathbf{h}_{jk}$ , respectively, for  $\bar{k} \neq k$ . The optimal resource allocation for the two-user MISO interference channel can only be achieved by precoding vectors that are linear combinations of MRT and ZF [JLD08]. This optimal structure is interesting from a game theoretical perspective, since it can be interpreted as a combination of the selfish MRT approach and the altruistic ZF approach [LELM09].

The multicell resource allocation problem in (7.1) is fundamentally different from the two-user MISO interference channel, since it enables joint transmissions and an arbitrary number of transmitters and receivers. But the following theorem provides a precoding characterization that turns out to be a similar combination of MRT and ZF.

*Theorem 7.1.* The optimal solution to (7.1) can be achieved if BS<sub>*j*</sub> selects  $\mathbf{v}_{jk} = \mathbf{0}_{N_j \times 1}$  for all  $k \notin \mathcal{D}_j$  and

$$\mathbf{v}_{jk} \in \text{span} \left( \{ \mathbf{h}_{jk} \} \cup \{ \mathbf{\Pi}_{\mathbf{h}_{j\bar{k}}}^\perp \mathbf{h}_{jk} \} \right) \quad \forall k \in \mathcal{D}_j. \quad (7.2)$$

*Proof.* The proof is given in Appendix 7.A.1. □

This theorem implies that (7.1) is solved by using

$$\mathbf{v}_{jk} = \underbrace{v_{jk}^{(k)} \frac{\mathbf{h}_{jk}}{\|\mathbf{h}_{jk}\|_2}}_{=\text{MRT}} + \sum_{\bar{k} \in \mathcal{C}_j \setminus \{k\}} v_{jk}^{(\bar{k})} \underbrace{\frac{\mathbf{\Pi}_{\mathbf{h}_{j\bar{k}}}^\perp \mathbf{h}_{jk}}{\|\mathbf{\Pi}_{\mathbf{h}_{j\bar{k}}}^\perp \mathbf{h}_{jk}\|_2}}_{=\text{ZF towards user } \bar{k}} \quad \text{for all } j \text{ and } k \in \mathcal{D}_j, \quad (7.3)$$

for some coefficients  $v_{jk}^{(\bar{k})} \in \mathbb{C}$ . This is a linear combination of MRT and  $|\mathcal{C}_j| - 1$  ZF vectors, each inflicting zero interference at user  $\bar{k} \in \mathcal{C}_j \setminus \{k\}$ . A special case of (7.3) is the system-wide ZF vector that inflicts zero interference to all co-users in  $\mathcal{C}_j \setminus \{k\}$  and only exists if  $N_j \geq |\mathcal{C}_j|$ .<sup>1</sup> This case can also be expressed as  $\mathbf{v}_{jk}$  (for  $k \in \mathcal{D}_j$ ) being parallel to

$$\mathbf{\Pi}_{\mathbf{H}_{jk}^{\text{interf}}}^\perp \mathbf{h}_{jk} \quad \text{where} \quad \mathbf{H}_{jk}^{\text{interf}} = \text{span} \left( \bigcup_{\bar{k} \in \mathcal{C}_j \setminus \{k\}} \{ \mathbf{h}_{j\bar{k}} \} \right). \quad (7.4)$$

The insights provided by Theorem 7.1 can be summarized as follows. Firstly, the optimal beamforming direction is a linear combination of the selfish MRT approach and altruistic interference control towards each co-user. Secondly, the optimal precoding vector belongs to a subspace that is defined using only local CSI (i.e., CSI for channels from BS<sub>*j*</sub> to users in  $\mathcal{C}_j$ ). The optimal choice within this subspace certainly depends on the decisions taken by other base stations, but Theorem 7.1 shows that the difficulty in multicell resource allocation is not the lack of CSI but the need for coordinated selection of the  $v$ -parameters; the magnitude of  $v_{jk}^{(\bar{k})}$  describes the (relative) importance of interference-avoidance towards MS <sub>$\bar{k}$</sub> , while the phase can be coordinated to enable joint interference cancellation. The distributed resource allocation strategy that we propose in Section 7.3 can be viewed as a heuristic selection of these  $v$ -parameters.

<sup>1</sup>Through joint multicell transmission, the total interference at a user can be zero although the interference caused by each base station is non-zero. In other words, multicell coordination makes more degrees of freedom available for zero-forcing.

### 7.2.2 Precoding Parametrization Based on Global CSI

While the precoding parametrization in Theorem 7.1 provides insight, it does not constitute any major reduction of the search-space (merely from  $N_j$  complex-valued parameters per transmitter-receiver pair to  $|\mathcal{C}_j|$  such parameters). The following theorem provides a novel explicit parametrization that uses much fewer parameters than the original search-space.

*Theorem 7.2.* The optimal solution to (7.1) can be expressed as  $\mathbf{v}_k = \sqrt{p_k} \bar{\mathbf{v}}_k$ . If  $q_l > 0 \forall l$  and  $\tau_{ik} > 0 \forall i, k$ , the positive parameters  $\{\mu_k\}_{k=1}^{K_r}$ ,  $\{\lambda_l\}_{l=1}^{L_p}$ , and  $\{\kappa_{ik}\}_{i=1}^{L_k} \forall k$  can be selected such that the optimal power allocation  $p_k$  and unit-norm precoding vectors  $\bar{\mathbf{v}}_k$  are given by

$$\bar{\mathbf{v}}_k = \frac{\left( \sum_{l=1}^{L_p} \frac{\lambda_l}{q_l} \mathbf{Q}_l + \sum_{i=1}^{L_k} \frac{\kappa_{ik}}{\tau_{ik}} \mathbf{T}_{ik} + \sum_{\bar{k} \neq k} \mu_{\bar{k}} \mathbf{D}_{\bar{k}}^H \mathbf{C}_{\bar{k}}^H \mathbf{h}_{\bar{k}} \mathbf{h}_{\bar{k}}^H \mathbf{C}_{\bar{k}} \mathbf{D}_{\bar{k}} \right)^\dagger \mathbf{D}_k^H \mathbf{h}_k}{\left\| \left( \sum_{l=1}^{L_p} \frac{\lambda_l}{q_l} \mathbf{Q}_l + \sum_{i=1}^{L_k} \frac{\kappa_{ik}}{\tau_{ik}} \mathbf{T}_{ik} + \sum_{\bar{k} \neq k} \mu_{\bar{k}} \mathbf{D}_{\bar{k}}^H \mathbf{C}_{\bar{k}}^H \mathbf{h}_{\bar{k}} \mathbf{h}_{\bar{k}}^H \mathbf{C}_{\bar{k}} \mathbf{D}_{\bar{k}} \right)^\dagger \mathbf{D}_k^H \mathbf{h}_k \right\|_2} \quad (7.5)$$

$$\text{and } [p_1 \dots p_{K_r}] = [\gamma_1 \sigma_1^2 \dots \gamma_{K_r} \sigma_{K_r}^2] \mathbf{M}^\dagger, \quad (7.6)$$

where

$$\gamma_k = \mu_k \mathbf{h}_k^H \mathbf{D}_k \left( \sum_l \frac{\lambda_l}{q_l} \mathbf{Q}_l + \sum_i \frac{\kappa_{ik}}{\tau_{ik}} \mathbf{T}_{ik} + \sum_{\bar{k} \neq k} \mu_{\bar{k}} \mathbf{D}_{\bar{k}}^H \mathbf{C}_{\bar{k}}^H \mathbf{h}_{\bar{k}} \mathbf{h}_{\bar{k}}^H \mathbf{C}_{\bar{k}} \mathbf{D}_{\bar{k}} \right)^\dagger \mathbf{D}_k^H \mathbf{h}_k \quad (7.7)$$

and the  $ij$ th element of  $\mathbf{M} \in \mathbb{R}^{K_r \times K_r}$  is

$$[\mathbf{M}]_{ij} = \begin{cases} |\mathbf{h}_i^H \mathbf{D}_i \bar{\mathbf{v}}_i|^2, & i = j, \\ -\gamma_j |\mathbf{h}_j^H \mathbf{C}_j \mathbf{D}_i \bar{\mathbf{v}}_i|^2, & i \neq j. \end{cases} \quad (7.8)$$

In addition, it is sufficient to select positive parameters that satisfy

$$\sum_k \mu_k + \sum_l \lambda_l + \sum_{i,k} \kappa_{ik} = 1. \quad (7.9)$$

*Proof.* The proof is given in Appendix 7.A.2.  $\square$

The characterization in Theorem 7.2 uses  $K_r + L$  parameters from  $[0, 1]$ , but we only need to select  $K_r + L - 1$  parameters since the last one is given by the unit sum constraint in (7.9). These parameters are actually Lagrange multipliers related to the optimal solution (see the proof in Appendix 7.A.2 for details) and there are important links between our parametrization and the idea of uplink-downlink duality in [WES06, YL07, BJBO11].

Our novel characterization only has a single parameter per user, although multiple base stations are involved. This reduces the number of

parameters compared with the prior work in [MJ11a, JLD08, SCP11, ZC10], where each base station has its own parameter for each user. As an example, consider the  $K_r$ -user MISO interference channel where the previous state-of-the-art characterization was given [SCP11] and uses  $K_r(K_r - 1)$  parameters from  $[0, 1]$ . In this scenario, Theorem 7.2 only requires  $2K_r - 1$  parameters (since  $L = K_t = K_r$  under per-transmitter power constraints). Thus, our characterization is advantageous whenever  $K_r \geq 3$ , and the benefit increases with  $K_r$ . In the special case of  $K_r = 2$ , recent work in [MJ11b, LKL11] only requires a single parameter; a similar reduction is not possible in our general multicell scenario without removing the support for arbitrary power and soft-shaping constraints. For general multicell systems,  $K_t(K_r - 1)$   $[0, 1]$ -parameters were used per transmitter-receiver pair in [MJ11a], which is also more than  $K_t + K_r - 1$  in our parametrization.

The parameter selection in Theorem 7.2 implicitly determines each user's performance. Corollary 7.1 provides some intuition to how the different parameters affect the performance.

*Corollary 7.1.* If  $g_k(\cdot)$  is differentiable, the parameters in Theorem 7.2 have the following impact on the performance of  $\text{MS}_k$ :

$$\begin{aligned} \frac{\partial}{\partial \mu_{\bar{k}}} g_k(\text{SINR}_k) & \begin{cases} \geq 0, & k = \bar{k}, \\ \leq 0, & k \neq \bar{k}, \end{cases} \\ \frac{\partial}{\partial \lambda_l} g_k(\text{SINR}_k) & \leq 0 \quad \forall l, \\ \frac{\partial}{\partial \kappa_{ik}} g_k(\text{SINR}_k) & \leq 0 \quad \forall i. \end{aligned} \tag{7.10}$$

*Proof.* Observe that Theorem 7.2 gives  $\text{SINR}_k = \gamma_k$ . Differentiation of the  $\gamma_k$ -expression in (7.7) gives the expressions in the corollary, in conjunction with the monotonicity of  $g_k(\cdot)$ .  $\square$

Since increasing  $\mu_k$  improves the performance for  $\text{MS}_k$  and degrades it for other users,  $\mu_k$  represents the system priority of  $\text{MS}_k$ . The  $\lambda$ - and  $\kappa$ -parameters are related to power and soft-shaping constraints, respectively, and should be small to boost performance; they should in fact be zero for inactive constraints. It is non-trivial which parameters to modify to improve system performance and fulfill all constraints. In fact, it is unlikely to find exact optimal solutions by trial-and-error parameter selection. Main applications of Theorem 7.2 are to search for good parameter values iteratively or to select them heuristically. An example of the former application is the search algorithm in [ZC10], which cannot guarantee global convergence but satisfies a necessary condition on optimality. The well-known signal-to-leakage-and-noise ratio (SLNR) beamforming strat-

egy<sup>2</sup> in [STS07,LJS<sup>+</sup>08,HSHS08,ZMM<sup>+</sup>08,ZG10a] corresponds to a certain heuristic selection of our parameters, and the regularized zero-forcing approach in [PHS05] resembles the optimal structure in Theorem 7.2. Thus, Theorem 7.2 explains why these strategies perform well and demonstrates that even better performance can be achieved by fine-tuning the parameters. We will propose new heuristic ways of selecting the parameters later in this chapter.

Finally, we observe that Theorem 7.2 will not produce feasible precoding strategies for all parameter selections. Feasibility can however be assured through a simple scaling.

*Corollary 7.2.* Let  $\mathbf{v}_1, \dots, \mathbf{v}_{K_r}$  be a resource allocation strategy suggested by Theorem 7.2. The modified resource allocation strategy with  $\tilde{\mathbf{v}}_k = \mathbf{v}_k/\sqrt{c} \ \forall k$  and  $c = \max(\max_l \sum_k (\mathbf{v}_k^H \mathbf{Q}_l \mathbf{v}_k)/q_l, \max_{i,k} (\mathbf{v}_k^H \mathbf{T}_{ik} \mathbf{v}_k)/\tau_{ik})$  will always be feasible (i.e., satisfy all constraints).

This modification only affects suboptimal and infeasible strategies since optimal strategies have  $c = 1$  (i.e., satisfy at least one constraint with equality, as proved in Theorem 5.2).

### 7.2.3 Characterization of the Pareto Boundary

The performance region  $\mathcal{R}$  (see Definition 5.2) is characterized by its upper boundary  $\partial^+ \mathcal{R}$ . This upper boundary surely contains the optimal solution to (7.1), as proved by Lemma 5.2. In fact, only a subset of the upper boundary is of interest, namely the Pareto boundary where the performance cannot be increased for any user without degrading for other users.

*Definition 7.1.* The *Pareto boundary*  $\partial \mathcal{R} \subseteq \mathcal{R}$  consists of all  $\mathbf{g} \in \mathcal{R}$  for which there is no  $\mathbf{g}' \in \mathcal{R} \setminus \{\mathbf{g}\}$  with  $\mathbf{g}' \geq \mathbf{g}$  (componentwise inequality).

Based on this definition, one can say that any efficient outcome of a multicell resource allocation lies on the Pareto boundary  $\partial \mathcal{R}$ . The parametrization in Theorem 7.2 also provides a characterization of  $\partial \mathcal{R}$ .

*Corollary 7.3.* Each Pareto optimal point  $\mathbf{g}^* \in \partial \mathcal{R}$  is attained by some precoding strategy  $\sqrt{p_1} \bar{\mathbf{v}}_1, \dots, \sqrt{p_{K_r}} \bar{\mathbf{v}}_{K_r}$  achieved by (7.5) and (7.6) for some selection of the parameters  $\{\mu_k\}_{k=1}^{K_r}$ ,  $\{\lambda_l\}_{l=1}^{L_p}$ , and  $\{\kappa_{ik}\}_{i=1}^{L_k} \forall k$  that satisfies  $\sum_k \mu_k + \sum_l \lambda_l + \sum_{i,k} \kappa_{ik} = 1$ . In addition, the conditions for full power usage in Theorem 5.2 need to be fulfilled.

*Proof.* Any given  $\mathbf{g}^* \in \partial \mathcal{R}$  is the optimal solution to (7.1) if  $f(\mathbf{g}) = \min_k g_k/g_k^*$ . Thus, Theorem 7.2 provides a parametrization for achieving this point.  $\square$

---

<sup>2</sup>This heuristic strategy has been suggested by multiple authors and is based on maximizing the ratio between the signal gain at the intended user and the noise plus the total interference leakage towards other users. The interference leakage was called “caused-interference” in [HSHS08] and “generating-interference” in [LJS<sup>+</sup>08].

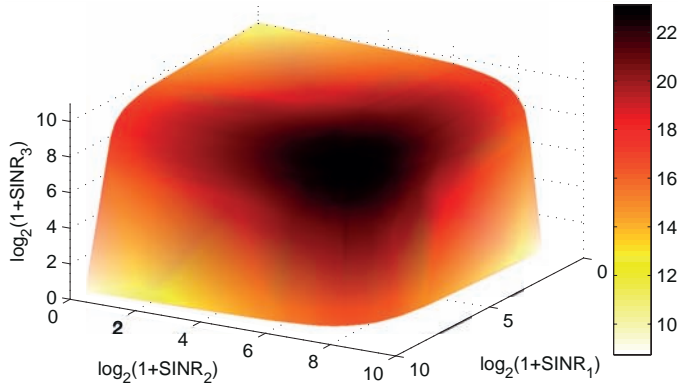


Figure 7.1: Rate region for a three-user MISO interference channel with four antennas per base station and per-transmitter constraints. The colorbar shows the sum rate. The region resembles a box with rounded edges.

In other words, there is a duality between characterizing the optimal solution to any multicell resource allocation problem and characterizing the Pareto boundary of the corresponding performance region. This explains why previous work in this area has concentrated on characterizing performance regions [JLD08, SCP11, ZC10].

The Pareto characterization in Corollary 7.3 can be used to simulate performance regions. Consider a MISO interference channel with  $K_t = K_r = 3$ ,  $N = 4$  transmit antennas, and an average SNR of 10 dB (under MRT). Figure 7.1 shows  $\mathcal{R}$  for a random uncorrelated Rayleigh fading channel realization and with the data rate  $g_k(\text{SINR}_k) = \log_2(1 + \text{SINR}_k)$  as performance measure. The region was generated using Corollary 7.3 by changing the five parameters in steps of 0.02 and filling the space between the achieved points. As it is hard to interpret 3D-plots, observe that the region resembles a box with rounded edges and that the colorbar shows the sum rate.

### 7.3 Low-Complexity Multicell Resource Allocation

In this section, we propose two low-complexity strategies for multicell resource allocation that exploit the precoding parametrization in the previous section. The first strategy requires joint coordination and computations by some central station, while the second strategy is distributed and designed to require very little backhaul signaling. Both strategies greatly reduce the computational complexity compared with the optimal solution to (7.1) in Chapter 6, while still showing close-to-optimal performance in

the evaluation in Chapter 8. In addition, asymptotic optimality in terms of multiplexing gain can be achieved in certain scenarios.

Theorem 7.2 parameterized the optimal solution to (7.1), thus good performance can be achieved by judicious selection of  $\{\mu_k\}_{k=1}^{K_r}$ ,  $\{\lambda_l\}_{l=1}^{L_p}$ , and  $\{\kappa_{ik}\}_{i=1}^{L_k} \forall k$ . An important observation is that (7.1) performs user selection and precoding design as a joint optimization problem. In the parametrization, this user selection is represented by having  $\mu_k > 0$  for all users  $k$  that are selected for transmission in the current scheduling slot. Thus, every heuristic parameter selection requires a separate scheduling mechanism. Herein, we adopt the state-of-the-art ProSched algorithm from [FGH06, FGH07].

For notational convenience, this section only considers per-transmitter power constraints (i.e.,  $L = K_t$  and  $L_k = 0$ )

$$\sum_{k=1}^{K_r} \mathbf{v}_k^H \mathbf{Q}_j^{\text{per-BS}} \mathbf{v}_k \leq q_j \quad \text{for } j = 1, \dots, K_t, \quad (7.11)$$

where  $\mathbf{Q}_j^{\text{per-BS}} = \text{diag}(\mathbf{0}_{N_1}, \dots, \mathbf{0}_{N_{j-1}}, \mathbf{1}_{N_j}, \mathbf{0}_{N_{j+1}}, \dots, \mathbf{0}_{N_{K_t}})$ .

In addition, we consider the weighted sum performance  $f(g_1, \dots, g_{K_r}) = \sum_{k=1}^{K_r} w_k g_k$  (with  $w_k \geq 0$ ) and user performance functions  $g_k(\cdot)$  that are concave. This structure holds for both data rates, mean squared errors (MSEs), and symbol error rates (SERs), as will be seen later on.

### 7.3.1 Centralized Resource Allocation

As the parametrization in Theorem 7.2 builds upon the duality between transmission in the downlink and in a virtual uplink, we call the centralized version of our strategy *centralized virtual SINR (CVSINR) resource allocation*. It is outlined as follows:

1. Consider weighted sum optimization  $f(g_1, \dots, g_{K_r}) = \sum_{k=1}^{K_r} w_k g_k$  for some collection of weights  $w_k \geq 0$ .
2. Allocate users  $\tilde{\mathcal{S}} \subseteq \{1, \dots, K_r\}$  for transmission using an appropriate algorithm (e.g., ProSched [FGH06, FGH07]).
3. Set  $\mu_k = w_k |\tilde{\mathcal{S}}| / (\sigma_k^2 \sum_{\tilde{k} \in \tilde{\mathcal{S}}} \tilde{w}_{\tilde{k}})$  if user  $k \in \tilde{\mathcal{S}}$  is scheduled, otherwise set  $\mu_k = 0$ .
4. Set  $\lambda_j = 1$  and calculate  $\mathbf{v}_k^{(\text{CVSINR})}$  using Theorem 7.2.
5. Rescale all  $\mathbf{v}_k^{(\text{CVSINR})}$ , according to Theorem 5.2, to satisfy all power constraints (and at least one with equality).

The CVSINR strategy first selects users and then calculates a transmit strategy in compliance with the single-stream beamforming optimality and conditions for full power usage in Chapter 5.3, and with the precoding parametrization in Theorem 7.2. The parameters  $\lambda_j, \mu_k$  are selected heuristically, and the details are provided later in this section.

The CVSINR strategy can be applied right way (and shows good performance in Chapter 8), but it is not guaranteed that the transmit power will be allocated efficiently; some base stations could in principle use very little power. This can be arranged by fixing the interference that each user experience  $z_k = \sum_{\bar{k} \neq k} |\mathbf{h}_k^H \mathbf{C}_k \mathbf{D}_{\bar{k}} \mathbf{v}_k^{(\text{CVSINR})}|^2$  and solving the following optimization problem

$$\begin{aligned}
& \underset{\substack{\mathbf{v}_1, \dots, \mathbf{v}_{K_r} \\ \chi_1, \dots, \chi_{K_r}}}{\text{maximize}} && \sum_{k=1}^{K_r} w_k g_k(\chi_k) \\
& \text{subject to} && \frac{|\mathbf{h}_k^H \mathbf{C}_k \mathbf{D}_k \mathbf{v}_k|^2}{\sigma_k^2 + z_k} \geq \chi_k \quad \forall k, \\
& && \sum_{\bar{k} \neq k} |\mathbf{h}_k^H \mathbf{C}_k \mathbf{D}_{\bar{k}} \mathbf{v}_{\bar{k}}|^2 \leq z_k \quad \forall k, \\
& && \sum_{k=1}^{K_r} \mathbf{v}_k^H \mathbf{Q}_j^{\text{per-BS}} \mathbf{v}_k \leq q_j \quad \forall j.
\end{aligned} \tag{7.12}$$

This problem is called *interference-constrained beamforming* [BZBO11] and will maximize the performance under the condition that the interference levels may not exceed those with the original CVSINR strategy. The following lemma shows that (7.12) can be solved efficiently, using convex optimization theory (e.g., interior-point methods [TTT03]).

*Lemma 7.1.* The semi-definite relaxation of (7.12) is

$$\begin{aligned}
& \underset{\substack{\mathbf{v}_1 \succeq \mathbf{0}, \dots, \mathbf{v}_{K_r} \succeq \mathbf{0} \\ \chi_1, \dots, \chi_{K_r}}}{\text{maximize}} && \sum_{k=1}^{K_r} w_k g_k(\chi_k), \\
& \text{subject to} && \frac{\text{tr}\{\mathbf{D}_k^H \mathbf{C}_k^H \mathbf{h}_k \mathbf{h}_k^H \mathbf{C}_k \mathbf{D}_k \mathbf{V}_k\}}{\sigma_k^2 + z_k} \geq \chi_k \quad \forall k, \\
& && \sum_{\bar{k} \neq k} \text{tr}\{\mathbf{D}_{\bar{k}}^H \mathbf{C}_{\bar{k}}^H \mathbf{h}_{\bar{k}} \mathbf{h}_{\bar{k}}^H \mathbf{C}_k \mathbf{D}_{\bar{k}} \mathbf{V}_{\bar{k}}\} \leq z_k \quad \forall k, \\
& && \sum_{k=1}^{K_r} \text{tr}\{\mathbf{Q}_j^{\text{per-BS}} \mathbf{V}_k\} \leq q_j \quad \forall j.
\end{aligned} \tag{7.13}$$

This problem is convex and has rank-one solutions  $\mathbf{V}_k^* = \mathbf{v}_k^* (\mathbf{v}_k^*)^H$ , where  $\mathbf{v}_k^*$  solves the original problem in (7.12).

*Proof.* The proof is given in Appendix 7.A.3.  $\square$

The resource allocation obtained by (7.12) will be called the *modified CVSINR resource allocation* strategy and its performance will be illustrated in Chapter 8. This centralized approach can be used to achieve an initial lower bound for the BRB algorithm in Chapter 6 and thereby improve its convergence speed.

### 7.3.2 Distributed Resource Allocation

The drawback of any centralized strategy, including the proposed CVSINR strategy, is that the resource allocation requires global CSI. In a system with many base stations and many active users, this requires huge amounts of backhaul signaling. In addition, joint CSI processing typically means large computational demands. Therefore, our main focus is to derive a low-complexity distributed version of the CVSINR strategy that only uses local CSI. It will be suboptimal in terms of performance, but have much more reasonable system requirements than centralized approaches.

The collective precoding vectors  $\mathbf{v}_k$  can be decomposed as  $\mathbf{v}_k = [\sqrt{p_{1k}}\bar{\mathbf{v}}_{1k}^T \cdots \sqrt{p_{K_t k}}\bar{\mathbf{v}}_{K_t k}^T]^T$ . Here,  $\bar{\mathbf{v}}_{jk} \in \mathbb{C}^{N_j \times 1}$  is the unit-norm precoding vector and  $p_{jk} \geq 0$  is the power allocated by BS<sub>*j*</sub> for transmission to MS<sub>*k*</sub> (only non-zero for  $k \in \mathcal{D}_j$ ). With this notation, weighted sum performance optimization with per-transmitter power constraints becomes

$$\begin{aligned} & \underset{\substack{\{\bar{\mathbf{v}}_{jk}\}_{j=1, k=1}^{K_t, K_r} \\ \{p_{jk}\}_{j=1, k=1}^{K_t, K_r}}}{\text{maximize}}}{\sum_{k=1}^{K_r} w_k g_k(\text{SINR}_k)} \\ & \text{subject to } \text{SINR}_k = \frac{\left| \sum_{j=1}^{K_t} \sqrt{p_{jk}} \mathbf{h}_{jk}^H \mathbf{C}_{jk} \mathbf{D}_{jk} \bar{\mathbf{v}}_{jk} \right|^2}{\sigma_k^2 + \sum_{\bar{k} \neq k} \left| \sum_{j=1}^{K_t} \sqrt{p_{j\bar{k}}} \mathbf{h}_{j\bar{k}}^H \mathbf{C}_{j\bar{k}} \mathbf{D}_{j\bar{k}} \bar{\mathbf{v}}_{j\bar{k}} \right|^2} \quad \forall k, \quad (7.14) \\ & \sum_{k=1}^{K_r} p_{jk} \leq q_j \quad \forall j, \\ & p_{jk} \geq 0, \|\bar{\mathbf{v}}_{jk}\|_2 = 1 \quad \forall j, k. \end{aligned}$$

An important question is how to maximize  $\text{SINR}_k$  in (7.14) in a distributed manner using only local CSI. Starting with the numerator, coherent signal reception can be achieved, for instance by synchronizing the joint transmissions such that  $\sqrt{p_{jk}} \mathbf{h}_{jk}^H \mathbf{C}_{jk} \mathbf{D}_{jk} \bar{\mathbf{v}}_{jk}$  is positive real-valued (or zero) for each BS<sub>*j*</sub>. Achieving coherent interference cancelation (i.e.,  $|\sum_{j=1}^{K_t} \sqrt{p_{j\bar{k}}} \mathbf{h}_{j\bar{k}}^H \mathbf{C}_{j\bar{k}} \mathbf{D}_{j\bar{k}} \bar{\mathbf{v}}_{j\bar{k}}|^2$  is small without enforcing that every term is

small) is more difficult under local CSI, if not impossible in large multiuser systems.<sup>3</sup> Without coherent interference cancelation, there are few reasons for joint transmission; it is more power efficient and reliable to only use the base station with the strongest link, although somewhat more unbalanced interference patterns may be generated. Therefore, we assume that each user is only served by one base station in our distributed strategy.<sup>4</sup> This assumption greatly reduces the synchronization requirements, while the performance loss may be small or even non-existent (see Chapter 8).

The resource allocation problem in (7.14) can be divided into three parts: 1) User selection; 2) Power allocation  $\{p_{jk}\}$ ; and 3) Beamforming directions  $\{\tilde{\mathbf{v}}_{jk}\}$ . Our distributed strategy solves them sequentially, only requiring local CSI at each base station in each part (i.e.,  $\mathbf{h}_{jk}$  is known at BS<sub>*j*</sub> for all users  $k \in \mathcal{C}_j$ ). In between each step, a small amount of signaling is used to inform each base station which users that are served by adjacent base stations (to enable interference coordination). Next, we describe the steps in detail.

### 7.3.3 Step 1: User Selection

The goal of this step is to select the set  $\mathcal{S}(j, n)$  with users that are served by BS<sub>*j*</sub> at the current scheduling slot  $n$ . The proposed scheme is based on the ProSched algorithm in [FGH06, FGH07], but generalized to take the interference generated on users served by other base stations,

$$\mathcal{A}(j, n) = \bigcup_{i \neq j} (\mathcal{S}(i, n) \cap \mathcal{C}_j), \quad (7.15)$$

into consideration. For a given set  $\mathcal{A}$ , the scheduling metric for user  $k$  is

$$\eta_{jk}^{(\mathcal{S}, \mathcal{A})} = w_k g_k \left( \frac{q_j \|\mathbf{h}_{jk}^H \tilde{\mathbf{P}}_{jk}^{(\mathcal{S}, \mathcal{A})}\|_2^2}{\sigma_k^2 |\mathcal{S}|} \right) \quad (7.16)$$

where  $\tilde{\mathbf{P}}_{jk}^{(\mathcal{S}, \mathcal{A})}$  denotes the projection matrix onto the null space of channels for all users in  $(\mathcal{S} \cup \mathcal{A}) \setminus \{k\}$ . Thus,  $\eta_{jk}^{(\mathcal{S}, \mathcal{A})}$  represents the performance with equal power allocation and zero-forcing precoding. To lower the computational complexity, the ProSched algorithm calculates  $\tilde{\mathbf{P}}_{jk}^{(\mathcal{S})}$  using efficient projection-based approximations (see [FGH07]). In the search for the scheduling set  $\mathcal{S}$  with the highest sum metric

$$\bar{\eta}_j^{(\mathcal{S}, \mathcal{A})} = \sum_{k \in \mathcal{S}} \eta_{jk}^{(\mathcal{S}, \mathcal{A})}, \quad (7.17)$$

<sup>3</sup>Iterative optimization can be used to achieve coherent interference cancelation, but it requires backhaul signaling and is sensitive to CSI uncertainty, delays, etc.

<sup>4</sup>If there are many subchannels, different base stations can be used on each of them.

the ProSched algorithm avoids the complexity of evaluating the sum metric for every possible  $\mathcal{S} \subseteq \mathcal{D}_j$  by performing a greedy tree search. Despite all simplifications, ProSched has shown good performance under reasonable computational complexity [FGH06, FGH07]. Our distributed ProSched algorithm exploits time correlation (i.e., that users that were scheduled at the previous scheduling slot are more probable to also be scheduled at the current slot) and selects  $\mathcal{S}(j, n)$  as follows:

1. Input  $\mathcal{S}^{\text{tmp}}(j, n) = \mathcal{S}(j, n - 1)$  and  $\mathcal{A}(j, n - 1)$ .
2. Use the “Tracking and Adaptivity”-procedure in [FGH07] to add and remove users from  $\mathcal{S}^{\text{tmp}}(j, n)$ , while zero interference is generated to users in  $\mathcal{A}(j, n - 1)$ . The sum metric is evaluated using (7.17). The final set needs to satisfy  $|\mathcal{S}^{\text{tmp}}(j, n) \cup \mathcal{A}(j, n - 1)| \leq N_j$ .<sup>5</sup>
3. Set  $\mathcal{S}(j, n) = \mathcal{S}^{\text{tmp}}(j, n)$  and send it to the central station.
4. Central station calculates  $\mathcal{A}(j, n)$  using (7.15) and sends it to BS<sub>*j*</sub>.

The main difference from the original ProSched algorithm is the existence of  $\mathcal{A}(j, n - 1)$ , which are users that BS<sub>*j*</sub> must coordinate interference towards. The algorithm exploits time correlation by taking new decisions based on previous ones; it tries to remove users from the selected set and then add other users. The user weights can be updated between scheduling slots, although not reflected in our notation. The initialization can be achieved in some arbitrary way, for example by selecting the strongest user as  $\mathcal{S}(j, 0) = \operatorname{argmax}_{k \in \mathcal{D}_j} \eta_{jk}^{\{\{k\}, \emptyset\}}$ . The last step of the algorithm prepares for the next scheduling slot and  $\mathcal{A}(j, n)$  will also be used in the next steps to adapt the precoding to the current user selection.

### 7.3.4 Step 2: Power Allocation

The difficulty in distributed power allocation is that the interference powers generated by other base stations are unknown. Fortunately, the proposed user selection is designed to make  $|\mathcal{S}(j, n) \cup \mathcal{A}(j, n)| \leq N_j$  so that zero-forcing precoding exists.<sup>6</sup> Power allocation based on zero-forcing simplifications has been shown to provide accurate results (e.g., in the context

<sup>5</sup>A feature of the approximate zero-forcing precoding in ProSched is that the sum metric is well-defined also for  $|\mathcal{S}^{\text{tmp}}(j, n) \cup \mathcal{A}(j, n - 1)| > N_j$ , but this corresponds to an interference-limited system and should be avoided.

<sup>6</sup>Since the user selection makes  $|\mathcal{S}^{\text{tmp}}(j, n) \cup \mathcal{A}(j, n - 1)| \leq N_j$  with  $\mathcal{A}(j, n - 1)$  instead of  $\mathcal{A}(j, n)$ , it might occasionally happen that  $|\mathcal{S}(j, n) \cup \mathcal{A}(j, n)| > N_j$ . This is either handled by having a central mechanism that removes users or by ignoring the weakest unserved users in  $\mathcal{A}(j, n)$  in the power allocation step. The latter will have limited impact on performance since most of the interference coordination comes from the beamforming directions and not from power allocation.

of the ProSched algorithm), although better precoding vectors are used in the end. This will be illustrated in Chapter 8.

Based on this assumption, the SINR of  $\text{MS}_k$  becomes

$$\text{SINR}_k = p_{jk} \underbrace{\frac{|\mathbf{h}_{jk}^H \bar{\mathbf{v}}_{jk}^{\text{ZF}}|^2}{\sigma_k^2}}_{=\rho_{jk}} \quad \forall k \in \mathcal{S}(j, n) \quad (7.18)$$

where  $\bar{\mathbf{v}}_{jk}^{\text{ZF}}$  is the unit-norm zero-forcing vector for users in  $\mathcal{S}(j, n) \cup \mathcal{A}(j, n)$ . For fixed  $\rho_{jk}$ , the power allocation can be solved as follows.

*Lemma 7.2.* For a given  $\text{BS}_j$ , some given constants  $\rho_{jk} > 0$ , and differentiable concave functions  $g_k(\cdot)$  with invertible derivatives, the power allocation problem

$$\begin{aligned} & \underset{p_{jk} \geq 0 \quad \forall k \in \mathcal{S}(j, n)}{\text{maximize}} && \sum_{k \in \mathcal{S}(j, n)} w_k g_k(p_{jk} \rho_{jk}) \\ & \text{subject to} && \sum_{k \in \mathcal{S}(j, n)} p_{jk} \leq q_j \end{aligned} \quad (7.19)$$

is solved by

$$p_{jk} = \max \left( \frac{1}{\rho_{jk}} g_k'^{-1} \left( \frac{\alpha}{w_k \rho_{jk}} \right), 0 \right) \quad (7.20)$$

where  $\frac{d}{dx} g_k(x) = g_k'(x)$  and  $\alpha \geq 0$  is selected to use full power.

*Proof.* This convex optimization problem is solved by standard Lagrangian techniques; see [BV04].  $\square$

The distributed power allocation depends on the inverse of the derivative of the user performance function  $g_k(\cdot)$ . To exemplify the structure, we let the performance functions either describe the data rate, MSE, or Chernoff bound<sup>7</sup> on the SER for an uncoded  $M$ -ary modulation:

$$g_k^{\text{rate}}(x) = \log_2(1+x) \quad \Rightarrow \quad g_k'^{-1}(y) = \frac{1}{y} - 1, \quad (7.21)$$

$$g_k^{\text{MSE}}(x) = -\frac{1}{1+x} \quad \Rightarrow \quad g_k'^{-1}(y) = \frac{1}{\sqrt{y}} - 1, \quad (7.22)$$

$$g_k^{\text{cSER}}(x) = -\frac{M-1}{M} e^{-xz} \quad \Rightarrow \quad g_k'^{-1}(y) = \frac{1}{z} \log_e \frac{(M-1)z}{My}. \quad (7.23)$$

In (7.23),  $z = 3/(M^2 - 1)$  for pulse amplitude modulation (PAM),  $z = \sin^2(\pi/M)$  for phase-shift keying (PSK), and  $z = 3/(2M - 2)$  for quadrature amplitude modulation (QAM) [SA98].

<sup>7</sup>The exact SER can also be used, but there are no closed-form expressions for the inverse of its derivative.

For these user performance functions, the power allocation in Lemma 7.2 has the waterfilling behavior, meaning that strong users receive more power than weak users. In addition, the system prioritizes users with large weights. Some users might be allocated zero or negligible power (below some threshold  $p^{\text{thres}}$ ). These users should immediately be removed from  $\mathcal{S}(j, n)$ , and adjacent base stations should be informed so that all  $\mathcal{A}(j, n)$  can be adjusted. This requires some extra signaling, but will avoid unnecessary interference coordination and improves the user selection in the next scheduling slot.

### 7.3.5 Step 3: Beamforming Directions

The parametrization in Theorem 7.2 provides the optimal precoding structure. Since at most one base station serves each user in our distributed approach, we have the following corollary.

*Corollary 7.4.* Assume that all  $\mathcal{S}(j, n)$  are disjoint and that BS<sub>*j*</sub> has a per-transmitter power constraint of  $q_j$ . For BS<sub>*j*</sub>, the optimal beamforming direction to user  $k \in \mathcal{S}(j, n)$  is given by

$$\bar{\mathbf{v}}_{jk} = \frac{\left(\frac{\lambda_j}{q_j} \mathbf{I}_{N_j} + \sum_{\bar{k} \in \mathcal{SA}(j, n) \setminus \{k\}} \mu_{\bar{k}} \mathbf{h}_{j\bar{k}} \mathbf{h}_{j\bar{k}}^H\right)^\dagger \mathbf{h}_{jk}}{\left\| \left(\frac{\lambda_j}{q_j} \mathbf{I}_{N_j} + \sum_{\bar{k} \in \mathcal{SA}(j, n) \setminus \{k\}} \mu_{\bar{k}} \mathbf{h}_{j\bar{k}} \mathbf{h}_{j\bar{k}}^H\right)^\dagger \mathbf{h}_{jk} \right\|_2}, \quad (7.24)$$

where  $\mathcal{SA}(j, n) = \mathcal{S}(j, n) \cup \mathcal{A}(j, n)$ , for some positive parameters  $\lambda_j$  and  $\{\mu_{\bar{k}}\}_{\bar{k}=1}^{K_r}$ .

To apply Corollary 7.4, the parameters  $\lambda_j$  and  $\mu_{\bar{k}}$  need to be selected heuristically. For this reason, recall that the parametrization is achieved using uplink-downlink duality. Thus,  $\lambda_j$  is inversely proportional to the SNR of the (virtual) uplink channels. As the parameter is user-independent, it is only affected by the transmit power of BS<sub>*j*</sub> and not of any noise parameter. Since  $\lambda_j$  is already multiplied with  $\frac{1}{q_j}$ , we select

$$\lambda_j^{(\text{heuristic})} = 1. \quad (7.25)$$

Next, we consider  $\mu_{\bar{k}}$  and recall from Section 7.2.2 that  $\mu_{\bar{k}}$  represents the priority of MS<sub>*k*</sub>, and whether or not the user is scheduled. The best priority indicators we have are the weights  $w_k$ , but we need to normalize them based on which users are scheduled. In addition,  $\mu_{\bar{k}}$  should be inversely proportional to the noise power  $\sigma_k^2$  of MS<sub>*k*</sub>, since this term could not be included in the user-independent  $\lambda_j$ -parameters. We therefore select

$$\mu_k^{(\text{heuristic})} = \begin{cases} \frac{w_k}{\sigma_k^2 \sum_{\bar{k} \in \mathcal{SA}(j, n)} \frac{w_{\bar{k}}}{|\mathcal{SA}(j, n)|}}, & \text{if } k \in \mathcal{SA}(j, n), \\ 0, & \text{otherwise,} \end{cases} \quad (7.26)$$

where  $\mathcal{SA}(j, n) = \mathcal{S}(j, n) \cup \mathcal{A}(j, n)$ . Observe that different base stations can have different heuristic values on  $\mu_k^{(\text{heuristic})}$ , representing different local user priorities.

### 7.3.6 Final DVSINR Strategy

The proposed strategy is named *distributed virtual SINR (DVSINR) resource allocation*, since the parametrization in Theorem 7.2 builds upon the duality between transmissions in the downlink and in a virtual uplink. It is summarized in Algorithm 7.1.

---

#### Algorithm 7.1 Distributed Virtual SINR (DVSINR) Resource Allocation

---

- 1: **input** power threshold  $p^{\text{thres}}$ .
  - 2: **for each** base station  $j$  at scheduling slot  $n$ :
  - 3:   set  $\mathcal{S}^{\text{tmp}}(j, n) = \mathcal{S}(j, n - 1)$ .
  - 4:   perform the “Tracking and Adaptivity”-procedure [FGH07] on  $\mathcal{S}^{\text{tmp}}(j, n)$  with the special rules in Section 7.3.3.
  - 5:   set  $\mathcal{S}(j, n) = \mathcal{S}^{\text{tmp}}(j, n)$  and send it to the central station.
  - 6:   achieve  $\mathcal{A}(j, n)$  from the central station.
  - 7:   calculate  $p_{jk}$  for  $k \in \mathcal{S}(j, n)$  using Lemma 7.2.
  - 8:   remove users with  $p_{jk} < p^{\text{thres}}$  from  $\mathcal{S}(j, n)$ .
  - 9:   send updates of  $\mathcal{S}(j, n)$  to the central station and attain updates of  $\mathcal{A}(j, n)$ .
  - 10:   calculate  $\lambda_j$  and  $\mu_k$  using (7.25) and (7.26).
  - 11:   calculate  $\bar{\mathbf{v}}_{jk}$  for  $k \in \mathcal{S}(j, n)$  using Corollary 7.4.
  - 12: **end**
- 

The proposed CVSINR and DVSINR strategies are both suboptimal, but for a given user selection they can achieve asymptotic optimality:

*Theorem 7.3.* Let  $\mathcal{S} \subseteq \{1, \dots, K_r\}$  be the users scheduled for transmission. If  $|\mathcal{S} \cap \mathcal{C}_j| \leq N_j$  for all  $j$ , then the CVSINR and DVSINR strategies achieve the largest possible multiplexing gain of  $|\mathcal{S}|$  (with probability one).

*Proof.* The proof is given in Appendix 7.A.4. □

This means that the weighted sum rate behaves as  $|\mathcal{S}| \log_2(q) + \text{constant}$  at high transmit power  $q$ . Thus, the absolute performance losses (i.e., rate offsets) of the CVSINR and DVSINR strategies are bounded compared with the optimal solution, and the relative loss goes to zero as constant/ $\log_2(q)$  with increasing transmit power.

## 7.4 Summary

The difficulty in multicell resource allocation is not the lack of CSI (the optimal precoding vectors are linear combinations of local CSI), but the coordination of scheduling and interference cancelation. The optimal solution was characterized using  $K_r + L - 1$  parameters between zero and one. But since the general resource allocation problem is NP-hard, we should expect the search for optimal parameters to also be very difficult. However, it is relatively easy to find heuristic parameter values that provide good performance. The well-known SLNR strategy corresponds to a heuristic selection of our parameters, which explains why many papers have achieved good performance with this strategy. The parametrization demonstrates that even better performance can be achieved by fine-tuning the parameters, which was done in our proposed CVSINR and DVSINR strategies for weighted sum performance optimization. The CVSINR strategy is centralized and the evaluation in Chapter 8 establishes its close-to-optimal performance. The distributed DVSINR strategy only requires backhaul signaling of scheduling decisions, and we note that coherent interference cancelation is not possible without extensive coordination signaling. Both strategies contain a scheduling step based on an extension of the ProSched algorithm from [FGH06, FGH07].

## 7.A Collection of Proofs

### 7.A.1 Proof of Theorem 7.1

Let an optimal solution to (7.1) be denoted  $\mathbf{v}_{jk}^*$  for all  $j, k$ . If  $k \notin \mathcal{D}_j$ , we can replace  $\mathbf{v}_{jk}^*$  with a zero-vector without affecting the performance, since  $\mathbf{v}_{jk}^*$  only appears as  $\mathbf{D}_{jk}\mathbf{v}_{jk}^*$  in the SINR expressions in (7.2) and since  $\mathbf{D}_{jk} = \mathbf{0}_{N_j}$  for these  $k$ .

For  $k \in \mathcal{D}_j$ , the following approach can be taken to replace  $\mathbf{v}_{jk}^*$  with a precoding vector  $\mathbf{v}_{jk}$  that fulfills (7.2) and reduces the power usage, without degrading the performance. Let  $\mathcal{B}_{jk} = \{\mathbf{h}_{jk}\} \cup_{\bar{k} \in \mathcal{C}_j \setminus \{k\}} \{\mathbf{\Pi}_{\mathbf{h}_{j\bar{k}}}^\perp \mathbf{h}_{jk}\}$  and observe that the vector  $\mathbf{v}_{jk}^*$  can be expressed as the linear combination

$$\mathbf{v}_{jk}^* = v_k \mathbf{h}_{jk} + \sum_{\bar{k} \in \mathcal{C}_j \setminus \{k\}} v_{\bar{k}} \mathbf{\Pi}_{\mathbf{h}_{j\bar{k}}}^\perp \mathbf{h}_{jk} + \sum_{n=\text{rank}(\mathcal{B}_{jk})+1}^N v_n \mathbf{a}_n \quad (7.27)$$

for some coefficients  $v_k \in \mathbb{C}$  and some orthogonal basis  $\{\mathbf{a}_n\}_{n=\text{rank}(\mathcal{B}_{jk})+1}^N$  of the orthogonal complement to  $\mathcal{B}_{jk}$ . Now, observe that

$$\mathbf{h}_{j\bar{k}} = \frac{\|\mathbf{h}_{j\bar{k}}\|_2}{\|\mathbf{\Pi}_{\mathbf{h}_{j\bar{k}}}^\perp \mathbf{h}_{jk}\|_2} \left( \mathbf{h}_{jk} - \mathbf{\Pi}_{\mathbf{h}_{j\bar{k}}}^\perp \mathbf{h}_{jk} \right)$$

for all  $\bar{k} \in \mathcal{C}_j \setminus \{k\}$  that are non-orthogonal to  $\mathbf{h}_{jk}$  (while orthogonal channels can be removed from  $\mathcal{B}_{jk}$ , since these directions only carry interference). Thus,  $\mathbf{h}_{j\bar{k}}^H \mathbf{a}_n = 0$  for all  $\bar{k} \in \mathcal{C}_j$  and all  $n = \text{rank}(\mathcal{B}_{jk}) + 1, \dots, N$ . Observe that  $\mathbf{v}_{jk}$  only appears in the SINR expressions in (7.2) as inner products  $\mathbf{h}_{j\bar{k}}^H \mathbf{C}_{j\bar{k}} \mathbf{D}_{jk} \mathbf{v}_{jk}$ . Since  $\mathbf{C}_{j\bar{k}} = \mathbf{0}_{N_j}$  if  $\bar{k} \notin \mathcal{C}_j$  (see the definition in (5.2)),  $\mathbf{v}_{jk}$  is (effectively) only multiplied with  $\mathbf{h}_{j\bar{k}}$  for  $\bar{k} \in \mathcal{C}_j$ . Therefore, exactly the same user performance is achieved by the precoding vector

$$\mathbf{v}_{jk} = v_k \mathbf{h}_{jk} + \sum_{\bar{k} \in \mathcal{C}_j \setminus \{k\}} v_{\bar{k}} \mathbf{\Pi}_{\mathbf{h}_{j\bar{k}}}^\perp \mathbf{h}_{jk}. \quad (7.28)$$

This vector will not increase any of the constraints, since it basically is the orthogonal projection of  $\mathbf{v}_{jk}^*$  onto the span of  $\mathcal{B}_{jk}$ . Thus, we have proved that the optimal solution to (7.1) can be achieved by  $\mathbf{v}_{jk} \in \text{span}(\mathcal{B}_{jk})$ .

### 7.A.2 Proof of Theorem 7.2

Denote the optimal user performance in (7.1) by  $g_k(\text{SINR}_k) = g_k^*$  (if the optimal solution is non-unique, we can take any of the possibilities) and let the corresponding SINRs be denoted  $\gamma_k = g_k^{-1}(g_k^*)$ . These  $\gamma_k$  are of course unknown, but we include them in the analysis and will later observe that the

same parametrization structure is achieved for any collection of  $g_1^*, \dots, g_{K_r}^*$ . In addition, we will find an alternative expression for  $\gamma_k$  that only depends on our parametrization. Now, observe that the optimal resource allocation also solves the convex feasibility problem

$$\begin{aligned} & \text{find } \mathbf{v}_1, \dots, \mathbf{v}_{K_r} \\ & \text{subject to } \frac{|\mathbf{h}_k^H \mathbf{D}_k \mathbf{v}_k|^2}{\sigma_k^2 + \sum_{\bar{k} \neq k} |\mathbf{h}_k^H \mathbf{C}_k \mathbf{D}_{\bar{k}} \mathbf{v}_{\bar{k}}|^2} \geq \gamma_k \quad \forall k, \\ & \sum_k \mathbf{v}_k^H \mathbf{Q}_l \mathbf{v}_k \leq q_l \quad \forall l, \\ & \mathbf{v}_k^H \mathbf{T}_{ik} \mathbf{v}_k \leq \tau_{ik} \quad \forall i, k. \end{aligned} \tag{7.29}$$

Using Lagrange multipliers  $\{\mu_k\}_{k=1}^{K_r}$ ,  $\{\lambda_l\}_{l=1}^{L_p}$ , and  $\{\kappa_{ik}\}_{i=1}^{L_k} \forall k$ , the Lagrangian of (7.29) becomes (similarly to [YL07, Proof of Proposition 1])

$$\begin{aligned} \mathcal{L} = & \sum_k \mu_k \sigma_k^2 - \sum_l \lambda_l - \sum_{i,k} \kappa_{ik} + \sum_k \mathbf{v}_k^H \left( \sum_{l=1}^{L_p} \frac{\lambda_l}{q_l} \mathbf{Q}_l + \sum_{i=1}^{L_k} \frac{\kappa_{ik}}{\tau_{ik}} \mathbf{T}_{ik} \right. \\ & \left. + \sum_{\bar{k} \neq k} \mu_{\bar{k}} \mathbf{D}_k^H \mathbf{C}_{\bar{k}}^H \mathbf{h}_{\bar{k}} \mathbf{h}_k^H \mathbf{C}_{\bar{k}} \mathbf{D}_k - \frac{\mu_k}{\gamma_k} \mathbf{D}_k^H \mathbf{h}_k \mathbf{h}_k^H \mathbf{D}_k \right) \mathbf{v}_k. \end{aligned} \tag{7.30}$$

The stationarity for  $\mathbf{v}_k$  (i.e.,  $\partial \mathcal{L} / \partial \mathbf{v}_k = \mathbf{0}$ ) and multiplication with a Moore-Penrose inverse gives

$$\begin{aligned} \mathbf{v}_k = & \left( \sum_{l=1}^{L_p} \frac{\lambda_l}{q_l} \mathbf{Q}_l + \sum_{i=1}^{L_k} \frac{\kappa_{ik}}{\tau_{ik}} \mathbf{T}_{ik} + \sum_{\bar{k} \neq k} \mu_{\bar{k}} \mathbf{D}_k^H \mathbf{C}_{\bar{k}}^H \mathbf{h}_{\bar{k}} \mathbf{h}_k^H \mathbf{C}_{\bar{k}} \mathbf{D}_k \right)^\dagger \\ & \times \mathbf{D}_k^H \mathbf{h}_k \underbrace{\frac{\mu_k}{\gamma_k} \mathbf{h}_k^H \mathbf{D}_k \mathbf{v}_k}_{=\text{scalar}}. \end{aligned} \tag{7.31}$$

Since the phase of  $\mathbf{v}_k$  will not affect the Lagrangian and since  $\frac{\mu_k}{\gamma_k} \mathbf{h}_k^H \mathbf{D}_k \mathbf{v}_k$  is a scalar, the optimal  $\mathbf{v}_k$  can without loss of generality be expressed as  $\mathbf{v}_k = \sqrt{p_k} \bar{\mathbf{v}}_k$  with  $\bar{\mathbf{v}}_k$  as in (7.5) and for some  $p_k \geq 0$ . To determine  $p_k$  for  $k = 1, \dots, K_r$ , observe that since we consider the optimal solution, all SINR constraints in (7.29) are satisfied with equality. These SINR equalities give  $K_r$  linear equations that can be expressed and solved as in (7.6). The achieved SINRs  $\gamma_k$  can be expressed as in (7.7) by multiplying (7.31) with  $\mathbf{h}_k^H \mathbf{D}_k$  from the left and remove  $\mathbf{h}_k^H \mathbf{D}_k \mathbf{v}_k$  from both sides. Observe that this expression only depends on our Lagrange multipliers and not on the unknown optimal user performance.

Finally, observe that (7.30) (and all equations in Theorem 7.2) is unaffected by a common scaling of all Lagrange multipliers. The sufficiency of

having unit parameter sum is proved by observing that for any optimal set of multipliers, we can rescale them to satisfy a unit parameter sum without affecting the optimality.

### 7.A.3 Proof of Lemma 7.1

The methodology in [WES08] and in Theorem 5.1 can be used to show the existence of rank-one solutions. If an optimization procedure still delivers a high-rank solution  $\mathbf{V}_k^*$ , we can find  $\mathbf{v}_k^*$  by maximizing  $\Re\{\mathbf{h}_k^H \mathbf{C}_k \mathbf{D}_k \mathbf{v}_k\}$  under the interference constraints  $|\mathbf{h}_{\bar{k}}^H \mathbf{C}_{\bar{k}} \mathbf{D}_k \mathbf{v}_k|^2 \leq \text{tr}\{\mathbf{D}_k^H \mathbf{C}_{\bar{k}}^H \mathbf{h}_{\bar{k}} \mathbf{h}_{\bar{k}}^H \mathbf{C}_{\bar{k}} \mathbf{D}_k \mathbf{V}_k^*\} \forall \bar{k} \neq k$  and power constraints  $\mathbf{v}_k^H \mathbf{Q}_j^{\text{per-BS}} \mathbf{v}_k \leq \text{tr}\{\mathbf{Q}_j^{\text{per-BS}} \mathbf{V}_k^*\} \forall j$ .

### 7.A.4 Proof of Theorem 7.3

We concentrate on the DVSINR strategy and assume that  $\text{BS}_j$  transmits to  $\mathcal{S}(j) \subseteq \mathcal{S}$ . At high transmit power, the waterfilling behavior in Lemma 7.2 makes the power allocation become  $p_{jk} = q_j/|\mathcal{S}(j)|$ . If  $|\mathcal{S} \cap \mathcal{C}_j| \leq N_j$ , then with probability one

$$\mathbf{h}_{jk} \notin \text{span}\left(\bigcup_{\bar{k} \in (\mathcal{S} \cap \mathcal{C}_j) \setminus \{k\}} \{\mathbf{h}_{j\bar{k}}\}\right) \quad (7.32)$$

for all  $k \in \mathcal{S}(j)$ . To achieve the multiplexing gain of  $|\mathcal{S}|$ , we need to show that all interference terms in (7.14) for the selected users are bounded as  $q_j \rightarrow \infty$ . This is sufficient since the signal gains increase linearly with  $q_j$ . In fact, we will show that  $\sqrt{q_j} \mathbf{h}_{jk}^H \mathbf{C}_{jk} \mathbf{D}_{j\bar{k}} \bar{\mathbf{v}}_{j\bar{k}} \rightarrow 0$  for  $k \neq \bar{k}$  when  $q_j \rightarrow \infty$  when using the DVSINR strategy. We use the eigen decomposition notation  $\sum_{\bar{k} \in (\mathcal{S} \cap \mathcal{C}_j) \setminus \{k\}} \mu_{\bar{k}}^{(\text{heuristic})} \mathbf{h}_{j\bar{k}} \mathbf{h}_{j\bar{k}}^H = \mathbf{U} \mathbf{\Lambda} \mathbf{U}^H$ , where  $\text{rank}(\mathbf{\Lambda}) = |\mathcal{S} \cap \mathcal{C}_j| - 1$ , to see that

$$\begin{aligned} \bar{\mathbf{v}}_{j\bar{k}} &= \frac{(\frac{1}{q_j} \mathbf{I}_{N_j} + \mathbf{U} \mathbf{\Lambda} \mathbf{U}^H)^{-1} \mathbf{h}_{j\bar{k}}}{\|(\frac{1}{q_j} \mathbf{I}_{N_j} + \mathbf{U} \mathbf{\Lambda} \mathbf{U}^H)^{-1} \mathbf{h}_{j\bar{k}}\|_2} \\ &= \frac{\left(q_j (\mathbf{I}_{N_j} - \sum_{m=1}^{\text{rank}(\mathbf{\Lambda})} \mathbf{u}_m \mathbf{u}_m^H) + \sum_{m=1}^{\text{rank}(\mathbf{\Lambda})} \frac{q_j}{\lambda_m q_j + 1} \mathbf{u}_m \mathbf{u}_m^H\right) \mathbf{h}_{j\bar{k}}}{\left\| \left(q_j (\mathbf{I}_{N_j} - \sum_{m=1}^{\text{rank}(\mathbf{\Lambda})} \mathbf{u}_m \mathbf{u}_m^H) + \sum_{m=1}^{\text{rank}(\mathbf{\Lambda})} \frac{q_j}{\lambda_m q_j + 1} \mathbf{u}_m \mathbf{u}_m^H\right) \mathbf{h}_{j\bar{k}} \right\|_2} \end{aligned} \quad (7.33)$$

where  $\lambda_m$  is the  $m$ th largest eigenvalue of  $\mathbf{U} \mathbf{\Lambda} \mathbf{U}^H$  and  $\mathbf{u}_m$  is the corresponding eigenvector. Observe that  $\mathbf{h}_{jk}^H \mathbf{C}_{jk} \mathbf{D}_{j\bar{k}} (\mathbf{I}_{N_j} - \sum_{m=1}^{\text{rank}(\mathbf{\Lambda})} \mathbf{u}_m \mathbf{u}_m^H) \mathbf{h}_{j\bar{k}} = 0$  since the bracketed term is the orthogonal projection matrix onto the subspace spanned by the co-user channels of the scheduled users (including

$\mathbf{h}_{jk}$ ). Therefore,

$$\begin{aligned}
& \sqrt{q_j} \mathbf{h}_{jk}^H \mathbf{C}_{jk} \mathbf{D}_{j\bar{k}} \bar{\mathbf{v}}_{j\bar{k}} \\
&= \frac{\sqrt{q_j} \mathbf{h}_{jk}^H \mathbf{C}_{jk} \mathbf{D}_{j\bar{k}} \left( \sum_{m=1}^{\text{rank}(\Lambda)} \frac{q_j}{\lambda_m q_j + 1} \mathbf{u}_m \mathbf{u}_m^H \right) \mathbf{h}_{j\bar{k}}}{\left\| \left( q_j (\mathbf{I}_{N_j} - \sum_{m=1}^{\text{rank}(\Lambda)} \mathbf{u}_m \mathbf{u}_m^H) + \sum_{m=1}^{\text{rank}(\Lambda)} \frac{q_j}{\lambda_m q_j + 1} \mathbf{u}_m \mathbf{u}_m^H \right) \mathbf{h}_{j\bar{k}} \right\|_2} \\
&= \frac{\mathbf{h}_{jk}^H \mathbf{C}_{jk} \mathbf{D}_{j\bar{k}} \left( \sum_{m=1}^{\text{rank}(\Lambda)} \frac{\sqrt{q_j}}{\lambda_m q_j + 1} \mathbf{u}_m \mathbf{u}_m^H \right) \mathbf{h}_{j\bar{k}}}{\left\| \left( \sqrt{q_j} (\mathbf{I}_{N_j} - \sum_{m=1}^{\text{rank}(\Lambda)} \mathbf{u}_m \mathbf{u}_m^H) + \sum_{m=1}^{\text{rank}(\Lambda)} \frac{\sqrt{q_j}}{\lambda_m q_j + 1} \mathbf{u}_m \mathbf{u}_m^H \right) \mathbf{h}_{j\bar{k}} \right\|_2} \rightarrow 0,
\end{aligned} \tag{7.34}$$

since the numerator is bounded when  $q_j \rightarrow \infty$  while the denominator grow without bound.

The same result (i.e., that the signal terms grows towards infinity while the interference terms approach zero) can be shown for CVSINR strategies using a similar approach.

## Chapter 8

# Evaluation of Strategies for Multicell Resource Allocation

In this chapter, we evaluate the performance of different multicell resource allocation strategies. The BRB algorithm from Chapter 6 is used to achieve optimal solutions and serves as a benchmark for the low-complexity strategies that were proposed in Chapter 7. The evaluation is divided into two parts. In Section 8.1, different aspects of the low-complexity strategies are illustrated and compared with the optimal solution. This evaluation is carried out on synthetic channels under simple Rayleigh fading assumptions, to emphasize resource allocation properties rather than channel assumptions. In Section 8.2, we evaluate the performance in actual multicell scenarios based on multiantenna channel measurements. Thus, the simulations include realistic fading distributions, path losses, and base station correlation. This evaluation both confirms that the proposed strategies achieve good performance under low computational complexity and reveals important properties of coordinated multicell transmission.

### 8.1 Evaluation on Simple Synthetic Channels

This section will illustrate aspects of optimal and suboptimal resource allocation strategies. First, we consider the performance behavior with different heuristic selections of beamforming directions. We consider a 4-user MISO interference channel with  $N_j = 4$  antennas per base station, where the channels  $\mathbf{h}_{jk}$  are modeled as uncorrelated Rayleigh fading. The average channel gain  $\mathbb{E}\{\|\mathbf{h}_{jk}\|_2^2\}/\sigma_k^2$  is  $N_j$  from the serving base station and  $N_j/2$  from all interfering base stations. We compare the DVSINR strategy (which builds upon the precoding parametrization in Chapter 7) with classic ZF and MRT precoding. The average sum rate is shown in Figure 8.1 as a function of the total transmit power (per base station). As

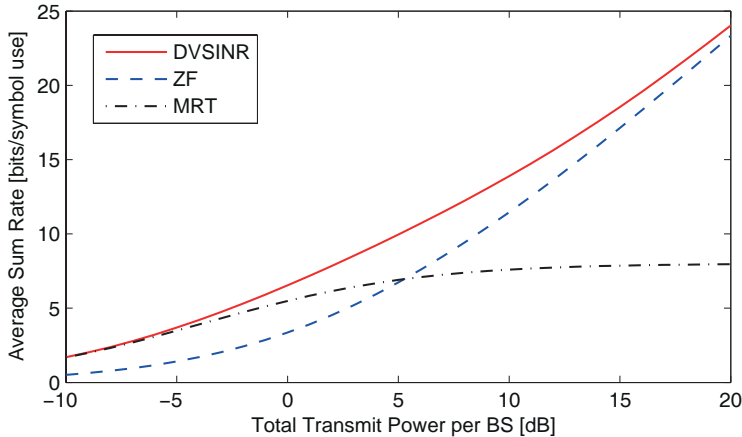


Figure 8.1: Average sum rate (over channel realizations) with DVSINR, MRT, and ZF in a 4-user MISO interference channel, as a function of the transmit power. MRT and ZF are good strategies at low and high SNR, respectively, while DVSINR shows good performance at all SNRs.

expected, MRT is good at very low SNR while ZF is good at high SNR. However, the DVSINR strategy is a more versatile heuristic strategy as it combines the respective asymptotic benefits of MRT and ZF, and clearly outperforms them at medium SNRs. This illustrates that the optimal precoding vectors are linear combinations of MRT and ZF vectors, as proved by Theorem 7.1. Observe that in this scenario, the DVSINR strategy is equivalent to the signal-to-leakage-and-noise ratio (SLNR) beamforming strategy of [STS07, ZMM<sup>+</sup>08].

Next, we investigate which percentages of the performance with optimal precoding and user selection that can be attained with low-complexity techniques. We separate the impact of these two parts of resource allocation by considering precoding with fixed user selection, and *vice versa*. The transmission scenario includes  $K_t = 2$  base stations (with  $N_j = 3$  antennas each) that jointly serve a set of  $K_r$  users. The channels  $\mathbf{h}_{jk}$  are modeled as uncorrelated Rayleigh fading and for each base station we assume that  $\mathbb{E}\{\|\mathbf{h}_{jk}\|_2^2\}/\sigma_k^2$  is  $N_j$  for half the users and  $N_j/2$  for the others, and *vice versa* for the other base station. In other words,  $K_r/2$  users are located in each of the cells but they are all close to the common cell edge.

The average sum rate with  $K_r = 6$  users and different precoding strategies is shown in Figure 8.2, as a function of the transmit power (per base station). The optimal precoding strategy is achieved using the BRB algorithm from Chapter 6. We consider both the original and the mod-

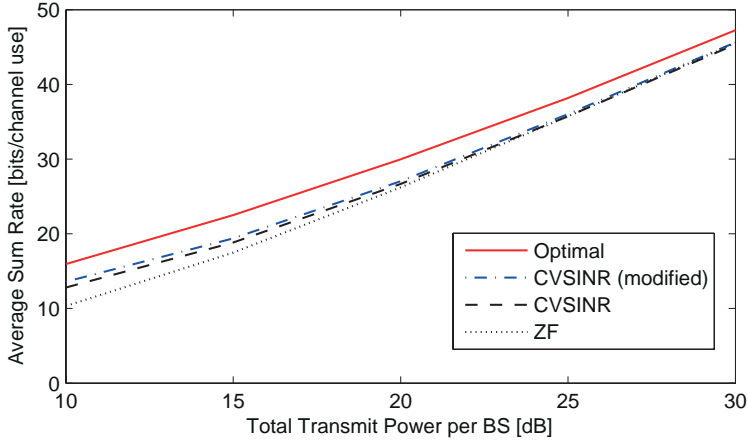


Figure 8.2: Average sum rate (over channel realizations) with different precoding strategies in a scenario with two base stations and six users close to the common cell edge. The low-complexity CVSINR strategy (without user selection) achieves a major part of the optimal performance, but can be further improved by solving a convex optimization problem.

ified version of the low-complexity CVSINR strategy from Chapter 7.3, where the modified version solves a convex optimization problem to enhance performance (without increasing the co-user interference). We also consider ZF precoding, which due to the per-base station power constraints is achieved by solving a convex optimization problem [WES08]. Depending on the transmit power, 80 – 95% of the optimal performance is achieved by the original CVSINR strategy.<sup>1</sup> This is remarkable since the CVSINR strategy only exploits the precoding parametrization in Theorem 7.2, without solving any mathematical optimization problem. The modified version increases the performance by a few percentage points, especially at low transmit power. However, our conclusion is that a major part of the maximal performance is achievable by heuristic utilization of the precoding parametrization, while optimization algorithms only are required to achieve the last few percentage points of the maximal performance. Iterative algorithms such as those in [TCJ08, ZWN08b, CACC08, NSGS10, VPW10] can be applied to approach the optimal value.

<sup>1</sup>We can expect all the heuristic strategies to have asymptotic optimality in this scenario, but the convergence is somewhat slow since the optimal solution also includes user selection (i.e., the per-base station power constraints sometimes makes it beneficial to serve fewer than six users when the transmit power is low), while the heuristic strategies always try to serve all users.

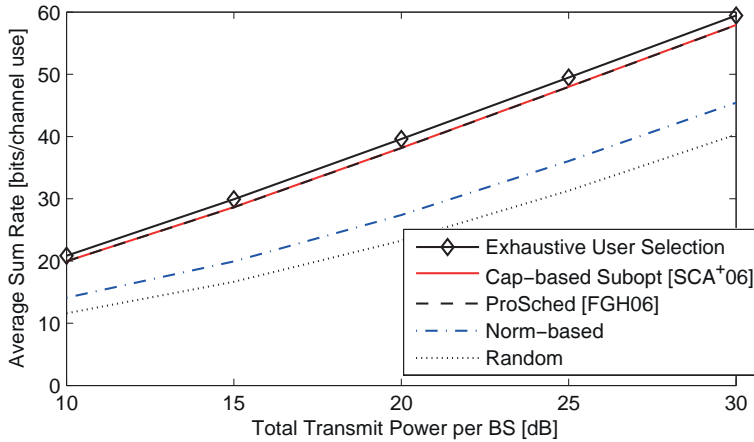


Figure 8.3: Average sum rate (over channel realizations) with CVSINR precoding and different user selection algorithms in a scenario with two base stations and six users close to the common cell edge. The low-complexity algorithms from [SCA<sup>+</sup>06, FGH06] achieve close-to-optimal performance and greatly outperform simple norm-based or random user selections.

The average sum rate with CVSINR precoding and different user selection schemes is shown in Figure 8.3. We consider  $K_r = 20$  users and vary the transmit power. The optimal user selection is based on exhaustive search, while the capacity-based suboptimal user selection algorithm was proposed in [SCA<sup>+</sup>06] and the ProSched algorithm in [FGH06, FGH07]. These are two quite similar greedy algorithms based on ZF precoding, but the ProSched algorithm has lower computational complexity as it avoids channel inversions by projection-based approximations. Irrespectively of the SNR, 96 – 97% of the optimal performance is achieved by the two greedy algorithms. This confirms that ZF-based user selection is efficient even in the low SNR regime, as long as the final precoding vectors are selected in a good way. It is hard to see any difference between the two algorithms, meaning that the complexity improvements of the ProSched algorithm comes at almost no cost. Figure 8.3 also shows the performance with norm-based user selection (the six strongest users are selected) and random user selection, which both performs rather poorly. We conclude that close-to-optimal user selection can be achieved by simple means, but the algorithm should take both channel gains and directions into account.

## 8.2 Evaluation on Channel Measurements

The theoretical performance of coordinated multicell transmission has been thoroughly studied on synthetic channels, assuming uncorrelated Rayleigh fading, simple large-scale fading models, and perfect base station synchronization (see e.g., [ZD04, TCJ08, ZWN08b, BSXZ10, VPW10]). These works have reported large improvements over single-cell processing. Especially cell edge users seem to benefit from multicell interference coordination. However, results obtained from numerical simulations are highly dependent on the assumptions in the underlying channel models. For example, it is common to model the channel characteristics between a user and multiple base stations as uncorrelated, although correlation appears in practice [JZOG07]. Along with other idealized assumptions (e.g., on fading distributions and path losses), such channel dependencies may affect the performance of any multicell system.

The purpose of this section is to evaluate the performance of the optimal and low-complexity resource allocation strategies on realistic multicell scenarios based on channel measurements. We consider the following six strategies:

1. **Optimal Resource Allocation:** This represents the optimal linear precoding strategy and is calculated using the BRB algorithm in Chapter 6. The implementation is based on the CVX toolbox of [GB10] and the YALMIP toolbox of [Löf04], which both use the numerical convex optimization solver SDPT3 from [TTT03].
2. **Optimal Resource Allocation with Incoherent Interference Reception:** This approach is similar to the optimal resource allocation, but under the additional assumption that base stations cannot cancel out each other's interference through joint transmission. This case is relevant since it is difficult to enable (robust) coherent interference cancellation over wide areas (as discussed in Chapter 5). Thus, this strategy becomes an upper bound for distributed resource allocation strategies. Mathematically, it solves the weighted sum performance problem in (7.14), but with  $\text{SINR}_k$  replaced by

$$\text{SINR}_k^{\text{incoherent}} = \frac{\left| \sum_{j=1}^{K_t} \sqrt{p_{jk}} \mathbf{h}_{jk}^H \mathbf{C}_{jk} \mathbf{D}_{jk} \bar{\mathbf{v}}_{jk} \right|^2}{\sigma_k^2 + \sum_{\bar{k} \neq k, j=1}^{K_t} \left| \sqrt{p_{j\bar{k}}} \mathbf{h}_{j\bar{k}}^H \mathbf{C}_{j\bar{k}} \mathbf{D}_{j\bar{k}} \bar{\mathbf{v}}_{j\bar{k}} \right|^2}. \quad (8.1)$$

3. **Centralized virtual SINR (CVSINR) strategy:** Proposed in Chapter 7.3.1 and combines the precoding parametrization in Theorem 7.2 with ProSched user selection.

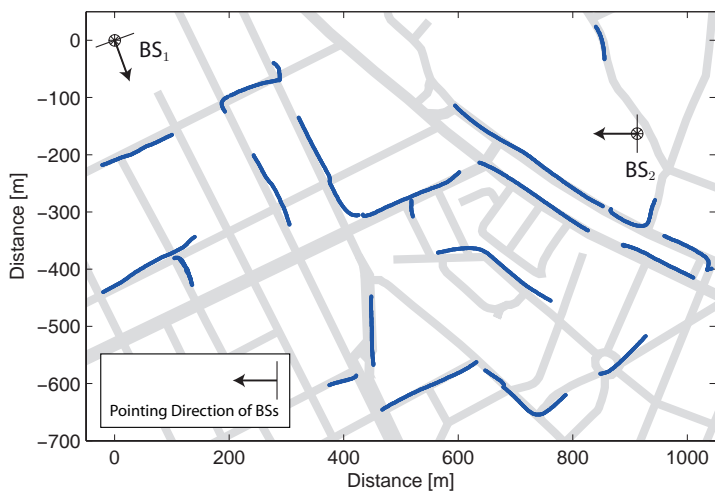
4. **Distributed virtual SINR (DVSINR) strategy:** Distributed version of CVSINR that exploits the precoding parametrization in Theorem 7.2 and a new distributed version of the ProSched user selection scheme (see Chapter 7.3.2).
5. **Coordinated ZF precoding:** Classic coordinated precoding approach where each base station performs independent power allocation and zero-forcing precoding using local CSI. The user selection is achieved using the distributed ProSched scheme (see Chapter 7.3.2) and each user is only served by one base station.
6. **Single-cell processing:** Performs resource allocation as if there is only one cell in the system. The average out-of-cell interference is included in the  $\sigma_k^2$ -terms. The resource allocation is based on the DVSINR strategy (pretending that  $K_t = 1$ ).

The evaluation is based on channel data collected in Stockholm, Sweden, using two base stations<sup>2</sup> with four-element uniform linear arrays (ULAs) with  $0.56\lambda$  antenna spacing and one user device. The user had a uniform circular array (UCA) with four directional antennas, but herein we average the signal over its antennas to create a single virtual omni-directional antenna. The system bandwidth was 9.6 kHz at a carrier frequency in the 1800 MHz band. The measurement environment can be characterized as typical European urban with four to six story high stone buildings. Figure 8.4 shows the measurement area with roads illustrated in light gray and blue routes showing the GPS coordinates of the user locations used for the simulations in this chapter. Further measurement details are available in [JZOG07]. The collected channel data is utilized to generate two evaluation scenarios where users are moving around in the area covered by both base stations:

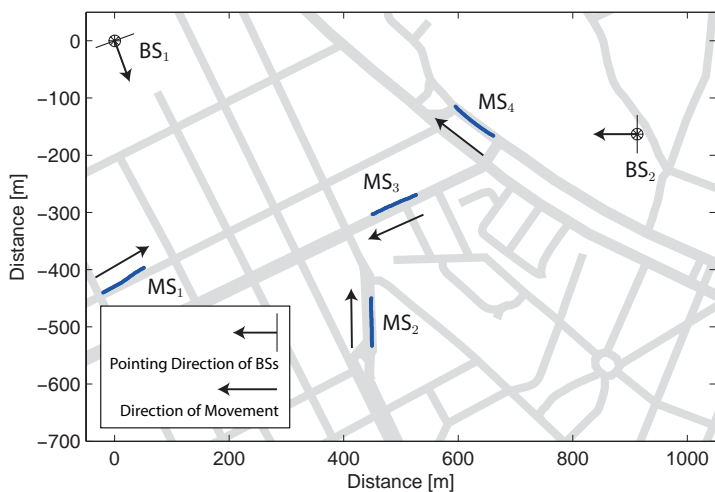
- **Scenario A:** The performance behavior is evaluated over different random user distributions. In each snapshot, users can be located anywhere on the measured routes in Figure 8.4a with uniform probability. To create balance, at least two users are placed to have their strongest channel gains ( $\|\mathbf{h}_{jk}\|_2^2$ ) from BS<sub>1</sub>, while at least two users have their strongest gains from BS<sub>2</sub>.
- **Scenario B:** To study the impact of base station coordination on individual users, four users are now placed at certain locations and moved as indicated in Figure 8.4b.

---

<sup>2</sup>Channel data from a third base station, co-located with BS<sub>1</sub>, was also measured in [JZOG07]. However, the overlap in coverage area between this base station and BS<sub>1</sub> and BS<sub>2</sub> in Figure 8.4 is small and therefore it is not used in our simulation.



(a) Routes in Scenario A.



(b) Routes in Scenario B.

Figure 8.4: The downlink performance evaluation is based on measurements in an urban environment. Two four-antenna base stations are serving multiple single-antenna users. These users are either randomly located on the measured routes marked in Scenario A or move along four fixed routes as in Scenario B.

In both scenarios, the performance will be evaluated as a function of the output power per base station (in dBm). The noise level is set to  $-131$  dBm (i.e., thermal noise and a few dBs of transceiver noise) and the measured path losses from the strongest base station varies between  $-37$  dB and  $-85$  dB for different user locations in Figure 8.4.

The performance measure is the weighted sum rate with weights

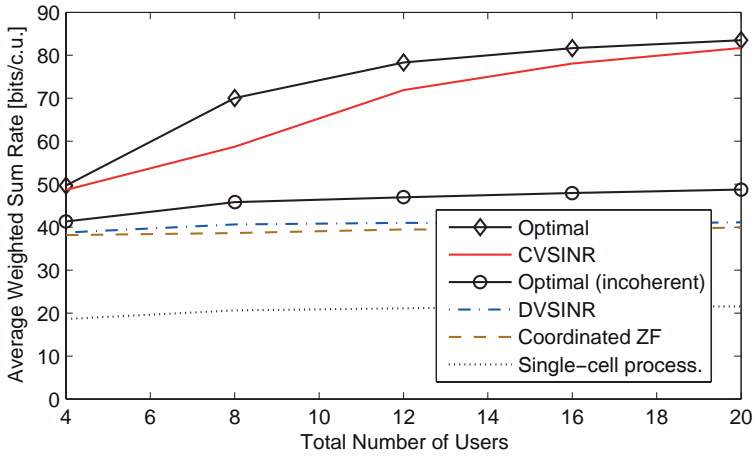
$$w_k = c_w / \mathbb{E} \left\{ \log_2 \left( 1 + \frac{K_t}{K_r \sigma_k^2} \max_j P_j \|\mathbf{h}_{jk}\|_2^2 \right) \right\}, \quad (8.2)$$

where  $c_w$  is a scaling factor making  $\sum_{k=1}^{K_r} w_k = K_r$ . This can be interpreted as a type of fairness balancing (with equal power allocation).

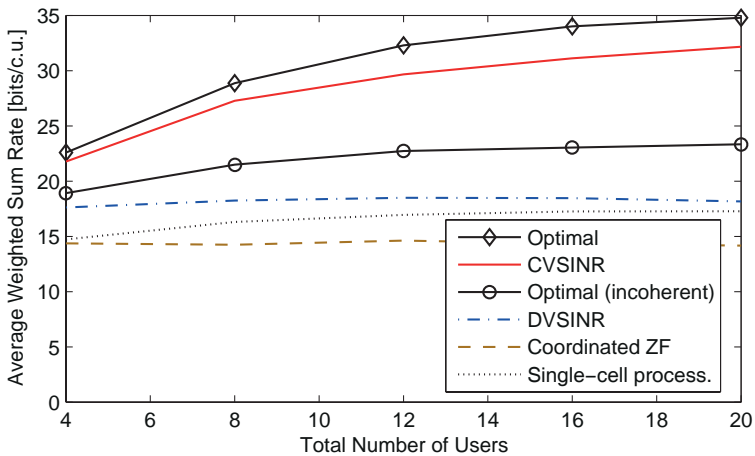
### 8.2.1 Results for Scenario A

The scheduling performance is evaluated in Figure 8.5 over different random user locations, each used for 10 channel realizations (i.e., using consecutive channel measurements). The average weighted sum rate is given as a function of the total number of users at 20 dBm and 0 dBm output power per base station. The proposed CVSINR strategy provides close-to-optimal performance, especially when the number of users increases. The gap to the optimal solution is remarkably small, given that CVSINR is a simple combination of ProSched scheduling and heuristic use of the precoding parametrization in Chapter 7.2.2—further parameter tweaking can certainly reduce the gap. The distributed strategies (DVSINR and coordinated ZF) stabilize on about half the performance of the centralized strategies, representing that only half the number of users can be simultaneously accommodated. One might think that this is due to that only one base station serves each user, but the actual explanation is that (non-iterative) distributed strategies cannot achieve coherent interference cancellation. This is understood by the comparably small difference from the optimal strategy under incoherent interference reception, and it confirms the discussion in Section 7.3.2. The proposed centralized and distributed strategies provide performance improvements over single-cell processing, and the differences increase rapidly with the output power.

Next, we want to study how multicell coordination impacts the performance of each user and we set  $K_r = 4$  to make sure that all six strategies consider the same set of users. In Figure 8.6, the cumulative distribution functions (CDFs) of the individual user rates are given for output powers of 0 dBm and 20 dBm. The proposed CVSINR strategy is very close to the optimal solution, in particular at high output power. The difference between the optimal solution and the DVSINR strategy increases with the SNR, but the distributed approach is close to the optimum under incoherent interference reception, which might be the most reasonable upper



(a) 20 dBm output power per base station.



(b) 0 dBm output power per base station.

Figure 8.5: Average weighted sum rate (over random user locations) for Scenario A with different number of users. The performance is shown for different resource allocation strategies.

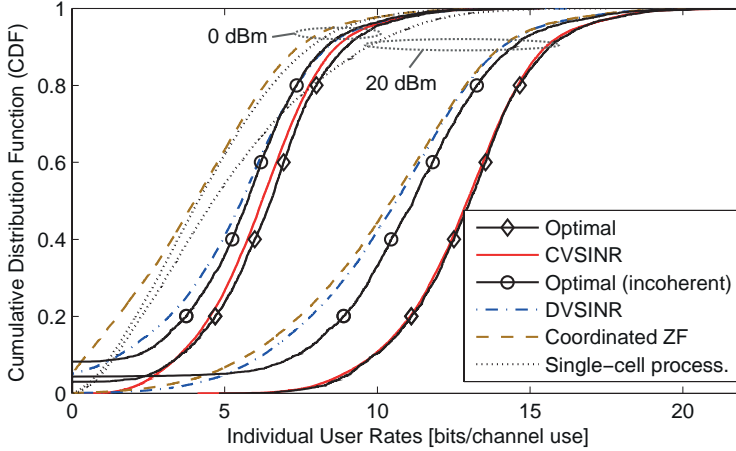


Figure 8.6: Cumulative distribution function of the individual user rates (over random user locations) for Scenario A with  $K_r = 4$  users. The performance is shown for different resource allocation strategies at 0 dBm and 20 dBm output power.

bound for distributed strategies. Both CVSINR and DVSINR provide great improvements over single-cell processing—especially at high output power. The primary reason is the interference coordination, which gives immediate improvements for cell edge users but also enables a power reallocation that all users can benefit from. The coordinated ZF strategy performs poorly at low output power, but approaches DVSINR at higher power. To summarize, users that move around in the cell will benefit from multicell coordination through higher average performance. In Scenario B, we will however see that users that are fixed at certain locations may experience performance degradations.

### 8.2.2 Results for Scenario B

For Scenario B, the average weighted sum rate (per channel use and over 750 channel realizations) is shown in Figure 8.7. Once again, the proposed CVSINR strategy provides close-to-optimal performance. As in Scenario A, there is a clear gap to the distributed approaches, explained by fewer degrees of freedom in the interference cancelation. However, both DVSINR and coordinated ZF precoding achieve the optimal multiplexing gain (see Theorem 7.3), while the performance of single-cell processing is bounded at high output power. Observe that the major gain over single-cell processing comes from interference coordination, while the difference between DVS-

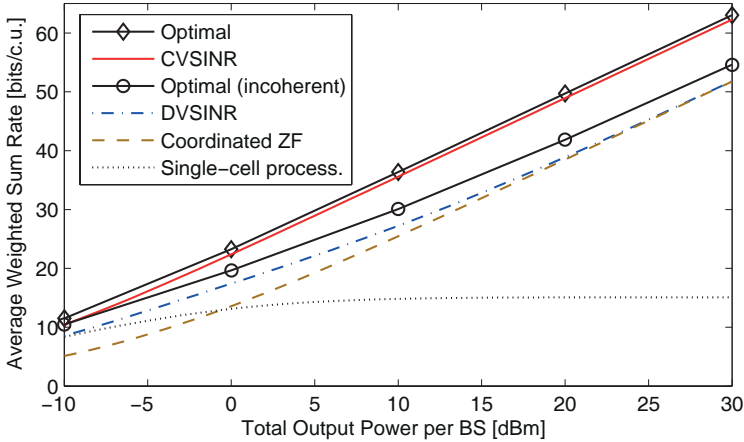


Figure 8.7: Average weighted sum rate as a function of the output power for Scenario B. The performance is shown for different resource allocation strategies, including the proposed CVSINR and DVSINR strategies.

INR and optimal joint transmission is comparably small (and bounded).

Figure 8.8 shows the average individual user rates for DVSINR (marked with triangles) and single-cell processing, as a function of the output power. Interestingly, the increased weighted sum rate with multicell coordination does not translate into a monotonic improvement of all user rates. Recall that the user locations are shown in Figure 8.4b. User 3 has almost equally strong channels from both base stations and therefore gain substantially from interference coordination. However, User 2 has a very weak link to BS<sub>2</sub> and sees a decrease in performance for output powers below 10 dBm. This is explained by BS<sub>1</sub> modifying its precoding to avoid causing interference to Users 3 and 4. In other words, cell edge users benefit from interference coordination, while users that are untroubled by interference (e.g., shadowed from neighboring cells) might see deteriorations.<sup>3</sup> The generic claim that multicell coordination improves both the total throughput and the fairness is therefore not necessarily true in practice. However, Scenario A showed that users that move around in the whole coverage area will on average benefit from multicell coordination.

The analysis has thus far considered perfect base station synchronization, which cannot be guaranteed in practice due to estimation errors, CSI acquisition and hardware delays, clock drifts, oscillator phase noise, doppler

<sup>3</sup>This drawback can be alleviated through coordinated user selection. Users that are located in similar directions should not be scheduled together, even if only some of them are troubled by interference.

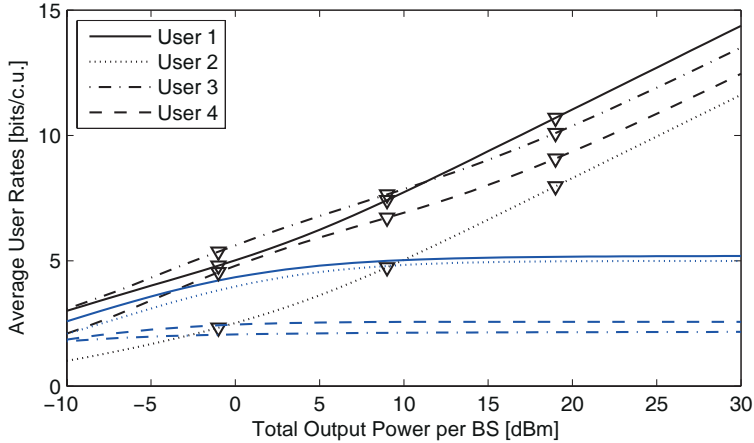


Figure 8.8: Average individual user rates for Scenario B with and without multicell coordination. The proposed DVSINR strategy (triangles) is compared with single-cell processing.

spread, and insufficient cyclic prefixes. We emulate these mismatches by letting the actual channels be  $\mathbf{h}_{jk}^{\text{actual}} = \mathbf{h}_{jk} e^{i\phi_{jk}}$  for some random phase deviations  $\phi_{jk} \in \mathcal{N}(0, \sigma_\phi^2)$  (where  $\sigma_\phi = 0$  means perfect synchronization). In Figure 8.9, the average weighted sum rate is shown as a function of the phase standard deviation  $\sigma_\phi$  (at 20 dBm output power). The optimal resource allocation and the CVSINR strategy are very sensitive to synchronization errors as they rely on coherent interference cancellation where the interfering signals from different base stations should cancel out perfectly. The DVSINR and coordinated ZF strategies are unaffected by such synchronization errors, and the gap to the optimal strategy based on incoherent interference reception reduces with  $\sigma_\phi$ . We conclude that tight synchronization is required to gain from centralized multicell coordination with joint transmission.

### 8.3 Summary

Multicell resource allocation is a very difficult problem to solve optimally, but the simulations on synthetic channels indicate that a very large portion of the optimal performance can be achieved by simple means. The precoding parametrization in Chapter 7 provides a clear structure of the optimal precoding directions (it is a combination of MRT and ZF) that can be exploited without having to solve any mathematical optimization problem—although, a convex problem can be solved for further improve-

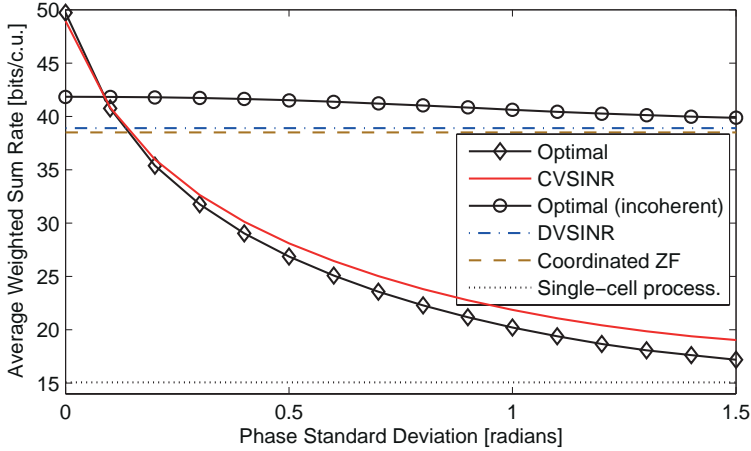


Figure 8.9: Weighted sum rate for Scenario B as a function of the phase standard deviation  $\sigma_k$  (at 20 dBm output power). The actual channels are modeled as  $\mathbf{h}_{jk}^{\text{actual}} = \mathbf{h}_{jk} e^{i\phi_{jk}}$ , where  $\phi_{jk} \in \mathcal{N}(0, \sigma_\phi^2)$ .

ments. User selection has also a great impact on the performance, but classic algorithms that maximize the performance greedily attain almost the optimal performance. There is a natural coupling between precoding and user selection; it is easier to find good precoding for spatially separated users, and easier to determine a good user set if a sound precoding strategy is used. While ideal resource allocation solves these problems jointly, successive solutions that first select users based on ZF precoding and then refine the precoding show very promising results.

The performance of multicell resource allocation was also evaluated on actual measured channels in a typical urban macro-cell scenario. Substantial performance gains over single-cell processing were observed for the proposed CVSINR and DVSINR strategies. The former is even close-to-optimal, while the latter performs closely to what can be expected from distributed strategies (since coherent interference cancellation is more or less impossible to achieve). This is remarkable since both CVSINR and DVSINR are just simple applications of the precoding parametrization in Chapter 7—further parameter tweaking and adaptation to special scenarios is possible.

Ideal joint transmission includes both coherent signal reception and coherent interference cancellation. While the former is quite robust, the interference cancellation is very sensitive to synchronization errors (since the sum of the interference is minimized, instead of each transmitter's contribution). The gain of joint transmission that only exploits coherent signal reception

is marginal, leading to the conclusion that joint transmission should only be used if tight synchronization can be guaranteed. In addition, we have confirmed that multicell coordination improves the average performance for users that are moving in the cell. But the overall signal/interference pattern is modified such that static users might experience performance degradations if they are located in certain parts of the cells (e.g., where the intercell interference is already small due to shadowing).

## Chapter 9

# Conclusions

The performance of multiantenna cellular communications greatly depends on the availability of channel state information and its utilization for channel-aware transmission design. This thesis considered the simplifying block fading model to emphasize three main components of downlink communications: 1) channel estimation; 2) channel feedback; and 3) resource allocation exploiting instantaneous channel information. In each of these areas, the thesis generalized system assumptions in prior work and provided novel mathematical results, along with supporting numerical examples. This chapter summarizes the main conclusions of the thesis, which provide insights on the design of efficient cellular systems.

In the area of channel estimation, we have shown the importance of directly estimating each quantity of interest, instead of only estimating the channel matrix and use it for calculating different quantities. We considered training-based MMSE estimation under general Rician statistics and showed under which conditions the optimal training strategy is easily obtained. These insights were utilized for proposing a low-complexity training strategy that performs well in the numerical evaluation, even under non-ideal statistics. This indicates that most of the potential gain of training optimization can be achieved by simple means.

In the area of channel feedback, we have shown that better performance is achieved by serving many users with one data stream each, than by multiplexing several streams to a smaller number of users. This is proved analytically under both quantization errors and estimation errors, and the conclusion is that each user should use its antennas for receive combining and interference rejection. This has positive implications on the hardware design of user devices and on the quantization complexity. In addition, feedback of the channel direction is shown to be of primary importance, while 2-3 bits of quality feedback is sufficient in many scenarios. The demands for accurate directional information increases with the SNR, but will not affect the number of uplink channel uses spent on CSI acquisition.

We proposed a generalized mathematical model for multicell systems to enable joint analysis of different levels of transmission coordination between base stations. This model reveals both the similarities and differences between cellular systems and the well-established research area of multiuser MIMO. Multicell user selection and precoding design were posed as a joint resource allocation problem, which unfortunately is NP-hard under most conditions. The optimal solution is therefore unattainable in practice, but it is still important to find the solution for benchmarking purposes. We derived an algorithm that guarantees optimal convergence, but with exponential complexity in the number of users. As a subproblem, it solves so-called fairness-profile optimization problems that avoid the high complexity by searching along one-dimensional curves in the user dimension space.

The thesis also showed that the multicell resource allocation problem becomes convex and can be solved in closed form if a certain set of parameters are fixed. This leads to a parametrization of the optimal solution, which both provides intuition and a foundation for designing low-complexity strategies through heuristic parameter selection. We proposed two such strategies, one requiring centralized resource allocation and another one suitable for distributed implementation with little backhaul signaling. The performance of these strategies was compared with the optimal solution using measured multicell channels in an urban macro-cell system. This evaluation showed that a remarkably large portion of the optimal performance can be achieved by low-complexity strategies. On the other hand, we observed that joint multicell transmission requires tight synchronization and that not all users will benefit from multicell coordination.

## 9.1 Future Work

There is an endless road of possible improvements and generalizations to the results of this thesis. Some extensions have intentionally been left out to make the thesis coherent, while other limitations were necessary to achieve analytical tractability or to avoid making assumptions that would affect the generality. However, several ideas for future work have been conceived in the process of writing the thesis:

- When channel statistics are exploited for improved CSI acquisition, the robustness to inaccurate statistical knowledge deserves attention. In the area of channel estimation, one can raise the fundamental question on how accurate the prior distribution should be in order to benefit from Bayesian estimation (compared with classic estimation without any prior). In addition, the length and structure of the optimal training sequence might be affected by including a power

constraint per training symbol (instead of only constraining the total training power).

- The downlink performance of multiuser FDD systems is limited by the feedback accuracy. In practice, this requires the development of large and adaptive codebooks that enable the best codeword to be found with low computational complexity. The feedback design is also influenced by hardware impairments that are often overlooked. In particular, those can create transmission noise that scales with the output power and greatly affects the asymptotic analysis since the practical multiplexing gain then becomes zero.
- There are many open problems in the design and deployment of cellular systems. For example, the selection of the dynamic cooperation clusters was not considered in the thesis. Although the optimal resource allocation problem is NP-hard, there are room for convergence improvements (especially for the upper bound in the BRB algorithm). The numerical analysis showed that close-to-optimal performance is possible to achieve by heuristic utilization of our precoding parametrization. However, the validity and robustness of these results remain to be analyzed in practical systems.



# Bibliography

- [ABH<sup>+</sup>07] H. Asplund, J.-E. Berg, F. Harrysson, J. Medbo, and M. Riback, “Propagation characteristics of polarized radio waves in cellular communications,” in *Proc. IEEE VTC’07-Fall*, 2007, pp. 839–843.
- [AFFM98] T. Asté, P. Forster, L. Féty, and S. Mayrargue, “Down-link beamforming avoiding DOA estimation for cellular mobile communications,” in *Proc. IEEE ICASSP’98*, 1998, pp. 3313–3316.
- [AM97] S. Amari and R. Misra, “Closed-form expressions for distribution of sum of exponential random variables,” *IEEE Trans. Rel.*, vol. 46, no. 4, pp. 519–522, 1997.
- [And09] N. Anderson, “Paired and unpaired spectrum,” in *LTE - The UMTS Long Term Evolution: From Theory to Practice*, S. Sesia, I. Toufik, and M. Baker, Eds. Wiley, 2009, ch. 23, pp. 551–583.
- [AYL07] C. Au-Yeung and D. Love, “On the performance of random vector quantization limited feedback beamforming in a MISO system,” *IEEE Trans. Wireless Commun.*, vol. 6, no. 2, pp. 458–462, 2007.
- [BBB91] V. Balakrishnan, S. Boyd, and S. Balemi, “Robust downlink beamforming based on outage probability specifications,” *Int. J. Robust and Nonlinear Control*, vol. 1, no. 4, pp. 295–317, 1991.
- [BBO10] E. Björnson, M. Bengtsson, and B. Ottersten, “Optimality properties and low-complexity solutions to coordinated multicell transmission,” in *Proc. IEEE GLOBECOM’10*, 2010.
- [BBO11a] E. Björnson, M. Bengtsson, and B. Ottersten, “Pareto characterization of the multicell MIMO performance region with

- simple receivers,” *IEEE Trans. Signal Process.*, may 2011, submitted, arXiv:1105.4880v1.
- [BBO11b] E. Björnson, M. Bengtsson, and B. Ottersten, “Receive combining vs. multistream multiplexing in multiuser MIMO systems,” in *Proc. IEEE Swe-CTW’11*, 2011, pp. 109–114.
- [BBZO11] E. Björnson, M. Bengtsson, G. Zheng, and B. Ottersten, “Computational framework for optimal robust beamforming in coordinated multicell systems,” in *Proc. IEEE CAM-SAP’11*, 2011.
- [BDMJ08] E. Björnson, P. Devarakota, S. Medawar, and E. Jorswieck, “Schur-convexity of the symbol error rate in correlated MIMO systems with precoding and space-time coding,” in *Proc. Nordic Radio Science and Commun. (RVK’08)*, 2008.
- [BG93] S. Boyd and L. E. Ghaoui, “Method of centers for minimizing generalized eigenvalues,” *Linear Algebra and Its Applications*, vol. 188, pp. 63–111, 1993.
- [BG06] M. Biguesh and A. Gershman, “Training-based MIMO channel estimation: a study of estimator tradeoffs and optimal training signals,” *IEEE Trans. Signal Process.*, vol. 54, no. 3, pp. 884–893, 2006.
- [BGS09] M. Biguesh, S. Gazor, and M. Shariat, “Optimal training sequence for MIMO wireless systems in colored environments,” *IEEE Trans. Signal Process.*, vol. 57, no. 8, pp. 3144–3153, 2009.
- [BHO07] E. Björnson, D. Hammarwall, and B. Ottersten, “Beamforming utilizing channel norm feedback in multiuser MIMO systems,” in *Proc. IEEE SPAWC’07*, 2007.
- [BHO09] E. Björnson, D. Hammarwall, and B. Ottersten, “Exploiting quantized channel norm feedback through conditional statistics in arbitrarily correlated MIMO systems,” *IEEE Trans. Signal Process.*, vol. 57, no. 10, pp. 4027–4041, 2009.
- [BHZ<sup>+</sup>08] E. Björnson, D. Hammarwall, R. Zakhour, M. Bengtsson, D. Gesbert, and B. Ottersten, “Feedback design in multiuser MIMO systems using quantization splitting and hybrid instantaneous/statistical channel information,” in *Proc. ICT Mobile and Wireless Communications Summit*, 2008.

- [BJBO11] E. Björnson, N. Jaldén, M. Bengtsson, and B. Ottersten, “Optimality properties, distributed strategies, and measurement-based evaluation of coordinated multicell OFDMA transmission,” *IEEE Trans. Signal Process.*, 2011, to appear.
- [Bjö07] E. Björnson, “Beamforming utilizing channel norm feedback in multiuser MIMO systems,” Master’s thesis, Lund University (in cooperation with KTH Royal Institute of Technology), 2007.
- [BJO10] E. Björnson, E. Jorswieck, and B. Ottersten, “Impact of spatial correlation and precoding design in OSTBC MIMO systems,” *IEEE Trans. Wireless Commun.*, vol. 9, no. 11, pp. 3578–3589, 2010.
- [BNO10] E. Björnson, K. Ntontin, and B. Ottersten, “Channel quantization design in multiuser MIMO systems: Asymptotic versus practical conclusions,” in *Proc. IEEE ICASSP’11*, 2010, pp. 3072–3075.
- [BO01] M. Bengtsson and B. Ottersten, “Optimal and suboptimal transmit beamforming,” in *Handbook of Antennas in Wireless Communications*, L. C. Godara, Ed. CRC Press, 2001.
- [BO08a] E. Björnson and B. Ottersten, “Exploiting long-term statistics in spatially correlated multi-user MIMO systems with quantized channel norm feedback,” in *Proc. IEEE ICASSP’08*, 2008, pp. 3117–3120.
- [BO08b] E. Björnson and B. Ottersten, “Pilot-based Bayesian channel norm estimation in Rayleigh fading multi-antenna systems,” in *Proc. Nordic Radio Science and Commun. (RVK’08)*, 2008.
- [BO08c] E. Björnson and B. Ottersten, “Post-user-selection quantization and estimation of correlated Frobenius and spectral channel norms,” in *Proc. IEEE PIMRC’08*, 2008.
- [BO09a] E. Björnson and B. Ottersten, “On the principles of multicell precoding with centralized and distributed cooperation,” in *Proc. WCSP’09*, 2009.
- [BO09b] E. Björnson and B. Ottersten, “Training-based Bayesian MIMO channel and channel norm estimation,” in *Proc. IEEE ICASSP’09*, 2009, pp. 2701–2704.

- [BO10] E. Björnson and B. Ottersten, “A framework for training-based estimation in arbitrarily correlated Rician MIMO channels with Rician disturbance,” *IEEE Trans. Signal Process.*, vol. 58, no. 3, pp. 1807–1820, 2010.
- [BOJ09] E. Björnson, B. Ottersten, and E. Jorswieck, “On the impact of spatial correlation and precoder design in MIMO systems with space-time block coding,” in *Proc. IEEE ICASSP’09*, 2009, pp. 2741–2744.
- [Böl04] H. Bölcskei, “Principles of MIMO-OFDM wireless systems,” in *Signal Processing for Mobile Communications Handbook*, M. Ibnkahla, Ed. CRC Press, 2004, ch. 12, pp. 12.1–12.22.
- [BS02] H. Boche and M. Schubert, “A general duality theory for uplink and downlink beamforming,” in *Proc. IEEE VTC’02-Fall*, 2002, pp. 87–91.
- [BSXZ10] C. Botella, T. Svensson, X. Xu, and H. Zhang, “On the performance of joint processing schemes over the cluster area,” in *Proc. IEEE VTC’10-Spring*, 2010.
- [BTGN09] A. Ben-Tal, L. E. Ghaoui, and A. Nemirovski, *Robust Optimization*. Princeton University Press, 2009.
- [BTN01] A. Ben-Tal and A. Nemirovski, *Lectures on modern convex optimization: analysis, algorithms, and engineering applications*. SIAM, 2001.
- [BTO<sup>+</sup>11] M. Boldi, A. Tölili, M. Olsson, E. Hardouin, T. Svensson, F. Boccardi, L. Thiele, and V. Jungnickel, “Coordinated multipoint (CoMP) systems,” in *Mobile and Wireless Communications for IMT-Advanced and Beyond*, A. Osseiran, J. Monserrat, and W. Mohr, Eds. Wiley, 2011, pp. 121–155.
- [BU09] J. Brehmer and W. Utschick, “Utility maximization in the multi-user MISO downlink with linear precoding,” in *Proc. IEEE ICC’09*, 2009.
- [BU10] J. Brehmer and W. Utschick, “Optimal interference management in multi-antenna, multi-cell systems,” in *Proc. Int. Zurich Seminar on Commun.*, 2010, pp. 134–137.
- [BV04] S. Boyd and L. Vandenberghe, *Convex Optimization*. Cambridge University Press, 2004.

- [BZBO11] E. Björnson, G. Zheng, M. Bengtsson, and B. Ottersten, “Robust monotonic optimization framework for multicell MISO systems,” *IEEE Trans. Signal Process.*, mar 2011, submitted, arXiv:1104.5240v2.
- [BZGO09] E. Björnson, R. Zakhour, D. Gesbert, and B. Ottersten, “Distributed multicell and multiantenna precoding: Characterization and performance evaluation,” in *Proc. IEEE GLOBECOM’09*, 2009.
- [BZGO10] E. Björnson, R. Zakhour, D. Gesbert, and B. Ottersten, “Cooperative multicell precoding: Rate region characterization and distributed strategies with instantaneous and statistical CSI,” *IEEE Trans. Signal Process.*, vol. 58, no. 8, pp. 4298–4310, 2010.
- [CACC08] S. Christensen, R. Agarwal, E. Carvalho, and J. Cioffi, “Weighted sum-rate maximization using weighted MMSE for MIMO-BC beamforming design,” *IEEE Trans. Wireless Commun.*, vol. 7, no. 12, pp. 4792–4799, 2008.
- [CHC04] B. Chalise, L. Haering, and A. Czylik, “Robust uplink to downlink spatial covariance matrix transformation for downlink beamforming,” in *Proc. IEEE ICC’04*, 2004, pp. 3010–3014.
- [CJ08] V. Cadambe and S. Jafar, “Interference alignment and degrees of freedom of the  $k$ -user interference channel,” *IEEE Trans. Inf. Theory*, vol. 54, no. 8, pp. 3425–3441, 2008.
- [CJKR10] G. Caire, N. Jindal, M. Kobayashi, and N. Ravindran, “Multiuser MIMO achievable rates with downlink training and channel state feedback,” *IEEE Trans. Inf. Theory*, vol. 56, no. 6, pp. 2845–2866, 2010.
- [CLW<sup>+</sup>03] D. Chizhik, J. Ling, P. Wolniansky, R. Valenzuela, N. Costa, and K. Huber, “Multiple-input-multiple-output measurements and modeling in Manhattan,” *IEEE J. Sel. Areas Commun.*, vol. 21, no. 3, pp. 321–331, 2003.
- [CMJH08] C.-B. Chae, D. Mazzarese, N. Jindal, and R. Heath, “Coordinated beamforming with limited feedback in the MIMO broadcast channel,” *IEEE J. Sel. Areas Commun.*, vol. 26, no. 8, pp. 1505–1515, 2008.
- [CS97] E. D. Carvalho and D. Slock, “Cramer-Rao bounds for semi-blind, blind and training sequence based channel estimation,” in *Proc. IEEE SPAWC’97*, 1997, pp. 129–132.

- [CS03] G. Caire and S. Shamai, "On the achievable throughput of a multi-antenna Gaussian broadcast channel," *IEEE Trans. Inf. Theory*, vol. 49, no. 7, pp. 1691–1706, 2003.
- [CSAH08] R. Chen, Z. Shen, J. Andrews, and R. Heath, "Multimode transmission for multiuser MIMO systems with block diagonalization," *IEEE Trans. Signal Process.*, vol. 56, no. 7, pp. 3294–3302, 2008.
- [CSCG07] B. Chalise, S. Shahbazpanahi, A. Czylik, and A. Gershman, "Robust downlink beamforming based on outage probability specifications," *IEEE Trans. Wireless Commun.*, vol. 6, no. 10, pp. 3498–3503, 2007.
- [CT91] T. Cover and J. Thomas, *Elements of Information Theory*. Wiley, 1991.
- [dFS08] R. de Francisco and D. Slock, "A design framework for scalar feedback in MIMO broadcast channels," *EURASIP J. on Adv. in Signal Process.*, 2008.
- [DHL<sup>+</sup>11] M. Dohler, R. Heath, A. Lozano, C. Papadias, and R. Valenzuela, "Is the PHY layer dead?" *IEEE Commun. Mag.*, vol. 49, no. 4, pp. 159–165, 2011.
- [DHST08] I. Dhillon, R. Heath, T. Strohmer, and J. Tropp, "Constructing packings in Grassmannian manifolds via alternating projection," *Experiment. Math.*, vol. 17, no. 1, pp. 9–35, 2008.
- [DLR08] W. Dai, Y. Liu, and B. Rider, "Quantization bounds on Grassmann manifolds and applications to MIMO communications," *IEEE Trans. Inf. Theory*, vol. 54, no. 3, pp. 1108–1123, 2008.
- [DPSB08] E. Dahlman, S. Parkvall, J. Sköld, and P. Beming, *3G Evolution: HSPA and LTE for Mobile Broadband*, 2nd ed. Academic Press, 2008.
- [DU05] F. Dietrich and W. Utschick, "Pilot-assisted channel estimation based on second-order statistics," *IEEE Trans. Signal Process.*, vol. 53, no. 3, pp. 1178–1193, 2005.
- [DY10] H. Dahrouj and W. Yu, "Coordinated beamforming for the multicell multi-antenna wireless system," *IEEE Trans. Wireless Commun.*, vol. 9, no. 5, pp. 1748–1759, 2010.

- [ECS<sup>+</sup>98] R. Ertel, P. Cardieri, K. Sowerby, T. Rappaport, and J. Reed, "Overview of spatial channel models for antenna array communication systems," *IEEE Personal Commun. Mag.*, vol. 5, no. 1, pp. 10–22, 1998.
- [EM04] Y. Eldar and N. Merhav, "A competitive minimax approach to robust estimation of random parameters," *IEEE Trans. Signal Process.*, vol. 52, no. 7, pp. 1931–1946, 2004.
- [ESV<sup>+</sup>10] K. Eriksson, S. Shi, N. Vučić, M. Schubert, and E. Larsson, "Globally optimal resource allocation for achieving maximum weighted sum rate," in *Proc. GLOBECOM'10*, 2010.
- [ETW08] R. Etkin, D. Tse, and H. Wang, "Gaussian interference channel capacity to within one bit," *IEEE Trans. Inf. Theory*, vol. 54, no. 12, pp. 5534–5562, 2008.
- [FG98] G. J. Foschini and M. J. Gans, "On limits of wireless communications in a fading environment when using multiple antennas," *Wireless Personal Commun.*, vol. 6, no. 3, pp. 311–335, 1998.
- [FGH06] M. Fuchs, G. D. Galdo, and M. Haardt, "Low complexity spatial scheduling ProSched for MIMO systems with multiple base stations and a central controller," in *Proc. ITG Workshop on Smart Antennas*, 2006.
- [FGH07] M. Fuchs, G. D. Galdo, and M. Haardt, "Low-complexity space-time-frequency scheduling for MIMO systems with SDMA," *IEEE Trans. Veh. Technol.*, vol. 56, no. 5, pp. 2775–2784, 2007.
- [GB10] M. Grant and S. Boyd, "CVX: Matlab software for disciplined convex programming," <http://cvxr.com/cvx>, May 2010.
- [Gev05] M. Gevers, "Identification for control: From the early achievements to the revival of experiment design," *European Journal of Control*, vol. 11, pp. 1–18, 2005.
- [GGLF08] B. Göransson, S. Grant, E. Larsson, and Z. Feng, "Effect of transmitter and receiver impairments on the performance of MIMO in HSDPA," in *Proc. IEEE SPAWC'08*, 2008.
- [GHH<sup>+</sup>10] D. Gesbert, S. Hanly, H. Huang, S. Shamai, O. Simeone, and W. Yu, "Multi-cell MIMO cooperative networks: A new look at interference," *IEEE J. Sel. Areas Commun.*, vol. 28, no. 9, pp. 1380–1408, 2010.

- [GJJV03] A. Goldsmith, S. Jafar, N. Jindal, and S. Vishwanath, "Capacity limits of MIMO channels," *IEEE J. Sel. Areas Commun.*, vol. 21, no. 5, pp. 684–702, 2003.
- [GK11] D. Gesbert and M. Kountouris, "Rate scaling laws in multicell networks under distributed power control and user scheduling," *IEEE Trans. Inf. Theory*, vol. 57, no. 1, pp. 234–244, 2011.
- [GKGØ07] D. Gesbert, S. Kiani, A. Gjendemsjø, and G. Øien, "Adaptation, coordination, and distributed resource allocation in interference-limited wireless networks," *Proc. IEEE*, vol. 95, no. 12, pp. 2393–2409, 2007.
- [GKH<sup>+</sup>07] D. Gesbert, M. Kountouris, R. Heath, C.-B. Chae, and T. Sälzer, "Shifting the MIMO paradigm," *IEEE Signal Process. Mag.*, vol. 24, no. 5, pp. 36–46, 2007.
- [GPS08] K. Gomadam, H. Papadopoulos, and C.-E. Sundberg, "Techniques for multi-user MIMO with two-way training," in *Proc. IEEE ICC'08*, 2008.
- [GSS<sup>+</sup>10] A. Gershman, N. Sidiropoulos, S. Shahbazpanahi, M. Bengtsson, and B. Ottersten, "Convex optimization-based beamforming," *IEEE Signal Process. Mag.*, vol. 27, no. 3, pp. 62–75, 2010.
- [HBO08a] D. Hammarwall, M. Bengtsson, and B. Ottersten, "Acquiring partial CSI for spatially selective transmission by instantaneous channel norm feedback," *IEEE Trans. Signal Process.*, vol. 56, no. 3, pp. 1188–1204, 2008.
- [HBO08b] D. Hammarwall, M. Bengtsson, and B. Ottersten, "Utilizing the spatial information provided by channel norm feedback in SDMA systems," *IEEE Trans. Signal Process.*, vol. 56, no. 7, pp. 3278–3293, 2008.
- [HBYB11] X. Hou, E. Björnson, C. Yang, and M. Bengtsson, "Cell-grouping based distributed beamforming and scheduling for multi-cell cooperative transmission," in *Proc. IEEE PIMRC'11*, 2011.
- [HCML10] H. Huh, G. Caire, S.-H. Moon, and I. Lee, "Multi-cell MIMO downlink with fairness criteria: The large system limit," in *Proc. IEEE ISIT'10*, 2010, pp. 2058–2062.

- [HH03] B. Hassibi and B. Hochwald, "How much training is needed in multiple-antenna wireless links?" *IEEE Trans. Inf. Theory*, vol. 49, no. 4, pp. 951–963, 2003.
- [Hja05] H. Hjalmarsson, "From experiment design to closed-loop control," *Automatica*, vol. 41, pp. 393–438, 2005.
- [HK81] T. Han and K. Kobayashi, "A new achievable rate region for the interference channel," *IEEE Trans. Inf. Theory*, vol. 27, no. 1, pp. 49–60, 1981.
- [HLW06] W. Hager, Y. Liu, and T. Wong, "Optimization of generalized mean square error in signal processing and communication," *Linear Algebra and its Applications*, vol. 416, pp. 815–834, 2006.
- [HP10] Y. Huang and D. Palomar, "Rank-constrained separable semidefinite program with applications to optimal beamforming," *IEEE Trans. Signal Process.*, vol. 58, no. 2, pp. 664–678, 2010.
- [HSG90] M. Honig, K. Steiglitz, and B. Gopinath, "Multichannel signal processing for data communications in the presence of crosstalk," *IEEE Trans. Commun.*, vol. 38, no. 4, pp. 551–558, 1990.
- [HSHS08] N. Hassanpour, J. Smee, J. Hou, and J. Soriaga, "Distributed beamforming based on signal-to-caused-interference ratio," in *Proc. IEEE ISSSTA '08*, 2008, pp. 405–410.
- [HTH<sup>+</sup>09] H. Huang, M. Trivellato, A. Hottinen, M. Shafi, P. Smith, and R. Valenzuela, "Increasing downlink cellular throughput with limited network MIMO coordination," *IEEE Trans. Wireless Commun.*, vol. 8, no. 6, pp. 2983–2989, 2009.
- [JAWV11] J. Jose, A. Ashikhmin, P. Whiting, and S. Vishwanath, "Channel estimation and linear precoding in multiuser multiple-antenna TDD systems," *IEEE Trans. Veh. Technol.*, vol. 60, no. 5, pp. 2102–2116, 2011.
- [JB07] E. Jorswieck and H. Boche, "Majorization and matrix-monotone functions in wireless communications," *Foundations and Trends in Communication and Information Theory*, vol. 3, no. 6, pp. 553–701, 2007.

- [Jin06] N. Jindal, "MIMO broadcast channels with finite-rate feedback," *IEEE Trans. Inf. Theory*, vol. 52, no. 11, pp. 5045–5060, 2006.
- [Jin08] N. Jindal, "Antenna combining for the MIMO downlink channel," *IEEE Trans. Wireless Commun.*, vol. 7, no. 10, pp. 3834–3844, 2008.
- [JJZ<sup>+</sup>08] P. Jiyong, L. Jiandong, L. Zhuo, Z. Linjing, and C. Liang, "Optimal training sequences for MIMO systems under correlated fading," *Journal of Systems Engineering and Electronics*, vol. 19, pp. 33–38, 2008.
- [JL10] E. Jorswieck and E. Larsson, "Monotonic optimization framework for the two-user MISO interference channel," *IEEE Trans. Commun.*, vol. 58, no. 7, pp. 2159–2168, 2010.
- [JLD08] E. Jorswieck, E. Larsson, and D. Danev, "Complete characterization of the Pareto boundary for the MISO interference channel," *IEEE Trans. Signal Process.*, vol. 56, no. 10, pp. 5292–5296, 2008.
- [JTS<sup>+</sup>08] S. Jing, D. Tse, J. Soriaga, J. Hou, J. Smee, and R. Padovani, "Multicell downlink capacity with coordinated processing," *EURASIP J. Wirel. Commun. Netw.*, 2008.
- [JZOG07] N. Jaldén, P. Zetterberg, B. Ottersten, and L. Garcia, "Inter- and intrasite correlations of large-scale parameters from macrocellular measurements at 1800 MHz," *EURASIP J. Wirel. Commun. Netw.*, 2007.
- [Kay93] S. Kay, *Fundamentals of Statistical Signal Processing: Estimation Theory*. Prentice Hall, 1993.
- [KBLS08] T. Kim, M. Bengtsson, E. Larsson, and M. Skoglund, "Combining long-term and low-rate short-term channel state information over correlated MIMO channels," *IEEE Trans. Wireless Commun.*, vol. 7, no. 7, pp. 2409–2414, 2008.
- [KCJ08] M. Kobayashi, G. Caire, and N. Jindal, "How much training and feedback are needed in MIMO broadcast channels?" in *Proc. IEEE ISIT'08*, 2008.
- [KDB09] M. Kobayashi, M. Debbah, and J. Belfiore, "Outage efficient strategies in network MIMO with partial CSIT," in *Proc. IEEE ISIT'09*, 2009, pp. 249–253.

- [KdFG06] M. Kountouris, R. de Francisco, and D. Gesbert, "Multiuser diversity - multiplexing tradeoff in MIMO broadcast channels with limited feedback," in *Proc. ACSSC'06*, 2006, pp. 364–368.
- [KdFG+07] M. Kountouris, R. de Francisco, D. Gesbert, D. Slock, and T. Sälzer, "Efficient metrics for scheduling in MIMO broadcast channels with limited feedback," in *Proc. IEEE ICASSP'07*, vol. 3, 2007, pp. 109–112.
- [KfV06] M. Karakayali, G. Foschini, and R. Valenzuela, "Network coordination for spectrally efficient communications in cellular systems," *IEEE Wireless Commun. Mag.*, vol. 13, no. 4, pp. 56–61, 2006.
- [KGS08] M. Kountouris, D. Gesbert, and T. Sälzer, "Enhanced multiuser random beamforming: Dealing with the not so large number of users case," *IEEE J. Sel. Areas Commun.*, vol. 26, no. 8, pp. 1536–1545, 2008.
- [KK08] M. Ku and D. Kim, "Tx-Rx beamforming with multiuser MIMO channels in multiple-cell systems," in *Proc. ICACT'08*, 2008, pp. 1767–1771.
- [KK10] S. Kaviani and W. Krzymien, "Multicell scheduling in network MIMO," in *Proc. IEEE GLOBECOM'10*, 2010.
- [KKGK09] F. Kaltenberger, M. Kountouris, D. Gesbert, and R. Knopp, "On the trade-off between feedback and capacity in measured MU-MIMO channels," *IEEE Trans. Wireless Commun.*, vol. 8, no. 9, pp. 4866–4875, 2009.
- [KKT07] D. Katselis, E. Kofidis, and S. Theodoridis, "Training-based estimation of correlated MIMO fading channels in the presence of colored interference," *Signal Processing*, vol. 87, pp. 2177–2187, 2007.
- [KKT08] D. Katselis, E. Kofidis, and S. Theodoridis, "On training optimization for estimation of correlated MIMO channels in the presence of multiuser interference," *IEEE Trans. Signal Process.*, vol. 56, no. 10, pp. 4892–4904, 2008.
- [KL10] E. Karipidis and E. Larsson, "Efficient computation of the Pareto boundary for the MISO interference channel with perfect CSI," in *Proc. WiOpt'10*, 2010, pp. 573–577.

- [KS04] J. Kotecha and A. Sayeed, “Transmit signal design for optimal estimation of correlated MIMO channels,” *IEEE Trans. Signal Process.*, vol. 52, no. 2, pp. 546–557, 2004.
- [KSP<sup>+</sup>02] J. Kermoal, L. Schumacher, K. Pedersen, P. Mogensen, and F. Frederiksen, “A stochastic MIMO radio channel model with experimental validation,” *IEEE J. Sel. Areas Commun.*, vol. 20, no. 6, pp. 1211–1226, 2002.
- [KTS<sup>+</sup>10] P. Komulainen, A. Tölli, B. Song, F. Roemer, E. Björnson, and M. Bengtsson, “CSI acquisition concepts for advanced antenna schemes in the WINNER+ project,” in *Proc. Future Network and Mobile Summit*, 2010.
- [KY12] B. Khoshnevis and W. Yu, “Bit allocation laws for multi-antenna channel quantization: Multi-user case,” *IEEE Trans. Signal Process.*, 2012, to appear.
- [LBG80] Y. Linde, A. Buzo, and R. Gray, “An algorithm for vector quantizer design,” *IEEE Trans. Commun.*, vol. 28, no. 1, pp. 84–95, 1980.
- [LDL11] Y.-F. Liu, Y.-H. Dai, and Z.-Q. Luo, “Coordinated beamforming for MISO interference channel: Complexity analysis and efficient algorithms,” *IEEE Trans. Signal Process.*, vol. 59, no. 3, pp. 1142–1157, 2011.
- [LELM09] E. Larsson, E. Jorswieck, J. Lindblom, and R. Mochaourab, “Game theory and the flat-fading Gaussian interference channel,” *IEEE Signal Process. Mag.*, vol. 26, no. 5, pp. 18–27, 2009.
- [LG01] L. Li and A. Goldsmith, “Capacity and optimal resource allocation for fading broadcast channels—part i: Ergodic capacity,” *IEEE Trans. Inf. Theory*, vol. 47, no. 3, pp. 1083–1102, 2001.
- [LH06] D. Love and R. Heath, “Limited feedback diversity techniques for correlated channels,” *IEEE Trans. Veh. Technol.*, vol. 55, no. 2, pp. 718–722, 2006.
- [LHL<sup>+</sup>08] D. Love, R. Heath, V. Lau, D. Gesbert, B. Rao, and M. Andrews, “An overview of limited feedback in wireless communication systems,” *IEEE J. Sel. Areas Commun.*, vol. 26, no. 8, pp. 1341–1365, 2008.

- [LHS03] D. Love, R. Heath, and T. Strohmer, “Grassmannian beamforming for multiple-input multiple-output wireless systems,” *IEEE Trans. Inf. Theory*, vol. 49, no. 10, pp. 2735–2747, 2003.
- [LHS04] D. Love, R. Heath, and T. Strohmer, “What is the value of limited feedback for MIMO channels?” *IEEE Commun. Mag.*, vol. 42, no. 10, pp. 54–59, 2004.
- [LJ07] J. Lee and N. Jindal, “High SNR analysis for MIMO broadcast channels: Dirty paper coding vs. linear precoding,” *IEEE Trans. Inf. Theory*, vol. 53, no. 12, pp. 4787–4792, 2007.
- [LJ10] A. Lozano and N. Jindal, “Transmit diversity vs. spatial multiplexing in modern MIMO systems,” *IEEE Trans. Wireless Commun.*, vol. 9, no. 1, pp. 186–197, 2010.
- [LJS+08] B. O. Lee, H. W. Je, I. Sohn, O.-S. Shin, and K. B. Lee, “Interference-aware decentralized precoding for multi-cell MIMO TDD systems,” in *Proc. IEEE GLOBECOM’08*, 2008.
- [LKL11] J. Lindblom, E. Karipidis, and E. Larsson, “Closed-form parameterization of the Pareto boundary for the two-user MISO interference channel,” in *Proc. IEEE ICASSP’11*, 2011, pp. 3372–3375.
- [Löf04] J. Löfberg, “YALMIP: A toolbox for modeling and optimization in MATLAB,” in *Proc. IEEE CACSD*, 2004, pp. 284–289.
- [Loy01] S. Loyka, “Channel capacity of MIMO architecture using the exponential correlation matrix,” *IEEE Commun. Lett.*, vol. 5, no. 9, pp. 369–371, 2001.
- [LTE10] *Evolved Universal Terrestrial Radio Access (E-UTRA); Physical Channels and Modulation (Release 9)*. 3GPP TS 36.213, Sep. 2010.
- [LTV05] A. Lozano, A. Tulino, and S. Verdú, “High-SNR power offset in multiantenna communication,” *IEEE Trans. Inf. Theory*, vol. 51, no. 12, pp. 4134–4151, 2005.
- [LWH07] Y. Liu, T. Wong, and W. Hager, “Training signal design for estimation of correlated MIMO channels with colored interference,” *IEEE Trans. Signal Process.*, vol. 55, no. 4, pp. 1486–1497, 2007.

- [LZ08] Z.-Q. Luo and S. Zhang, "Dynamic spectrum management: Complexity and duality," *IEEE J. Sel. Topics Signal Process.*, vol. 2, no. 1, pp. 57–73, 2008.
- [LZX<sup>+</sup>10] J. Li, H. Zhang, X. Xu, X. Tao, T. Svensson, C. Botella, and B. Liu, "A novel frequency reuse scheme for coordinated multi-point transmission," in *Proc. IEEE VTC'10-Spring*, 2010.
- [MAMK09] M. Maddah-Ali, A. Mobasher, and A. Khandani, "Fairness in multiuser systems with polymatroid capacity region," *IEEE Trans. Inf. Theory*, vol. 55, no. 5, pp. 2128–2138, 2009.
- [MBG<sup>+</sup>11] P. Marsch, S. Brück, A. Garavaglia, M. Schulist, R. Weber, and A. Dekorsy, "Clustering," in *Coordinated Multi-Point in Mobile Communications: From Theory to Practice*, P. Marsch and G. Fettweis, Eds. Cambridge, 2011, ch. 7, pp. 139–159.
- [MCS06] M. McKay, I. Collings, and P. Smith, "Capacity and SER analysis of MIMO beamforming with MRC," in *Proc. IEEE ICC'06*, 2006.
- [ME10] B. Makki and T. Eriksson, "On the average rate of quasi-static fading channels with ARQ and CSI feedback," *IEEE Commun. Lett.*, vol. 14, no. 9, pp. 806–808, 2010.
- [MF70] R. Mueller and G. Foschini, "The capacity of linear channels with additive Gaussian noise," *The Bell System Technical Journal*, pp. 81–94, 1970.
- [MF08] P. Marsch and G. Fettweis, "On multicell cooperative transmission in backhaul-constrained cellular systems," *Ann. Telecommun.*, vol. 63, pp. 253–269, 2008.
- [MF09] P. Marsch and G. Fettweis, "On downlink network MIMO under a constrained backhaul and imperfect channel knowledge," in *Proc. IEEE GLOBECOM'09*, 2009.
- [MF11] P. Marsch and G. Fettweis, "Static clustering for cooperative multi-point (CoMP) in mobile communications," in *Proc. IEEE ICC'11*, 2011.
- [MJ11a] R. Mochaourab and E. Jorswieck, "Optimal beamforming in interference networks with perfect local channel information," *IEEE Trans. Signal Process.*, vol. 59, no. 3, pp. 1128–1141, 2011.

- [MJ11b] R. Mochaourab and E. Jorswieck, "Walrasian equilibrium in two-user multiple-input single-output interference channels," in *Proc. IEEE ICC'11*, 2011.
- [MO79] A. Marshall and I. Olkin, *Inequalities: Theory of Majorization and Its Applications*. Academic Press, 1979.
- [MYG05] X. Ma, L. Yang, and G. Giannakis, "Optimal training for MIMO frequency-selective fading channels," *IEEE Trans. Wireless Commun.*, vol. 4, no. 2, pp. 453–466, 2005.
- [MZC06] M. Mohseni, R. Zhang, and J. Cioffi, "Optimized transmission for fading multiple-access and broadcast channels with multiple antennas," *IEEE J. Sel. Areas Commun.*, vol. 24, no. 8, pp. 1627–1639, 2006.
- [NEHA08] B. L. Ng, J. Evans, S. Hanly, and D. Aktas, "Distributed downlink beamforming with cooperative base stations," *IEEE Trans. Inf. Theory*, vol. 54, no. 12, pp. 5491–5499, 2008.
- [NMB09] H. Nooralizadeh, S. Moghaddam, and H. Bakhshi, "Optimal training sequences in MIMO channel estimation with spatially correlated Rician flat fading," in *Proc. IEEE ISIEA'09*, 2009, pp. 227–232.
- [NSGS10] F. Negro, S. Shenoy, I. Ghauri, and D. Slock, "Weighted sum rate maximization in the MIMO interference channel," in *Proc. IEEE PIMRC'10*, 2010, pp. 684–689.
- [OCVJP05] C. Oestges, B. Clerckx, D. Vanhoenacker-Janvier, and A. Paulraj, "Impact of fading correlations on MIMO communication systems in geometry-based statistical channel models," *IEEE Trans. Wireless Commun.*, vol. 4, no. 3, pp. 1112–1120, 2005.
- [Oes06] C. Oestges, "Validity of the Kronecker model for MIMO correlated channels," in *Proc. IEEE VTC'06-Spring*, 2006, pp. 2818–2822.
- [PC06] D. Palomar and M. Chiang, "A tutorial on decomposition methods for network utility maximization," *IEEE J. Sel. Areas Commun.*, vol. 24, no. 8, pp. 1439–1451, 2006.
- [PCL03] D. Palomar, J. Cioffi, and M. Lagunas, "Joint Tx-Rx beamforming design for multicarrier MIMO channels: a unified framework for convex optimization," *IEEE Trans. Signal Process.*, vol. 51, no. 9, pp. 2381–2401, 2003.

- [PDF<sup>+</sup>08] S. Parkvall, E. Dahlman, A. Furuskär, Y. Jading, M. Olsson, S. Wänstedt, and K. Zangi, “LTE-advanced - evolving LTE towards IMT-advanced,” in *Proc. IEEE VTC’08-Fall*, 2008.
- [PGH08] A. Papadogiannis, D. Gesbert, and E. Hardouin, “A dynamic clustering approach in wireless networks with multi-cell cooperative processing,” in *Proc. IEEE ICC’08*, 2008.
- [PHS05] C. Peel, B. Hochwald, and A. Swindlehurst, “A vector-perturbation technique for near-capacity multi-antenna multi-user communication—part I: Channel inversion and regularization,” *IEEE Trans. Commun.*, vol. 53, no. 1, pp. 195–202, 2005.
- [PLZL07] J. Pang, J. Li, L. Zhao, and Z. Lü, “Optimal training sequences for MIMO channel estimation with spatial correlation,” in *Proc. IEEE VTC’07-Fall*, 2007, pp. 651–655.
- [PP08] K. Petersen and M. Pedersen, “The matrix cookbook,” <http://www2.imm.dtu.dk/pubdb/p.php?3274>, Oct. 2008.
- [PPV10] Y. Polyanskiy, H. Poor, and S. Verdú, “Channel coding rate in the finite blocklength regime,” *IEEE Trans. Inf. Theory*, vol. 56, no. 5, pp. 2307–2359, 2010.
- [PSC05] S. Pillai, T. Suel, and S. Cha, “The Perron-Frobenius theorem: some of its applications,” *IEEE Signal Process. Mag.*, vol. 22, no. 2, pp. 62–75, 2005.
- [RC98] G. Raleigh and J. Cioffi, “Spatio-temporal coding for wireless communication,” *IEEE Trans. Commun.*, vol. 46, no. 3, pp. 357–366, 1998.
- [RHS07] V. Raghavan, R. Heath, and A. Sayeed, “Systematic codebook designs for quantized beamforming in correlated MIMO channels,” *IEEE J. Sel. Areas Commun.*, vol. 25, no. 7, pp. 1298–1310, 2007.
- [RJ08a] N. Ravindran and N. Jindal, “Limited feedback-based block diagonalization for the MIMO broadcast channel,” *IEEE J. Sel. Areas Commun.*, vol. 26, no. 8, pp. 1473–1482, 2008.
- [RJ08b] N. Ravindran and N. Jindal, “Multi-user diversity vs. accurate channel feedback for MIMO broadcast channels,” in *Proc. IEEE ICC’08*, 2008, pp. 3684–3688.

- [RL06] T. Ren and R. La, “Downlink beamforming algorithms with inter-cell interference in cellular networks,” *IEEE Trans. Wireless Commun.*, vol. 5, no. 10, pp. 2814–2823, 2006.
- [RTSH11] M. Rossi, A. Tulino, O. Simeone, and A. Haimovich, “Non-convex utility maximization in Gaussian MISO broadcast and interference channels,” in *Proc. IEEE ICASSP’11*, 2011, pp. 2960–2963.
- [Rud76] W. Rudin, *Principles of Mathematical Analysis*. McGraw-Hill, 1976.
- [SA98] M. Simon and M. Alouini, “A unified approach to the performance analysis of digital communication over generalized fading channels,” *Proc. IEEE*, vol. 86, no. 9, pp. 1860–1877, 1998.
- [Say02] A. Sayeed, “Deconstructing multiantenna fading channels,” *IEEE Trans. Signal Process.*, vol. 50, no. 10, pp. 2563–2579, 2002.
- [SB04] M. Schubert and H. Boche, “Solution of the multiuser downlink beamforming problem with individual SINR constraints,” *IEEE Trans. Veh. Technol.*, vol. 53, no. 1, pp. 18–28, 2004.
- [SB05] M. Schubert and H. Boche, “QoS-based resource allocation and transceiver optimization,” *Foundations and Trends in Communication and Information Theory*, vol. 2, no. 6, pp. 383–529, 2005.
- [SB11a] N. Shariati and M. Bengtsson, “How far from Kronecker can a MIMO channel be? Does it matter?” in *Proc. European Wireless*, 2011.
- [SB11b] N. Shariati and M. Bengtsson, “Robust training sequence design for spatially correlated MIMO channels and arbitrary colored disturbance,” in *Proc. IEEE PIMRC’11*, 2011.
- [SCA<sup>+</sup>06] Z. Shen, R. Chen, J. Andrews, R. Heath, and B. Evans, “Low complexity user selection algorithms for multiuser MIMO systems with block diagonalization,” *IEEE Trans. Signal Process.*, vol. 54, no. 9, pp. 3658–3663, 2006.
- [SCG06] X. Shang, B. Chen, and M. Gans, “On the achievable sum rate for MIMO interference channels,” *IEEE Trans. Inf. Theory*, vol. 52, no. 9, pp. 4313–4320, 2006.

- [Sch88] E. Scheuer, "Reliability of an  $m$ -out-of- $n$  system when component failure induces higher failure rates in survivors," *IEEE Trans. Rel.*, vol. 37, no. 1, pp. 73–74, 1988.
- [SCP11] X. Shang, B. Chen, and H. V. Poor, "Multiuser MISO interference channels with single-user detection: Optimality of beamforming and the achievable rate region," *IEEE Trans. Inf. Theory*, vol. 57, no. 7, pp. 4255–4273, 2011.
- [SD08] M. B. Shenouda and T. Davidson, "Probabilistically-constrained approaches to the design of the multiple antenna downlink," in *Proc. Asilomar'08*, 2008, pp. 1120–1124.
- [SD09] M. B. Shenouda and T. Davidson, "Nonlinear and linear broadcasting with QoS requirements: Tractable approaches for bounded channel uncertainties," *IEEE Trans. Signal Process.*, vol. 57, no. 5, pp. 1936–1947, 2009.
- [SGB99] A. Scaglione, G. Giannakis, and S. Barbarossa, "Redundant filterbank precoders and equalizers part I: Unification and optimal designs," *IEEE Trans. Signal Process.*, vol. 47, no. 7, pp. 1988–2006, 1999.
- [SGH08] H. Skjveling, D. Gesbert, and A. Hjørungnes, "Low-complexity distributed multibase transmission and scheduling," *EURASIP J. on Adv. in Signal Process.*, 2008.
- [SH04] W. Santipach and M. Honig, "Asymptotic capacity of beamforming with limited feedback," in *Proc. IEEE ISIT'04*, 2004, p. 290.
- [SH05] M. Sharif and B. Hassibi, "On the capacity of MIMO broadcast channels with partial side information," *IEEE Trans. Inf. Theory*, vol. 51, no. 2, pp. 506–522, 2005.
- [SH06] W. Santipach and M. Honig, "Capacity of beamforming with limited training and feedback," in *Proc. IEEE ISIT'06*, 2006, pp. 376–380.
- [SH07] J. Shi and M. Ho, "MIMO broadcast channels with channel estimation," in *Proc. IEEE ICC'07*, 2007, pp. 1042–1047.
- [Sha48] C. Shannon, "A mathematical theory of communication," *Bell System Technical Journal*, vol. 27, pp. 379–423, 623–656, 1948.

- [SLF09] C. Shen, T. Liu, and M. Fitz, "On the average rate performance of hybrid-ARQ in quasi-static fading channels," *IEEE Trans. Commun.*, vol. 57, no. 11, pp. 3339–3352, 2009.
- [SP09] L. Sanguinetti and H. Poor, "Fundamentals of multi-user MIMO communications," in *New Directions in Wireless Communications Research*, V. Tarokh, Ed. Springer US, 2009, pp. 139–173.
- [SSH04] Q. Spencer, A. Swindlehurst, and M. Haardt, "Zero-forcing methods for downlink spatial multiplexing in multiuser MIMO channels," *IEEE Trans. Signal Process.*, vol. 52, no. 2, pp. 461–471, 2004.
- [SSPS09] O. Simeone, O. Somekh, H. V. Poor, and S. Shamai, "Downlink multicell processing with limited-backhaul capacity," *EURASIP J. on Adv. in Signal Process.*, 2009.
- [Str03] R. Stridh, "Smart antennas in wireless networks: System issues and performance limits," Ph.D. dissertation, KTH Royal Institute of Technology, 2003.
- [STS07] M. Sadek, A. Tarighat, and A. Sayed, "A leakage-based precoding scheme for downlink multi-user MIMO channels," *IEEE Trans. Wireless Commun.*, vol. 6, no. 5, pp. 1711–1721, 2007.
- [SWB10] C. Studer, M. Wenk, and A. Burg, "MIMO transmission with residual transmit-RF impairments," in *Proc. ITG/IEEE Workshop on Smart Antennas (WSA)*, 2010.
- [SZ01] S. Shamai and B. Zaidel, "Enhancing the cellular downlink capacity via co-processing at the transmitting end," in *Proc. IEEE VTC'01-Spring*, vol. 3, 2001, pp. 1745–1749.
- [TAKT05] H. Tuy, F. Al-Khayyal, and P. Thach, "Monotonic optimization: Branch and cut methods," in *Essays and Surveys in Global Optimization*, C. Audet, P. Hansen, and G. Savard, Eds. Springer US, 2005.
- [TBH08] M. Trivellato, F. Boccardi, and H. Huang, "On transceiver design and channel quantization for downlink multiuser MIMO systems with limited feedback," *IEEE J. Sel. Areas Commun.*, vol. 26, no. 8, pp. 1494–1504, 2008.

- [TBT07] M. Trivellato, F. Boccardi, and F. Tosato, "User selection schemes for MIMO broadcast channels with limited feedback," in *Proc. IEEE VTC'07-Spring*, 2007, pp. 2089–2093.
- [TCJ08] A. Tölli, M. Codreanu, and M. Juntti, "Cooperative MIMO-OFDM cellular system with soft handover between distributed base station antennas," *IEEE Trans. Wireless Commun.*, vol. 7, no. 4, pp. 1428–1440, 2008.
- [Tel99] E. Telatar, "Capacity of multi-antenna Gaussian channels," *European Trans. Telecom.*, vol. 10, no. 6, pp. 585–595, 1999.
- [TO96] T. Trump and B. Ottersten, "Estimation of nominal direction of arrival and angular spread using an array of sensors," *Signal Processing*, vol. 50, no. 1-2, pp. 57–69, 1996.
- [TPK09] A. Tölli, H. Pennanen, and P. Komulainen, "On the value of coherent and coordinated multi-cell transmission," in *Proc. IEEE ICC'09*, 2009.
- [TPW11] A. Tajer, N. Prasad, and X. Wang, "Robust linear precoder design for multi-cell downlink transmission," *IEEE Trans. Signal Process.*, vol. 59, no. 1, pp. 235–251, 2011.
- [TTT03] R. Tütüncü, K. Toh, and M. Todd, "Solving semidefinite-quadratic-linear programs using SDPT3," *Mathematical Programming*, vol. 95, no. 2, pp. 189–217, 2003.
- [Tuy00] H. Tuy, "Monotonic optimization: Problems and solution approaches," *SIAM J. Optim.*, vol. 11, no. 2, pp. 464–494, 2000.
- [TV05] D. Tse and P. Viswanath, *Fundamentals of Wireless Communication*. Cambridge University Press, 2005.
- [VB09] N. Vučić and H. Boche, "Robust QoS-constrained optimization of downlink multiuser MISO systems," *IEEE Trans. Signal Process.*, vol. 57, no. 2, pp. 714–725, 2009.
- [VBS09] N. Vučić, H. Boche, and S. Shi, "Robust transceiver optimization in downlink multiuser MIMO systems," *IEEE Trans. Signal Process.*, vol. 57, no. 9, pp. 3576–3587, 2009.
- [VLS05] V. Veeravalli, Y. Liang, and A. Sayeed, "Correlated MIMO wireless channels: capacity, optimal signaling, and asymptotics," *IEEE Trans. Inf. Theory*, vol. 51, no. 6, pp. 2058–2072, 2005.

- [VLV07] S. Venkatesan, A. Lozano, and R. Valenzuela, "Network MIMO: Overcoming intercell interference in indoor wireless systems," in *Proc. IEEE ACSSC'07*, 2007, pp. 83–87.
- [VP07] M. Vu and A. Paulraj, "MIMO wireless linear precoding," *IEEE Signal Processing Magazine*, vol. 24, no. 5, pp. 86–105, 2007.
- [VPW10] L. Venturino, N. Prasad, and X. Wang, "Coordinated linear beamforming in downlink multi-cell wireless networks," *IEEE Trans. Wireless Commun.*, vol. 9, no. 4, pp. 1451–1461, 2010.
- [VT03] P. Viswanath and D. Tse, "Sum capacity of the vector Gaussian broadcast channel and uplink-downlink duality," *IEEE Trans. Inf. Theory*, vol. 49, no. 8, pp. 1912–1921, 2003.
- [VVH03] H. Viswanathan, S. Venkatesan, and H. Huang, "Downlink capacity evaluation of cellular networks with known-interference cancellation," *IEEE J. Sel. Areas Commun.*, vol. 21, no. 5, pp. 802–811, 2003.
- [WCLaE10] P. Weeraddana, M. Codreanu, M. Latva-aho, and A. Ephremides, "Weighted sum-rate maximization for a set of interfering links via branch and bound," in *Proc. Asilomar'10*, 2010.
- [WCWKM11] K.-Y. Wang, T.-H. Chang, and C.-Y. C. W.-K. Ma, A. So, "Probabilistic SINR constrained robust transmit beamforming: A Bernstein-type inequality based conservative approach," in *Proc. IEEE ICASSP'11*, 2011, pp. 3080–3083.
- [WES06] A. Wiesel, Y. Eldar, and S. Shamai, "Linear precoding via conic optimization for fixed MIMO receivers," *IEEE Trans. Signal Process.*, vol. 54, no. 1, pp. 161–176, 2006.
- [WES08] A. Wiesel, Y. Eldar, and S. Shamai, "Zero-forcing precoding and generalized inverses," *IEEE Trans. Signal Process.*, vol. 56, no. 9, pp. 4409–4418, 2008.
- [WHOB06] W. Weichselberger, M. Herdin, H. Özcelik, and E. Bonek, "A stochastic MIMO channel model with joint correlation of both link ends," *IEEE Trans. Wireless Commun.*, vol. 5, no. 1, pp. 90–100, 2006.
- [Win84] J. Winters, "Optimum combining in digital mobile radio with cochannel interference," *IEEE J. Sel. Areas Commun.*, vol. 2, no. 4, pp. 528–539, 1984.

- [WJ01] J. Wallace and M. Jensen, "Measured characteristics of the MIMO wireless channel," in *Proc. IEEE VTC'01-Fall*, vol. 4, 2001, pp. 2038–2042.
- [WJ09a] K. Werner and M. Jansson, "Estimating MIMO channel covariances from training data under the Kronecker model," *Signal Processing*, vol. 89, no. 1, pp. 1–13, 2009.
- [WJ09b] P. Wu and N. Jindal, "Coding versus ARQ in fading channels: How reliable should the PHY be?" in *Proc. IEEE GLOBECOM'09*, 2009.
- [WSS06] H. Weingarten, Y. Steinberg, and S. Shamai, "The capacity region of the Gaussian multiple-input multiple-output broadcast channel," *IEEE Trans. Inf. Theory*, vol. 52, no. 9, pp. 3936–3964, 2006.
- [XCL10] X. Xu, X. Chen, and J. Li, "Handover mechanism in coordinated multi-point transmission/reception system," *ZTE Communications*, no. 1, pp. 31–35, 2010.
- [YBB11] J. Yang, E. Björnson, and M. Bengtsson, "Receive beamforming design based on a multiple-state interference model," in *Proc. IEEE ICC'11*, 2011.
- [YBO<sup>+</sup>04] K. Yu, M. Bengtsson, B. Ottersten, D. McNamara, P. Karlsson, and M. Beach, "Modeling of wide-band MIMO radio channels based on NLoS indoor measurements," *IEEE Trans. Veh. Technol.*, vol. 53, no. 3, pp. 655–665, 2004.
- [YG06] T. Yoo and A. Goldsmith, "On the optimality of multi-antenna broadcast scheduling using zero-forcing beamforming," *IEEE J. Sel. Areas Commun.*, vol. 24, no. 3, pp. 528–541, 2006.
- [YJG07] T. Yoo, N. Jindal, and A. Goldsmith, "Multi-antenna downlink channels with limited feedback and user selection," *IEEE J. Sel. Areas Commun.*, vol. 25, no. 7, pp. 1478–1491, 2007.
- [YL07] W. Yu and T. Lan, "Transmitter optimization for the multi-antenna downlink with per-antenna power constraints," *IEEE Trans. Signal Process.*, vol. 55, no. 6, pp. 2646–2660, 2007.
- [YRT09] C.-H. Yu, K. Ruttik, and O. Tirkkonen, "Approximate rate quantization of adaptive modulation and coding with near-optimum throughput," in *Proc. IEEE PIMRC'09*, 2009, pp. 157–161.

- [Zab95] S. Zabell, "Alan Turing and the central limit theorem," *The American Mathematical Monthly*, vol. 102, no. 6, pp. 483–494, 1995.
- [ZC10] R. Zhang and S. Cui, "Cooperative interference management with MISO beamforming," *IEEE Trans. Signal Process.*, vol. 58, no. 10, pp. 5450–5458, 2010.
- [ZCA<sup>+</sup>09] J. Zhang, R. Chen, J. Andrews, A. Ghosh, and R. Heath, "Networked MIMO with clustered linear precoding," *IEEE Trans. Wireless Commun.*, vol. 8, no. 4, pp. 1910–1921, 2009.
- [ZD04] H. Zhang and H. Dai, "Cochannel interference mitigation and cooperative processing in downlink multicell multiuser MIMO networks," *EURASIP J. Wirel. Commun. Netw.*, vol. 2, pp. 222–235, 2004.
- [ZG07] R. Zakhour and D. Gesbert, "A two-stage approach to feedback design in multi-user MIMO channels with limited channel state information," in *Proc. IEEE PIMRC'07*, 2007.
- [ZG10a] R. Zakhour and D. Gesbert, "Distributed multicell-MISO precoding using the layered virtual SINR framework," *IEEE Trans. Wireless Commun.*, vol. 9, no. 8, pp. 2444–2448, 2010.
- [ZG10b] R. Zakhour and D. Gesbert, "Team decision for the cooperative MIMO channel with imperfect CSIT sharing," in *Proc. ITA '10*, 2010.
- [ZG11] R. Zakhour and D. Gesbert, "Optimized data sharing in multicell MIMO with finite backhaul capacity," *IEEE Trans. Signal Process.*, 2011, to appear.
- [ZH10] R. Zhang and L. Hanzo, "Joint and distributed linear precoding for centralised and decentralised multicell processing," in *Proc. IEEE VTC'10-Fall*, 2010.
- [Zha05] F. Zhang, *The Schur Complement and Its Applications*. Springer, 2005.
- [ZHKA09] J. Zhang, R. Heath, M. Kountouris, and J. Andrews, "Mode switching for the multi-antenna broadcast channel based on delay and channel quantization," *EURASIP J. on Adv. in Signal Process.*, 2009.

- [ZJOP09] X. Zhang, E. Jorswieck, B. Ottersten, and A. Paulraj, "On the asymptotic optimality of opportunistic norm-based user selection with hard SINR constraint," *EURASIP J. on Adv. in Signal Process.*, 2009.
- [ZKAH11] J. Zhang, M. Kountouris, J. Andrews, and R. Heath, "Multi-mode transmission for the MIMO broadcast channel with imperfect channel state information," *IEEE Trans. Commun.*, vol. 59, no. 3, pp. 803–814, 2011.
- [ZL04] Y. Zhang and K. Letaief, "Multiuser adaptive subcarrier-and-bit allocation with adaptive cell selection for OFDM systems," *IEEE Trans. Wireless Commun.*, vol. 3, no. 5, pp. 1566–1575, 2004.
- [ZL06] S. Zhou and B. Li, "BER criterion and codebook construction for finite-rate precoded spatial multiplexing with linear receivers," *IEEE Trans. Signal Process.*, vol. 54, no. 5, pp. 1653–1665, 2006.
- [ZMM<sup>+</sup>08] H. Zhang, N. Mehta, A. Molisch, J. Zhang, and H. Dai, "Asynchronous interference mitigation in cooperative base station systems," *IEEE Trans. Wireless Commun.*, vol. 7, no. 1, pp. 155–165, 2008.
- [ZO95] P. Zetterberg and B. Ottersten, "The spectrum efficiency of a base station antenna array system for spatially selective transmission," *IEEE Trans. Veh. Technol.*, vol. 44, no. 3, pp. 651–660, 1995.
- [ZT03] L. Zheng and D. Tse, "Diversity and multiplexing: A fundamental tradeoff in multiple-antenna channels," *IEEE Trans. Inf. Theory*, vol. 49, no. 5, pp. 1073–1096, 2003.
- [ZWN08a] G. Zheng, K.-K. Wong, and T.-S. Ng, "Robust linear MIMO in the downlink: A worst-case optimization with ellipsoidal uncertainty regions," *EURASIP J. on Adv. in Signal Process.*, 2008.
- [ZWN08b] G. Zheng, K.-K. Wong, and T.-S. Ng, "Throughput maximization in linear multiuser MIMO-OFDM downlink systems," *IEEE Trans. Veh. Commun.*, vol. 57, no. 3, pp. 1993–1998, 2008.